Joanne Caddy
BSc (HONS) Applied Biosciences

The Non-Genomic Effects Of The PPAR-γ Ligand Rosiglitazone On Intracellular Calcium Concentrations In Mammalian Monocytic And Smooth Muscle Cells

A DOCTORAL THESIS
UNIVERSITY OF WALES

University of Wales Institute, Cardiff
School of Health Sciences

Submitted November 2009

Submitted in fulfilment of the requirements for the award of Doctor of Philosophy, UWIC

Director of Studies:
Dr Richard Webb
(School of Health Sciences, UWIC)

Supervisors:
Dr Andrew Thomas
(School of Health Sciences, UWIC)
&
Dr Derek Lang
(Welsh Heart Research Institute, Cardiff University)

The research within this thesis was undertaken under the auspices of the University of Wales Institute, Cardiff

Abstract

Thiazolidinediones such as rosiglitazone are used in the treatment of Type-2 Diabetes, and are ligands for peroxisome proliferator-activated receptor-gamma (PPARγ), a ligand-activated transcription factor that regulates expression of genes involved in glucose and lipid metabolism. However, rosiglitazone is known to exert PPARγ-independent effects alongside its classical receptor-dependent effects. This study investigated the PPARγ-independent effects of rosiglitazone on intracellular calcium (Ca^{2+}_i) signalling in cultured monocytic and vascular smooth muscle cells

Rosiglitazone rapidly (5-30min) inhibited the Ca^{2+} sequestration activity of the ER-resident Ca^{2+} pump enzyme SERCA2b in a dose-dependent manner (IC_{50}~2μM). 10μM Rosiglitazone triggered rapid increases in $[Ca^{2+}]_i$; however, restoration to basal levels occurred within 72h. Consequently, cell viability was not adversely affected by rosiglitazone treatment.

Initiation of the unfolded protein response (UPR) was identified as the mechanism underpinning rosiglitazone's Ca^{2+} homeostatic restorative properties. Rosiglitazone induced alternate splicing of the UPR transcription factor XBP-1, which led to increased mRNA and protein expression of SERCA2b (shown via bioinformatics analysis to be a UPR target gene), and increased ER Ca^{2+}-ATPase activity in rosiglitazone-treated cells.

In tissue (rabbit aortic ring) samples, 10μM rosiglitazone induced transient (within 1h) non-significant losses in vasorelaxatory sensitivity to sodium nitroprusside, but extended treatment (4-24h) increased sensitivity beyond that of vehicle-treated samples. Thus, at cell and tissue levels, this data suggests that rosiglitazone initially causes increased $[Ca^{2+}]_i$ due to inhibition of SERCA2b, but extended incubation induces - via upregulation of UPR target genes - the restoration of Ca^{2+} homeostasis, and possibly even improvements in function in some contexts.

Clearly, the data presented in this *in vitro* study must be treated tentatively, and more research is needed before these potentially beneficial effects can be firmly identified as being clinically significant. Nevertheless, the data obtained here may constitute preliminary evidence that, alongside its PPARγ-dependent effects, rosiglitazone may exert functional improvements on the vasculature.

DECLARATION

This work has not previously been accepted in substance for any degree and is not being currently submitted in candidature for any degree.

Signed……(candidate)

Date……

STATEMENT 1

This thesis is the result of my own investigations, except where otherwise stated. Where correction services have been used, the extent and nature of the correction is clearly marked in a footnote(s).

Other sources are acknowledged by footnotes giving explicit references. A bibliography is appended.

Signed……(candidate)

Date……

STATEMENT 2

I hereby give consent for my thesis, if accepted, to be available for photocopying and for inter-library loan, and for the title and summary to be made available to outside organisations.

Signed……(candidate)

Date……

Acknowledgements

I would first and foremost like to thank Dr Richard Webb, my Director of Studies, for his continued help, guidance and support throughout my entire studies, but most importantly towards the latter months when his support became invaluable. I would also like to thank my PhD supervisors, Dr Andrew Thomas and Dr Derek Lang for their help over the last few years. In particular, I would like to extend my sincere thanks to Dr Lang for allowing me to carry out some of my research in his lab at the Welsh Heart Research Institute and for his tremendous help, during this time and throughout. Although not part of my supervisory team, I would also like to say a special thanks to Dr Keith Morris for his constant help and encouragement and for always making me smile during difficult times.

The experimental work in this thesis was also assisted from time to time by members of the UWIC Cardiff School of Health Science technical staff, namely Steve, Paul, Gareth and Leighton and I would like to extend my gratitude to them for their help.

Special thanks go to Cathryn, Lee, Hannah, Lowri, Rowena and Neenu, fellow academic associates and good friends, for being there for me continuously throughout the last few years and who have made the whole PhD experience one I will never forget. Thanks also go to my good friends and family outside of UWIC who have wholeheartedly supported me throughout my entire studies.

Lastly, I must say special thanks to the most important people. Thanks go to my parents for their constant belief in me and for instilling in me that anything is possible and that if you work hard enough you will always succeed. Thanks go to Chris for his unwavering love, support and patience throughout my entire studies, for being the one person I could always turn to and for putting up with my constant moaning throughout the difficult times. Finally, this thesis is dedicated to Ben, my as-yet unborn son, who‟s constant wriggling and kicking over the last few months has reminded me that there are many good times ahead and whose impending arrival has focussed my efforts on completing this PhD and on one day making him proud of what his mum has achieved.

List of Figures

Abbreviations

ACh – Acetylcholine

AChR - acetylcholine receptor

ADOPT - „A Diabetes Outcome Progression Trial"

ADP – Adenosine diphosphate

AGE - Advanced glycosylation end-products

ALT – Alanine aminotransferase

Anova – One way analysis of variance

A7r5 – Rat aortic vascular smooth muscle cell line

Ask1 - apoptosis signal-regulating kinase 1

ATF-2 – Activating transcription factor-2

ATF-4 – Activating transcription factor-4

ATF-6 – Activating transcription factor-6

ATP – Adenosine tri-phosphate

BiP – Binding protein

BLAST - Basic Local Alignment Search Tool

BSA – Bovine Serum Albumin

Ca^{2+} - „free" intracellular ionic calcium

$CaCl_2$ – Calcium chloride

CaM -Calmodulin

Ca^{2+}CaM - Calcium calmodulin complex

cGMP- cyclic Guanosine 3,5-monophosphate

CPA - Cyclopiozonic acid

COX-2 - Cyclooxygenase-2

CRAC – Ca^{2+}-release activated Ca^{2+} channel

CT – Cycle threshold

CV - Cardiovascular

CVD – Cardiovascular disease

DAG - Diacylglycerol

d-cAMP - dibutyryl-cyclic AMP

DMEM – Dulbecco"s Modified Eagle Medium

DMSO - Dimethyl sulfoxide

DREAM – „Diabetes Reduction Assessment with ramipril and rosiglitazone Medication" trial

eIF2α - eukaryotic initiation factor-alpha

eNOS – endothelial nitric oxide synthase

ER – Endoplasmic reticulum

ERSE - ER stress enhancer

FCS - Foetal Calf Serum

GTP - guanosine 5-triphosphate

GAPDH - Glyceraldehyde Phosphate Dehydrogenase

GCRs - G protein-coupled receptors

HODE – Hydroxyoctadecadienoic acid

hSPCA - Human secretory Pathway Ca^{2+}ATPases

IL4 - Interleukin-4

IL6 – Interleukin-6

IFN-γ - Interferon-γ

iNOS - inducible nitric oxide snthase

IP_3 – Inositol tri-phosphate

IP_3R - Inositol tri-phosphate receptors

Ire1 - Inositol requiring enzyme-1

p38 MAPK – p38 Mitogen activated protein kinase

JNK - c-Jun N-terminal kinase

KCl – Potassium chloride

LDL – Low density lipoprotein

LPS – Liposaccharide

MLCK - myosin light chain kinase

MM6 – Monomac 6 (monocytic cell line)

Mn^{2+} - Manganese ions

mRNA – messenger ribonucleic acid

MI – Myocardial infarction

NCX - sodium calcium exchanger

NF-κB – Nuclear factor kappa B

NFκB - Nuclear factor kappaB

NICE - National Institute of Clinical Excellence

NO – Nitric oxide

PBS – Phosphate buffered saline

PE – Phenylephrine

PERK - Protein kinase-like ER kinase

PGE_2 – prostaglandin E_2

PKG - phosphokinase G

PIP_2 - Phosphatidylinositol (4,5)-biphosphate

PLCβ - Phospholipase Cβ

PLN - Phosholamban

15d-PGJ2 - 15-deoxy-$\Delta^{12,14}$-prostaglandin J_2

PPARs –Peroxisome proliferator-activated receptors

PPRE – Peroxisome proliferator response element

PM – Plasma membrane

PMCA - Plasma membrane Ca^{2+}ATPase

PMR1- Yeast hSPCA

PSG - penicillin-streptomycin-glutamine

RAGE – Receptor for advanced glycosylation end-products

RECORD – „Rosiglitazone evaluated for cardiovascular outcomes in oral agent therapy for type 2 diabetes" trial

RPMI – Roswell Park Memorial Institute

RTKs - Receptor tyrosine kinase

RT-PCR – Reverse transcription polymerase chain reaction

RXR - 9-cis retanoic acid receptor

RyR – Ryanodine receptors

SERCA – Sarco(endo)plasmic reticulum Ca^{2+}ATPase

sGC - soluble guanylate cyclase

SLN - Sarcolipin

SNP – Sodium nitroprusside

SPCAs - Secretory Pathway Ca^{2+}ATPases

SR – Sarcoplasmic reticulum

STIM1 - Stromal interactacting molecule 1

T2D – Type 2 Diabetes Mellitus

TNFα - Tumour necrosis factor-alpha

TRAIL - Tumour necrosis factor-related apoptosis-inducing ligand

TRAF2 – TNF receptor-associated factor 2

TZD – Thiazolidinedione

UPR – Unfolded protein response

UPRE – Unfolded protein response element

VSMC – Vascular smooth muscle cell

Contents

Chapter 2: An investigation into the effect of rosiglitazone on intracellular Ca^{2+} homeostasis in monocytic and vascular smooth muscle cells.

Chapter 3: Elucidation of the mechanism for restoration of calcium homeostasis in rosiglitazone-treated monocytic and vascular smooth muscle cells

Chapter One

General Introduction

1.0 Introduction

1.1 Type 2 diabetes

1.1.1 Introduction to Type 2 diabetes

Type 2 diabetes mellitus (T2D) is an increasingly common disorder in which patients fail to respond effectively to endogenously produced insulin, leading to hyperglycaemia and other metabolic distrurbances. T2D is a serious condition and is associated with numerous life-threatening and disabling complications. T2D is strongly associated with cardiovascular disease due to the comparative nature of onset of both conditions.

The complications associated with T2D can be subdived into two groups: the macrovascular and the microvascular complication. Macrovascular complications are those which affect the larger arteries of the body, for example the development of atherosclerosis, which then leads to further damage and disease of the cardiovascular system as a whole. Microvascular complications are those affecting the smaller vessels of the body including the eyes, kidneys and peripheral nerves, producing devastating consequences such as blindness due to retinopathy, renal failure due to nephropathy and substantial nerve damage due to neuropathy respectively.

The increased prevalance of T2D over the last decades, from an estimated 30 million in 1985 to over 150 million in 2000 (Gruber *et al*, 2006) seems set to continue with predictions that the number of people globally with T2D will rise to well over 300 million by the year 2025 (Heine *et al*, 2006). Currently, 23 million people in the EU have T2D, and prevalence is increasing year-by-year (http://www.heartstats.org). According to the UK National Heart Forum, around 3% of British adults have diagnosed diabetes. However, it is estimated that around half of diabetes cases may be undiagnosed**,** putting the total prevalence at around 6% of adults (http://www.heartforum.org.uk). In broad agreement with these figures, the Welsh Assembly Government reports that in Wales, an estimated 140,000 people (or 4.4% of the population) have T2D, a figure somewhat higher than their quoted UK average of 3.8% (http://www.wales.nhs.uk).

Aside from the personal toll T2D and its complications have on patients, the economic toll they have on society is equally as devastating, with massive treatment costs for the NHS and the loss of income generated as a result of sickness and death in the increasingly susceptible population. As described above, cardiovascular disease (CVD) is a major complication of diabetes, and is a major cause of death both in the EU in general (2 million deaths per year (http://www.heartstats.org), and specifically in Wales, where it is responsible for 36.3% of all deaths, or 11,287 deaths per year (http://www.wales.nhs.uk). In 2006, production losses due to mortality and morbidity associated with CVD cost the UK over £8.2 billion, with around 55% of this cost due to death and 45% due to illness in those of working age. However, it should also be noted that the informal care of people with these diseases contributes greatly to the overall financial burden. For example, the cost of informal care for people with CVD in the UK was over £8.0 billion in 2006 (http://www.heartstats.org). In total, it is estimated that T2D and its complications cost the UK economy £29 billion a year (more than any other EU country). This figure of £29 billion includes the economic burden of informal care for people with CVD by their relatives (http://www.heartforum.org.uk).

Thus, T2D/CVD and the associated health and economic burden constitute one of the most important public health and economic issues affecting not only Wales and the UK, but the whole world.

1.1.2 T2D and insulin resistance

Insulin is a polypeptide hormone produced by the β cells of the Islets of Langerhans within the pancreas, consisting of two peptide chains (cleaved from a larger single polypeptide pre-proinsulin, and linked by disulphide bonds). Insulin is an anabolic hormone, which normally effects glycaemic control via increasing glucose uptake into muscle and adipose tissue, and via reducing glucose production through gluconeogenesis or glycogenolysis in the liver. Insulin resistance, which is the failure of the body cells to respond effectively to insulin is key to the metabolic consequences of T2D (Saltiel, 2001).

The failure of muscle cells to respond to insulin and take up glucose, the failure of fat depots to respond to insulin (causing its normal anti-lipolytic effects to be replaced by increased lipolysis and fatty acid release into the circulation), and the failure to

suppress gluconeogenesiss in the liver summarise the metabolic disturbances initiated in the development of insulin resistance. They are followed by subsequent increased secretion of insulin by the β-cell, which leads to hyperinsulinaemia; however, cells soon become desensitised to constantly elevated insulin levels, and further aggravation of insulin resistance results, until finally the β cell fails (Saltiel, 2001).

T2D and its complications are multi-factorial: several factors are required for the disease to fully develop. Thus, variables such as sedentary behaviour and obesity are independent risk factors for T2D and its complications: for example, as an independent risk factor, obesity exacerbates the detrimental effects of other factors such as inadequate physical activity, smoking or genetic predisposition. (Saltiel, 2001; see fig 1.1). The association between obesity and T2D can be explained as follows: it should be noted that visceral adipocytes (which are obviously present in excess in obese individuals) are not just passive fat stores; they secrete many signalling factors („adipokines"), and these interfere with - amongst other things - the liver's ability to break down insulin. This then contributes to hyperinsulinaemia, insulin desensitisation and thus T2D (Rabe *et al*, 2008).

As a result of insulin resistance, glucose and lipids are spurned by cells, and so are found at elevated levels within the circulation, conditions known as „hyperglycaemia" and „dyslipidaemia" respectively (Kumar, 1997). At this point it is worth introducing the concept of T2D as an inflammatory disease. Inflammation is conventionally viewed as the initial acute phase of the body"s defence against invading potential pathogens; in response to the presence of the foreign body, local vasodilatation occurs, and white blood cells are recruited to the site, with neutrophils and monocytes migrating through the blood vessel wall, and phagocytosing and destroying the potential pathogen (Bray, 1986). However, while acute inflammation predominantly involves neutrophils and is classed as lasting up to a couple of days in duration, in certain conditions, chronic inflammation involving predominantly monocyte-macrophages can persist for months or years (Lakhani, 2003). T2D is increasingly being seen as a chronic inflammatory disease because of the associations seen between hyperglycaemia, dyslipidaemia and inflammation in diabetic tissues.

Non-enzymatic glycation of proteins leads to the formation of irreversible products knowns as advanced glycosylation end-products (AGEs) (Singh *et al*, 2001). Formation of AGEs is associated with pro-inflammatory signalling events; on occupancy, the AGE receptor (RAGE; (Bierhaus *et al*, 1998), a member of the immunoglobulin superfamily of receptors, triggers intracellular signalling pathways such as activation of the proinflammatory transcription factor Nuclear factor kappaB (Thornally, 1998; Brownlee, 1995).

Dyslipidaemia is also linked to inflammation – for example, Dogra *et al* reported that in subjects with insulin resistane, increases in plasma markers of inflammation such as Interleukin-4 (IL-4) and fibrinogen correlated with circulating levels of non-esterified fatty acids (Dogra *et al*, 2002). Also, it has been reported that increased levels of pro-inflammatory markers such as CRP or reduced levels of anti-inflammatory markers such as adiponectin, predict the development of Type 2 diabetes (Ziegler, 2005). As will be discussed subsequently, inflammation is inextricably linked to the pathophysiology of both T2D and many diabetic complications.

1.1.3 T2D and modern lifestyles

Perhaps the most intriguing theory about how T2D originated, and why it has become prevalent in modern society, was one originally formulated by James Neel in 1962 (Neel, 1962). Neel suggested that "*the diabetic genotype is, to employ a somewhat colloquial but expressive term, a "thrifty" genotype, in the sense of being exceptionally efficient in the intake and utilization of food*". Neel regarded early humans as generally having lived under conditions of feast or famine. When faced with feasting, individuals who possessed a "quick insulin trigger" to use Neel's term released large amounts of insulin to facilitate more efficient storage of food and minimize urinary glucose loss. We now live in a period where the composition of the diet has changed beyond recognition in the last few decades, with a higher percentage of the daily intake being composed of energy-rich saturated fats (Eizirik *et al*, 2007). As farming developed and food became relatively more abundant, the development of diabetes was probably held in check by the fact that people remained active, and early crops produced food of a relatively low glycaemic index. It was not until the modern era when due to people‟s generally sedentary lifestyles, the abundance of highly processed fatty/carbohydrate-rich diets, and the onset of obesity

that the symptoms of insulin resistance/T2D (as described above) began to manifest themselves (Miller *et al*, 1994). Additionally, this dietary change, combined with increased life expectancy, has meant that the stresses imposed on long-living cells such as the pancreatic β-cell have become greater (Eizirik *et al*, 2007). In summary, therefore, the high frequency of high-energy meals mean that the consequent episodes of postprandial hyperinsulinemia, once a genetic benefit, now occur excessively often, leading to insulin resistance, beta cell failure, and eventual fully-fledged T2D.

1.1.4 Macrovascular and microvascular complications of T2D

Although T2D and its two categories of complications are often referred to as distinct conditions, it has been recognised for more than a decade that these conditions have common genetic and environmental antecedents, i.e., they have sprung from a "common soil." Thus, it is now known that adverse environmental conditions, related to less-than-optimal nutrition earlier in life are associated with an enhanced risk of both diabetes and cardiovascular disease many decades later (Stern, 1995). More recently, inflammation has been identified as a common theme that runs through the pathophysiology of T2D and its complications (Ziegler, 2005). In his review article, Ziegler states that it is well documented that chronic inflammatory processes play an important role in the causation of atherosclerotic CVD, and that inflammatory mediators play a paramount role in the initiation, progression, and rupture of atherosclerotic plaques. However, as described previously, evidence has emerged suggesting that inflammation is also involved in the development of Type 2 diabetes – for example, increased levels of pro-inflammatory markers such as CRP or reduced levels of anti-inflammatory markers such as adiponectin predict the development of Type 2 diabetes. Thus, Ziegler claimed that the evidence suggests that inflammation is the bridging link between T2D and its complications such as atherosclerosis and microvascular perturbations – taken together, these linked conditions have been termed „the metabolic syndrome“ (Ziegler, 2005), while Henry Pownell of Baylor College of Medicine, Texas has even suggested the term „Metabolic Axis of Evil“ in a similar context (http://www.bcm.edu – see fig. 1.1b). Therefore, it follows that interventions by agents with anti-inflammatory properties may reduce the risk of both T2D and its complications – the importance of this conclusion will be discussed in a later section.

(a)

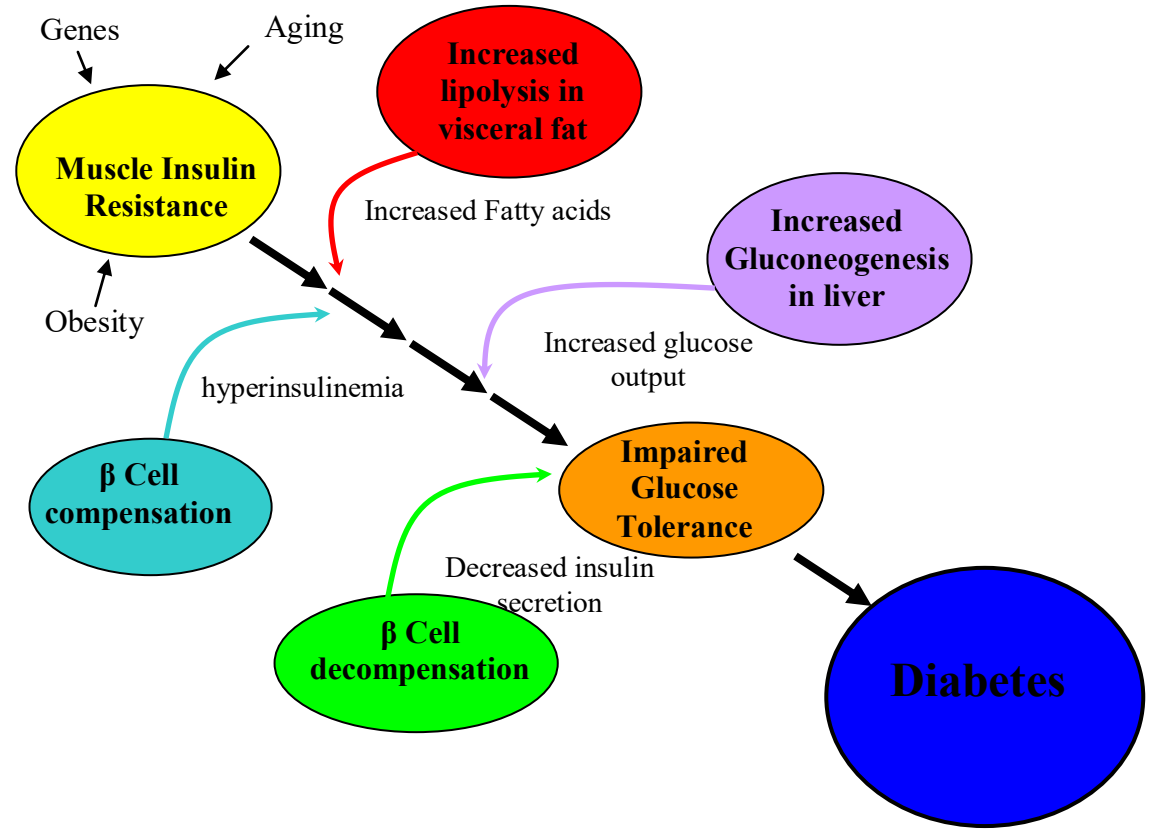

(b)

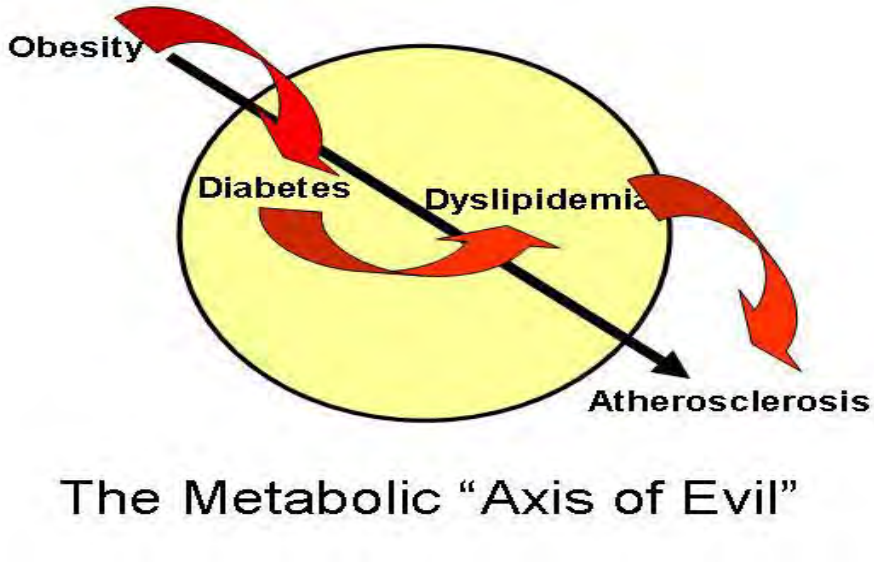

Fig 1.1 –(a) Metabolic development of type 2 diabetes (adapted from Saltiel *et al*, 2001) and **(b) 'The Metabolic axis of evil'** – how obesity and diabetes promote development of diabetic complications such as atherosclerosis (adapted from http://www.bcm.edu**)** both T2D and its complications.

Macrovascular -

T2D and Heart failure: Numerous studies have highlighted the association between T2D and heart failure (Nichols *et* al 2004; Bell, 2003; Thrainsdottir *et al* 2005). Indeed, patients with cocomittent T2D and heart failure have poorer outcomes than those patients with heart failure but no diabetes (Gustafsson *et al*, 2004; Varela-Roman *et al*, 2005). (NB. Heart failure (HF) is defined as a condition in which a problem with the structure or function of the heart impairs its ability to supply sufficient blood flow to meet the body's needs (http://www.dorlands.com). It should not be confused with cardiac arrest, or with the adverse CV events reported by Nissen & Wolski, 2007).

T2D and Atherosclerosis: Atherosclerosis in its simplest terms is the build-up - over a period of decades - of fatty deposits called atheromas on the walls of the arteries. Diabetic patients are often exposed to extended periods of hyperglycaemia and dyslipidaemia, and this has now been classed as a major contributor to the pathogenesis of atherosclerosis in these patients (Aronson and Rayfield, 2002). Cardiovascular disease was the cause of over 75% of hospitalisations of people with complications associated with T2D and atherosclerosis alone is responsible for over 80% of all deaths of T2D patients in North America (Aronson and Rayfield , 2002).

In line with Ziegler‟s suggestion (see above), it has been stated that athersclerosis can be seen as an „unintended consequence of a normal physiological inflammatory response“ (Lodish, 2004). Under normal circumstances, blood flows smoothly through the lumen of an artery – this is known as „laminar flow“. However, damage can occur within the walls of an artery due to build-up of lipid (packaged in circulating lipoprotein particles) and/or glycated proteins, and this can trigger the body‟s inflammatory defences. The class of white blood cells known as monocytes are very important in the development of atherosclerosis („atherogenesis“) because once the artery wall has become damaged, monocytes initially adhere to the endothelium, and subsequently migrate into the artery wall. Here, they differentiate into macrophages, where they can endocytose large amounts of cholesterol and other lipids from various lipoprotein particles that also accumulate within the damaged arterial wall. The imported cholesterol is esterified into cholesteryl ester lipid droplets, and the resulting lipid-filled macrophages are called „foam cells“. Thus, the early stages in the development of an atheroscerotic plaque are the development and

accumulation of lipid-filled foam cells, and the subsequent formation of the so-called „fatty streak". This fatty streak grows bigger as the disease progresses, forming an atherosclerotic plaque. Cells within the core of the plaque die, leaving an accumulation of cholesteryl esters and unesterified cholesterol covered by a fibrous cap composed of smooth muscle cells and collagen. As the disease progresses further, this fibrous cap can rupture, forming an unstable plaque, formation of large blod clots within the artery lumen and ultimately vessel occlusion (see fig 1.2). This can lead to ischaemia and consequently tissue damage in downstream tissues whose blood supply has been affected, and thus to events such as myocardial infarctions (in the case of vessels supplying the heart), or strokes (in the case of vessels supplying the brain).

Finally, it should be noted that increased arterial stiffness, which is significantly greater in individuals with T2D compared to controls (McEniery *et al*, 2008), accelerates atherosclerosis by increasing the propensity for the blood to develop pools and eddy currents. In the normally compliant aorta, blood flow occurs throughout most of the cardiac cycle; in contrast, in a perfectly stiff aorta, the entire stroke volume would be expelled in systole and no low-velocity diastolic flow will occur. This will encourage thrombus growth and subsequent formation and organization of an atheromatous plaque.

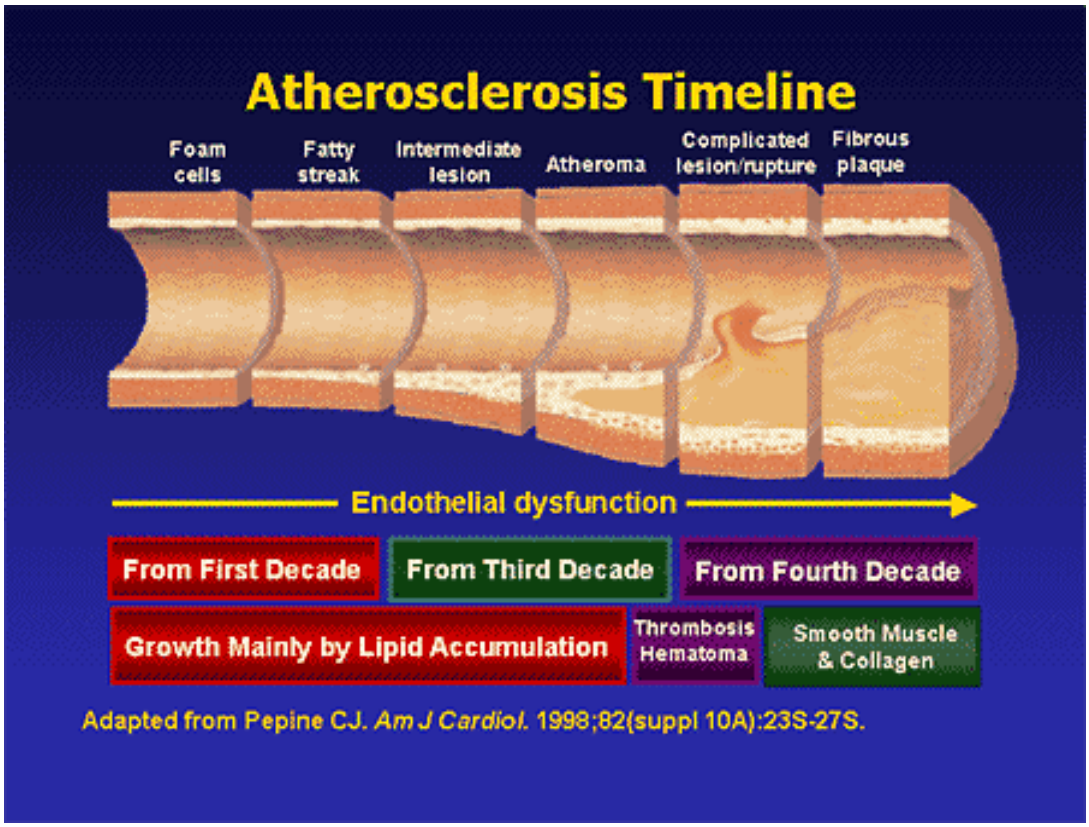

Fig 1.2 Development of athersclerosis over time (Taken from The Evolution of Type 2 Diabetes: A Staged Approach to Reducing Macrovascular Risk by Richard S. Beaser, MD; Faculty: Enrique Caballero, MD; Robert E. Heinig, MD, accessed at http://www.medscape.com)

Microvascular complications

In addition to atherosclerosis, T2D can also bring about pathogenic complications within the microvasculature. Unlike erythrocytes, which retain their biconcave disc shape but are sufficiently deformable to be able to pass through the smallest of the body‟s microcapillaries, circulating leukocytes – and particularly monocytes – can take on a variety of shapes, including the sending-out of pseudopodia during activation (ie. the response to a perceived threat, for example pseudopodia formation in order to carry out phagocytosis and engulf a potential pathogen during an inflammatory response). Pseudopodium formation has been shown to be the most notable physical parameter that determines the activation of monocytes (Mazzoni & Schmid-Schonbein, 1996). Pseudopodia are stiffer than the main cell body and consequently, circulation of hyperactivated monocytes may lead to a greater risk of entrapment of cells within small blood vessels (Schroder *et al*, 1991). Once again, therefore, inflammation can be identified as a common theme linking T2D and its complications (Ziegler, 2005).

Patients with T2D have an increased tendency to have hyper-activated monocytes, which results in a reduced cell deformabilty and an increased propensity for cells to become trapped in the microvasculature leading to microvascular complications (Miyamoto *et al*, 1997). On a biochemical level, cell deformability occurs in numerous cell types including monocytes due to changes in the cell cytoskeleton. Depolymerisation and polymerisation of the abundant cytoskeletal protein Actin (and conformational change between globular or G-actin and filamentous or F-actin in the presence of ATP) can result in changes to the cell cytoskeleton (Lodish, 2004), making monocytes more or less rigid and hence having a major influence on cell motility/transport in the microvasculature.

Diabetic microangiopathy is a collective term used to describe damage to cells of the microvasculature, leading to occlusion, ishemia or organ damage mainly to the kidney and retina but also to the peripheral nerves and skin (Brownlee, 2001). Diabetic nephropathy, or more simply diabetic kidney disease, occurs in approx 30-40% of diabetic patients. It has increased dramatically and is now the major cause of end-stage renal disease necessitating renal replacement therapy (Ritz *et al*, 1999).

Diabetic retinopathy, or diabetic eye disease, occurs in ~3/4 of the diabetic population (in those patients who have had established diabetes for 15 years or more) (Sheetz & King, 2002), and is the most common cause of blindness in the developed world (Kahn & Moorhead, 1973). It is caused by persistent hyperglycaemia leading to damage to intraretinal blood vessels and eventual retinal ishemia (Chappey *et al*, 1997). Diabetic neuropathy, or diabetic nerve disease, is experienced by approximately 50% of diabetic patients (Dyck *et al*, 1993) and is characterised by the glycation of certain cytoskeletal proteins for example tubulin and actin, leading to axonal atrophy and degeneration (Dyck *et al*, 1996).

Hyperglycaemia and the formation of AGE products, and dyslipidaemia and the build-up of lipoprotein particles (particularly oxidised lipoprotien particles), both constitute pro-inflammatory events that play a major role in the development of the diabetic microangiopathy events described above. This is because monocytes respond to their presence by mounting inflammatory responses, becoming hyperactivated, and thus becoming trapped in the microvasculature.

Finally, it has been proposed that inflammation, and particularly monocyte hyperactivation (which have been discussed here as components of microvascular complications) may also be primary factors in macrovascular complications such as atherosclerosis. Actin polymerisation as a consequence of such hyperactivation has been shown to promote recruitment and infiltration of monocytes through the vascular endothelium, initiating the formation of atherosclerotic plaques (Luscinskas *et al*, 1994). Furthermore, there is also evidence that chronic monocyte hyperactivation may play a crucial role in plaque destabilisation and subsequent thrombogenesis (Miller *et al*, 2003).

1.2 PPARgamma (PPARγ)

Transcription factors are DNA-binding proteins which function to activate or repress expression of eukaryotic protein-encoding genes (Lodish, 2004). Peroxisome proliferator-activated receptors (PPARs) are a group of ligand-activated transcription factors that play an important role in the modulation of expression of genes involved in the regulation of metabolic processes including glucose homeostasis and adipogenesis (Touyz & Schiffrin, 2006). There are three members of the PPAR family, namely PPARα, β/δ and γ. PPARα was the first member of the family to be

identified and is involved in controling the expression of genes regulating lipid and lipoprotein metabolism (Touyz & Schiffrin, 2006). PPARα is expressed in tissues including the heart, liver, kidney and skeletal muscle. It is activated by the binding of unsaturated fatty acids and by hypolipidemic agents such as members of the fibrate family of drugs (Desvergne *et al*, 1999). PPARβ/δ is ubiquitously expressed (Ferré 2004) and its ligands include polyunsaturated fatty acids and prostaglandins (Berger *et al*, 1999). The PPARγ gene is located on chromosome 3 at position 3p25 (Greene *et al*, 1995) and PPARγ is expressed in tissues such as adipose tissue, large intestine and selected immune cells including monocytes and macrophages (Ferré 2004) as well as endothelial and vascular smooth muscle cells (Law *et al*, 2000). PPARγ has been subject to intensive study over recent years, more so than the other isoforms.

1.2.1 PPARγ ligands

PPARγ, as previously described, is a ligand-dependent transcription factor (see Fig.1.2). Originally termed an „orphan receptor" because it itself was characterised several years before any of its ligands were characterised (Murphy and Holder, 2000). PPARγ is now known to be activated by binding of a number of naturally occuring ligands including many unsaturated fatty acids such as oleate, linoleate and arachidonic acid as well as the prostanoid 15-deoxy-$\Delta^{12,14}$-prostaglandin J_2 (15d-PGJ_2) (Ferré *et al*, 2004).

The role of natural PPARγ ligands in T2D

The essential fatty acids linoleic acid, linolenic acid, arachidonic acid and eicosapentaenoic acid have been shown to bind PPARγ at micromolar concentrations *in vitro*; however it is unlikely that they are found intracellularly at these relatively high concentrations *in vivo* (Willson *et al*, 2000). It is considered more likely that 15-lipoxygenase-catalysed conversion of fatty acids to eicosanoids is responsible for PPARγ activation *in vivo*, and that therefore metabolites of fatty acids/fatty acid derivatives such as 9-HODE, 13-HODE and 15d-PGJ2 (metabolites of linoleic acid and Prostaglandin D2 respectively) are more plausible candidates for natural PPARγ ligands – ie. compounds which can activate PPARγ at physiological concentrations (Willson *et al*, 2000). It may be speculated that the enzymes that generate these ligands from fatty acids, and the PPARγ receptor with which they interact, have evolved to regulate the physiological response to dietary intake of fatty acids, and hence that the PPARγ/natural PPARγ-ligand system now plays a central role in

regulating the storage and catabolism particularly of fats. Clearly, this places this system in an advantageous position in the context of compensation for the metabolic disruptions due to defective insulin signalling seen in T2D. For this reason, PPARγ has been the target of much clinical attention over the past decade or so..

The role of synthetic PPARγ ligands in T2D

Synthetic PPARg ligands include a class of drugs known as the thiazolidinediones (TZDs). When these drugs were initially developed and marketed as oral anti-hyperglycaemic agents, it was not initially known that their mechanism of action was via PPARγ binding (Willson *et al*, 2000). However, it is now well-established that TZDs‟ mode of action is to improve glucose tolerance by increasing insulin sensitivity via activation of PPARγ (Murphy and Holder,2000). The first member of the TZD family to be marketed for use was Troglitazone, but this drug was withdrawn from use as it caused liver toxicity (Wise, 1997). Other members of the family which are currently in clinical use include pioglitazone and rosiglitazone. TZDs will be discussed in more detail in Section 1.3.

1.2.2 Genomic transcriptional regulation of PPARγ target genes

Fig 1.3 shows how PPARs dimerise with the cofactor 9-cis retanoic acid receptor (RXR) before binding to a specific region of a target gene, the peroxisome proliferator response element (PPRE). PPARs consists of four domains namely A/B, C, D and E/F. The A/B contains the N-terminus and contains a ligand-dependent transcriptional activating function (AF-1). The C domain constitutes the DNA-binding domain that recognises and bind to a PPRE, a specific DNA sequence consisting of repeating hexanucluotide sequence AGGTCA separated by one or two nucleotides, on target genes. The D domain modulates the DNA binding ability of PPAR while the E/F domain, the ligand-binding domain allows the PPAR to bind to or dimerise with the cofactor RXR and also contains another ligand-dependent transcription activating factor (ATF-2) (Diradourian *et al*, 2005).

In its inactive state, i.e. in the absence of PPARγ ligands, the PPARγ/RXR heterodimer is prevented from undergoing transcriptional activation due to the formation of high affinity complexes with co-repressor proteins. This causes the PPARγ/RXR/corepressor complex to be distanced from the target gene promoter, thus ensuring it is remains in an inactive state prior to ligand binding. However,

upon ligand binding, a conformational change of this complex leads to dissociation of repressor proteins from the complex, facilitating binding of the PPARγ/RXR dimer to the PPRE of the target gene (Smith, 2003). Binding and interaction of the activated PPAR/RXR heterodimer with the PPRE leads to transcription of numerous genes involved in lipid metabolism.

1.2.3 Non-genomic transcription transrepression

The above mechanism of action is responsible for PPARγ ligands" role in glycaemic control (Murphy and Holder, 2000). However, PPARγ ligands have also been shown to play a role in inhibition of the inflammatory response in monocytes and macrophages (Jiang *et al*, 1998; Ricote *et al*, 1998). However, as the concentration of PPARγ-ligands required to exert these anti-inflammatory effects appear to be much higher than their relative dissociation constants, speculation arose as the necessity of PPARγ in the observed anti-inflammatory response (Chawla *et al*, 2001). It has therefore become apparent that PPARγ, aside from its ability to regulate transcription upon ligand binding via association with the PPRE, also has the ability to regulate cell behaviour by „non-genomic" mechanism(s), not requiring the binding of PPAR to DNA. Such non-genomic transcriptional transrepresion may be facilitated by direct protein:protein interaction of the nuclear receptor with other transcriptional factors such as NF-kB, interfering with their ability to bind with their own response elements (Genolet *et al*, 2004 - see fig 1.4).

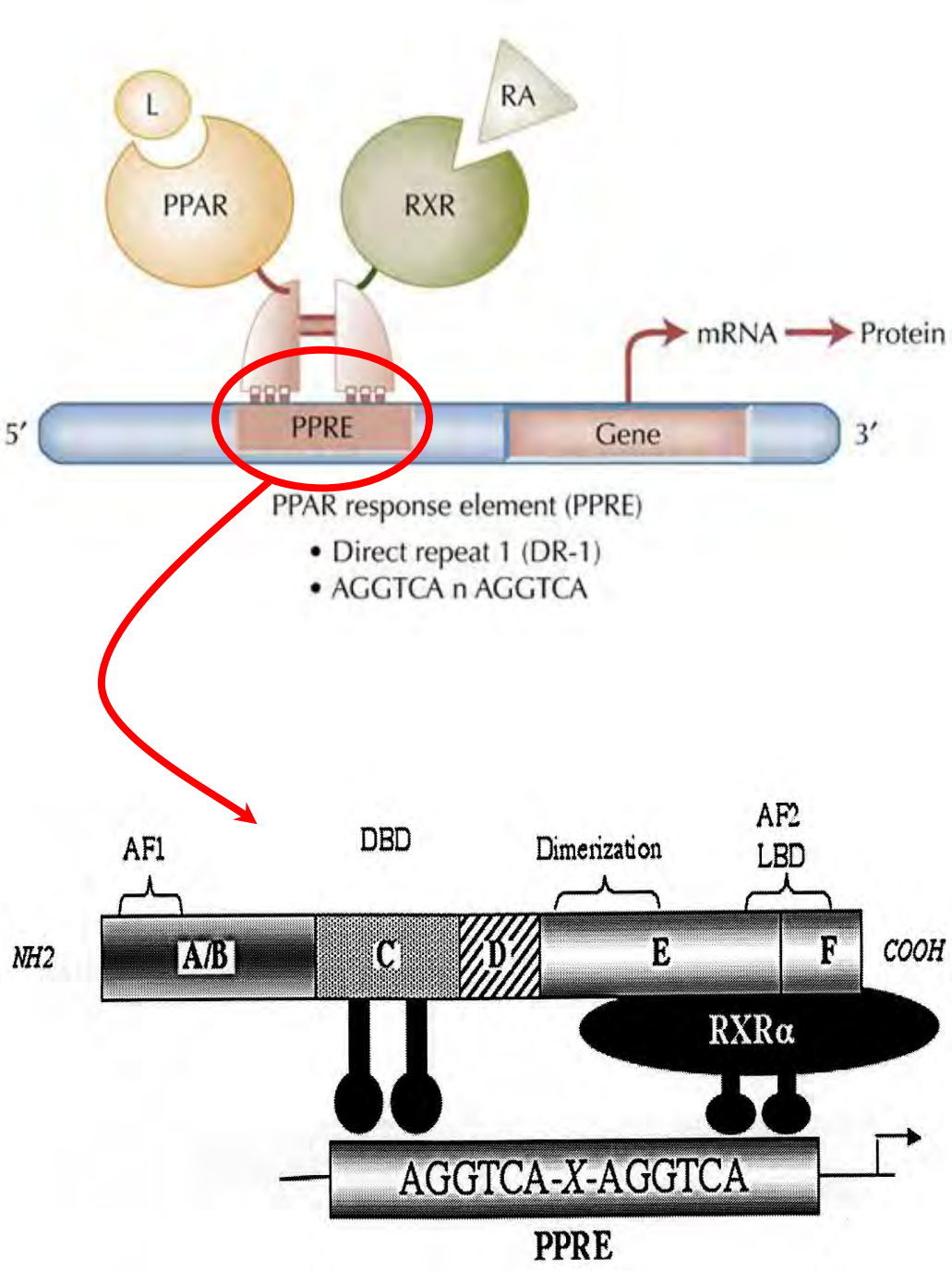

Fig 1.3 PPAR structure and activation. AF1: activating function-1, DBD: DNA binding domain, AF-2: avtivating factor-2, LBD: ligand-binding domain, RXR: 9-cis retinoic acid receptor, PPRE: peroxisone proliferator response element (adapted from Marx, 2002 and Diradourian *et al*, 2005)

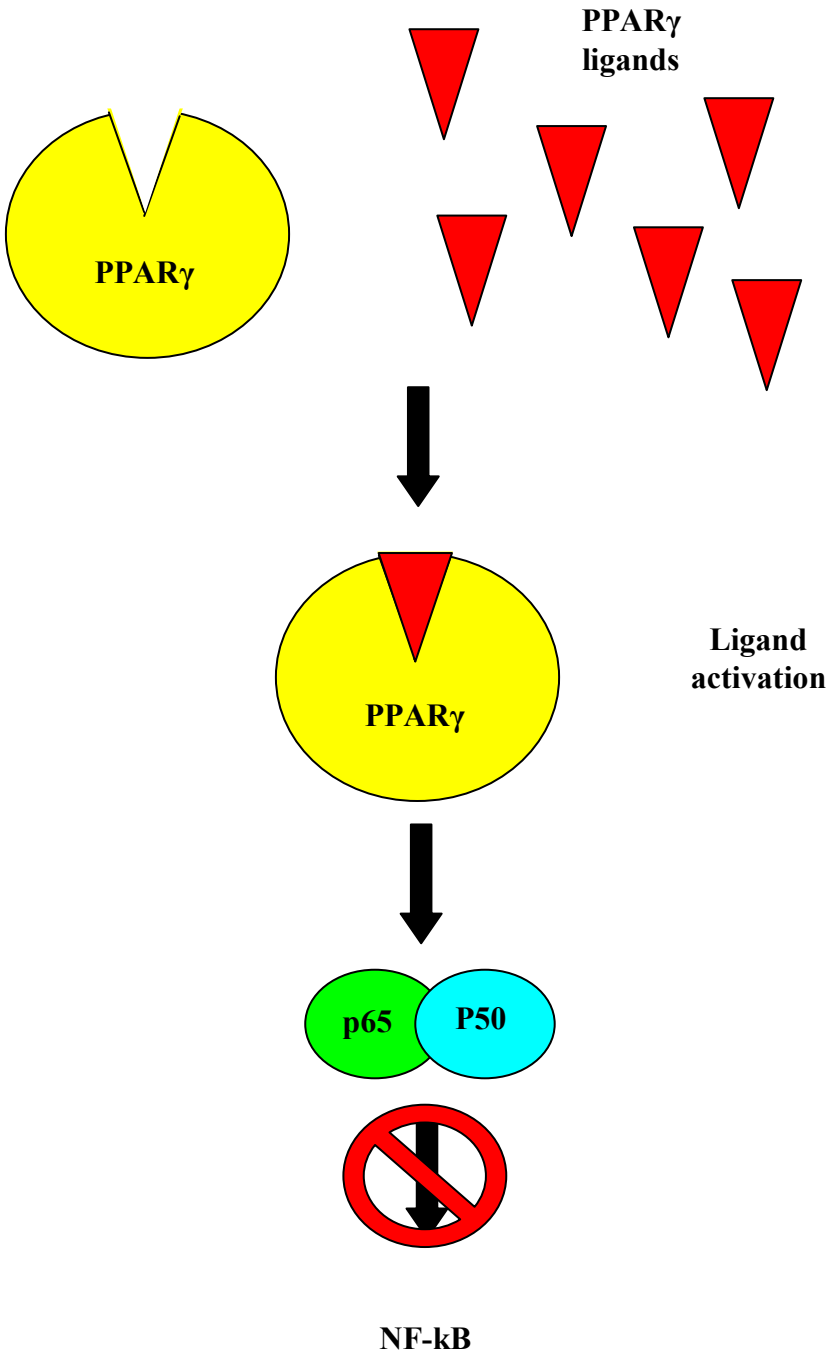

Fig 1.4 PPARγ transrepression. PPARγ repress gene transcription of other pathways such as nuclear factor-kB (NF-kB) (Adapted from Chirelli & Di Marzio, 2008).

Numerous studies have been conducted in order to determine that PPARγ ligand"s have this additional „non-genomic role" and whether this is the mechansim responsible for their apparent anti-inflammatory actions. Chawla *et al* stimulated wild-type and PPARγ-deficient macrophages with liposaccharide (LPS) and measured the inhibition of cytokine secretion on addition of PPARγ ligands. LPS-induced production of the pro-inflammatory cytokines tumour necrosis factor-alpha (TNF-α) and interleukin-6 (IL-6) were identical in both wild type and PPARγ-deficient macrophages. Treatment of these cells with 15d-PGJ2 and various TZDs inhibited the above inflammatory response equally in both cell types, indicating that PPARγ is not required for the mediation of the anti-inflammatory properties of 15d-PGJ2 or the TZDs (Chawla *et al*, 2001). The group also stimulated the wild type and mutated macrophages with interferon-γ (IFN-γ) and determined the gene expression of the inflammatory mediators inducible nitric oxide snthase (iNOS) and cyclooxygenase-2 (COX-2) in the absence and presence of both natural and synthetic PPARγ ligands. Again IFN-γ stimulation led to the equivalent levels of mRNA expression on iNOS and COX-2 in both wild type and PPARγ-dependent macrophages and treatment with PPARγ ligands inhibited the aforementioned expression to the same extent in both cell types.

In a similar study conducted on human blood monocytes, stimulation with LPS led to increased mRNA expression of the inflammatory mediators COX-2, IL-1, IL-6, TNF and GM-CSF (Hinz *et al*, 2003). Treatment of these cells with 15d-PGJ2 resulted in almost complete inhibition of the expression of these inflammatory mediators. Interestingly, comparative treatment with ciglitazone did not produce any downregulation of gene expression. However the effects observed with 15d-PGJ2 were still apparent in the presence of the PPARγ inhibitor (BADGE) indicating that the observed effects were indeed PPARγ-independent.

1.3 TZDs

1.3.1 Discovery and mode of action

As described above, TZDs are a relatively new class of anti-hyperglycaemic agents whose mode of action is to improve glucose tolerance by increasing insulin sensitivity via activation of PPARγ (Murphy & Holder, 2000). The first member of the TZD family to be marketed for use was Troglitazone, but this drug was withdrawn from use as it caused liver toxicity (Wise, 1997). Other members of the

family which are currently in clinical use include pioglitazone, rosiglitazone and ciglitazone; the main focus of the present study is rosiglitazone (marketed under the brand name Avandia). In 2000, rosiglitazone received marketing authorisation for clinical use in Europe (Home *et al*, 2009), while similar authorisation was granted in 1999 in the USA (Nissen & Wolski, 2007).

TZDs such as rosiglitazone exert their effects by an entirely diffent mechanism to the then pre-existing diabetic medications, the biguanides such as metformin and the insulin secretagogues, the sulfonylureas. TZDs do not affect insulin secretion but elicit improvements in glycaemic control via a reduction of insulin resistance, while metformin and the sulfonylureas work by reducing hepatic glucose output (Smith, 2003). TZDs differ from other available oral anti-diabetic agents, because their function is to improve insulin sensitivity though a combination of increasing the effect of insulin on glucose uptake into skeletal muscle, via cessation of glucose production in the liver and by increasing the secretion of insulin from pancreatic β-cells (Camp 2003). Their actions are summarized in fig 1.5.

Thus, the TZDs bring about their actions by targeting the nuclear receptor PPARγ as described in 1.2. Thus by activating this molecular target, TZDs control the switching on and off of genes involved in glycaemic control and induce numerous clinical advantages such as normalisation of glycaemia as well as mediating anti-inflammatory effects. TZD-induced activation of PPARγ in adipose tissue causes enhanced glucose uptake, lipid storage and a decreased release of free fatty scids (FFA). Following TZD administration, enhanced insulin activity is observed not only in adipose tissue but also in the liver and skeletal muscle, the three main tissues which are affected by insulin resistance. (Smith, 2003).

The first TZD approved and marketed for use in the treatment of T2D was troglitazone (Romazin), but the drug was subsequently voluntarily withdrawn from use in the UK by its manufacturer GSK in December 1997 (Wise, 1997) and eventually also in the USA in March 2000 due to the manifestation of severe liver toxicity in a proportion of patients using this therapy (Kohlroser *et al*, 2000). Since then, two other members of the TZD family, rosiglitazone (Avandia) and

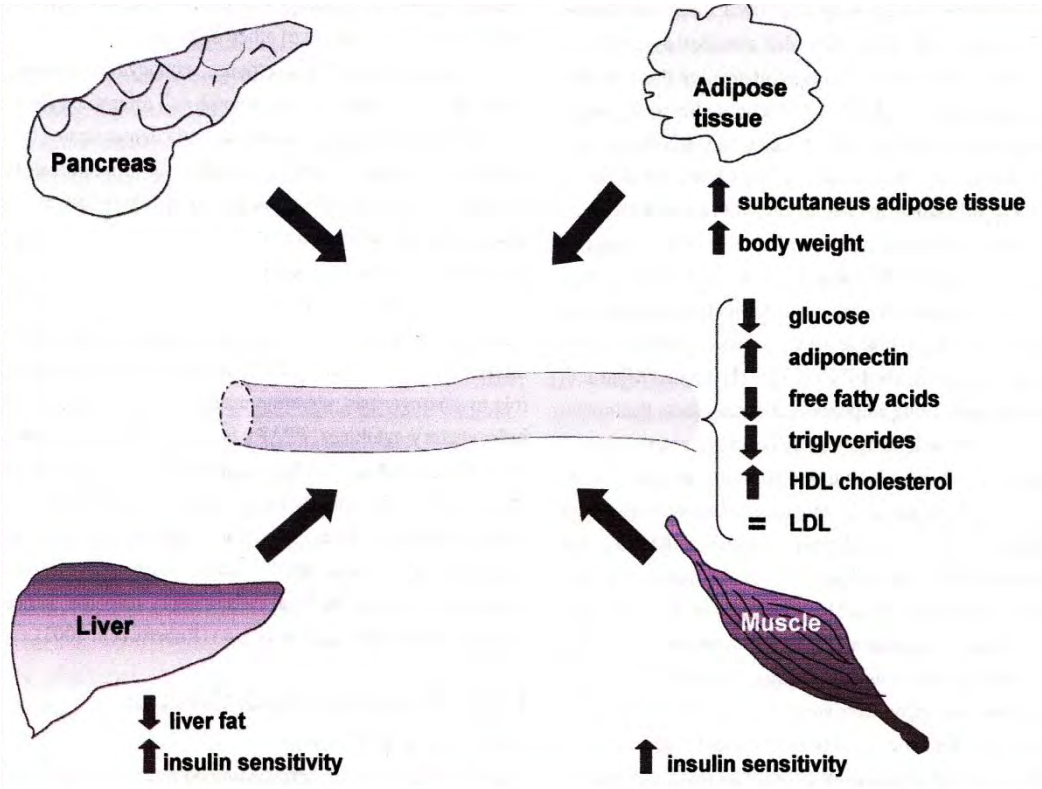

Fig 1.5 The clinical effects of Thiazolidinediones (Adapted from Chiarelli & Di Marzio, 2008)

pioglitazone (Actos), have been approved for use and are still currently on the market. Clinical trial data and patient monitoring shows that these drugs do not cause the hepatic toxicity seen previously with troglitazone (Kahn *et al*, 2006). Fig 1.6 shows (a) the incidence of liver abnormalities (consistent with elevated alanine aminotransferase (ALT) levels in clinical trials with troglitazone, rosiglitazone and pioglitazone compared to placebo and (b) the incidence of severe hepatitis, liver transplant and death related to troglitazone, rosiglitazone or pioglitazone therapy in type 2 diabetic patients. However, there has been much recent debate (see eg the meta-analysis of Nissen & Wolski, 2007) about the association of the use of these drugs with cardiac toxicity and cardiovascular (CV) events (NB. This will be discussed in detail in section 1.3.4).

1.3.2 TZD administration and success rates: clinical trial data

The TZDs can be administered on their own in a monotherapy approach, or alternatively alongside other antidiabetic drugs such as metformin, sulfonylureas and insulin in combination therapy. GlaxoSmithKline, the manufacturers of Avandia (rosiglitazone), state that the drug is indicated in the treatment of T2D:

- as monotherapy in patients inadequately controlled by diet and exercise for whom metformin is inappropriate because of contraindications/intolerance;
- as dual oral therapy in combination with metformin in patients with insufficient glycaemic control despite administration of maximum dose of monotherapy with metformin;
- as dual oral therapy with sulphonylurea, only in patients showing intolerance to/having contraindications to metformin, with insuffiecient glycaemic control despite monotherapy with sulfonyurea;
- as triple oral therapy in combination with metformin and sulfonylurea in patients who show insufficient glycaemic control despite dual oral therapy (GSK summaries of product characteristics factsheet: Avandia 4mg & 8mg film-coated tablets, 2009).

Rosiglitazone and pioglitazone have both had clinical success when used in monotherapy and have been found to greatly improve insulin sensitivity and glycaemic control in individuals with T2D via reduction of plasma glucose and insulin levels, ultimately resulting in reduced HbA1c levels *(*Chiarelli & Di Marzio,

2008*)*. Both drugs have also been successful in combination therapy, demonstrating additional improvements in glycaemic control versus monotherapy (Camp 2003).

(a)

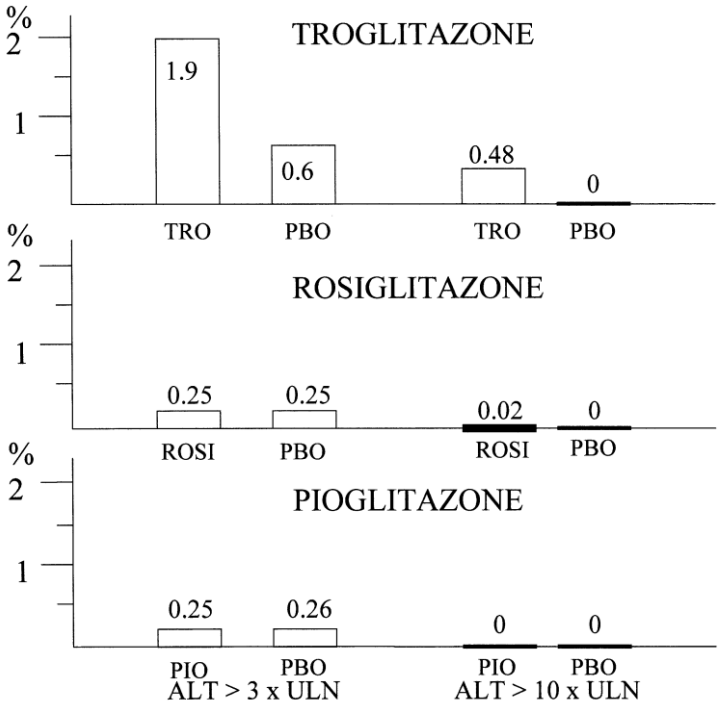

(b)

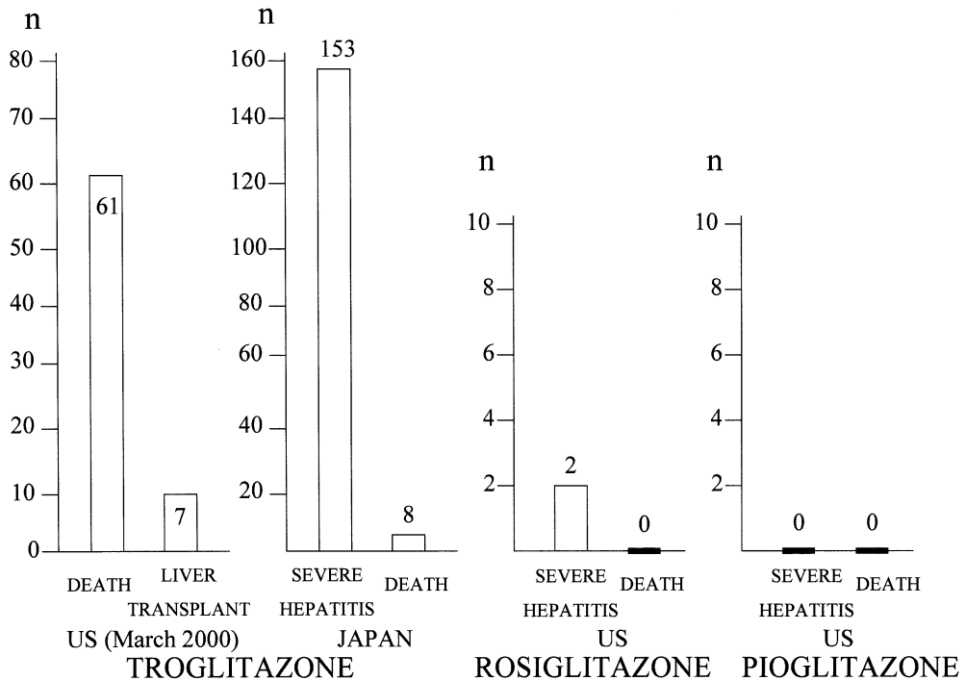

Fig 1.6(a) Comparison of the incidence (%) of elevated alanine aminotransferase (ALT) levels in controlled clinical trials. Troglitazone (TRO, n = 2 510), rosiglitazone (ROSI, n = 3 314) and pioglitazone (PIO, n = 1 526) are shown compared to placebo (PBO).ULN: upper limit of normal range (b).Comparison of reported cases (n) of severe hepatitis, liver transplant and death related to troglitazone, rosiglitazone or pioglitazone therapy in type 2 diabetic patients (taken from Scheen, 2001).

There have been numerous clinical trials involving rosiglitazone, analyzing its impact on aspects such as glycaemic control and durability and cardiovascular and renal outcomes. The outcomes of some of the larger scale clinical trials are summarized below.

The ADOPT study

One major study, namely „A Diabetes Outcome Progression Trial" is more commonly referred to as the ADOPT study (Kahn *et al*, 2006). This multi-center, randomized, double-blind clinical trial evaluated and compared rosiglitazone (a TZD), metformin (a biguanide) and glyburide (a sulfonylurea) for their effectiveness and durability in improving glycaemic control when used in a monotherapy approach in recently diagnosed T2D patients. 4360 patients were randomly assigned one of the three drugs and their glycaemic control was assessed over a 4 year period. The primary outcome of the study was the time taken for each therapy to fail to maintain a set plasma glucose level (180mg/dL). Secondary outcomes were plasma fasting glucose levels and glycated haemaglobin, insulin sensitivity and β-cell function. The results of the study showed that the cumulative incidence of monotherapy failure at 5 years was lower in rosiglitazone (15%) than in metformin (21%) or glyburide (34%). However, glyburide was associated with a decreased risk of adverse cardiovascular events than rosiglitazone or metformin, whose risks were found to be comparable. Rosiglitazone was also found to increase weight gain and cause edema more frequently than the other drugs. The conclusion of the trial was than rosiglitazone had a slower progression to monotherapy failure than metformin or glyburide. While the study was not designed specifically to determine cardiovascular outcomes, retrospectively rosiglitazone"s risk of CV events was determined to be equivalent to previous studies using metformin.

The DREAM study

Another trial, „the Diabetes Reduction Assessment with ramipril and rosiglitazone Medication" or (DREAM) trial compared the effects of ramipril (an ACE inhibitor) and rosiglitazone on cardiovascular and renal outcomes in a non-diabetic cohort of >5000 people with specific risk factors of diabetes, namely impaired glucose tolerance or impaired fasting glucose (The DREAM Trial Investigator, 2008). Patients were randomly assigned to a treatment regime: ramipril versus placebo or rosiglitazone versus placebo and cardiovascular and renal outcomes assessed over a

three year period. The study showed that ramipril did not significantly reduce the risk of primary outcome of diabetes i.e. cardiorenal events, or death compared with placebo, but did reduce postload glucose levels and reduced impaired glucose tolerance and impaired glucose tolerance to normal. In contrast, rosiglitazone reduced the primary outcome by 60%, with significant decreases in fasting glucose and postload glucose levels. Ramipril was found to be ineffective in altering cardiorenal outcomes. Rosiglitazone, alongside causing a reduction in diabetes, also reduced the risk of adverse renal outcomes but not cardiorenal outcomes. Rosiglitazone was however deemed to increase the risk of heart failure (NB. Heart failure (HF) is a condition in which a problem with the structure or function of the heart impairs its ability to supply sufficient blood flow to meet the body's needs. (http://www.dorlands.com). It should not be confused with cardiac arrest, or with the adverse CV events reported by Nissen & Wolski, 2007).

The RECORD study

Another recent multi-centre, randomized open-label trial, was the „Rosiglitazone evaluated for cardiovascular outcomes in oral agent therapy for type 2 diabetes" or RECORD study. The RECORD study group conducted their study on 4447 patients with T2D, suffering from inadequate glycaemic control and previously receiving either metformin or sulfonylurea. They were randomised to receive either their original medication plus rosiglitazone (2220 patients) or a combination of metformin and sulfonylurea (2227 patients). The primary end point of the study was hospitalisation or death from cardiovascular events. Publication of interim results in the light of concerns regarding rosiglitazone"s association with adverse cardiovascular outcomes, revealed that there was no apparent increase in risk of death from rosiglitazone therapy but there was an association with the drugs use and increased risk of heat failure (Home *et al*, 2007). Publication of the full study in 2009, confirmed the association of rosiglitazone therapy with increased risk of heart failure, but proved inconclusive as to the effects of the drug on the risk of MI. However it was also concluded that there was no significant increase in the risk of overall cardiovascular morbidity or mortality when compared with other anti-hyperglycaemic agents (Home *et al*, 2009). These studies are described in greater detail later in this section.

1.3.3 Non genomic effects of TZDs

As discussed previously, PPARγ agonists including the TZDs have been shown to exert receptor-independent effects alongside their traditional receptor-dependent effects. The determination of TZD-induced PPARγ-independent effects have been based on the following criteria.

- TZD concentrations required to elicit observced effects were much higher than reported EC50 values;
- the order of efficacy for the TZDs (tro>Pio>Rosi) to produce observed effects was the opposite to their binding efficiencies;
- non-TZD agonists produced little or no effect;
- TZD effects were not blocked upon additon of PPARγ antagonists;
- the rapidity of the observed responses;
- effects were apparent in the absence of PPARγ expression or of PPREs in gene promoter regions;
- effects were still observed in the presence of transcriptional and translational inhibitors (Feinstein *et al*, 2005).

There is therefore a need to elucidate the mechanism(s) by which TZDs may exert effects independent of PPAR-γ activated gene expression. As well as the transrepression effects exerted on other transcription factors such as NFkB (as described above), so-called "non-genomic" effects of PPAR-γ ligands have been shown to influence intracellular signals such as changes in cytosolic calcium ion concentrations ($[Ca^{2+}]_i$) or protein kinase activity (Takeda *et al*, 2001; Marx *et al*, 1998; Goetze *et al*, 2002).

Thus, amongst the „non-genomic" effects observed is rosiglitazone's potential to influence deviations in $[Ca^{2+}]_i$. Previous work in our laboratory by Singh *et al* discovered that incubation of isolated mononuclear cells with rosiglitazone induced rapid significant increases (within 5 minutes) in $[Ca^{2+}]_i$ from basal values and that this elevation persisted for up to 1hr following incubation (Fig 1.7) (Singh *et al*, 2005). The rapid nature of the elevation allows distinction of this effect from the traditional „genomic" effects which take much longer to produce an effect. The author also observed that, while mononuclear cells responded to the agonist f-MLP via a very rapid (<5s) increase in $[Ca^{2+}]_i$ producing a "calcium spike", that pre-incubation of these cells with rosiglitazone for 30 minutes prior to f-MLP stimulation

led to a significantly larger increase in $[Ca^{2+}]_i$, which was initiated from an elevated basal level. The "calcium spike" seen with f-MLP alone is induced by stimulation of inositol tri-phosphate receptors (IP_3R) calcium channels in the ER membrane by the second messenger IP_3, (whose synthesis at the PM by phospholipase C is triggered by occupancy of f-MLP of its congruent G-protein-coupled receptor, see section 1.4.2) leading to a mobilization of Ca^{2+} into the cytoplasm. Importantly, Singh *et al* proposed that:

a) The fact that this fMLP-induced "calcium spike" is retained following pre-incubation with rosiglitazone;
b) The fact that incubation with rosiglitazone alone induced a less rapid (within 1-5min) increase in $[Ca^{2+}]_i$, which was sustained for at least 1h (see Fig 1.7)

suggested that this further increase is due not to mobilization of Ca^{2+} from the ER but to unchecked leakage of Ca^{2+} from the ER, perhaps due to some effect on the Ca^{2+} pumps that normally sequester Ca^{2+} back into the ER, for example the housekeeping Ca^{2+}ATPase SERCA2b (Singh *et al*, 2005). The current study aimed to extend this observation so as to elucidate in more detail the effects of rosiglitazone on $[Ca^{2+}]_i$ signalling/homeostasis, a system which will be described in section 1.4.

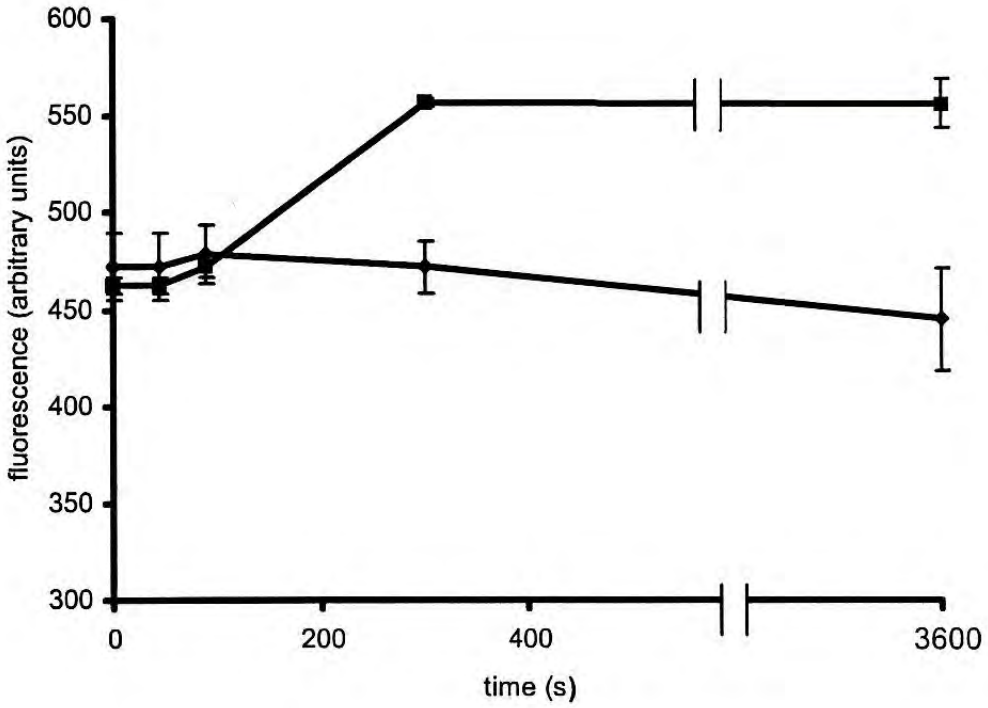

Fig 1.7: The effect of rosiglitazone on intracellular Ca^{2+} concentrations. Ca^{2+}-dependent fluorescence of Fluo-3 in mononuclear cells after incubation for the indicated times with (squares) and without (circles) 20μM rosiglitazone (Taken Singh *et al,* 2005, with permission)

1.3.4 Rosiglitazone and Cardiovascular Outcomes

The last few years has produced much debate over the safety of two members of the TZD family, namely rosiglitazone (Avandia) and pioglitazone (Actos) with numerous publications suggesting an association between rosiglitazone treatment and increased risk of myocardial infarction and risk of death from cardiovascular disease (Nissen & Wolski, 2007; Singh *et al*, 2007; Psaty and Furberg, 2007).

Nissen and Wolski conducted a meta-analysis of available published literature and clinical trial data aiming to assess the effect of rosiglitazone, versus a placebo or other non-TZD therapy, on cardiovascular outcomes. The meta-analysis encompasses data from 42 trials and inclusion criteria included trials where rosiglitazone treatment was of duration greater than 24 weeks. Interim results from two of the three large scale trials, the DREAM and the ADOPT trials, were included in this meta-analysis. The third trial, the RECORD trial, had not released interim results at this time and was not included. The results of the meta-analysis showed that rosiglitazone was associated with an increased risk of myocardial infarction (odds ratio 1.43, 95% confidence interval (CI), 1.03-1.98; p=0.03) and increase in risk of death from cardiovascular outcomes which was seen to show borderline significance (odds ratio 1.64, 95% confidence interval, 0.98-2.74; p=0.06).

Publication of Nissen *et al*"s meta-analysis led the authors of RECORD to feel compelled to publish an interim report into their findings (Home *et al*, 2007). As previously discussed, the RECORD study group conducted their study on a T2D patient cohort with inadequate glycaemic control and previously receiving either metformin or sulfonylurea. They were randomised to receive either their original medication plus rosiglitazone or a combination of metformin and sulfonylurea. The primary end point of the study was hospitalisation or death from cardiovascular events. The study found that while there was a small increase in myocardial infarction and a small decrease in death from cardiovascular causes, there was no statistically significant difference between rosiglitazone-treated and non-treated groups regarding myocardial infarction (HR 1.16, 95%CI, 0.75-1.81, p= 0.50) and death from cardiovascular causes (HR 0.83, 95% CI, 0.51-1.36, p=0.46). In contrast, the authors did concede that there were more patients with heart failure following rosiglitazone treatment than in the control group (HR, 215, 95% CI, 1.30-3.57,

p=0.003), an observation highlighted by the previously published meta-analysis by Nissen & Wolski.

However, despite Home *et al*"s insistence that their results showed that the proposed link between rosiglitazone treatment and decreased cardiovascular outcomes was inconclusive, addition of the RECORD data to Nissen & Wolski"s meta-analysis still showed an increased risk of myocardial infarction (odds ratio, 1.33, 95% CI; 1.02-1.72) (Psaty & Furberg, 2007). Furthermore, a meta-analysis conducted by Singh *et al* of four randomised controlled trials (including DREAM, ADOPT and RECORD (interim data only)) and three systematic reviews, concluded that rosiglitazone therapy for 12 months or more was associated with a significantly inceased risk of myocardial infarction (relative risk 1.42, 95% CI; 1.06-1.91, p=0.02) and heart failure (relative risk 2.09, 95% CI; 1.52-2.88, p=<0.001) without significantly increasing the risk of cardiovascular mortality (relative risk 0.90, 95% CI; 1.63-1.26, p=0.53) (Singh *et al*, 2007).

In 2009, Home *et al* published the completed RECORD trial data. In this report they confirm that while addition of rosiglitazone to pre-existing glucose-lowering therapy in T2D patients increases the risk of heart failure (HR 2.10, 95% CI, 1.35-3.27, p=0.001), and that their data remains inconclusive to the effect of the drug on risk of myocardial infarction (HR1.14, 95% CI, 0.80-1.63, p=0.47), rosiglitazone therapy does not increase the risk of cardiovascular morbidity or mortality compared with comparable non-TZD anti-hyperglycaemic drugs (HR 0.84, 95% CI, 0.59-1.18, p=0.32) (Home *et al*, 2009).

Publication of another key study has re-ignited the rosiglitazone safety debate. A recent Canadian study compared the risk of acute MI, heart failure and death in T2D patients treated with rosiglitazone and pioglitazone (Juurlink *et al*, 2009). In their retrospective cohort study, ~40,000 patients over the age of 66 on rosiglitazone or pioglitazone therapy for a six year period were analysed for the above cardiovascular events. Pioglitazone was found to be associated with a lower risk of primary outcome i.e. death or admission to hospital for either acute myocardial infarction or congestive heart failure than rosiglitazone (adjusted HR 0.83, 95% CI, 0.76 to 0.90).Also pioglitazone appeared to exert a lower risk of congestive heart failure (adjusted HR 0.77, 95% CI, 0.69 to 0.87) and a lower risk of death from all causes

(adjusted HR 0.86, 95% CI, 0.75 to 0.98) than rosiglitazone treatment. Interestingly the study failed to find any significant difference in risk of MI with pioglitazone as compared with rosiglitazone (adjusted HR 0.95, 95% CI, 0.81 to 1.11). The authors conclusion is that pioglitazone is associated with a significant reduced risk of heart failure and death than rosiglitazone and that because the latter drug appears to have no other clinical advantages over the former, then continued administration of the drug cannot be justified (Juurlink *et al*, 2009).

When considering the whole issue of TZD therapy and cardiovascular safety, it is also worth noting that several studies have suggested that non-TZD anti-hyperglycaemic therapies including metformin, sulfonylureas and insulin may all be associated with an increased risk of heart failure when compared with patients with no exposure to these drugs (Koro *et al*, 2005; Maru *et al*, 2005; Nichols *et al*, 2005).

This research provides further emphasis of the principle that drug choices should be considered by health care practitioners purely on a patient-to-patient basis, taking into consideration all medical contraindications of the individual concerned and the potential risk each particular drug may pose opposed to the consequences of not administering any drugs at all.

Current National Institute of Clinical Excellence (NICE) guidelines for the administration of PPARγ agonist (including TZDs) published in an NHS guide „Management of Type 2 Diabetes" states that

• People should be offered a thiazolidinedione as oral combination therapy if:
  - they are unable to take metformin and insulin secretagogues as combination therapy; or
  - the HbA1c level remains unsatisfactory despite an adequate trial of metformin with insulin secretagogues.

The above section highlights the potential side-effects associated with use of rosiglitazone. Given Singh *et al*'s research showing that rosiglitazone induces a disruption in calcium homeostasis in monocytic cells, and the above data showing how rosiglitazone therapy may potentiate adverse cardiovascular events, the possibility exists that these „side-effects" may be linked to aberrant Ca^{2+} homeostasis

in cardiac tissues. This highlights the importance of maintaining tight Ca^{2+} control in the heart by the homeostatic mechanisms discussed in section 1.4.

Source	N	Study population	Relative risk* of MI	Proportion experiencing MI	Relative risk of CV death (95% CI)	Proportion experiencing CV death
Meta analysis (1**)	27847	Any patient included in 1 of the eligible studies – includes patients with T2D, prediabetes, Alzheimer's and psoriasis	OR 1.43 (1.03-1.98) ***	Cont: 0.62% Rosi: 0.60%	OR 1.64 (0.98-2.74)	Cont: 0.23% Rosi: 0.36%
Meta analyis 2 (+ RECORD)	32294	See above	OR 1.33 (1.02-1.72) ***	–	Not reported	-
RECORD (interim) vs met & sul	4447	T2D with no CVD	HR 1.16 (0.75-3.80)	Cont: 1.7% Rosi: 1.9%	HR 0.83 (0.51-1.36)	Cont: 1.6% Rosi: 1.3%
DREAM vs placebo	5269	Pre-diabetics with no CVD	HR 1.66 (0.73-3.80)	Cont: 0.3% Rosi: 0.6%	HR 1.20 (0.52-2.77)	Cont: 0.4% Rosi: 0.5%
ADOPT vs met	4351	Recently diagnosed diabetics with no CVD	HR 1.23 (0.68-2.22)	Cont: 1.7% Rosi: 1.9%	HR 1.30 (0.35-4.86)	Cont: 0.3% Rosi: 0.3%
vs glib			HR 1.52 (0.79-2.94)	Cont: 1.0% Rosi: 1.6%	HR 0.58 (0.19-1.78)	Cont: 0.6% Rosi: 0.3%
RECORD (2009) vs met & sul	4447	T2D with no CVD	HR 1.14 (0.80-1.63)		HR 0.84 (0.59-1.18)	

Fig 1.8 Summary of the meta-analyses and the large prospective clinical trials
CI – confidence interval, CV – cardiovascular, CVD – cardiovascular disease, HR – hazard ratio, MI – myocardial infarction, OR – odds ratio, met – metformin, sul – sulfonylurea, Glib – glibenclamide
* The risk of an event in the treatment group compared to the risk of that event in the control group. An OR (or HR) of 1.43 means that the risk of an MI is 43% higher among patient on rosiglitazone than in patients not on rosiglitazone.
** Meta analysis (1) = Nissen *et al*, 2007, Meta-analysis (2) = Singh *et al*, 2007
*** Significant result
Adapted from NPS limited fact sheet: Rosiglitazone and cardiovascular risk (downloaded from http://www.nps.org.au/_data/assets/pdf_file/0020/17057/rosiglitazone-cvrisk.pdf)

1.4 The Intracellular Ca^{2+} Signalling/Homeostasis System

Calcium: Approx 99% of the calcium found in the human body exists in its crystalline or mineral form, bound within the skeleton and teeth, with the majority of the remainder, in its ionised or buffered form, being found in blood and extracellular fluid (Sherwood *et al*). Only a very small fraction of this calcium - some 0.1% - exists as „free" intracellular ionic calcium "Ca^{2+}" (Kass & Orrenius, 1999). The intracellular concentration of free ionic calcium "$[Ca^{2+}]_i$" has to be kept low due to the chemistry of the Ca^{2+} ion. Ca^{2+} ions can form up to 8 co-ordinate bonds with electron donors, and in the aqueous environment within cells, rapidly forms bonds to phosphate, carboxyl and carbonyl groups leading to the formation of insoluble calcium phosphates and carboxylates. This formation of calcium precipitates becomes problematic as it renders the phosphates and carboxylates present in proteins, phospholipids and nucleic acids useless and unable to participate in cellular processes such as energy provision/storage. In future, in this study "Ca^{2+}" will be used to refer to the free divalent ion form.

As an aside, it is interesting to note that it has been suggested that cellular Ca^{2+} signalling/homeostasis could have originated primarily for the purpose of defence against the „calcium holocaust" (Jaiswal, 2001). This theory proposes that when life was originating on earth, calcium was abundant in the igneous rocks present in the earth's hot crust and was unavailable for use by living matter. As the earth cooled, various chemical and biological reactions caused the extracellular free calcium levels to rise on the earth's surface. This caused a serious problem, since calcium at high concentration causes organellar damage and protein and nucleic acid aggregation, and leads to precipitation of phosphates (which are necessary for all energy transactions in the cell). Each of these events would cause instant death of the cell. Therefore, it was essential for cells to contain or handle calcium in a manner such that it was no longer harmful. This could have been the basis for the selective pressure that led to the evolution of calcium pumps and internal calcium stores, by which cells could maintain their cytosolic free calcium at tolerable levels.

Intracellular Ca^{2+}: Ca^{2+} is now one of the most widely used and important intracellular second messenger in cell biology, and is central to the mediation of many varied cellular signalling processes. In fact, it is involved in almost all cellular events: including cell growth and proliferation, metabolism, contraction and

relaxation, cell secretion and motility and gene expression (Lipskaia *et al,* 2007; Groenendyk *et al* 2004).

However Ca^{2+} is different from other cell messengers in that it is essential for life (due to its indispensable participation in many vital cell signaling processes), yet can also be cytotoxic if allowed to accumulate in the main body of a cell. Therefore Ca^{2}+ can reach high intracellular concentrations due to its ability to cause precipitation of phosphates as described above and since phosphate is critically tied in with the cell‟s energy storage/utilisation, Ca^{2+} levels have to be kept low. Intracellular Ca^{2+} levels are usually kept in the magnitude of ~100nM which is much lower than extracellular levels which may reach ~2mM (Clapham, 1995). As Ca^{2+} cannot be metabolised it is imperative that the cell constantly regulates this important cation via a series of Ca^{2+}-binding proteins, and via either sequestration of Ca^{2+} into intracellular organelle stores or removal of Ca^{2+} from the cell.

1.4.1 Role of the ER and calcium storage

The endoplasmic reticulum (ER) is an organelle found in eukaryotic organisms that consists of a network of fluid-filled membranes distributed throughout the cytoplasm. Its has numerous functions including amongst others, the folding, glycosylation and transport of synthesised proteins. The ER is the main site of intracellular Ca^{2+} storage and as such plays a vital role in establishing and maintaining Ca^{2+} homeostasis (Berridge 2002). The ER has a very large surface area, much larger than the plasma membrane, and also permeates much of the cell, making it an ideal candidiate for Ca^{2+} storage as by the actions of the ER, Ca^{2+} can either be accumulated or mobilised quickly and efficiently.

1.4.2 Calcium signalling

Calcium signalling is induced in a slightly different manner in non-excitable cells such as monocytes, to that in excitable cells such as muscle cells. In non-excitable cells, two mechanisms exist which both ultimately lead to the formation of the molecule inositol (1,4,5)-triphosphate (IP_3). IP_3 is formed upon hydrolysis of phosphatidylinositol (4,5)-biphosphate (PIP_2), an inositol lipid precursor which is stored in the plasma membrane. The first mechanism by which IP_3 is released is through activation of the G protein-coupled receptors (GCRs), which are also known as seven transmembrane domain receptors. This class of receptor spans the plasma

membrane and extracellular ligand binding to this receptor induces a conformational change and activation of a GTP binding protein which subsequently activates phospholipase Cβ (PLCβ), instigating the hydrolysis of PIP_2 to IP_3 and diacylglycerol (DAG) (see Fig 1.9).

The alternate mechanism of IP_3 release involves receptor tyrosine kinase (RTKs) which also leads to the formation of DAG and IP_3. Briefly, RTKs are single transmembrane –spanning receptors which upon ligand binding, become activated by dimerisation and autophosphorylate of their tyrosine residues. PLCγ translocates and binds to the phosphorylated tyrosine residues where it stimulates the catalysation of PIP_2 into DAG and IP_3 (Clapham, 1995).

IP_3 diffuses though the cell where it binds to IP_3 receptors (IP_3R), which are ligand-gated Ca^{2+} channels in the ER Membrane (Ferris *et al,* 1989). Binding of IP_3 to its receptor causes a conformational change and subsequent opening of channels made up of IP_3R tetramers in the ER/SR membrane, allow Ca^{2+} to diffuse down the concentration gradient into the cytoplasm, and thus trigger a cellular response

Under conditions of prolonged stimulation, a second phase of response is initiated in which the released Ca^{2+} activates TRP/CRAC channels in the plasma membrane and potentiates the entry of Ca^{2+} from outside the cell via plasma membrane via an until recently unknown mechanism. It has since been discovered that decreases in ER Ca^{2+} are detected by an ER trans-membrane protein known as stromal interactacting molecule 1 (STIM1) (Zhang *et al*, 1995). STIM1 upon sensing Ca^{2+} depletion subsequently translocates from the ER membrane to near the PM where it binds with ORAI1, a pore-forming protein found in the Ca^{2+}-release activated Ca^{2+} (CRAC) channel, a store-operated Ca^{2+} channel (SOC) in the plasma membrane, initiating Ca^{2+} entry into the cell via the CRAC channel (reviewed in Frischauf *et al*, 2008). Nevertheless, the primary source of cytosolic free calcium is intracellular – ie. from the ER/SR – with influx of extracellular Ca^{2+} being a secondary Ca^{2+} source usually only used during prolonged cellular stimulation (Lipskaia *et al* 2007). Although it is not the main focus of the current study, for completion‟s sake it should be briefly noted that in excitable cells, in addition to the events described above, Ca^{2+} enters via voltage-dependent Ca^{2+} channels and activates ryanodine receptors (RyR) stimulating the

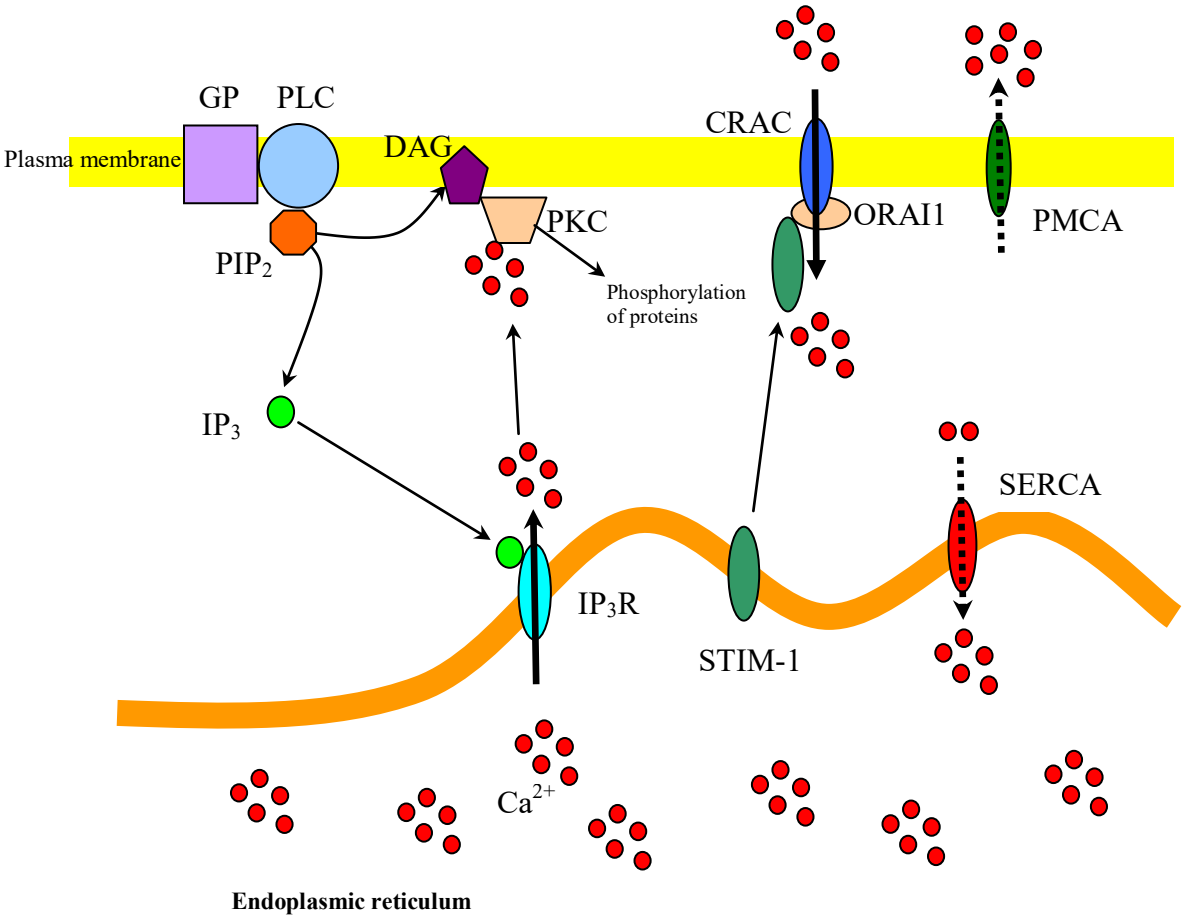

Key

GP- G-protein
PLC – Phosholipase C
DAG – Diacylglycerol
PKC – Protein Kinase C
PIP_2 – Phosphatidylinositol (4,5)-biphosphate
IP_3 – Inositol (1,4,5)-triphosphate
IP_3R – Inositol (1,4,5)-triphosphate receptor
Ca^{2+} - Calcium
CRAC – Ca^{2+}-release activated Ca^{2+} channel
ORAI1 - Pore-forming protein found in the CRAC channel
PMCA – Plasma Membrane Ca^{2+}ATPase
STIM-1 - stromal interactacting molecule 1
SERCA – Sarco(endo)plasmic reticulum Ca^{2+}ATPase

Fig 1.9 A summary of Calcium signalling and homeostatic mechanisms

Calcium Signaling: mobilization of Ca^{2+} from internal and extracellular sources (Ca^{2+} movement depicted by solid arrows). Ligand binding to the G-protein receptor activates Phospholipase C which coverts PIP_2 into DAG and IP_3. IP^3 binds to receptors on IP_3R channels initiating Ca2+ efflux from the ER via the IP3R channel. STIM 1 detects decreased ER Ca^{2+} levels and translocated from the ER membrane to bind with ORAI1, the pore forming componest of the CRAC channel, initiating Ca^{2+} influx from the extracellular environment. Elevated cytoplasmic Ca^{2+} causes protein kinase C to translocate to the PM where it is activated by DAG to induce phosphorylation of numerous proteins/enzymes.

Calcium Homeostasis: sequestration of Ca^{2+} back into the ER or expelled from the cell (Ca^{2+} movement depicted by dashed arrows). Following cell signaling events requiring Ca^{2+} mobilization, the PMCA pumps Ca^{2+} out of the cell while SERCA pumps Ca^{2+} back into the ER, both resulting in restoration of basal Ca^{2+} levels (approx 100nM).

release of Ca^{2+} from the Sarcoplasmic reticulum (SR) (Clapham 1995). Nevertheless, both excitable and non-excitable cells do employ broadly comparable Ca^{2+} signalling systems. The current study will employ non-excitable cells in all practical investigations.

1.4.3 Calcium homeostasis

Section 1.4.2 highlighted the initiation of cell signalling events upon cell stimulation resulting in the mobilisation of calcium from intracellular stores. However as $[Ca^{2+}]_i$ are required to be kept low, the ions have to be removed from the cytoplasm following cessation of Ca^{2+}-dependent cell signlling events. This section summarises the cellular actions undertaken to return the cell back to its resting state i.e. its calcium homeostatic mechansim.

After cell stimulation when Ca^{2+} levels are high, Ca^{2+} is pumped into the ER/SR, against its concentration gradient, by the P-type ATPase calcium pump, Sarco-endoplasmic Reticulum Calcium ATPase (SERCA). Alternatively, Ca^{2+} can be transported out of the cell via the plasma membrane transporter proteins such as the sodium-calcium exchanger (NCX) or the plasma membrane Ca^{2+}ATPase (PMCA) pump enzymes (Berridge, 1997).

1.4.4 P-type ATPase Calcium Pumps

The establishment and maintenance of ion gradients across the plasma membrane and across internal Ca^{2+} stores is vital in order for Ca^{2+} to be successfully used as a signaling molecule. The P-type ATPase family of pump enzymes, of which there are several hundred (Axelsen and Palmgren, 1998 - See Fig 1.10), are responsible for ATP-dependent active transport of charged substrates across a diverse range of cellular membranes. Their name comes from their mechanism of action, in that phosphorylation of an aspartate residue in the active site upon ATP hydrolysis, results in conformational changes at multiple sites in the protein. The presence of two conformationally different forms of the protein, namely E1 (the unphosphorylated form) and E2 (the phosphorylated form), shows how the affinity of the protein for its substrate(s) alters during this conformational shift, allowing the protein to function effectively as a pump.

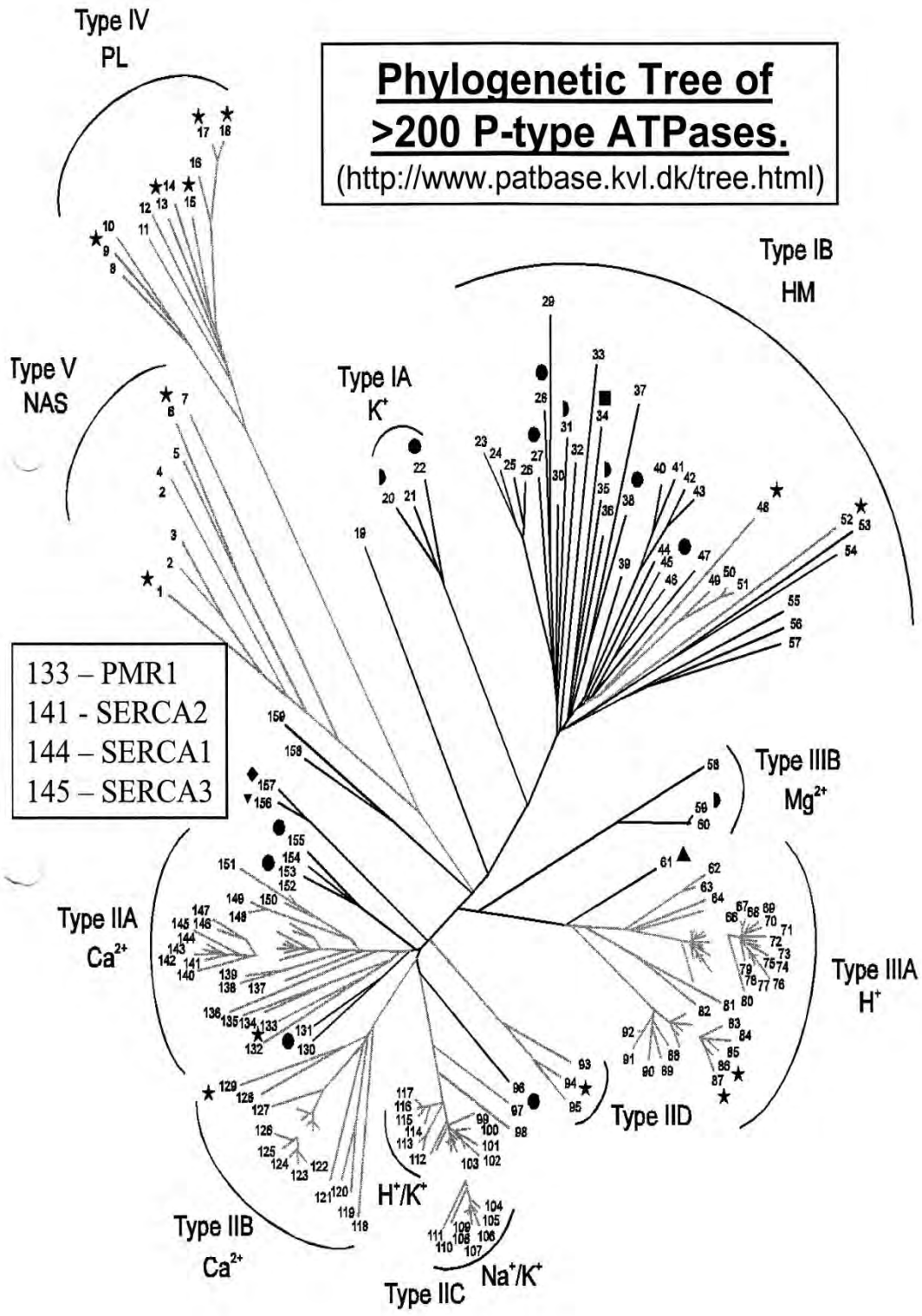

Fig 1.10 Phylogenetic tree showing the vast array of P-Type ATPases, including those mentioned in the study, namely the SPCA PMR1 and SERCA isoform 1-3.

The three main types of Ca^{2+}-transporting mammalian P-type ATPases are the plasma membrane calcium ATPases (PMCAs), the secretory pathway calcium ATPase (SPCAs) and the sarcoplasmic/endoplasmic reticulum calcium ATPAses (SERCAs). In the case of the SERCA enzymes that are the object of the present study, binding of two Ca^{2+} ions to the E1 form of the protein on the cytosolic side of the ER membrane is followed by subsequent ATP hydrolysis and phosphorylation of the protein, initiating a conformational change and the formation of the E2 version of the protein. The Ca^{2+} affinity of the E2 protein rapidly decreases, resulting in the release of the Ca^{2+} ions on the luminal side of the ER membrane. Subsequent dephosphorylation then allows the protein to revert back to its original conformation (East 2000). This is summarized in fig 1.11.

Plasma membrane calcium ATPases (PMCAs)

The main role of the PMCA, alongside the sodium calcium exchanger (NCX), is maintenance of the 10,000 fold Ca^{2+} gradient across the plasma membrane by pumping Ca^{2+} out of the cell in an energy dependent process. The PMCAs are thought to contain 10 transmembrane domains with both the NH_2 and COOH termini locating on the cytosolic side of the plasma membrane (Strehler, 2001). There are four known PMCAs (PMCA 1-4) each encoded by four separate genes (ATP2B1-4) and while PMCA is ubiquotously expressed, the isoforms are expressed in different regions of the body. Alternate splicing of these genes has produced more than 20 splice variants (Strehler, 2001). Following activation by phosphorylation of the aspartate residue as described above, PMCAs are further activated by the binding of Ca^{2+}/calmodulin (Wuytack *et al*, 1992). While to date no significant human disease has found to be associated with mutations in PMCAs, research in mice models shows that homozygous loss of PMCA1 is lethal (Prasad *et al*, 2004), homozygous loss of PMCA2 leads to deafness and balance disorders (Kozel *et al*, 1998) and homozygous loss of PMCA4 leads to male infertility (Okunade *et al*, 2004).

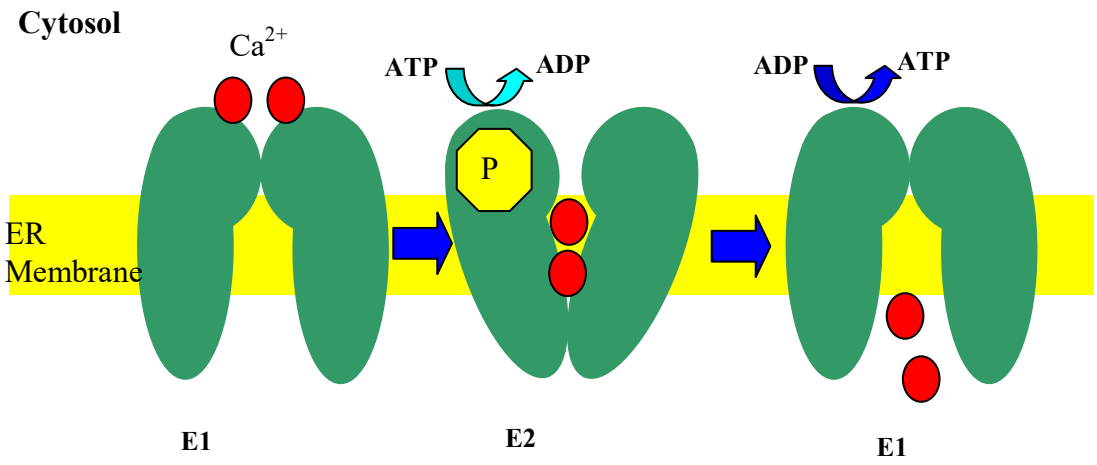

Key
ER – Endoplasmic Reticulum
ATP – Adenosine tri-phosphate
ADP – Adenosine diphosphate
Ca^{2+} - Calcium
E1 – Initial configuration of the P-type ATPase
E2 _ Configuration of the P-type ATPase upon binding of ATP

Fig 1.11 - Simple representation of the conformation shift from the E1 conformation of the SERCA P-type ATPase to the E2 conformation. The conformation shift upon binding of Ca^{2+} and ATP and the subsequent deposition of Ca^{2+} on the opposite side of the lumen following a return to the E1 conformation upon dephosphorylation are shown.

Secretory Pathway Ca^{2+}ATPases (SPCAs)

In comparison with PMCA and SERCA, very little research had been conducted on the mammalian secretory pathway ATPases. These were originally designated as hSPCA Ca^{2+} pumps in humans, due to the homology between these human genes and PMR1, a Ca^{2+} transporting pump originally cloned from the yeast *Saccharomyces cerevisiae* (Rudolph *et al*, 1989), and were later found to be P-type Ca^{2+}ATPases located in the Golgi apparatus and possessing properties distinct from the well known Ca^{2+}ATPases, the PMCAs and the SERCAs (Sorin *et al*, 1997). For example, unlike SERCA, hSPCA enzymes can transport Mn^{2+} in addition to Ca^{2+} (Xiang *et al*, 2005). Also, the stoichiometry of the hSPCA reaction cycle is such that 1 cation is transported for every ATP molecule hydrolysed (in contrast to the 2xCa^{2+}:1xATP stiochiometry seen with SERCA enzymes (Vanoevelen *et al*, 2005)).

Mutations of the SPCA genes can have deleterious consequences: for example, it has been shown that possessing only a single copy of the ATP2c1 gene which encodes for human SPCA, leads to Hailey-Hailey disease (Hu *et al*, 2000, Sudbrak et al, 2000), a disorder of the keratinocyte caused by defective Ca^{2+} homeostasis, thus providing further evidence for the role of the SPCA as a vital cellular Ca^{2+} pump in its own right.

Sarcoplasmic/endoplasmic reticulum calcium ATPase (SERCA)

SERCA calcium pumps are 110kDa proteins that span the membrane of the ER (and the SR in muscle cells). Two distinct X-ray crystallography studies have allowed elucidation of the crystal structure of SERCA1a (the skeletal muscle isoform of the enzyme family) in either the E1 conformation (Toyoshima *et al*, 2000) or the E2 conformation (Toyoshima *et al,* 2002). The cytoplasmic region consists of three well-separated domains with the phosphorylation site (Asp351) in the central catalytic domain, and the adenosine-binding site on another domain. In the E1 conformation, two Ca^{2+} ions are located side-by-side in the transmembrane domain, which comprises ten α-helices (Toyoshima *et al*, 2000). When the enzyme was held in the E2 conformation by the SERCA-specific inhibitor thapsigargin (Sagara & Inesi, 1991), large conformation differences could be seen compared to E1 – for example, the three cytoplasmic domains gather to form a single headpiece, and six of the ten transmembrane helices exhibit large-scale rearrangements. These rearrangements

ensure the release of Ca^{2+} ions into the lumen of the ER/SR, and on the cytoplasmic side create a pathway for entry of new Ca^{2+} ions (Toyoshima *et al*, 2002).

In vertebrates, SERCA proteins are encoded by three distinct genes found on three separate chromosomes but alternate splicing of these genes allows the formation of more than 10 SERCA isoforms (reviewed in East, 2000). (NB. As heterologous expression studies in which different SERCA isoforms were expressed in COS cells demonstrated broadly similar enzyme activities for SERCA1a, SERCA2a, SERCA2b and SERCA3 (Lytton *et al*, 1992), it is reasonable to assume that the basic structure of all SERCA isoforms are similar).

SERCA1: SERCA1, the most widely studied of the SERCA isoforms, was originally identified almost 40years ago as a "Ca^{2+} pump" enzyme expressed in fast-twitch skeletal muscle (MacLennan, 1970). Alternate splicing gives rise to two isoforms, SERCA1a and SERCA1b that differ only in a 42bp exon present in the former and absent in the latter (Brandl *et al*, 1987). SERCA1a is located in adult fast twitch skeletal muscle while SERCA1b is found in neonatal muscle and it appears that it takes a period of between 1 and 14 days after birth for the complete transition to encoding the adult isoform rather than the neonatal (Brandl *et al*, 1987). In their initial investigation, Lytton *et al* conducted functional comparisons of SERCA isoforms by overexpressing each isoform in COS cells. Microsomes prepared from cells transfected with SERCA1 were found to have the greatest Ca^{2+} pumping capacity of the SERCA isoforms, as detested by the high levels of calcium uptake/turnover and ATP hydrolysis when locked in the E2 conformation compared with other SERCAs (Lytton *et al*, 1992)

SERCA2: The SERCA2 transcript was originally cloned from neonatal muscle (Brandl *et al*, 1987). SERCA2 splice variants include SERCA2a and SERCA2b. SERCA2a is expressed in cardiac and slow twitch skeletal muscle (Lytton & MacLennan, 1988) and was found to have a Ca^{2+} transport capacity and Ca^{2+}-dependent ATP hydrolysis consistent with other SERCA isoforms (Lytton *et al*, 1992). SERCA2b is ubiquitously expressed in nearly all tissues and is the dominant ER Ca^{2+}ATPase in non-muscle tissue (Gunteski-Hamblin *et al*, 1988).

Interestingly, in contrast to other SERCAs, SERCA2b was demonstrated to have the lowest Ca*2*+ transporting capacity and ATP hydrolysis of all isoforms (Lytton *et al*, 1992). Following alternate splicing of the SERCA 2 gene, SERCA2b contains an additional 49-50 amino acid residues in its C-terminus to that of SERCA 2a (Gunteski-Hamblin *et al*, 1998). The extended C-terminus of SERCA2b leads to the formation of an additional eleventh trans-membrane domain and the localization of the C-terminus in the ER lumen (Campbell *et al*, 1992), where it has been found to interact with and be modulated by, the accessory protein calreticulin (John *et al*, 1998). Due to the ubiquitous nature of SERCA2b expression compared with other SERCA isoforms, its comparatively low Ca^{2+} pumping capacity and research showing that inhibition of SERCA leads to cellular apoptosis, it is thought that SERCA2b performs a critical „housekeeping" function in correcting non-specific leakage of Ca^{2+} from the ER/SR (Prasad *et al*, 2004). Recent research has discovered a third SERCA2 isoform, namely SERCA2c, which has been found to be expressed in cardiac muscle (Dally *et al*, 2006).

SERCA 3: SERCA3 was originally identified as an additional SERCA isoform expressed in non-muscle tissue (Burk *et al*, 1989); more recent studies have characterized several splice variants include SERCA3a,b and c and is usually found in only certain tissue including lymphocytes, mast cells, platelets and some endothelial and epithelial cells (reviewed in East, 2000). SERCA3 isoforms are rarely found alone but more usually in combination with other SERCA isoforms, commonly SERCA2b. Functional comparison of SERCA3 with other isoforms showed that it had a very high Ca^{2+} transporting capacity and average ATP hydrolysis rates (Lytton *et al* 1992).

SERCA and disease

In order to further assess the true functional capacity of each of the SERCA isoforms, it is necessary to render the gene/protein inactive via gene knockout studies. Such investigations confirm what happens on a cellular basis in the absence of a „working" gene/expressed protein and also allows us to see which disease states may occur in animal models as a result.

SERCA1: SERCA1 null mutants, ie mice containing no functional copy of the SERCA1 gene, have bred in the laboratory. These offspring were born live but

rapidly developed breathing difficulties leading to cyanosis and death (Pan *et al*, 2003). Histological analysis of diaphragm muscle tissue showed evidence of hypercontraction due to impaired muscle fibre relaxation and analysis of lung tissue showed hypercellularity and epithelial damage consistent with failure of alveoli expansion and respiratory failure. Wild-type offspring had none of the above problems indicating that in mice, SERCA1 while not producing embryonic lethality, is essential for neonatal survival.

Mutation of the SERCA1a gene in humans leads to Brody‟s disease, a rare but painful disorder that induces severe cramping and impairment of skeletal muscle relaxation in sufferers (Periasamy *et al*, 2007). The mutation is not fatal and skeletal muscle contraction and relaxation does still occur suggesting that upregulation of other SERCA isoforms may compensate for the loss of SERCA1a (reviewed in Shull, 2000) which does not seem to occur in other animal models such as mice.

SERCA2: Gene knockout studies were carried out where by a mutant SERCA2 gene, incapable of expressing SERCA2 transcripts/protein was created in a mouse model. Subsequent breeding of heterozygous mice produced both heterozygous and wild type offspring but not homozygous mutants, suggesting the importance of at least one functional copy of the SERCA2 gene in sustaining life. While appearing outwardly healthy, the heterozygous offspring carrying only one functional copy of the SERCA2 gene, were found to have decreased SERCA2 mRNA, protein and activity, ultimately resulting in impaired cardiac contractility and overall cardiac function (Periasamy *et al*, 1999).

Mutations of SERCA2 gene expression are much rarer and more severe in nature. Complete deletion of the SERCA2 gene is lethal while mutations affecting only one copy of the SERCA2 gene causes a non-lethal yet distressing skin disease, known as Darrier‟s disease, which is characterised by keritinisation of the squamous epithelial cells. Interestingly, despite SERCA2a being expressed in cardiac muscle, cardiac function is not impaired in single gene mutations. This suggests that one copy of the SERCA2 gene is sufficient to sustain cardiac function (although functioning would be somewhat diminished) (Periasamy *et al*, 2007).

SERCA3: SERCA3 is one of only two non-muscle isoforms but unlike SERCA2b it is not ubiquitously expressed. Knockout of the SERCA3 isoform in a mouse model gave rise to healthy homozygous offspring (Liu *et al*, 1997) and loss of the SERCA3 gene appeared not to directly result in major disease in animal studies. This is probaly due to the limited distribution of SERCA3 and to potential compensation by SERCA2b which is often co-expressed alongside SERCA3 (Periasamy *et al*, 2007). However, SERCA3 is expressed in vascular endothelial cells and it was discovered that acetylcholine-induced endothelium-dependent relaxation was reduced in aortic ring tissue taken from SERCA3 null mutant mice (Liu *et al*, 1997). Ca^{2+} imaging also showed decreased Ca^{2+} and reduced Ca^{2+} sequestration into acetylcholine-sensitive stores in SERCA3 deficient mice. The above data suggests SERCA3 may play an important role in Ca^{2+} in the vascular smooth muscle cell.

SERCA3 is expressed in pancreatic β-cells and combined with the discovery of reduced Ca^{2+}ATPase activity in rat diabetes models (Levy *et al*, 1998), the absence of SERCA3 has been proposed to be implicated in impaired glucose homeostasis and thus contribute to diabetes. However, despite aberations in Ca^{2+} signalling, loss of SERCA3 has been shown to have no effect on serum insulin and glucose levels (Arredouani *et al*, 2002) and therefore it is proposed to not be essential in glucose homeostatic mechansims and that loss of activity of this isoform does not cause diabetes (Prassad *et al*, 2004).

Modulators of SERCA activity/SERCA or Ca^{2+} accessory proteins

Phospholamban: Phosholamban (PLN) is a peptide made up 52 amino acids and is expressed in cardiac, smooth and slow-twitch skeletal muscle. PLN is an inhibitor of SERCA2 activity in its unphosphorylated form (East 2000) by interfering with their ability to bind to Ca^{2+}, inhibiting at low but not high [Ca^{2+}] (Tada *et al*, 1989; Simmerman *et al* 1996). Phosphorylation of PLN reverses its inhibitory affect as it can no longer effectively bind to SERCA2. SERCA1, can also be potentially inhibited by PLN despite PLNs lack of expression in fast-twitch muscle and indeed PLNs inhibitory actions have been modelled in SERCA1a (Toyoshima *et al* 2003).

Sarcolipin: Sarcolipin (SLN) is a peptide made up of 31 amino acids which resembles PLN in its inhibitory actions of SERCA1. SLN regulates SERCA

independently and also in association with PLN (Asashi *et al*, 2003). The effects of SLN and PLN are thought to be additive.

Calreticulin: Calreticulin is an ER resident chaperone protein aiding in the correct folding and sorting of proteins in this organelle. It also functions to bind/buffer ER Ca^{2+} and is therefore involved in Ca^{2+} homeostastic processes such as calcium storage and subsequent release from the ER, SERCA function and SOC entry (reviewed in Groedendyk *et al*, 2004). Calreticulin deficiency has been found to be embryonically lethal resulting from significant impairments in cardiac development (Mesaeli *et al*, 1999) and as Ca^{2+} release from the ER is calreticulin-dependent may suggest that as Ca^{2+} signalling is also impaired in these embryos therefore abherrant Ca^{2+} homeostasis may play a role in this lethality (Mesaeli *et al*, 1999).

1.4.5 Calcium and diabetes: complications

There is a wealth of data to support the view that increased cytoplasmic Ca^{2+} concentrations is involved at all points in the development of T2D and its associated complications, from the production of insulin by the β-cell onwards. For example, increased cytosolic Ca^{2+} stimulates insulin exocytosis by the β-cell through Ca^{2+}dependent protein kinase pathways. This is because SERCA3's physical interaction with the Insulin Receptor Substrate ensures that insulin is not secreted unless elevations in glucose specifically stimulate insulin secretion by disruption of this interaction (Borge & Wolf, 2003). This led to the suggestion that – as seen in a subset of the T2D population (or in Goto-Kakizaki rats, a non-obese model for type 2 diabetes) – disruptions in SERCA3 expression may be responsible for unchecked insulin secretion from the β cell, and thus hyperinsulinaemia (Borge & Wolf, 2003).

Also, elevated $[Ca^{2+}]_{cyto}$ is associated with decreased cellular insulin sensitivity and is thus indirectly contributing to the pathogenesis of insulin resistance in T2D (Balasubramanyam *et al,* 2001). Cellular Ca^{2+} accumulation as seen in cells from T2D has been reported to result from disruptions in several components of the $[Ca^{2+}]_i$ system, including (a) reduction in PMCA ATPase activity, (b) modulation of Na^+/Ca^{2+} exchange and (c) increased Ca^{2+} influx across the plasma membrane (Balasubramanyam *et al*, 2001).

It is possible that much of the impact of T2D can be linked to specific effects on SERCA enzymes. For example, Clarke *et al* have suggested that diabetic hyperglycaemia leads to glycosylation of transcription factors, and reduced expression of many genes, including SERCA2 (Clark *et al*, 2003). As a long-lived enzyme, SERCA2's turnover rate is slow (Ferrington *et al*, 1998), and so it is particularly susceptible to post-translational modifications, which can also occur due to reactive oxygen species given off during diabetes-associated inflammation, atherosclerosis - this direct inhibitory effect is heightened in hypercholesterolaemia (due to increased oxidative stress) (Adachi *et al*, 2001). Moreover, direct attachment of AGE to SERCA2a causes inhibition of Ca^{2+} pumping (Bisadee *et al*, 2004). In support of this, Belke *et al* have shown reduced SERCA activity in diabetic mice, and shown that this is linked to decreased relaxation and cardiovascular dysfunction (Belke *et al*, 2004).

Finally, disruptions in Ca^{2+} homeostasis have been found to be associated with conditions such as hypertension, cardiac dysfunction and microvascular diabetic complications (Advani *et al*, 2004; Belke *et al*, 2004; Singh *et al*, 2005). Hypertension is associated with a rise in cytoplasmic Ca^{2+} which results in impaired glucose metabolism, coupled with a rise in blood pressure, a reduction in insulin sensitivity and an increased potential for the development of insulin resistance (Randriamboavonjy *et al* 2008). Hyperactivation of monocytes has been shown to increase cytoskeletal rigidity while decreasing cell deformability resulting in microchannel occlusion and potentially life-threatening microvascular complications (Singh *et al* 2005). Platelet function in diabetic patients is also impaired, displaying excessive adhesiveness, aggregation and generation of thrombus, all suggested to be due to disruption of calcium homeostasis and resultant decrease in Ca^{2+}ATPase activity (Randriamboavonjy *et al* 2008).

1.5 Aims

Thus, in conclusion to this introductory chapter, the general aims of the present study will be stated:-

a) **To investigate rosiglitazone's effect on cellular calcium homeostasis, and to determine the mechanism(s) by which these effects are achieved:** Rosiglitazone has been established by Singh (Singh *et al*, 2005) amongst

others, to have a rapid effect on $[Ca^{2+}]_{cyto}$ (<5 mins) due to an as yet unknown mechanism. As aberrant Ca^{2+} homeostasis contributes to the development of T2D and to the progression of its associated complications, an understanding of the effects the diabetic anti-hyperglycemic agent rosiglitazone may elicit on Ca^{2+} homeostasis could be of clinical importance. Therefore, this study aims to utilize enzyme assays, Ca^{2+}activable fluorescent dye measurements, gene and protein expression studies, and cell viability/apoptosis assays to determine the effects of rosiglitazone on intracellular calcium homeostasis, cell growth and proliferation. This work is conducted in monocytes and vascular smooth muscle cells – 2 cell types associated with T2D complications (Chapter 2) and ultimately aims to determine the mechanism by which the drug elicits the effects previously observed (Chapter 3).

b) To investigate whether rosiglitazone's effects in cellular models could be observed in intact tissue:

As described above, T2D has been linked by many authors to an increased prevalence of cardiovascular disease and in particular atherosclerosis. Also, TZD therapy has been linked in many studies with improvements in endothelial function and subsequent improvements in cardiovascular function. Therefore, this study aims to carry out isometric tension recordings to determine rosiglitazone"s effects on vascular smooth muscle relaxation in aortic tissue, and to determine whether these effects can be attributed to the drugs" proposed mechanism of action on a cellular level - as deduced in Chapter 3 (Chapter 4).

c) In this way, it is hoped in a broader sense that insights will be gained into both the applied clinical and the pure cell biological aspects of this area of study. Specifically, light may be shed on the following two topics:

a. A contribution to the ongoing debate as to whether rosiglitazone should be prescribed clinically in the treatment of T2D and its complications.
b. An elucidation of the mechanisms by which the cells under investigation in the present study respond to agents that disrupt their $[Ca^{2+}]_i$ systems.

Chapter 2

An investigation into the effect of rosiglitazone on intracellular Ca^{2+} homeostasis in monocytic and vascular smooth muscle cells.

2.1.1 Introduction

As described in the previous chapter, Ca^{2+} is a very important second messenger and is central to an abundance of varied and vital cellular functions (Shull *et al*, 2000). Conversely, sustained elevation of intracellular levels of this cation is associated with numerous deleterious and damaging effects, and even cell death (Deng *et al,* 2005). Nevertheless, as described in Chapter 1, controlled, transient, discrete releases of Ca^{2+} into the cytoplasm have been shown to be involved in vital cell signalling processes.

In order for this second messenger to carry out its diverse signalling activities, the maintenance of Ca^{2+} gradients between the cell and its extra-cellular milieu and between the cytoplasm and intracellular Ca^{2+} stores is essential (Shull *et al*, 2000), as discussed in chapter 1.

Rises in $[Ca^{2+}]_{cyto}$ are often attributed to agonist-induced release of Ca^{2+} from the ER (over and above the constant small-scale non-specific leakage of Ca^{2+} from the ER). For example, Ca^{2+} release from the ER has been shown to be induced by agents including lipopolysacharide (LPS), cholera toxin (CT), dibutyryl-cyclic AMP (d-cAMP) and prostaglandin E_2 (PGE_2) (Bagley *et al* 2004). In non-pathological situations, excess Ca^{2+} is rapidly removed from the cytoplasm into the internal stores such as the ER by the actions of ER-resident SERCA Ca^{2+} pump enzymes. Many agents cause elevations in $[Ca^{2+}]_{cyto}$, however not by inducing leakage of Ca^{2+} from the ER but by interfering with the ability of the cell to return this Ca^{2+} to the ER, by partial or complete inhibition of SERCA enzymes. One such example is the sesquiterpene lactone thapsigargin, a classical SERCA inhibitor which has been used extensively in the laboratory for many years (Thastrup *et al*, 1989; Treiman *et al*, 1998). Cyclopiozonic acid (CPA), an indole tetramic acid isolated from *Penicillium cyclopium*, is another agent used in the laboratory as a Ca^{2+}ATPase inhibitor (Seidler *et al* 1989).

Many pathological conditions are known to invoke marked and sustained adaptations in $[Ca^{2+}]_{cyto}$ (Deng *et al,* 2005), in numerous diseases including diabetes (Advani *et*

al, 2004). In fact, disrupted Ca^{2+} homeostasis may, depending upon the cell type involved, be associated with the development of many diabetic complications including - amongst others - hypertension and cardiac dysfunction (Advani *et al*, 2004; Belke *et al*, 2004; Bisadee *et al*, 2004). The above homeostatic disruption may be at least partly due to malfunctioning of the resident SERCA Ca^{2+}ATPase pump. There is a great deal of evidence suggesting the deleterious effects of decreased or impaired SERCA functioning in numerous cell types.

As discussed in chapter one, SERCA2b is known as the „housekeeping" Ca^{2+} pump enzyme of non-muscle and smooth muscle cells (Scapagnini *et al*, 2004). Many studies have reported decreased SERCA2b expression and/or activity in diabetes (Bisadee *et al*, 2004; Clark *et al*, 2003; Zhong *et al*, 2001). For example, platelets from patients with T2D have also been shown to become hyperactivated and as a consequence have a greater potential to aggregate and lead to an increased thrombogenic risk (Randriamboavonjy *et al*, 2008). This was again found to be inactivation of SERCA2b and increased platelet $[Ca^{2+}]_{cyto}$.

With the continuing evidence for the involvement of increased $[Ca^{2+}]_{cyto}$ in the pathophysiology of T2D and its complications (Advani *et al*, 2004) came the demonstration in our laboratory that the anti-hyperglycaemic drug rosiglitazone, used in the treatment of T2D, itself leads to increased $[Ca^{2+}]_{cyto}$ in monocytes (Singh *et al* 2005). Monocyte hyper-activation and its associated increase in cytoskeletal rigidity leads to diabetic microvascular complications (Miyamoto *et al* 1997). However, Singh *et al* showed that the increase in $[Ca^{2+}]_{cyto}$ produced upon stimulation with rosiglitazone, actually led to decreased actin polymerisation (Singh *et al* 2005) due to effects on the Ca^{2+}-dependent actin disassembly protein gelsolin (Atkin, 2008). This would be expected to result in increased cell deformability, and hence could potentially provide a beneficial role in a clinical setting. The timescale of the response and the nature of the increase led the authors to propose that the mechanism behind this increased $[Ca^{2+}]_{cyto}$ may be due to a disruption in Ca^{2+} homeostasis (possibly due to SERCA2b inhibition) and not initiation of a Ca^{2+} signalling cascade (Singh *et al* 2005). However, it was not clear whether the putative effects of rosiglitazone in this regard are limited to inhibition of SERCA2b, or rather that rosiglitazone disrupts the function of all Ca^{2+} pumps, or of all ER resident proteins. To elucidate how widespread these effects are, the yeast ER/Golgi Ca^{2+}/Mg^{2+} pump

PMR1 (Sorin *et al*, 1997) was selected as a useful model system. Yeast cells do not express SERCA Ca^{2+} pumps in their ER, but instead express PMR1 in both their ER and the Golgi. The human homologue of PMR1 can only be found in the Golgi. Figure 2.1.1 shows how the various SERCA and PMR1 isoform sequences compare to each other.

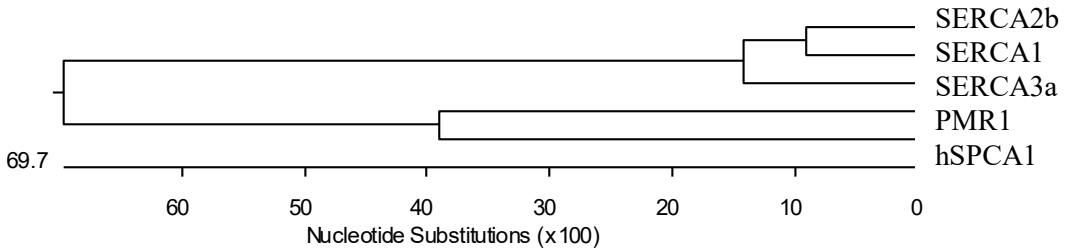

Fig 2.1.1 Phylogenetic tree comparing SERCA and PMR1 sequencing

Through its actions as a second messenger, Ca^{2+} is intensely involved in the regulation of cell growth and proliferation. Therefore it stands to reason that disruptions in calcium signalling/homeostasis, and consequently agents that cause such disruptions, can and do have profound effects on cell mortality. For example, Thapsigargin has been extensively identified as an agent that induces apoptosis via activation of CCAAT/enhancer-binding protein-homologous protein (CHOP) (Yamaguchi *et al,* 2004; Chen *et al*, 2007). CHOP is a transcription factor induced during times of ER stress (ER stress is discussed in more detail in chapter 3, and so will not be discussed in detail here). CHOP deletion in pancreatic B-cells of diabetic mice prevents cell apoptosis and promotes cell survival, indicating that its actions are a critical component in linking protein misfolding observed in ER stress with cell apoptosis (Song *et al*, 2008).

Given reports that rosiglitazone can disrupt Ca^{2+} homeostasis (Singh *et al*, 2005), it may be surmised that rosiglitazone may have an impact upon cell growth and survival. However, literature regarding rosiglitazone‟s effect on apoptosis are varied and therefore to date, inconclusive. Rosiglitazone treatment has been shown to induce apoptosis in non-small-cell lung cancer cells (A549 cells) at concentrations similar to this study (Kim *et al*, 2007). Rosiglitazone, and a natural PPARγ ligand, 15d-PGJ2, have both been found to induce apoptosis at similar concentrations in the colorectal cancer cell line HT-29 (Lin *et al*, 2007). Rosiglitazone also inhibited cell growth and initiated apoptosis in the gastric cancer cell line SGC-7901 in a dose-

dependent fashion (He *et al*, 2008). The majority of literature linking rosiglitazone with increases in apoptosis suggest that its actions are PPARγ-dependent, with the exception of the latter study which suggests the involvement of both PPARγ-dependent and independent mechanisms. However one study has shown that rosiglitazone induces apoptosis in a PPAR-γ-independent manner by increasing the sensitivity of human renal cancer cells to tumor necrosis factor-related apoptosis-inducing ligand (TRAIL) (Kim *et al*, 2008).

Alternatively, numerous studies have been conducted which associate rosiglitazone treatment with a decrease in apoptosis and subsequent increased cellular protection/survival. Rosiglitazone treatment has been shown to be anti-apoptotic and cytoprotective in hippocampal and dorsal root ganglion neuronal cells and PC12 cells (Fuenzalida *et al*, 2007), and in human primary T-cell lymphoma tissue (Yang *et al*, 2007), again apparently via PPARγ–dependent mechanisms. While much of the literature provides *in vitro* evidence, an *in vivo* study involving patients on rosiglitazone therapy for 4-8 weeks showed decreased apoptosis in peripheral polymorphonuclear leukocytes extracted from patients following completion of the treatment regime (Farah *et al*, 2008).

Evidence that disruptions in $[Ca^{2+}]_i$ play a role in the development and pathogenesis of disease such as T2D (see eg. Balasubramanyam *et al*, 2001), combined with the potential of the anti-diabetic drug rosiglitazone to induce changes in $[Ca^{2+}]_i$ (see eg. Singh *et al*, 2005), has highlighted the importance of tight regulatory control of this cation, and identified a potential intervention point at which therapeutic strategies could be targeted. However, as there is a paucity in the current literature on exactly how rosiglitazone may exert changes in cellular Ca^{2+} signalling/homeostasis, the mechanism(s) underpinning such changes and thus the cellular consequences of rosiglitazone treatment, the current study aims to investigate these areas in the hope that this may provide a valuable insight into any potential clinical advantages of this drug.

2.1.2 Aims

Thus, the specific aims of this chapter were;

- to identify/detect the presence of the ER-resident „housekeeping Ca^{2+} pump" enzyme SERCA2b in MM6 and A7r5 cell derived microsomes, and to detect the presence of the ER/Golgi Ca^{2+}/Mg^{2+} pump PMR1 in yeast cell derived microsomes (Sorin *et al*, 1997).

- to investigate the effect of rosiglitazone and other inhibitors on SERCA2b/PMR1 Ca^{2+}ATPase activity in MM6/A7r5 and yeast cell derived microsomes

- to investigate the effect of rosiglitazone on intracellular Ca^{2+} concentrations in MM6, A7r5 and yeast cells.

- to determine the effect of rosiglitazone on cell growth and apoptosis in MM6 and A7r5 cells.

2.2 Methods

2.2.1 Materials

Rosiglitazone was provided by Dr. T. Willson (GlaxoWellcome), and prepared as stock concentration (10mM) solutions in dimethyl sulfoxide (DMSO) before being stored as aliquots at -80°C. All other chemicals were purchased from Sigma-Aldrich (Sigma-Aldrich Company Ltd, Dorset, UK) unless stated otherwise.

2.2.2 Cell lines and preparation of tissue culture media

The human monocytic cell line Mono Mac 6 (MM6 cells) was obtained from the German collection of Micro-organisms and Cell Cultures (DSM ACC 124; Braunschweig, Germany). The MM6 cell line was originally derived from the peripheral circulation of a 64-year-old male patient suffering from acute monocytic leukaemia. MM6 cells characterise mature monocytes as they retain and express both phenotypical and functional abilities of these original cells (Ziegler-Heitbrock *et al*, 1988).

MM6 cells were grown in suspension in Roswell Park Memorial Institute 1640 media (RPMI). This was supplemented with 10% heat-inactivated Foetal Calf Serum (FCS) (Labtech International; France), 1% 200mM L-glutamine, 1% non-essential amino acids, 1% sodium pyruvate and 1% penicillin (50IU/ml)/streptomycin (100µg/ml) (all media supplements were obtained from Gibco BRL; Paisley, UK).

The rat aortic vascular smooth muscle cell line (A7r5 cells) was obtained from the European Collection of Cell Cultures (ECACC). The A7r5 cell line is an adherent cell line derived from the thoracic aorta of embryonic BDIX rats. This cell line is representative of adult smooth muscle and retains its contractile ability which is usually lost in passaged smooth muscle cells (Kimes *et al*, 1976).

A7r5 cells were grown in DMEM media supplemented with 10% heat-inactivated FCS, 2mM l-glutamine and 4g/L glucose (all media supplements were obtained from Gibco BRL; Paisley, UK).

Both cell lines were cultured at 37°C in a humidified atmosphere with 5% CO_2 to obtain optimal growth and proliferation.

2.2.3 Cell sub-culturing and harvesting

MM6 cells were cultured in 75cm^3 vented tissue culture flasks and were sub-cultured (passaged) when cell growth reached 80% confluence (i.e. 0.8 - 1.2 X 10^6 cells/ml). The doubling time of this cell line was 2 days, therefore cells were sub-cultured every 3 days at a density of 0.3 - 0.5 X 10^6 cells/ml and incubated at 37°C in a humidified atmosphere with 5% CO_2. For all experiments, no cells were maintained above 25 passages as after this time period, the cells tend to lose their original phenotypic properties (Zeigler-Heitbrock *et al*, 1988).

A7r5 cells were grown in 75-150cm^3 vented tissue culture flasks. Cells were sub-cultured at 70-80% confluence (at a ratio of 1:3) every 3-4 days. For sub-culturing, media was removed, the cells were washed with filter sterilised PBS and detached from flask wall by addition of 5-10ml 0.25% trypsin for 5-10 minutes at 37°C. The cell suspension was then centrifuged at 1500g for 5 minutes to pellet the cells. The cell pellet was then resuspended in fresh media, diluted appropriately and seeded into fresh tissue culture flasks.

2.2.4 Determination of cell viability by Trypan blue exclusion

Cell viability tests were conducted prior to sub-culturing, when incubating with reagents e.g. rosiglitazone, and immediately before any experimentation. Viability of cells was assessed by the Trypan blue exclusion method. Upon addition of this reagent, cells containing compromised membranes retain the trypan blue dye within the cytoplasm, whereas cells with intact membranes resist uptake of the dye. Cells were incubated with 0.4% *w/v* Trypan blue for approximately 10 minutes and then observed under the microscope. The percentage of cells observed that remained unstained indicated the percentage of viable cells within the culture.

2.2.5 Cultivation and growth of *Saccharomyces cerevisiae*

Saccharomyces cerevisiae strain FY1679-11D was obtained from Dr J. Richard Dickinson (School of Biosciences, Cardiff University). The yeast was stored at 4°C on Sabouraud glucose agar. Inocula were then cultivated in Sabouraud's broth at 30°C for 48 hours. The doubling time of this yeast strain was approximately 2 hours

at 30°C and an adequate yield of cells was achieved in 36-48 hours (Campbell & Duffus, 1988).

2.2.6 Preparation of microsomal samples

2.2.6.1 Preparation of spheroplasts

As yeast cells have an extremely rigid cell wall, a procedure known as spheroblasting, which is enzymatic degradation of the cell wall, was conducted to gain access to the contents of the cell. 100ml of the 48hr FY1679-11D yeast culture was centrifuged in two 50ml centrifuge tubes at 2500RPM (1500g) for 5 mins. The supernatant was discarded and a further 50ml yeast culture added and the centrifugation repeated. After discarding the supernatant, 1ml of Potassium Phosphate/Sorbitol buffer (Potassium Phosphate 10mM; Sorbitol 1.2M; pH 7.2) was added to the cell pellet. Cell were transferred to 2ml microcentrifuge tubes and spun at 12,000RPM for 3 minutes. After removing the supernatant, the pellet was resuspended in 0.846ml Potassium phosphate/sorbitol buffer before addition of 3µl β-Mercaptoethanol and 151µl Lyticase (1000U/ml). The tubes were placed in a shaker/water bath at 30°C overnight. Digestion was confirmed by measuring absorbance at 600nm of 30µl aliquots dissolved in 970µl, dH_2O using a Perkin-Elmer Lambda. The tubes were then spun at 6000RPM for 3 mins at 4°C to remove the Lyticase and β-Mercaptoethanol. The supernatant was again discarded and the spheroblast pellet resuspended in 500µl Buffer A (10mM Tris HCl; 0.5mM $MgCl_2$; pH 7.5) for undergoing homogenisation and subcellular fractionation (Ulug, 2004 MSc dissertation).

2.6.6.2 Preparation of MM6 cells for Subcellular Fractionation

40mls of MM6 cell suspension was centrifuged at 350RCF for 7 minutes. A further 40mls cell suspension was added and the suspension spun again at 350RCF for a further 7 minutes. The supernatant was discarded and the cell pellet stored on ice prior to immediate microsome preparation.

2.6.6.3 Subcellular Fractionation and isolation of yeast and MM6 microsomes

Differential centrifugation (subcellular fractionation) of MM6 and yeast cells was employed in order to obtain „microsomes", small vesicles containing the ER portion of the cell only, with other cell organelles and membranes removed. Microsome preparation from yeast spheroplasts or from MM6 cells was conducted according to the method of Maruyama & Maclennan (Maruyama & Maclennan, 1988) with some minor adaptations. MM6 cells or yeast spheroplasts were swollen on ice for 10minutes after addition of 2.5ml Buffer A (see above) containing 10µl protease inhibitor (Sigma, Poole, Dorset). Cells were then homogenised with 10 strokes in a glass Dounce homogenizer on ice and the homogenate diluted with an equal volume of Buffer B (0.5M Sucrose; 6mM β-Mercaptoethanol; 40µM $CaCl_2$; 300mM KCl; 10mM Tris HCl; pH 7.5). A small aliquot of the homogenate was retained. The remaining suspension was centrifuged at 9800RPM (1000g) for 20 minutes in a Sorvall SS-34 Centrifuge in order to pellet the nuclei and mitochondrial fraction. (Pellet was resuspended in buffer A and retained). 2.2ml of both Buffer A and Buffer B was added to the supernatant, along with 2.12ml KCl (2.5M). The supernatant was centrifuged at 70,000 RPM (100,000g) for 1 hour at 4°C in a Sorvall Ultracentrifuge. The supernatant containing the plasma membrane and cytoplasmic fraction was retained. The pellet containing the microsomal fraction was suspended in ~250µl Buffer C (0.25M Sucrose; 0.15M KCl; 3mM β-Mercaptoethanol; 20µM $CaCl_2$; 10mM Tris HCl; pH 7.5), aliquoted into small microcentrifuge tubes and snap-frozen in liquid nitrogen prior to storage, alongside the other retained fractions, at -80°C.

2.2.6.4 Preparation of A7r5 cells for Subcellular Fractionation

A7r5 cells were cultured in 150cm^3 tissue culture flasks as described above. The cells were washed in PBS, trypsinised (a small aliquot was removed for cell count) and then spun at 1500g for 5 minutes as described in cell subculturing above. The cell pellet was briefly kept on ice and subcellular fractionation conducted (see below).

2.2.6.5 Subcellular Fractionation and isolation of A7r5 microsomes

Microsome preparation from adherent A7r5 cells was conducted according to the method of Papp *et al* (Papp *et al,* 1992). The cell pellet produced upon cell

trypsinisation (see above) was resuspended in 5ml wash buffer (50µM EGTA; 160mM KCl; 17mM K-Hepes; pH 7.0) and the suspension spun at 1500g for 5 minutes. The pellet was resuspended in 2ml ice cold Lysis buffer (10mM KCl; 10mM K-Hepes; 100µM DTT; 50µM EDTA; 50µM EGTA; pH 7.0) and 10µl pre-aliquoted protease inhibitor added. Cells were homogenised with 50 strokes in a glass Dounce homogensizer on ice, then sonicated on ice for 20 seconds (setting 3) and spun at 12,400RPM (16,000g) for 10 minutes in a Sorval SS-34 Centrifuge. The supernatant was transferred to a Sorvall Ultracentrifuge tube prior to addition of ~8-9ml Lysis buffer (enough to fill the tube) and then ultracentrifugation at 43,217RPM (100,000g) for 1 hour at 4°C in a Sorvall Ultracentrifuge. The pellet was resuspended in ~250µl Resuspension buffer (10mM KCl; 10mM K-Hepes; 100µM DTT; pH 7.0) and snap-frozen in liquid nitrogen, prior to storage at -80°C.

2.2.7 Protein estimation of microsomal preparations

The protein content of the microsomes was assessed using the BioRad DC protein assay (BioRad Laboratories Ltd, Hertfordshire, UK), which utilises a colorimetric method following detergent solubilisation of protein samples. A series of protein standards (0-1mg/ml) were made up by dissolving Bovine Serum Albumin (BSA) in Phosphate Buffered Saline (PBS). 10µl of protein standard or microsomal sample was added to a micro-titre plate, 20µl reagent S was added to 1ml of reagent A and then 25µl of this reagent As was added to each well. 200µl reagent B was then added, mixed by pipetting and left to incubate for 15 minutes for any colouration to develop. Degree of colouration was read at an absorbance of 620nm using Dynex Revelations ELISA instrumentation (Dynex, UK) and subsequent protein concentration determined.

2.2.8 Western blot analysis

To determine whether SERCA2b and PMR1 were present, microsomal samples were subjected to Western blot analysis using primary antibodies directed against SERCA2b or PMR-1.

2.2.8.1 Protein separation by polyacrylamide gel electrophoresis

Denaturing gel electrophoresis was performed using NuPAGE electrophoresis system, lithium dodecyl sulphate (LDS) sample buffer, reducing agent (dithiothreitol), Multimark™ multicoloured molecular weight standard and the XCell II ™ Mini-Cell and PowerEase ™ power pack (NOVEX, Frankfurt, Germany). The gel used was a 10% polyacrylamide 1.0mm gel.

Electrophoresis was performed using 32.5µg protein in each case. All protein samples were made up to 50µl using 12.5µl LDS sample buffer, 5µl reducing agent and an appropriate amount of ultra-pure water. The samples were then vortexed, pulse centrifuged and heated for 5 minutes at 95°C to ensure denaturation of the proteins. The polyacrylamide gel wells were then rinsed using MOPS (3-(N-morpholino) propane sulphonic acid (MOPS) running buffer to remove any unpolymerised acrylamide. 10µl of heated protein sample was then added to each well. To verify blotting and electrophoresis, the pre-stained molecular marker MultiMark™ was added to one lane to verify electrophoresis, while Magimark™, an ECL-conjugated molecular weight marker, was also added to another well to verify the blotting procedure. Electrophoresis was then carried out at 200 V for 1 hour.

2.2.8.2 Electrophoretic transfer of proteins

Electrophoretic transfer of proteins was performed using Xcell II Surelock™ blot module and reagents, all obtained from NOVEX. The nitrocellulose membrane was rinsed in deionised water and NuPAGE transfer buffer. The electrophoresed gel was removed from its case and placed on filter paper, the membrane was then placed on the top followed by another filter paper. This membrane/gel/filter paper unit was then sandwiched between several pre-soaked blotting pads and placed on top of the cathode plate in the blotting unit. The anode plate was then fixed and the blot unit placed into the blot module. The blot module was then filled with transfer buffer, and the outer chamber was filled to two thirds its depth with ice-cold deionised water. The proteins were then electrophoretically transferred at 30 V for 1 hour at room temperature.

2.2.8.3 Western immuno-blot development

All western blot procedures were performed as per manufacturers‟ instructions. Following blotting, the transfer membrane was removed from the blot module and washed for 5 minutes in 20ml of TBS/Tween washing buffer (Tris buffer saline /Tween 20; 2.4g Tris base, 8g NaCl, to pH 7.6 with HCl, with 0.1% (*v/v)* Tween 20).

The membrane was blocked with 5% skimmed milk–Tris-buffered saline containing 0.1% Tween 20 (TBST) for 1 hour at room temperature to prevent non-specific binding. It was then incubated overnight (~16 hours) at 4°C with anti-SERCA2 antibody (1:500 dilution). The following day, the membrane was washed 3 times by immersion in fresh aliquots of TBS/Tween washing buffer followed by incubation with the horseradish peroxidase (HRP)-labelled secondary donkey anti-goat IgG antibody (1:2000 dilution) for 2 hours. Immunogenic proteins were detected by luminol-enhanced chemiluminescence.

To detect immunogenic proteins, the membrane was incubated with Supersignal® West Dura Substrate (Pierce, Rockford Illinois), a Luminol-enhanced chemiluminescent reagent, for 5 minutes. Proteins were visualized and densitometrically quantitated using AC-1 Bioimaging and Vision WorksLS Software systems (UltraVioletProducts Ltd, Cambridge, UK)

2.2.9 Measurement of Ca^{2+}ATPase activity

Ca^{2+}-dependent ATP hydrolysis was measured using the coupled enzyme assay described by East (East, 1994). Microsomal samples (2-50µg protein) were incubated at 25°C in 2.5ml buffer (100 mM KCl, 40 mM Hepes; pH 7.2) containing ATP (2mM, phosph(enol)pyruvate (2.5 mM), NADH (0.25 mM), pyruvate kinase (7.5 U) and lactate dehydrogenase (8.0U). ATP synthesis following depletion during Ca^{2+}ATPase activity was coupled by pyruvate kinase and lactate dehydrogenase to oxidation of NADH. This was measured at A340 using a Lambda25 spectrophotometer and UV Winlab software (Perkin Elmer, UK). ATPase activity (µmol of ATP hydrolysed/mg of total protein/min; expressed as IU) was measured following a 30 min pre-incubation of microsomal samples with either DMSO (0.1%v/v), rosiglitazone (0-20µM), thapsigargin (100 nM) or cyclopiazonic acid (10µM). Background activity was measured for approx 2-3mins prior to the addition of calcium. Ca^{2+}ATPase activity was defined as the activation observed following addition of calcium.

2.2.9.1 Optimisation of Ca^{2+}ATPase activity assay

The above experiment was conducted in the presence of varying free Ca^{2+} concentrations (pCa^{2+} 3.10-7.07). Free Ca^{2+} concentrations were calculated using

„CACONC" software kindly provided by Professor A.G. Lee (Southampton University). The software calculates the free Ca^{2+} concentration after taking into account the presence of the various ligands and ions that bind to Ca^{2+} and thus reduce its availability in the reaction mixture (e.g. EGTA, ATP, H^{+}).

2.2.10 Isolation of human peripheral mononuclear cells.

The isolation of peripheral blood mononuclear cells was achieved by the following method. Peripheral mononuclear cells were used as they proved to be a more reliable model for measurement of intracellular calcium than cultured monocytes. Approximately 40 ml of EDTA-anti-coagulated blood was obtained from healthy volunteers (NB. Ethical approval was obtained from the UWIC Research and Ethics Committee (UREC) before commencement of this part of the study – see Appendix). 7 ml of heparinised blood was carefully layered over 7 ml of Ficoll-Hypaque (Hypaque-sodium diatrizoate (3, 5-bis (acetylamino)-2, 4, 6-triiodobenzoic acid sodium) with a specific gravity 1.077g/ml. The tubes were then centrifuged at 400 g for 30 min. The mononuclear cell suspension was carefully removed from the Ficoll-Hypaque interface, washed three times in PBS and resuspended in Roswell Park Memorial Institute (RPMI) 1640 for use in all the experiments. Cell numbers were determined using a Beckman Coulter meter Model Ac. T 5diff (Beckman Coulter UK Ltd, High Wycome, UK). In all cases, cell viability was > 95% as measured by trypan blue staining (see above).

2.2.11 Measurement of intracellular Ca^{2+} concentrations

$[Ca^{2+}]_i$ was measured in peripheral mononuclear cells, A7r5 cells and yeast spheroplasts by the method of Elsner *et al*. (Elsner *et al*., 1993), with some minor modifications. Briefly, the fluorescence of the Ca^{2+} indicator Fluo-3 was used as an indicator of $[Ca^{2+}]_i$ following preincubation with DMSO (0.1%), rosiglitazone (1 or 10μM) or thapsigargin (100nM) for 1 hour.

2.2.11.1 Measurement of intracellular Ca^{2+} concentrations in mononuclear cells

Cell suspensions (1.5×10^6 ml in RPMI 1640 medium) were incubated with either DMSO, rosiglitazone or thapsigargin as stated above for 1 hour. Cell suspensions were incubated with 3 μM Fluo-3 AM for 45 min at 37 °C. Cells were washed twice and resuspended in PBS prior to analysis via flow cytometry. Measurement of

intracellular Ca^{2+} in monocytic cells was conducted using a Cytomics FC500MPL flow cytometer (λ_{ex} = 488nm; λ_{em} = 530nm; Beckman Coulter, Buckinghamshire, UK). FACS gates were set on cells labeled with fluo-3. For acquisition of Fluo-3 labelled events, a dot-plot was created for fluorescence detector fl-1 (x-axis) vs fluorescence detector 2 fl-2 (y-axis). A total of 10,000 cells were analysed during each event.

2.2.11.2 Measurement of intracellular Ca^{2+} concentrations in A7r5 and yeast cells

In contrast to the flow cytometric methodology employed for mononuclear cell samples, intracellular Ca^{2+} concentrations were determined in A7r5 and yeast cell samples by use of a multi-well fluorimeter. Approx 5 x 10^3 cells were seeded into each well of a 96 well plate suitable for reading in multi-well fluorimeter. Cells were then incubated with DMSO, rosiglitazone, cyclopiazonic acid or thapsigargin as described above for 1 hour. Cells were incubated with 3 µM Fluo-3 AM for 45 min at 37 °C then washed twice with PBS. Wells were filled with 200µl PBS and plate was read on a Perkin Elmer fusion HT multi-well fluorimeter with a Fluorescein filter (FITC) (Perkin Elmer, UK) as described in 2.2.13. The emission filter was 520nm and excitation 490nm.

2.2.12 Determination/measurement of cell growth in MM6 and A7r5 cells

To monitor the effect of rosiglitazone on cell growth, MM6 and A7r5 cells were cultured under standard conditions (see 2.2.3) prior to treatment with DMSO (0.1% v/v), rosiglitazone (1 or 10µM) or thapsigargin. In MM6 cells, a cell count (using a haemocytometer) was performed following treatment with the above reagents for 14 consecutive days – this time period was selected because it is the minimum duration required for rosiglitazone to begin to exert its beneficial effects in human patients *in vivo* (Marx *et al*, 2003). However, due to their adherent nature, and therefore the need to trypsinise every 3 days, A7r5 cells were incubated for 72 hours only with a cell count performed on initial cell seeding and again after 72 hour incubation).

2.2.13 Determination/measurement of apoptosis inMM6 and A7r5 cells

To monitor the effect of rosiglitazone on apoptosis, MM6 and A7r5 cells were cultured under standard conditions (see 2.2.3) prior to treatment with DMSO (0.1%), rosiglitazone (1 or 10μM) or thapsigargin for 0-14 days (A7r5 24hrs only). Cellular apoptosis was analysed (as per manufacturers‟ instructions) using a Caspase-Glo 3/7 assay (Promega), which utilises luminescence to detect two markers of apoptosis in mammalian cells, namely caspase-3 and caspase-7, to determine the extent of apoptosis in each sample (Thornberry *et al*, 1997). 2 x 10^4 cells in a volume of 100μL (or 100μl tissue culture media alone as a blank), were pipetted into a white-walled multi-well plate (96-well plate), to this was added 100μl Caspase-Glo 3/7 reagent. Contents were gently mixed and left to incubate at room temperature for approximately 30 minutess. Subsequent luminescence was read in a Dynex luminometer.

2.2.14 Statistical analysis

All data were expressed as mean ± SEM unless otherwise stated. The students t-test was used to compare the differences between means of two samples, while one-way analysis of variance (ANOVA) was used to compare group data. Statistical analysis was performed using Minitab version 14 (Minitab Inc, PA, USA) software. Significance was reached when differences were seen to be $p<0.05$.

2.3 Results

2.3.1 Determination of SERC2b expression in monocytic and vascular smooth muscle microsome preparations

To confirm the presence of SERCA2b in the cells of interest to the study, western blotting experiments were conducted on subcellular fractions prepared from MM6 and A7r5 cells, using anti-SERCA2b antibodies. SERCA2b expression was confirmed by the presence of an immunogenic band at ~110kDa in the microsomal fractions of the cells only (Fig 2.2.1).

2.3.2 Determination of PMR1 expression in yeast microsome preparations

To confirm the presence of PMR1 in yeast cells, western blotting experiments were conducted on subcellular fractions prepared from yeast spheroplasts, using anti-PMR1 antibodies. PMR1 expression was confirmed by the presence of an immunogenic band at ~100kDa in the microsomal fractions of the cells only (Fig 2.2.2).

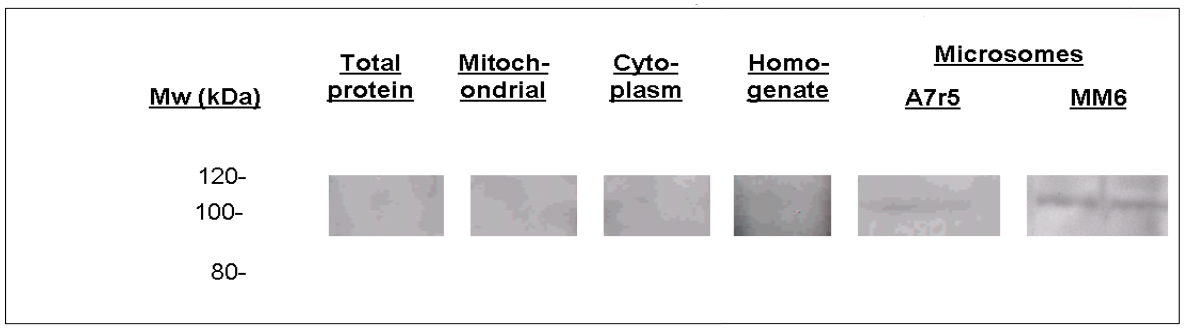

Fig 2.3.1: Western Blot detection of SERCA2b MM6 and A7r5 cells.
Western Blot experiments were carried out on MM6 subcellular fractions and also A7r5 microsomes. Microsome preparations were probed with anti-SERCA2b antibodies (1:1000) and HRP-linked donkey anti-goat 2^{o} antibodies (1:1000). The image shown is representative of 3 different experiments

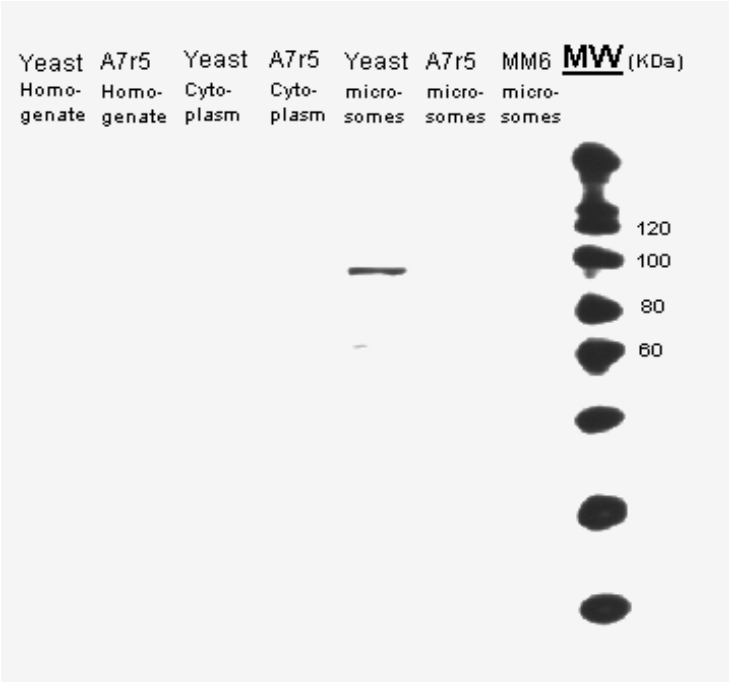

Fig 2.3.2: Western Blot detection of PMR1 in yeast cells.
Western Blot experiments were carried out on yeast sub cellular fractions and also MM6 and A7r5 microsomes. Microsome preparations were probed with anti-PMR1 antibodies (1:1000) and HRP-linked 2^{o} antibodies (1:1000). The image shown is representative of 3 different experiments

2.3.3 Investigation into the effects of rosiglitazone, and other 'classical SERCA inhibitors', on SERCA2b Ca^{2+}ATPase activity in MM6 and A7r5 microsomes

Microsomes from MM6 or A7r5 cells were incubated for 30 mins at 25°C with DMSO (0.1%v/v), rosiglitazone (1-20µM), thapsigargin (100nM) or cyclopiazonic acid (10µM) and their Ca^{2+}ATPase activity measured (and compared to untreated microsomes) by means of the coupled enzyme assay described in 2.2.9.

2.3.3.1 Optimisation: Effect of calcium concentration on Ca^{2+}ATPase activity

Coupled enzyme assays were conducted on microsomes in the presence of various free Ca^{2+} concentrations over the range pCa^{2+} 3.1 to 7.07 (calculated using „CACONC" software). As can be seen from fig 2.3.3, the optimum pCa^{2+} was established to be 4.82. In microsomes isolated from A7r5 and MM6 cells, optimum Ca^{2+}-dependent ATPase activities were identified (at ~pCa 4.82) of 0.143±0.038 and 0.054±0.013 IU respectively. Ca^{2+} dependencies for the A7r5 and MM6 preparations were almost identical to that of SR preparations from rabbit skeletal muscle (Eckstein-Ludwig, *et al*, 2003; Krishna *et al*, 2001). Thus, $[Ca^{2+}]_i$ required for maximal and half-maximal activation for Ca^{2+}ATPase activity in our experiments is in approximate agreement with previously published values for SERCA enzymes of ~40mM and ~0.3mM respectively (Eckstein-Ludwig, *et al* ,2003; Krishna *et al*, 2001). A free Ca^{2+} concentration of pCa 4.82 (which corresponds to ~15µM) was used in all subsequent experiments.

Therefore, given the detection of SERCA2b via Western blot in microsomal samples, together with the similarity of the Ca^{2+}-dependence in this case compared to previously published data, it seems likely that the enzyme responsible for the Ca^{2+}ATPase activity seen in the present study is SERCA2b, and it will henceforth be referred to as such.

2.3.3.2 The effects of thapsigargin and cyclopiazonic acid on SERCA2b Ca^{2+}ATPase activity in MM6 and A7r5 cells

As fig 2.3.5 shows, incubation with DMSO had no effect on SERCA2b activity (103.9±9.6% maximal activity, $p>0.05$, $n=3$). Conversely incubation with thapsigargin and CPA resulted in complete SERCA2b inhibition in both cell types. Ca^{2+}ATPase activities were reduced from 100±22.0% (MM6) and 100±26.6% (A7r5) to -8.1±9.9% basal (MM6) and 3.7±10.0% basal (A7r5) following incubation with 100nM thapsigargin, and to 3.4±5.2% basal (MM6) and 1.0±7.6% basal (A7r5) following incubation with 10µM CPA. The negative value seen here effectively corresponds to zero and is due to minor fluctuations in control samples. The inhibition of SERCA2b observed upon addition of CPA and thapsigargin observed here provides further evidence for the presence of the Ca^{2+}ATPase in the microsomal samples.

2.3.3.3 The effect of rosiglitazone on SERCA2b Ca^{2+}ATPase activity in MM6 and A7r5 cells

Incubation of MM6 and A7r5 cell derived microsomes with rosiglitazone led to a dose-dependent inhibition of SERCA2b Ca^{2+}ATPase activity as can be seen in fig 2.3.4. In MM6 microsomes, Ca^{2+}ATPase activity was reduced from 100±17.36% in the absence of rosiglitazone to -10.6±8.47% basal in the presence of 20µM rosiglitazone. In A7r5 microsomes, corresponding activities were reduced from 100% in the absence of rosiglitazone to -2±3.1% in the presence of 20µM rosiglitazone. IC_{50} values for rosiglitazone were 1.9µM for MM6 microsomes and 2.9µM for A7r5 microsomes (ANOVA $p=0.05$, $R^2 = 0.944$).

These values were determined using the quadratic equation:

$$Y=ax^2 – bx + c$$

For MM6, curve-fit software gave an equation of $y=0.00475x^2 – 0.12497 + 0.72523$
As at half-maximal inhibition, $y=0.5$, this equation could be re-arranged:

$$0=0.00475x^2 - 0.12497x + 0.22523$$

Using the formula $x = -b \pm \sqrt{(b^2 - 4ac)}/2a$, this equation could then be solved to give a value for x of:-

$$x = 0.12497 \pm \sqrt{((0.12497)^2 - 4 (0.00475 \times 0.22523))}/2 \times 0.00475$$

$$x = 0.12497 \pm 0.01134/0.00950$$

$$x = 1.9\mu M \text{ (or } 14.34\mu M)$$

For A7r5, curve-fit software gave an equation of $y=0.00589x^2 - 0.17501x + 0.95357$

As at half-maximal inhibition, y=0.5, this equation could be re-arranged:

$$0=0.00589x^2 - 0.17501x + 0.45357$$

Using the formula $x = -b \pm \sqrt{(b^2 - 4ac)}/2a$, this equation could then be solved to give a value for x of:-

$$x = 0.17501 \pm \sqrt{((0.17501)^2 - 4 (0.00589 \times 0.45357))}/2 \times 0.00589$$

$$x = 0.17501 \pm 0.14100/0.01178$$

$$x = 2.9\mu M \text{ (or } 26.83\mu M)$$

2.3.4 The effects of rosiglitazone and cyclopiazonic acid on PMR1 Ca^{2+}ATPase activity in yeast cells

As fig 2.3.6 shows, incubation with rosiglitazone appeared to have no inhibitory effect on PMR1 activity (46±23 nmol/mg/min following treatment with rosiglitazone compared with 18±13 nmol/mg/min basal). If anything an increase was observed but this was not found to be statistically significant. However, incubation with CPA induced complete inhibition of PMR1 with Ca^{2+}ATPase activity reduced from 100±75.8% control to ±-4.3±7.1% control).

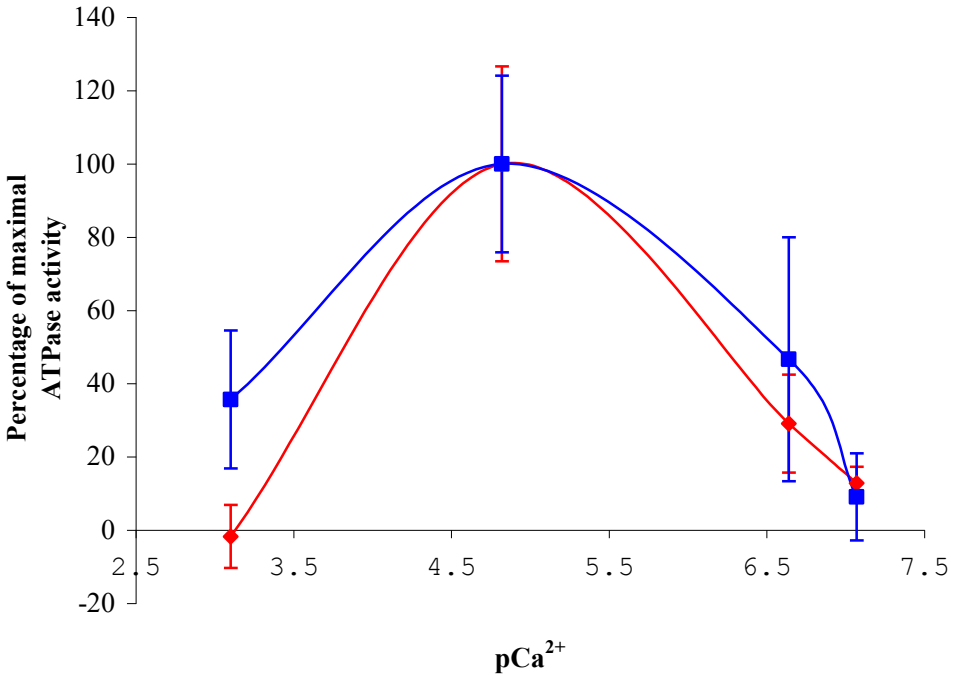

Fig 2.3.3: Calcium dependence of ATPase activity

Microsomes were prepared from MM6 and A7r5 cells and the effect of varying calcium concentrations on their resident Ca^{2+}ATPase pump activity determined. (MM6 microsomes – blue line, A7r5 microsomes - red line). Values are expressed as mean±SEM (n= 3 - 20).

(a)

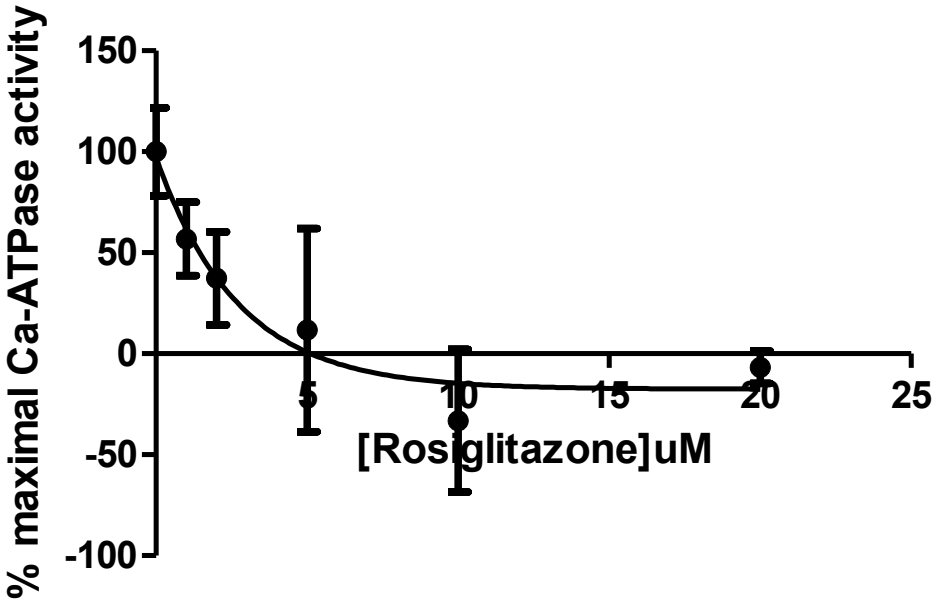

(b)

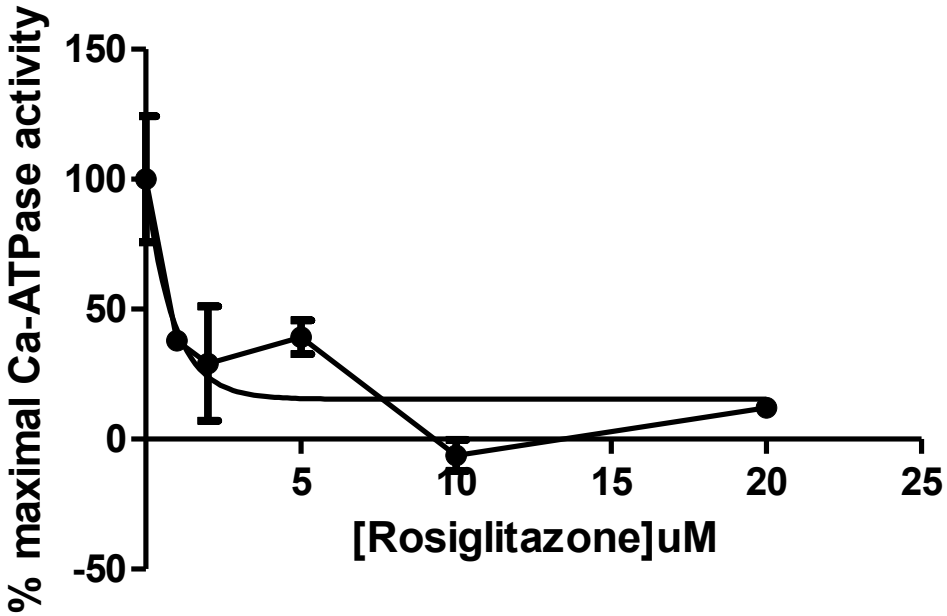

Fig 2.3.4: Effect of rosiglitazone on SERCA2b Ca^{2+}ATPase activity in (a) MM6 and (b) A7r5 microsomes. Microsomes prepared from a) MM6 and b) A7r5 cells were incubated with rosiglitazone (1-20μM) to determine the effect on their resident Ca^{2+}ATPase pump activity. Values are expressed as mean±SEM (n= 3-27).

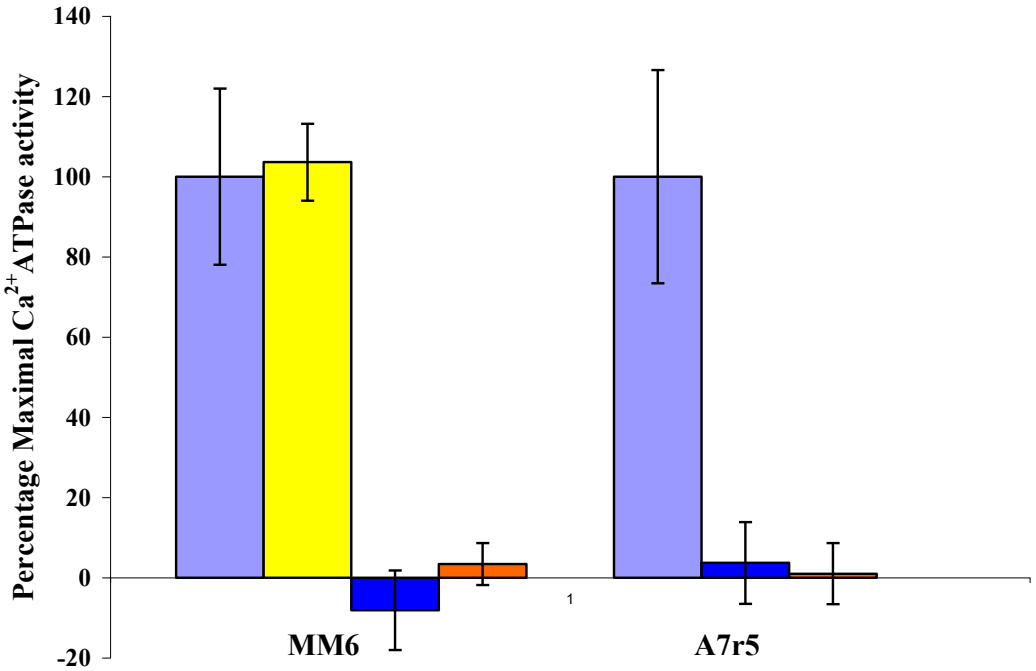

Fig 2.3.5: Effect of thapsigargin and cyclopiazonic acid on SERCA2b Ca^{2+}ATPase activity in MM6 and A7r5 microsomes

Microsomes prepared from a) MM6 and b) A7r5 cells were incubated with DMSO (0.1% v/v), thapsigargin (100nM) or CPA (10µM) and Ca^{2+}ATPase pump activity measured. (Purple bar = control, yellow bar = DMSO (0.1% v/v), Blue bar = thapsigargin (100nM), orange bar = CPA). Values are expressed as mean±SEM (n= 3-27).

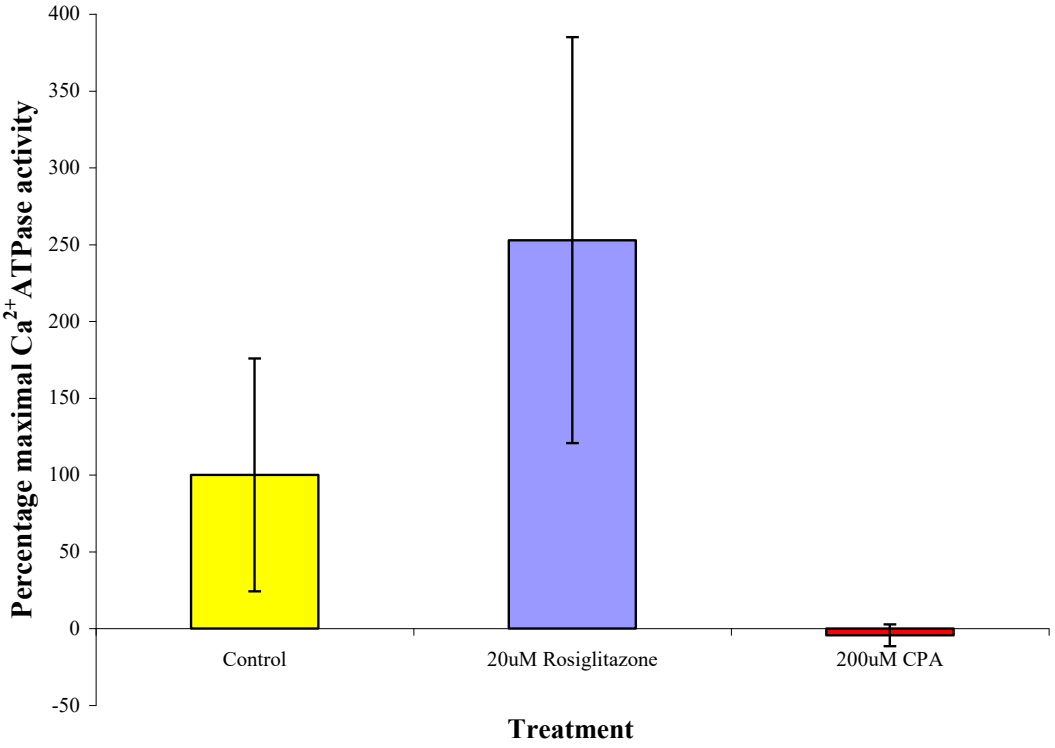

Fig 2.3.6: Effect of rosiglitazone on PMR1 Ca^{2+}ATPase activity in yeast cell derived microsomes

Microsomes prepared from yeast cells were incubated with rosiglitazone (20µM) or CPA (200µM) and the Ca^{2+}ATPase pump activity was measured. Values are expressed as mean±SEM (n= 3).

2.3.5 The effect of rosiglitazone on intracellular calcium concentrations in yeast spheroblasts

To investigate intracellular Ca^{2+} concentrations in yeast, spheroplasts were treated with DMSO (0.1% v/v/ - control), rosiglitazone (10µM) or CPA (10µM) for 45 min prior to 45 min incubation with the Ca^{2+}-fluorescent dye fluo-3. As fig 2.3.7 shows, treatment with rosiglitazone had no effect on Ca^{2+}dependent fluo-3 fluorescence in yeast spheroplasts (92.3±2.8% compared with a basal of 100±3.6%, n=2, p= >0.05). In contrast, incubation with CPA elicited a decrease in Ca^{2+}dependent fluo-3 fluorescence in yeast spheroplasts (from 100±3.6% basal to 73.9±4.8%, n= 2, p= <0.05).

2.3.6 Effect of rosiglitazone on intracellular Ca^{2+} concentrations in mononuclear cells

Isolated mononuclear cells were treated with DMSO (0.1%) or rosiglitazone (1 or 10µM) for 0-72 hours and incubated with the Ca^{2+}-fluorescent dye fluo-3 for 45 min. Data were normalised to basal due to inter-batch variability for ease of interpretation. As Fig. 2.3.8 shows, pre-incubation with 10µM rosiglitazone brought about a rapid but small increase in $[Ca^{2+}]_{cyto}$ within 1 hour (121.2 ± 2.9% basal; n=8; $p<0.05$). 24 hour incubation continued to show statistically significant elevation in $[Ca^{2+}]_{cyto}$ (140.5 ± 9.5% basal; n=3; $p<0.05$), which returned to basal after 72 hr treatment (92.3 ± 7.8% basal; n=6; $p>0.05$). Incubation with 1µM rosiglitazone elicited no increase in $[Ca^{2+}]_{cyto}$ following any treatment duration (n=15).

2.3.7 Effect of rosiglitazone on intracellular Ca^{2+} concentrations in vascular smooth muscle cells

A7r5 cells were treated with DMSO (0.1%), rosiglitazone (1 or 10µM) or thapsigargin (100nM) for 0-72 hours and incubated with the Ca^{2+}-fluorescent dye fluo-3 for 45 min, before reading of fluorescence using a multi-well fluorimeter. All data were normalised to basal due to inter-batch variability for ease of interpretation.

As fig 2.3.9 shows, treatment with all reagents except DMSO produced an initial statistically significant increase in intracellular calcium concentration after 1hr

(1μM: 116±9.3% basal; 10μM: 117±8.8% basal; thapsigargin: 137±8.28% basal, $n \geq 6$; $p<0.05$ v. DMSO in all cases) which dropped rapidly (within 4-24hrs) to levels apparently lower than basal (although not statistically significant from basal in the cases of 1μM and 10μM rosiglitazone) (1μM 92±13.1% basal; 10μM 92±5.5% basal; thapsigargin 105±9.5% basal, $n \geq 6$; $p<0.05$ v. DMSO for thapsigargin-treated samples, but not for rosiglitazone-treated samples). Finally, intracellular Ca^{2+} concentrations returned to approximately basal levels following 72 hour treatment in the case of the rosiglitazone-treated samples (1μM 100±8.9% basal; 10μM 99±3.9% basal;, $n \geq 6$; $p>0.05$ v. DMSO in all cases). In contrast, intracellular Ca^{2+} levels in thapsigargin-treated cells were elevated slightly with borderline statistical significance above basal levels (108±8.7% basal; $n \geq 6$; $p=0.14$) – as will be discussed in the subsequent sections 2.3.8. and 2.3.9, the inability of these cells to maintain $[Ca^{2+}]_I$ at low levels may be a reflection of cytotoxic effects of thapsigargin treatment for 72h.

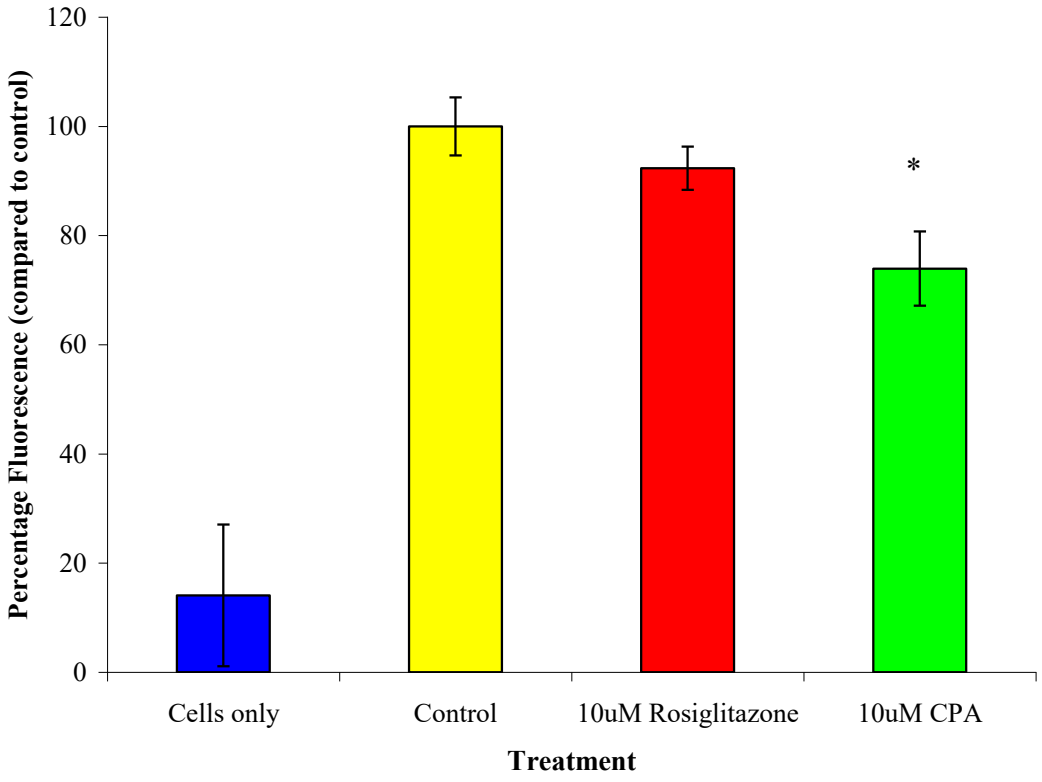

Fig 2.3.7: The effect of rosiglitazone on intracellular calcium concentration in yeast spheroplasts

Yeast spheroplasts were incubated for 45 min with either 10µM rosiglitazone (red bar) or 10µM CPA (green bar) prior to 45 min incubation with the Ca^{2+} fluorescent dye, Fluo-3. Cell only (spheroplasts; blue bar) were not incubated with fluo-3. Values are expressed as the mean± SEM (n= 2).

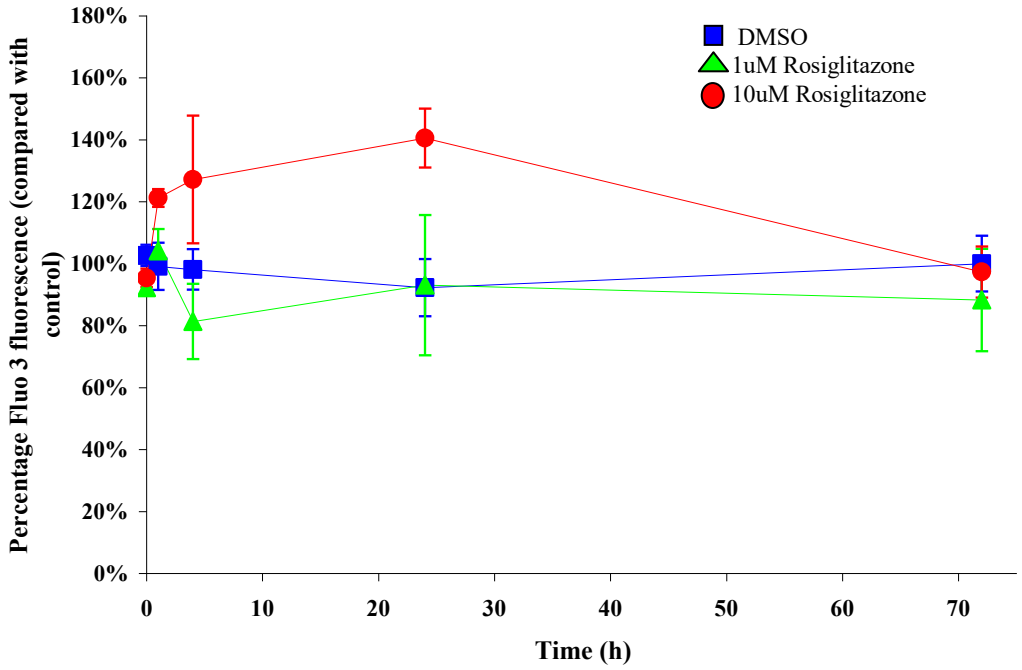

Fig 2.3.8: The effect of rosiglitazone in intracellular calcium concentration in mononuclear cells

Isolated mononuclear cells were incubated for 0-72hrs with either 0.1% DMSO (blue squares), 1µM rosiglitazone (green triangles) or 10µM rosiglitazone (red circles) prior to incubation with the Ca^{2+} fluorescent dye, Fluo-3. Values are expressed as percentage fluorescence compared to control (mean± SEM; n= 3 – 5).

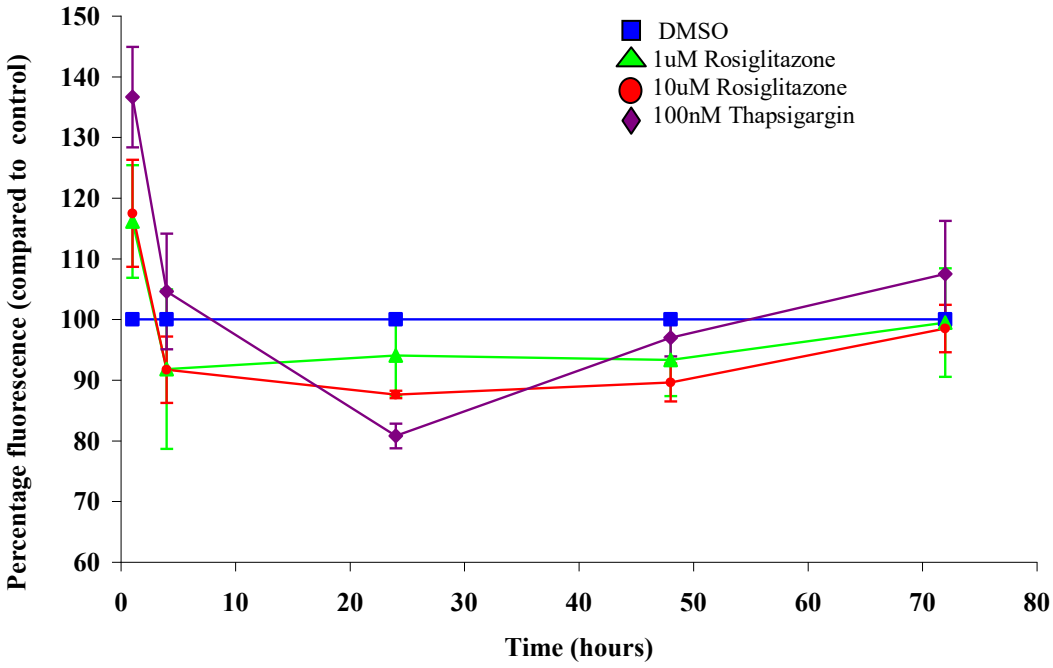

Fig 2.3.9: The effect of rosiglitazone in intracellular calcium concentration in A7r5 cells

A7r5 cells were incubated for 0-72hrs with either 0.1% DMSO (blue squares), 1µM rosiglitazone (green triangles), 10µM rosiglitazone (red circles) or 100nM thapsigargin (purple diamonds) prior to incubation with the Ca^{2+} fluorescent dye, Fluo-3. Values are expressed as the percentage fluorescence compared to DMSO (mean±SEM; n= 2-4).

2.3.8 Investigattion of the effect of rosiglitazone and thapsigargin on cell growth

MM6 and A7r5 cells were treated with DMSO (0.1%), rosiglitazone (1 or 10μM) or thapsigargin (100nM) for up to 14 days. Cell counts were conducted every 24 hours for 14 days for MM6 cells (after 72 hours only for A7r5 cells). As can be seen from fig 2.3.10, DMSO and rosiglitazone appeared to have no effect on cell growth in either cell line during the study"s duration. Thapsigargin, on the other hand, seemed to have a marked detrimental effect on cell growth with complete death of the entire population within 8 days in MM6 cells, and a 61% decrease in the number of viable cells compared with control following 72 hour treatment in A7r5 cells (39.0±2.9% compared with basal, $n = 3$, $p<0.05$).

2.3.9 Investigation of the effect of rosiglitazone and thapsigargin on apoptosis

MM6 and A7r5 cells were treated with DMSO (0.1%), rosiglitazone (1 or 10μM) or thapsigargin (100nm) for up to 14 days (24 hours only for A7r5 cells). Following incubation, cells were subjected to a Caspase-glo 3/7 apoptosis assay which measures apoptosis markers via luminescence. As can be seen from fig 2.3.11 treatment of monocytic cells with 1μM rosiglitazone initiates a very small non-significant increase in apoptosis (1667±123 RLU cf. 1109±445 RLU, or ~1.5-fold; $n=3$; $p>0.05$) while 10μM causes a slightly larger, significant increase (3382±992 RLU cf. 1109±445 RLU, or ~3-fold; $p<0.05$). In both cases, apoptotic levels reached a plateau of apoptosis after treatment for 24 hours, 72 hours or 14 days, which suggests that in a rosiglitazone-treated cell population, the population can tolerate these slightly elevated levels of cell death, and that rosiglitazone does not induce widespread cell death of the entire cell population. In support of this interpretation, these slight increases in apoptosis do not cause significant changes in overall cell viability, as the cell count data in Fig 2.3.10 attests.

In contrast, treatment with thapsigargin shows a very large increase in apoptosis at 24 hours (513±81.9% basal, $n = 3$, $p<0.05$). Although this appears to revert to basal after 72hours (79.2±13.3% basal, $n = 3$, $p>0.05$), it is likely that this decrease in signal is due to the fact that incubation with thapsigargin for this time scale has already caused large-scale cell death within the cell population (see fig 2.3.10a), and that therefore the thapsigargin-treated sample contains less than half as many cells than its control counterpart. As the apoptotic signal remains at approximately control

levels despite this smaller number of viable cells in the sample, it may be concluded that any surviving cells are in the process of initiating or undergoing apoptosis. Thus, this discrepancy in cell number, rather than any recovery within the thapsigargin-treated sample, is likely to be responsible for the apparent decrease in absolute magnitude of the apoptotic signal detected.

Treatment with either concentration of rosiglitazone for the shorter duration of 24 hours did not appear to induce apoptosis in A7r5 cells (1μM rosiglitazone 84.9±1.3% basal, 10μM rosiglitazone 87.8±0.5% basal, $n = 3$, $p<0.05$). This is supported by the A7r5 cell count being unaffected by 24 hour incubation with these reagents (see fig 2.3.10b), whereas comparable incubation with thapsigargin causes a 2-fold increase in apoptosis (204.0±3.5% basal, $n = 3$, $p<0.05$), providing an explanation for the decreased cell counts seen in this cell line following incubation with the reagent (fig 2.3.10b).

(a)

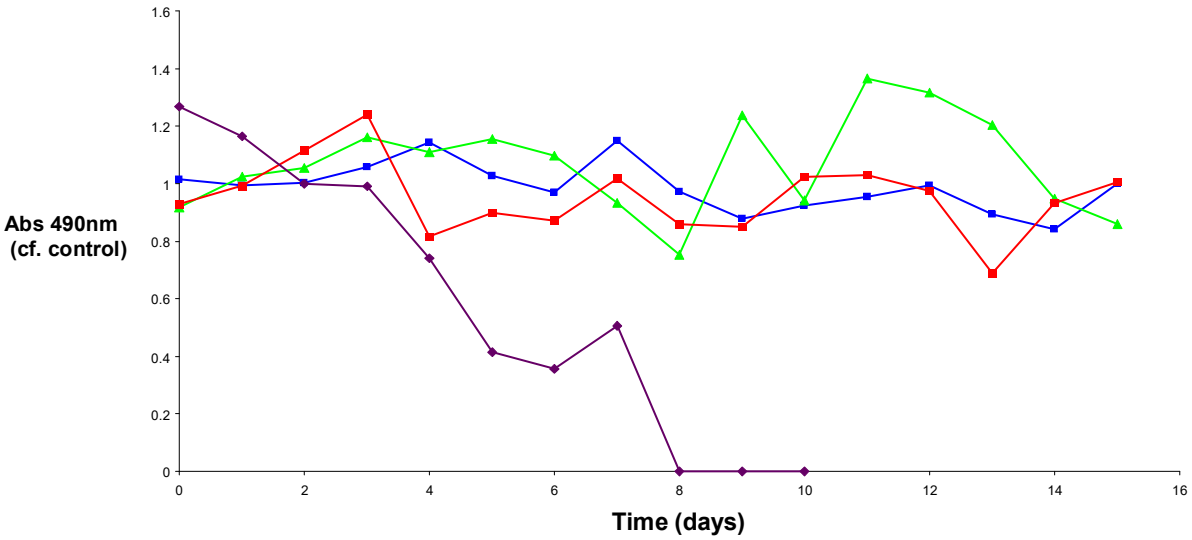

(b)

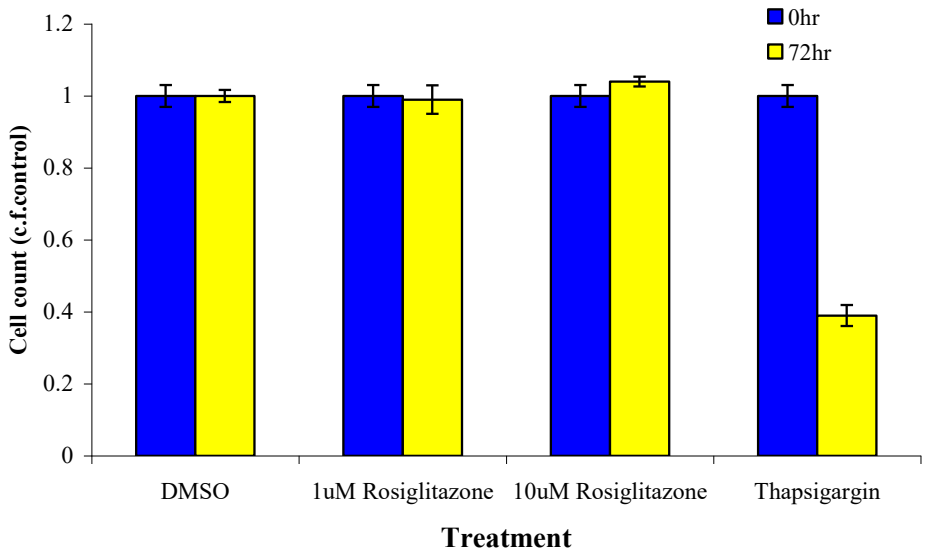

Fig 2.3.10: Effect of rosiglitazone on cell growth
(a) monocytes (b) vascular smooth muscle
MM6 or A7r5 cells were incubated for 0-72hrs with either DMSO (0.1% v/v – blue squares), rosiglitazone (1µM – green triangle or 10µM – red squares) or thapsigargin (100nM – purple diamonds). Cell counts were performed every 24 hours for 14 days for MM6 cells and at 0 and 72 hrs for A7r5 cells. Values are expressed as cell count compared with control (mean±SEM n= 3).

(a)

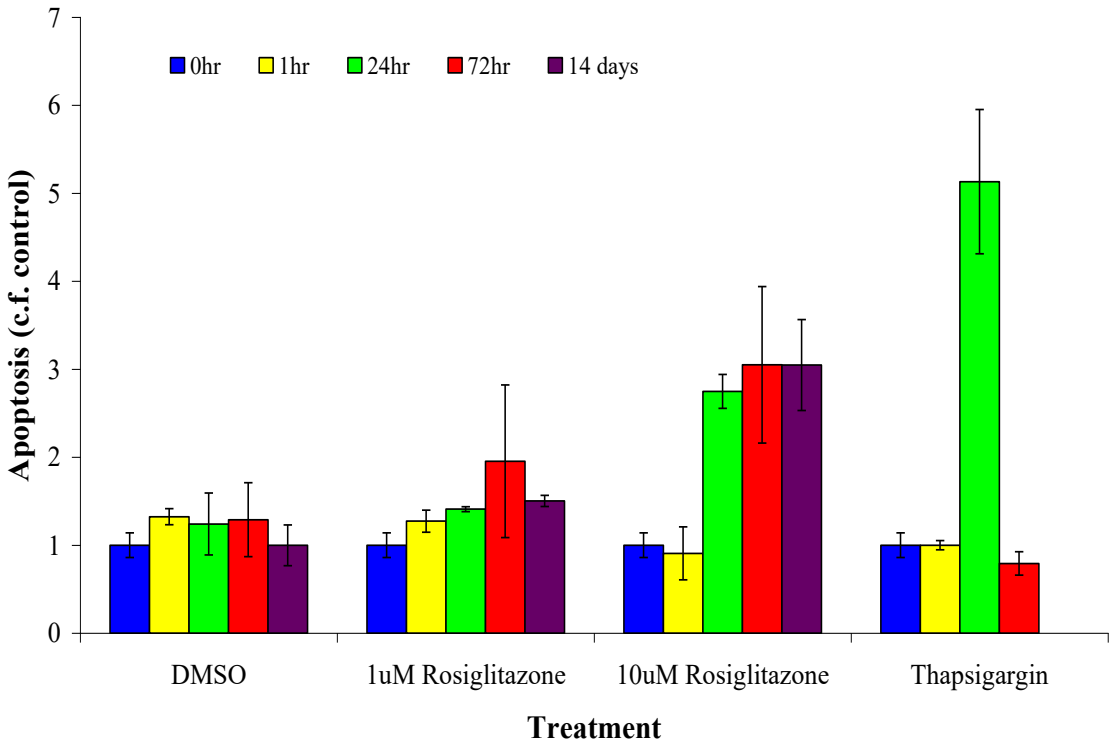

(b)

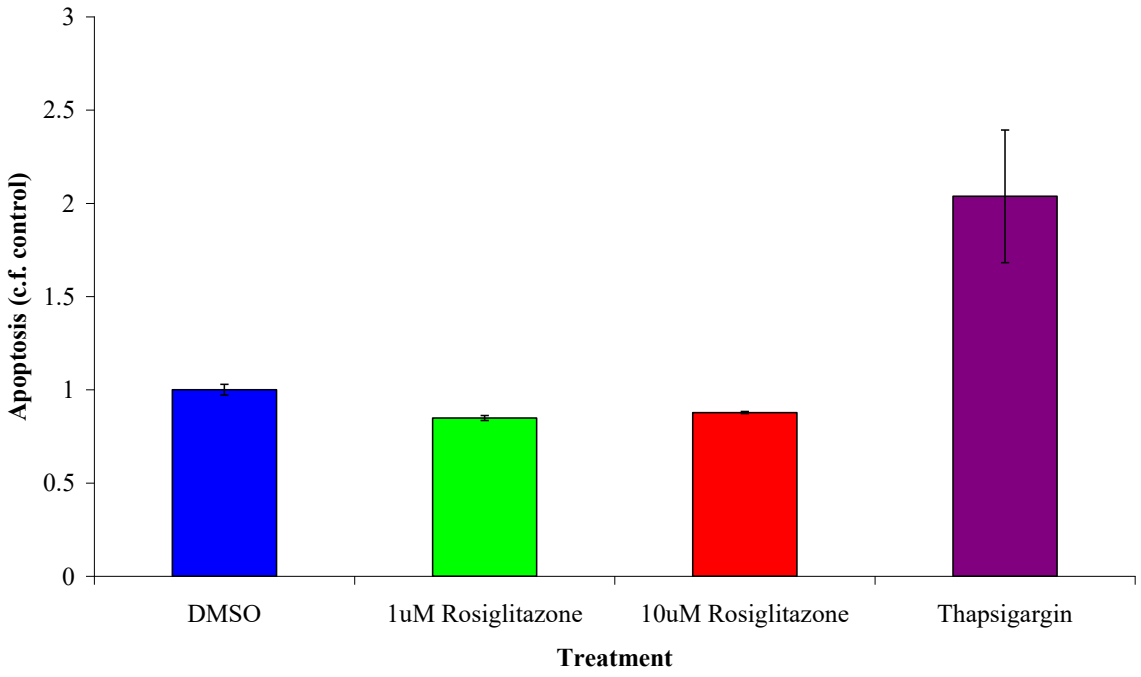

Fig 2.3.11: Effect of rosiglitazone on apoptosis
(a) monocytes (b) vascular smooth muscle
MM6 or A7r5 cells were incubated for 0-14 days (MM6) or 0-24 hrs (A7r5) with either DMSO (0.1% v/v), rosiglitazone (1 or 10μM) or thapsigargin (100nM). A luminescence based apoptosis assay was performed at 0, 1, 24, 72 hours and 14 days for MM6cells and at 0 and 24 hours for A7r5 cells. Values are expressed as the mean±SEM (n= 3).

2.4 Discussion

Intracellular Ca^{2+} signalling is essential to cell survival and as such $[Ca^{2+}]_i$ is tightly and meticulously regulated by all eukaryotic cells. Disturbances in Ca^{2+} signalling resulting in increased intracellular Ca^{2+} are features of many pathological conditions, but can also be induced by numerous pharmacological agents. This chapter investigated the effect of various agents including the anti-diabetic TZD rosiglitazone on *in-vitro* calcium signalling in three distinct cell types. Data is presented here detailing the acute effects of these agonists on the resident ER Ca^{2+}ATPase pump, and also their effects on intracellular $[Ca^{2+}]$ and on cell survival over an extended time period (14 days).

Ca^{2+} entering the cytoplasm from the cell exterior or via intracellular organelle stores for cell signalling events must be removed back into stores or pumped out of the cell for cell viability. The former reaction is brought about, dependent upon cell type, by the Ca^{2+}ATPases SERCA2b (in mammalian cells) and PMR1 (in yeast). SERCA2b is ubiquitously expressed in nearly all mammalian cell types (Strehler & Treiman, 2004) while PMR1 is expressed in yeast cell ER/Golgi (Rudolph *et al*, 1989). Sub-cellular fractionation of cultured monocytic MM6 cells and VSMCs, and subsequent immuno-blotting, established the presence of SERCA2b in microsomal fractions only. This showed that the microsomes contained ER derived calcium ATPases and that the predominant ATPase in this fraction was the „housekeeping pump" SERCA2b. Comparative immuno-blotting of yeast cell derived microsomes again showed the microsomal fraction to contain Ca^{2+}ATPases however in this case, the predominant Ca^{2+}ATPase was seen to be PMR1.

Studies previously conducted in our laboratory showed that the subcellular fractionation conditions employed in this study, do produce microsomes enriched with ER, as demonstrated by detection of the ER marker proteins Calnexin (MM6) and Kar2 (yeast) in microsomal fractions only, and the loss of the cytoplasmic marker protein Actin from microsomal fractions (Ulug, 2004 MSc dissertation). Calnexin is an integral ER membrane protein in monocytes, while Kar2 is the equivalent in yeast cells. Actin is ubiquitously expressed in all eukaryotic cells and is found only in the cytoplasm. Immunoblotting identified a pattern of increasing

concentration of Kar2 in yeast cells and Calnexin in MM6 cells following each step of the subcellular fractionation process, with the greatest concentration being found in the microsomal fraction of each cell type (Ulug, 2004 MSc dissertation). Conversely, each step of the fractionation process saw decreasing levels of the cytoplasm associated protein actin, suggesting that the purified microsomal fraction is devoid of cytoplasmic proteins.

Previous studies in our laboratory established a relationship between incubation of monocytic cells with rosiglitazone and increases in $[Ca^{2+}]_i$ (Singh *et al*, 2005). The timescale involved in the response led to the assumption that the drug may interact with SERCA2b, inhibiting the replenishment of ER Ca^{2+} stores by the „housekeeping" Ca^{2+} pump SERCA2b following non-specific leakage of Ca^{2+} into the cytoplasm. The present study has shown that incubation with rosiglitazone for 30 minutes induced a decrease in Ca^{2+}ATPase activity in both monocytic and smooth muscle cells and established that this was due to a dose-dependent inhibition of SERCA2b. Partial inhibition was achieved in the concentration range of 1 -5µM while >10µM lead to complete SERCA2b pump inhibition. IC_{50} values for rosiglitazone"s inhibition of SERCA2b were 1.9 and 2.9µM for MM6 and A7r5 microsomes respectively. Interestingly, these values are very similar to each other, and also to those previously determined for rosiglitazone"s Ca^{2+}-dependent actin cytoskeletal remodelling actions, (IC50 = 3.72 µM) (Singh *et al*, 2005).

Numerous studies have utilised thapsigargin and CPA in the investigation of their Ca^{2+}ATPase inhibitory actions. The classical SERCA inhibitors have been employed in numerous cell types inducing - amongst others - neurones (Wang *et al* 2002), vascular smooth muscle cells (Missaen *et al* 2001; Wu *et al* 2001) and leukocytes such as monocytes (Launay *et al*, 2003). This study has shown that incubation of MM6 and A7r5 microsomes with the reagents thapsigargin and CPA resulted in complete inhibition of SERCA2b, while vehicle (DMSO) alone produced no change in SERCA2b activity. Importantly, the decline of Ca^{2+}ATPase activity in MM6 and A7r5 microsomes following pre-incubation with the known SERCA inhibitors thapsigargin (Thastrup *et al*, 1989) and CPA (Missiaen *et al*, 2002) is similar to that observed in sarcopasmic reticulum preparations from rabbit skeletal muscle (data not shown), which would be expected to express the SERCA isoform SERCA1a. This data provides further evidence, alongside immuno-blotting, that human cultured

monocytic MM6 cells and cultured mammalian VSMCs not only express SERCA2b, but express an enzyme which pumps Ca^{2+} with a similar Ca^{2+}-dependence to that previously reported for SERCA enzymes (Eckstein-Ludwig et al, 2003; Krishna et al, 2001), and is similarly sensitive to inhibition by agents known to act on SERCA2b (Thastrup *et al,* 1989; Missiaen *et al*, 2002).

Thus, in summary, it can be concluded that the A7r5 and MM6 experiments described in this chapter show that SERCA2b is expressed and is active in these cell lines, and that therefore in this instance, rosiglitazone may potentially contribute to a disruption in intracellular Ca^{2+} homeostasis by inhibition of SERCA2b‟s Ca^{2+}ATPase activity within the ER of these cells.

Incubation of yeast microsomes with rosiglitazone did not lead to a decrease in Ca^{2+}ATPase activity from basal values; neither did incubation with the SERCA inhibitor thapsigargin (data not shown). A significant decrease in Ca^{2+}ATPase activity was seen, however, on incubation with CPA, a known PMR1 inhibitor (Sorin *et al*, 1997). This data alongside the immunoblotting experiment provides evidence that the predominant Ca^{2+} pump in yeast is PMR1, and that this pump is active, and is insensitive to some reagents that inhibit SERCA enzymes (eg. thapsigargin), but sensitive to others (eg. CPA).

No significant effect on yeast cell calcium homeostasis was observed following incubation with rosiglitazone (10µM); however incubation with CPA (10µM) for 90 minutes caused a reduction in Ca^{2+}-dependent fluo-3 fluorescence compared with control in wild type yeast cells. Interestingly, parallel studies in our laboratory have shown that CPA had no effect on Ca^{2+}-dependent fluo-3 fluorescence in a yeast strain devoid of PMR1, indicating that the disruption seen in Ca^{2+} homeostasis in wild-type cells is due to CPA‟s interaction with/inhibition of PMR1 (Akhondi, 2008, BSc dissertation).

In combination, the above data has shown that while rosiglitazone inhibits SERCA2b in monocytic and vascular smooth muscle cells resulting in altered calcium homeostasis, no inhibitory effect on PMR1 or change in calcium homeostasis were observed in rosiglitazone-treated yeast cells. This provides evidence to support the idea that rosiglitazone‟s mode of action is direct and specific inhibition of SERCA2b.

Following on from this, it may be concluded that either the delivery pathways by which rosiglitazone arrives at the mammalian ER are not present in yeast cells, or that rosiglitazone is correctly trafficked to the ER, but on arrival the specific nature of its interaction solely with SERCA2b (rather than more generalised disruption of all ER resident proteins) means that PMR1 is not affected, and therefore yeast cell Ca^{2+} homeostasis is not disrupted.

The investigation of rosiglitazone's effects on $[Ca^{2+}]_i$ in monocytes and VSMCs in this study produced some intriguing results. In monocytes, 10μM rosiglitazone induced a small but rapid increase in $[Ca^{2+}]_i$ which peaked at 24 hours before returning to basal values after 72 hours. 1μM rosiglitazone appeared to have no discernible effect on $[Ca^{2+}]_i$ in this cell type. In VSMCs, both concentrations of the drug led to an initial rapid rise in $[Ca^{2+}]$ which subsequently dropped and remained below basal until eventually being restored to basal values following incubation for 72 hours. This data supports the Singh *et al*'s observations of rapid rosiglitazone-induced $[Ca^{2+}]_i$ increases (Singh *et al*, 2005) but also builds on this by showing that upon extended incubation (72hrs – 14 days) with the agonist, the monocyte and VSMC appear to have the ability to restore calcium homeostasis. However, it is apparent that the two cell lines have slightly different mechanisms in restoring the normal „status quo", which could well be due to their differing cell type, function and their toleration to $[Ca^{2+}]_i$. Briefly, it appears that the monocyte being a non-contractile cell has the ability to tolerate small increases in cytoplasmic calcium without causing cellular damage, while the VSMC, as a contractile cell is unable to tolerate even minor increases in Ca^{2+} without compromising cellular activity and survival, and so must expel any Ca^{2+} that leaks into the cytoplasm due to rosiglitazone-mediated inhibition of SERCA2b. This will be discussed in more detail in chapter 5.

The data obtained - both in the current study and more generally - on the apoptotic effect of rosiglitazone treatment is varied. It has been shown in this study that in both mammalian cell types, incubation with either concentration of rosiglitazone does not alter cell growth (as assessed by cell counting over periods of up to 14 days). This contrasts starkly with thapsigargin which has been shown to have dramatic consequences on cell growth by rapidly inducing apoptosis to such an extent that cell numbers within the cell population decrease to effectively zero within

less than one week (Fig 2.3.10). In monocytes, 1μM rosiglitazone was shown to induce very minor non-significant levels of apoptosis (1.5-fold increase at 14 days) while 10μM induces a slightly larger degree of apoptosis (3-fold increase at 14 days) which is statistically significant but not large enough to induce any significant change in growth of the cell population as a whole. Any population of cells will contain a small proportion of cells undergoing apoptosis (usually approximately 5% under healthy conditions) and, while treatment of monocytes with 10μM Rosiglitazone did induce a marginal (~3-fold) increase in apoptosis above this basal level, haemocytometer cell counting indicated that 2 weeks rosiglitazone treatment was not sufficient to diminish the growth of the cell population as a whole (NB. MTS assay data showed that cell viability was also unaffected (data not shown)). Finally, in vascular smooth muscle cells, no rosiglitazone-induced increases in apoptosis were observed (albeit over a shorter duration of experiment).

However, the discovery that rosiglitazone may have potential benefits in cancer therapy due to its ability to prevent cell proliferation and induce apoptosis would seem to contradict the data presented here. Indeed numerous studies have provided evidence for a link between rosiglitazone treatment and increased apoptosis (Lin *et al*, 2007; Kim *et al*, 2007; He *et al*, 2008 and Kim *et al*, 2008), while it appears to be disputed whether these effects are PPARγ-dependent or independent. Conversely, there is a wealth of data promoting rosiglitazone as potentially cytoprotective/anti-apoptotic. While some of the in-vitro studies discussed here are in line with drug concentrations and timescale used in the present study, it is important to note that this is not the case in many cancer studies where the rosiglitazone concentrations used are much higher and treatment durations are longer. Also, the literature covers a wide variety of cell and tissue types and it is therefore of the upmost importance to remember that different cell types may respond differently to various drug regimes or stimuli. Indeed while it is the case that in cancer therapy, it is important that a drug kills the cell, in other conditions such as in diabetes, it is beneficial for drug therapy to reduce inflammation and cell death and therefore tissues respond differentially in many therapeutic settings.

In summary, it appears that - at least in the monocyte and the smooth muscle cell - rosiglitazone therapy for up to 14 days (72hrs for VSMC) does not have serious adverse effects on cell growth, viability or survival, whereas thapsigargin treatment

reduces cell growth and induces apoptosis. This is an important observation in the light of research suggesting that rosiglitazone takes 2 weeks to exert non-genomic effects in vivo in human subjects (Marx *et al*, 2003).

The current concerns regarding the overall cardiovascular safety of rosiglitazone was discussed in detail in Chapter 1. While it is important to note that the data presented in this chapter was conducted purely in stand-alone *in vitro* cellular models, and so is only of limited applicability to the *in vivo*/clinical situation, the data shows that rosiglitazone does influence $[Ca^{2+}]_i$ in the monocytic and smooth muscle cell, but that it appears to elicit a restoration of $[Ca^{2+}]^i$ with little or no concurrent apoptotic/cell viability effect issues.

Finally, however, given the cardiac nature of the recently aired concerns over rosiglitazone and patient safety (Nissen *et al*, 2007), and as regulation of $[Ca^{2+}]_i$ in cardiomyocytes is of the utmost importance for cardiac function, it is possible that rosiglitazone may potentially adversely affect Ca^{2+} homeostatic regulation specifically within cardiac cells. This may provide an explanation for why the observed cardiovascular complications do not seem to be apparent in other cell types, and therefore in other parts of the body. This issue will be discussed in more detail in future chapters.

2.4.1 Summary

This chapter has established the presence of the ER resident Ca^{2+}ATPase pump SERCA2b in both MM6 monocytic and A7r5 smooth muscle cells and of the Golgi-bound Ca^{2+}ATPase PMR1 in yeast cells. Rosiglitazone was shown to have a dose-dependent inhibition on the Ca^{2+} sequestration activity of SERCA2b in both MM6 and A7r5 cells but to have no effect on PMR1 in yeast cells, thus suggesting its inhibitory effects are specific to SERCA2b. Rosiglitazone was also shown to have an effect on $[Ca^{2+}]_i$ initiating a rapid increase within 1hr followed by a return to basal values within 72hrs in MM6 cells. In A7r5 cells, the same rapid increase was observed but this dropped below basal with in 4 hours only to return to basal within 72 hrs. The data suggests that rosiglitazone causes an initial increase in $[Ca^{2+}]_i$ due to inhibition of SERCA2b but that extended incubation with rosiglitazone induces the restoration of Ca^{2+} homeostasis in both cell types. As earlier data had suggested (Singh et al, 2005),

rosiglitazone's mode of action seems to be SERCA2b-specific, and this was supported in the current study by the demonstration that no changes in $[Ca^{2+}]_i$ were observed in comparable experiments in yeast cells. Finally, rosiglitazone was shown to induce only a small increase in apoptosis (between 1.5 and 3-fold compared with basal) in MM6 cells and had no pro-apoptotic effect on A7r5 cells. This, in addition to cell count data showing that rosiglitazone has no overall effect on cell growth in either cell line, suggests that at the concentrations used in this study, rosiglitazone does not affect cell viability in monocytic or vascular smooth muscle cells.

Chapter 3

Elucidation of the mechanism for restoration of calcium homeostasis in rosiglitazone-treated monocytic and vascular smooth muscle cells

3.1 Introduction

As previously discussed, there is a wealth of information regarding the roles that Ca^{2+} plays in the cell types of relevance to this study, and the subsequent impact that disruption of cellular handling of this important cation can have on human health and disease. Since Ca^{2+} is involved in such a plethora of cellular responses, regulation of intracellular calcium homeostasis is essential to normal cell functioning, and any disruptions in this regulation may have dire consequences to the cell.

As the endoplasmic reticulum is central to the regulation of cellular Ca^{2+}, disturbances in ER function or so-called „ER stress" has been the focal point for much recent research. Thus, there has been a great deal of research conducted in recent years concerning the involvement of ER stress in the development and incidence of numerous diseases. For example, ER stress is evident in Diabetes, Alzheimer"s disease and Parkinson"s disease, as well as many other debilitating disorders. Much of the research conducted on the effects of ER stress in literature of importance to this study centres around its effects on the pancreatic β cell (Song *et al*, 2008; Weber *et al*, 2003; *Weber et al*, 2004; Chambers *et al*, 2006). However, ER stress has also been implicated in many other cell types and with many diabetic complications, for example diabetic retinopathy (Oshitari *et al*, 2008).

3.1.1 ER Stress and the cellular 'fight or flight response' – the Unfolded Protein Response (UPR)

As previously discussed (see chapter 1), the role of the endoplasmic reticulum (ER) in the rapid release and subsequent sequestration and storage of intracellular calcium is essential to cell survival, because it mediates many essential calcium-dependent cell processes such as growth, proliferation and signalling events. However, the ER is also responsible for many other important aspects of cellular physiology. For instance, another essential role of the ER is the processing, folding and subsequent export of proteins that have been synthesised by ER-bound ribosomes (Lodish, 2004). Precise protein folding is facilitated via the production of di-sulphide bonds and binding of calcium-dependent chaperone proteins such as glucose-regulated 78kDa protein (eg. Grp 78; also known as binding protein (BiP), which belongs to a family of proteins known as the heat shock 70 proteins (Zhang *et al*, 2004)) in the

highly oxidative environment that is maintained within the lumen of the ER (Xu *et al*, 2005). Thus, chaperone proteins such as Grp 78 are vital in ensuring that such incorrectly folded proteins accumulating in the ER do leave the ER by binding permanently to them (Zhang *et al*, 2004).

When ER function is disturbed, via any of a number of mechanisms including alterations in glucose or calcium regulation, or via viral infections (Xu *et al*, 2005), the ER becomes overwhelmed with accumulated unfolded proteins. Under such conditions of ER stress, the cell responds by initiating a response known as the unfolded protein response (UPR) (Sidrauski *et al*, 1998). The response is two-fold. Firstly, there is increased transcription and up-regulation of many different UPR genes that can restore the ER‟s ability to function. Secondly, there is an inhibition of translation of any proteins not involved in the former response. This is to prevent the entry of vast quantity of proteins into the ER until the increased gene up-regulation results in production of the products of the UPR genes mentioned above, and thus resolution of the original ER stress.

The UPR centres around three trans-membrane proteins, namely activating transcription factor 6 (ATF6), Protein kinase-like ER kinase (PERK) and Ire1 (inositol requiring enzyme-1) (Fig 3.1.1). These proteins are normally held in place and inactivated by the chaperone protein Grp 78 (BiP), but the influx of unfolded proteins into the ER causes BiP to dissociate from these proteins, releasing and activating them as follows:-.

i) ATF6 translocates to the Golgi, where it is cleaved by proteases into a transcription factor which activates the upregulation of UPR target genes (Shang *et al*, 2004).

ii) Activated PERK phosphorylates eukaryotic initiation factor-alpha (eIFα), inactivating it and preventing mRNA translation into proteins (Hirota *et al*, 2006). (However, several mRNAs do still get translated, but these are generally only those directly involved in regulating UPR genes (eg. activating transcription factor 4 (ATF4), which is similar to ATF6 in that it is a UPR-inducible transcription factor involved in the upregulation of UPR target genes (Shang *et al*, 2004).

iii) Ire1 becomes dimerized, autophosphorylated and activated as an endoribonuclease, and can then initiate mRNA splicing of transcription factor X box protein-1 (XBP-1), and subsequent production of the active form of this transcription factor ($XBP\text{-}1_s$) (Xu *et al*, 2005). $XBP\text{-}1_s$ then subsequently binds to gene promoters bearing either or both of two cis-acting elements – the ER stress enhancer (ERSE), and the Unfolded Protein response Element (UPRE; Ma *et al*, 2001) – to induce upregulation of UPR genes (Shang, 2004). Ire1 is a bifunctional enzyme that acts as both a kinase and an endonuclease; its kinase activity is involved in the phosphorylation and therefore activation of proteins such as TRAF2, which itself mediates phosphorylation of proteins involved in the UPR (Chawla & Niwa 2005). Meanwhile, XBP-1 is activated by Ire1‟s endonuclease activity to bind to UPREs and/or ERSEs as shown in fig 3.1.2.

UPR genes can be split into in 3 categories: adaptation, alarm & apoptosis, with UPRE-bearing (or ERSE-bearing) genes being mostly involved in adaptation (Wu *et al*, 2005).

a) **Adaptation genes** are those which bring about restoration of ER homeostasis, and are usually genes whose products are involved in ER functions such as protein synthesis, folding and trafficking. Some examples of proteins encoded for by UPRE/ERSE-bearing genes are as follows:

- Protein Disulfide Isomerase (PDI or ERp72) catalyses protein folding by linking pairs of free sulphydryl (SH) groups via disulphide bonds (S-S). Its upregulation reduces the large number of unfolded proteins in the ER of a cell undergoing ER stress. (Lee *et al* 2003).
- Heat-shock protein 90 (HSP90 or GRP94), Calreticulin & BiP (Grp78) are Ca^{2+}-dependent chaperones which maintain correct folding of newly-synthesised proteins. Their upregulation „mops up“ the large number of unfolded proteins in the ER of a cell undergoing ER stress (Thuerauf *et al*, 2001).
- Similarly, SERCA2b as a „housekeeper Ca^{2+} pump“ supports BiP function by ensuring that the $[Ca^{2+}]$ in the ER lumen is kept high. Thus,

importantly in the context of the current study, SERCA2b has been shown to contain both ERSEs (Thuerauf *et al,* 2001) and UPREs (Caspersen *et al*, 2000).

b) **Alarm genes**. Ire1‟s kinase activity works via several protein phosphorylation cascades (eg. TRAF2 (Chawla and Niwa 2005)) to activate host defence inflammatory mechanisms against whatever extracellular stimulus it was that initially caused the ER stress - for example NF-kB (Wu *et al*, 2005). Interestingly, previous work in our laboratory has shown that the NFkB-dependent gene RAGE was activated by the classical ER stressor tunicamycin (L. Atkin, personal communication).

c) **Apoptosis genes** are only activated if the ER stress is either persistent or excessive. For example, the promoter of the CHOP gene contains response elements for XBP-1 (amongst other UPR response elements) (Wu *et al*, 2005), and when activated by persistent/excessive ER stress via XBP-1, CHOP can itself affect the expression of genes containing the CHOP response element [A/G]-[A/G]-[A/G]-T-G-C-A-A-T-[A/C]-C-C-C. These CHOP-regulated genes encode proteins like caspase-11 [Endo *et al*, 2006] and bcl-2 (McCullough *et al*, 2001), which are involved in apoptosis.

Thus, the UPR is a process which ultimately either leads to cell survival via the initiation of the above protective and restorative events, or to cell death if the UPR is activated for any length of time and protective measures fail to restore normal cell physiology (Weber *et al*, 2004b). In this respect, Ire1 is a fundamental protein in the ER stress response as it is involved in all cellular responses, and could therefore potentially hold the key to the cytoprotective versus cytotoxic actions following ER stress. Firstly, it helps the cell to adapt to short-term stress through upregulation of UPR genes via activation of XBP-1 as previously discussed. Secondly, via activation of TRAF2, which ultimately leads to the production of NF-κB, it sounds a warning to the cell that ER stress is taking place (Xu *et al*, 2005). Finally, following prolonged cellular stress, it activates signalling pathways involved in the apoptotic process, for example apoptosis signal-regulating kinase 1 (Ask1) which subsequently activates c-Jun N-terminal kinase (JNK) and p38MAPK leading to cell apoptosis (Wu *et al* 2005). The unfolded protein response can also lead to apoptosis via initiation of the

caspases, or by prolonged activation of PERK which leads to subsequent upregulation of the apoptosis-inducing transcription factor C/ERB homologous protein (CHOP) (Oshitari *et al*, 2008) whose target genes include caspase-11 (Endo et al, 2006).

Therefore, the UPR can either lead to the restoration of normal cell physiology, or – in the case of prolonged or severe ER stresses – to induction of cell death via apoptosis.

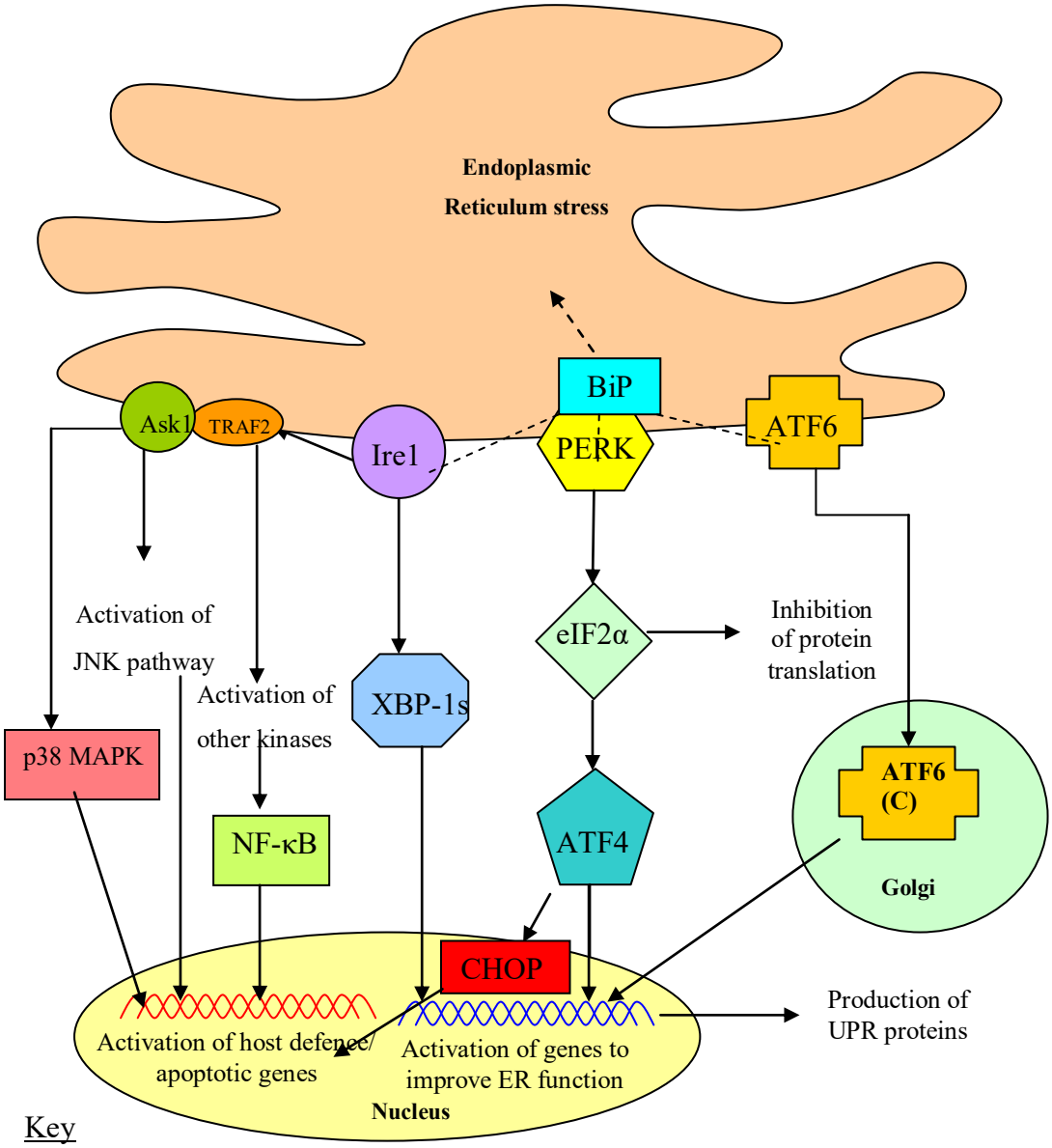

Key

BiP – Binding protein
Ask1 - apoptosis signal-regulating kinase 1
TRAF2 –
XBP-1 - X box protein-1
eIF2α - eukaryotic initiation factor-alpha
ATF4 – Activating transcriptionfactor 4
JNK - c-Jun N-terminal kinase
PERK - Protein kinase-like ER kinase
Ire1 - Inositol requiring enzyme-1
XBP-1s - X box protein-1 (spliced)
NF-κB – Nuclear factor kappa B
ATF6 - Activating transcription factor 6
ATF6(c) - Activating transcription factor 6 (cleaved)
p38 MAPK – p38 Mitogen activated protein kinase
UPR – Unfolded protein response

Fig 3.1.1: Activation of the unfolded protein response.
Cellular stresses such as increased $[Ca^{2+}]_{cyto}$ leads to activation of the unfolded protein response. This centres around the actions of ER stress in causing BiP to release the ER luminal domains of three important trans-membrane proteins: Ire1, PERK and ATF6. The chain reaction that is set in motion following activation of these proteins ultimately leads to activation of genes to improve cell function or to activation of apoptosis initiating genes and cell death.

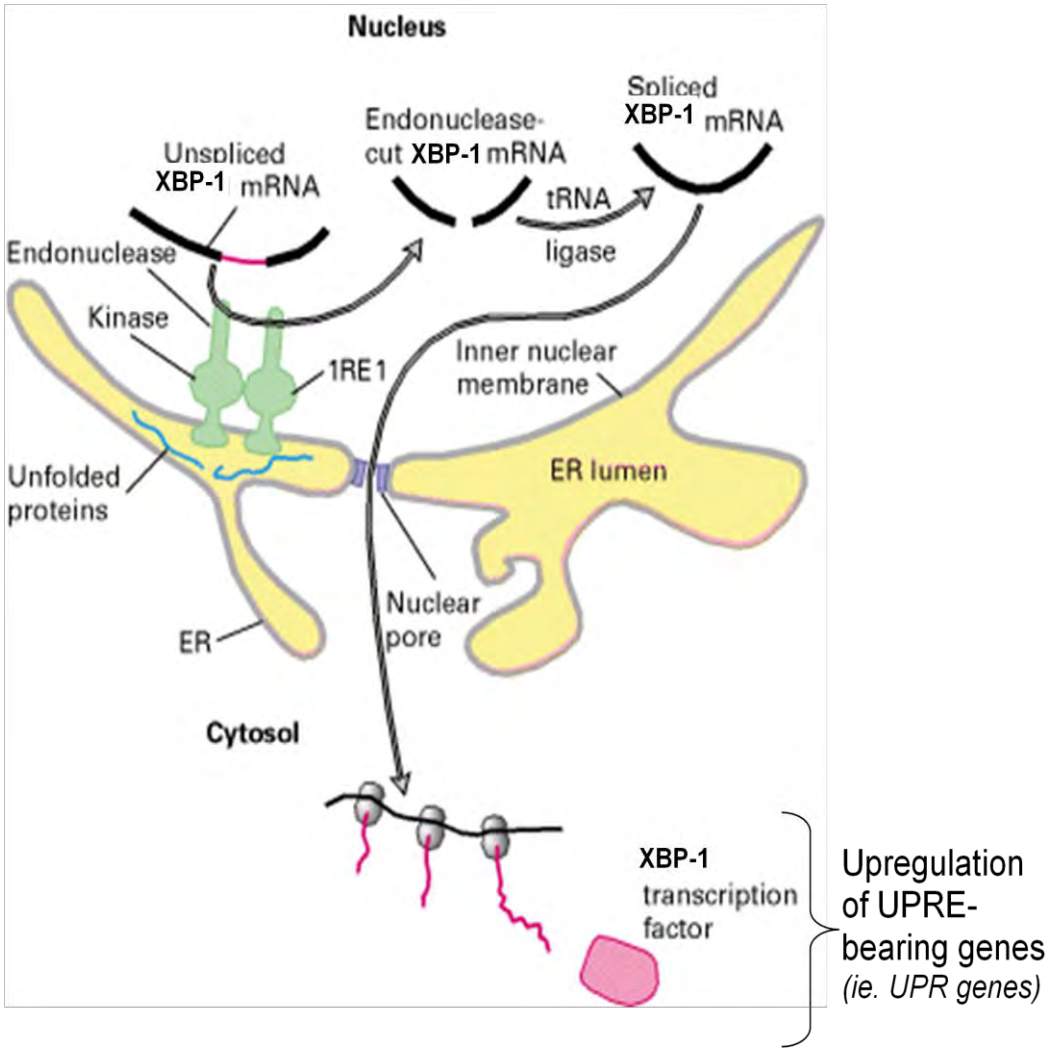

Key

ER – Endoplasmic reticulum
IRE1 – Inositol requiring enzyme 1
mRNA – Messenger ribonucleic acid
tRNA – Transfer ribonucleic acid
XBP-1 – X Box protein-1
UPRE – Unfolded protein response elements

Fig 3.1.2: Activation of XBP-1 by Ire1's endonuclease activity and its subsequent binding to UPREs and/or ERSEs (Adapted from Chawla & Niwa, 2005)

3.1.2 PPAR-γ ligands and the UPR

Aside from their anti-hyperglycaemic functions, PPARγ ligands (both natural and synthetic) have also been shown to elicit anti-inflammatory responses which appear to be mediated via the induction of ER stress (Weber *et al*, 2004b). For example, natural PPARγ ligands such as Δ12-prostaglandin J_2 (Δ12-PGJ_2) and 15-deoxy-$\Delta^{12,14}$-prostaglandin J_2 (15d-PGJ_2) have been shown to induce the unfolded protein response (Odani *et al*, 1996; Weber *et al*, 2004b; Chambers *et al*, 2007). The part PPARγ plays in this process remains to be fully elucidated; however, the inhibition of cytokine signalling that results in decreased inflammation appears to be a PPARγ-independent mechanism that is likely to involve the UPR (Weber *et al*, 2004a). Interestingly, prolonged UPR activation of pancreatic βcells by PGJ_2 has been shown to induce apoptosis (Chambers *et al,* 2006).

However, to date there appears to be a paucity in the literature regarding the effects of the synthetic PPARγ ligands on ER stress. Ciglitazone and troglitazone (and also ciglitazone and troglitazone derivatives lacking PPARγ ligand-binding activity) have been shown to lead to PERK activation and hence ER stress, by a PPARγ-independent mechanism in rat liver epithelial cells (Gardner *et al* 2005). Conversely, however Rosiglitazone has also been shown to reduce mitochondrial dysfunction-induced ER stress markers (Koh *et al*, 2007). In the light of data previously obtained in our laboratory (Singh *et al*, 2005) and the data presented in Chapter 2, the data presented in this chapter will investigate the hypothesis that, due to its effects on intracellular Ca^{2+}, rosiglitazone may be inducing UPRs in the monocytic and VSMC cells under investigation in the study.

3.1.3 Aims

In chapter 2, it was demonstrated that incubation with rosiglitazone caused rapid disruption to cellular calcium homeostasis and an increased cytoplasmic calcium concentration ($[Ca^{2+}]_{cyto}$) in monocytes and vascular smooth muscle cells. This was suggested to be due to inhibition of the ER Ca^{2+}ATPase enzyme SERCA2b because by virtue of its extra M11 transmembrane domain (see Chapter 1), SERCA2b functions as the cell‟s "housekeeper Ca^{2+} pump" enzyme (John *et al*, 1998), and so its inhibition would be expected to result in unchecked non-specific leakage of Ca^{2+} from the ER into the cytoplasm. However, extended incubation (72 h) with rosiglitazone appeared to restore the cells‟ ability to regulate storage and utilisation of Ca^{2+}. The aim of this chapter was to elucidate the mechanism behind the apparent

restoration of calcium homeostasis observed in these cells following extended incubation with rosiglitazone. Given that UPRs can ultimately lead to restoration of normal cellular physiology (see section 3.1.1), it was proposed that this may be due to the cell responding to ER stress imposed by rosiglitazone treatment by initiation of an unfolded protein response. We speculated that one mechanism by which the cell might overcome the observed rosiglitazone-induced disruption in calcium homeostasis may be via increased expression of SERCA2b, so that newly-synthesised SERCA2b molecules may compensate for those SERCA2b molecules that have been inhibited by rosiglitazone. Therefore, we speculated that SERCA2b itself may be a UPR-inducible gene, whose upregulation during a UPR may be involved in restoration of normal cell physiology

Therefore the specific aims of this chapter were;

- to use an RT-PCR-based assay system to measure XBP-1 activation (ie. expression of the active XBP-1 splice variant XBP-1_s), in order to establish whether rosiglitazone causes sufficient ER stress to induce a UPR;

- to use bioinformatics analysis, semi-quantitative real-time RT-PCR and western blot assays in order to establish whether SERCA2b is a UPRE-bearing UPR-inducible gene and, if so, to use SERCA2b as an example of a UPR gene to investigate the effect of rosiglitazone on the expression of UPR target genes in general;

- to determine how rosiglitazone-induced modulations lead to restoration of normal cellular function; e.g. to study the effects of rosiglitazone on SERCA2b activity to determine whether this could explain the restorative effects exerted by extended rosiglitazone treatment (72hrs) on calcium homeostasis.

3.2 Methods

3.2.1 Materials

All reagents were purchased from Sigma-Aldrich (Poole, Dorset, UK) unless otherwise stated. Western Blotting equipment/reagents and fluo-3 were obtained from Invitrogen (Paisley, UK) and real-time PCR consumables/reagents were obtained from Applied Biosystems (Warrington, UK).

3.2.2 Cell Culture

MM6 monocytic cells and A7r5 VSMCs were maintained in culture as described in section 2.2. Samples were treated with DMSO (0.1%), Rosiglitazone (1 or 10μM), thapsigargin (100nM) or tunicamycin (10μg/ml) for durations of 1, 4, 24, 48 and 72 hours. Following these treatments, A7r5 cells were trypsinised as described in section 2.2, to remove them from their culture flasks.

3.2.3 Extraction of RNA from MM6 monocytic and A7r5 smooth muscle cells

RNA was extracted from cells, after treatments as described above, following the TRIzol method as per the manufacturer‟s instructions (Invitrogen, Paisley, UK). $1x10^6$ to $5x10^6$ cells were pipetted into a 15ml sterile centrifuge tube and spun at 300g for 10 minutes. The supernatent was removed, 1ml TRIzol reagent was added and the cell pellet re-suspended by pipetting. The suspension was then vortexed for ~10sec before being transferred to a 1.5ml RNase-free micro-centrifuge tube and stored at -80°C. On defrosting, the tubes were thawed, vortexed and left to incubate for 5min. 200μl chloroform was added to each tube, tubes were shaken vigorously for 15sec**,** incubated for 3 min at 15-30°C and then spun in pre-cooled micro-centrifuge at 12000g for 15 min at 4°C. At this stage the mixture separated into a lower red, phenol-chloroform phase, an interphase and a colourless upper aqueous phase. The aqueous phase (approx 500μl) was transferred to a fresh 1.5ml centrifuge tube containing 500μl isopropanol and incubated for 10 minutes at 15-30°C. The tubes were then spun in a pre-cooled micro-centrifuge at 12000g for 15 min at 4°C and the supernatant removed. The RNA pellet was washed by adding 1ml 75% ethanol, the tubes were vortexed and spun in pre-cooled micro-centrifuge at 7500g for 5 min at 4°C. Alternatively, samples were stored at this stage by freezing at -80C after addition of ethanol. On defrosting, tubes were spun as described above, ethanol removed, a further 500μl of ethanol added and tubes re-spun at 7500g for five min. As much ethanol as possible was removed from the tube by pipette and then the

pellet was allowed to air dry for approx 30mins before being re-dissolved in 30-50µl RNase free dH_20. At this point the RNA were either quantified and cDNA conversion undertaken, or were stored at -80°C.

RNA was quantified and checked for purity using a GeneQuant Pro RNA/DNA calculator (Amersham Biosciences, UK). The RNA purity of samples was established via measurement of the ratio of their absorbances at 260nm and 280nm and only samples with a purity of >1.8 were used in further experiments. Extracted RNA was also analysed using agarose gel electrophoresis (as described in section 3.2.4) using 1% denaturing agarose gels to confirm that the preparation contained high-quality RNA.

3.2.4 Conversion of RNA to cDNA

RNA was converted to cDNA using the High-Capacity cDNA archive kit according to the manufacturer"s instructions (Applied Biosystems). RNA was diluted to 30mg/ml to give a final volume of 50µl and added to a 0.2ml dome capped PCR tube. 2x master mix was prepared on ice (10µl 10xRT Buffer, 4µl 25x dNTP mixture, 10µl 10x random primers, 5µl multiscribe RT (50U/µl) and 21µl RNase-free water per sample) and added to the RNA prior to mixing by gentle pipetting. The tubes were then placed in a Gene amp PCR system 2700 thermocycler (Applied Biosystems, Warrington, UK) and the RNA reverse transcribed to cDNA by incubating at 10°C for 10 minutes followed by 37°C for 2 hours.

3.2.5 Bioinformatics analysis of the SERCA2 promoter

A Bioinformatics analysis was conducted, using the Basic Local Alignment Search Tool (BLAST) application of the Pub Med database (http://blast.ncbi.nlm.nih.gov/Blast.cgi - accessed most recently 23-10-09), in order to detect certain important sequences within the SERCA2 promoter (Accession No:NC_000012.10), and so determine whether SERCA2b is either a PPARγ target gene and/or an ER stress-responsive UPR target gene. Firstly, given the need to discriminate between PPARγ-dependent and PPARγ-independent mechanisms, a search was carried out in the SERCA2 promoter for the PPRE sequence AGGTCAnAGGTCA (Murphy & Holder, 2000). Secondly a search was conducted for the following response elements for the UPR transcription factor XBP-1: the Unfolded Protein Response Element ("UPRE") **GACAGCGTGTC** (Ma *et al*, 2001),

and the ER Stress Response Element ("ERSE") **CCAAT**n9**CCACA** (Yoshida *et al*, 1998). Sequence analyses and alignments were performed using DNASTAR™ software (Lasergene, version 7; DNASTAR Inc., Madison, WI).

3.2.6 Use of RT-PCR-based assays to measure XBP-1 activation in MM6 monocytic cells

The expression of XBP-1 (spliced or unspliced) was measured by RT-PCR in a method adapted from Shang (Shang, 2005). As described in section 3.1.1, XBP-1 is activated via an alternative splicing event: Ire1's endoribonuclease activity excises a 44bp segment from within exon 4 of the unspliced XBP-1 mRNA species ($XBP\text{-}1_u$; Accession No: NM_005080.3) to generate a spliced mRNA ($XBP\text{-}1_s$; Accession No: NM_001079539.1) encoding the active form of the protein (Xu *et a*l, 2005). Shortly after the initial demonstration of this splicing event, Shang published an RT-PCR-based assay by which XBP-1 splicing could be monitored, and thus the induction of ER stress assessed (Shang, 2005). This method used primers designed to hybridise to sequences upstream (nucleotides 375-395, within exon 3) and downstream (nucleotides 798-818 [unspliced sequence] or nucleotides 754-774 [spliced sequence], both within exon 4) of the splice site, and so allowed the detection of distinct PCR products of length 442bp ($XBP\text{-}1_u$) or 398bp ($XBP\text{-}1_s$) when cDNA from control samples (when $XBP\text{-}1_u$ predominates) or cDNA from samples undergoing ER stress (when $XBP\text{-}1_s$ predominates) were used as templates in PCR reactions.

3.2.6.1 PCR

The following primers were used in PCR reactions involving cDNA samples obtained from MM6 samples treated with Rosiglitazone (1µM or 10 µM; 1-72h), or with tunicamycin (10µg/ml; 1-72h) or thapsigargin (100nM; 1-72h) as positive controls: XBP-1 mRNA sense primer 5'- CCTTGTAGTTGAGAACCAGG -3', anti-sense primer 5'- GGGGCTTGGTATATATGTGG-3'). Mastermix was prepared using the following reagents. For each sample 2.5µl 10x PCR buffer, 0.75µl 50mM $MgCl_2$, 0.5µl 10mM dNTP mixture, 0.2µl Taq DNA polymerase, 19.05µl distilled water, 0.5µl forward (sense) primer and 0.5µl reverse (anti-sense) primer were pipetted into a 0.2ml dome capped PCR tube and mixed thoroughly. 1µl cDNA from (3.2.1) was added to the master mix and the contents mixed by gentle pipetting. Thermocycling was as follows: 5 minutes at 95°C (melting), followed by 30 cycles

of 1 minute at 95°C (melting), 1 minute at 56°C (annealing) and 1 minute at 72°C (extension) with a final elongation step of 7 minutes at 72°C. The programme used consisted of 30 cycles because this had previously been determined to be during the exponential growth stage of the amplification reaction (data not shown).

3.2.6.2 Agarose gel electrophoresis

PCR products were analysed by electrophoresis on a 2% agarose gel. A 100 bp DNA ladder was run alongside samples to act as a fragment length marker. Gels were stained in Ethidium bromide (1µg/ml) for 45 minutes and then de-stained in distilled water for a further 45mins. Bands were visualised using a UV transilluiminator and then densitometry analysis was conducted to quantify the different splice variants of the UPR transcription factor XBP-1, using AC-1 Bioimaging and Vision WorksLS Software system (Ultra Violet Products Ltd, Cambridge, UK). Densitometry data of the various splice variants was subsequently analysed to determine XBP-1 activation, by means of the following formula:

$$\mathbf{[XBP\text{-}1(s) + 0.5\ XBP\text{-}1(h)]/[XBP\text{-}1(s) + XBP\text{-}1(h) + XBP\text{-}1(u)]},$$

where XBP-1(s) is a 398bp PCR product representing spliced XBP-1, and XBP-1(u) is a 442bp PCR product representing unspliced XBP-1 (Shang, 2005; XBP-1(h) is an approximately 450bp PCR product representing hybrid XBP-1 cDNA species). All samples were analysed in triplicate.

3.2.7 Use of RT-PCR-based assays to measure XBP-1 activation in A7r5 vascular smooth muscle cells

In contrast to the situation with human XBP-1 mRNA, where the NCBI have assigned separate Accession Numbers on their database for spliced and unspliced XBP-1 (NM_001079539.1 and NM_005080.3 respectively), rat XBP-1 mRNA is entered in the NCBI database as a single Accession No: NM_001004210.1, which corresponds to spliced XBP-1. This precluded use of the type of RT-PCR-based assay previously used for MM6 cells samples (Shang, 2005) for A7r5 cells. Instead, the approach of Kubisch *et al* was adopted, whereby a set of primers that specifically hybridise only with XBP-1(s) were designed and used (Kubisch *et al*, 2006). The forward primer spans XBP-1‟s splice site, and so will only anneal to a template containing spliced XBP-1, producing a 550bp PCR product that could be identified

via agarose gel elecrophoresis. Since the primer only anneals to XBP-1(s), the appearance of a band visible at 550 bps would indicate that the sample concerned had been derived from cells undergoing ER stress.

3.2.7.1 PCR (2)

mRNA and cDNA samples were prepared as previously described. However, in contrast to the previous experiment, where previously designed primers were used (Shang, 2005), in this case, primers were designed specifically for use in this experiment. Thus, the following primers were used in PCR reactions: XBP-1(s) mRNA sense primer 5'- GAG TCC GCA GC*A GGT G -3', anti-sense primer 5'- GTG TCA GAG TCC ATG GGA -3') *[* Designates position of rat XBP-1 splice site].*

T_m calculations were performed to check that the primer sets was viable, using the Wallace formula: $T_m = 4(G+C)\ 2(A+T)$

	T_m XBP-1(S) (°C)	T_m 18S-rRNA (°C)
Forward Primer	54	*74
Reverse Primer	56	*74

- *T_m of Primer is high due to its high G-C content

The primers chosen were all between 19 to 22 nucleotides long and the primers T_m were between 54-62°C (except for the housekeeper primers due to their high G-C nucleotide content). The primers did not have any palindrome content as to not form any hairpin loops amongst themselves.

Mastermix was prepared using the following reagents. For each sample 2.5µl 10x PCR buffer, 0.75µl 50mM $MgCl_2$, 0.5µl 10mM dNTP mixture, 0.2µl Taq DNA polymerase, 19.05µl distilled water, 0.5µl forward (sense) primer and 0.5µl reverse (anti-sense) primer were pipetted into a 0.2ml dome capped PCR tube and mixed thoroughly. 1µl cDNA from (3.2.1) was added to the master mix and the contents mixed by gentle pipetting. Thermocycling was as follows: for 18s rRNA (housekeeper) - 6 minutes at 95°C (melting), and 28 cycles of 1 minute at 95°C (melting), 1 minute at 74°C (annealing) and 1 minute at 72°C (extension) before a final 7 minute 72°C (Prolonged extension) step; for XBP1(s) - 6 minutes at 95°C (melting), and 28 cycles of 1 minute at 95°C (melting), 1 minute at 74°C (annealing) and 1 minute at 72°C (extension) before a final 7 minute 72°C (Prolonged extension) step. The programme used consisted of 28 cycles because this had previously been

determined to be during the exponential growth stage of the amplification reaction for both gene-of-interest and housekeeper gene (data not shown).

3.2.7.2 Agarose gel electrophoresis

Analysis of PCR products were carried out as previously using 2% agarose gel electrophoresis, followed by densitometric analysis using VisionWorks-LS software.

3.2.8 Semi-quantitative measurement of SERCA2b mRNA expression via real-time RT-PCR

SERCA2b mRNA expression was analysed semi-quantitatively relative to the housekeeping gene Glyceraldehyde Phosphate Dehydrogenase (GAPDH) via use of Real time RT-PCR and Taqman Gene Expression Assays for SERCA2b and GAPDH (Applied Biosystems, Warrington, UK – see below for further details). 10µl Taqman Universal Master Mix and 1µl Taqman Gene Expression Assay (SERCA2b or GAPDH as appropriate) were pipetted into each well of a 96-well PCR plate. 9µl of diluted cDNA was added to the well to a final DNA content of 10ng), the plate sealed with an optical plate cover and then spun at 1500g for 5 mins to mix contents. The plate was then analysed using an Applied Biosystems 7500 Real-time PCR System which amplifies the genes of interest, namely SERCA2b and GAPDH, from the cDNA. Thermocycling was as follows: 2 mins at 50°C then 10 mins at 95°C (initial denaturation), followed by 50 cycles of 15sec at 95°C (denaturation) and 60 sec at 60°C (annealing/extension). All experiments were conducted in triplicate.

SERCA2b mRNA expression in both MM6 and A7r5 samples was analysed using Taqman Gene Expression Assay Hs01566028_g1 as previously described (Shah *et al*, 2004). Primer and probe sequences were as follows.
Forward primer: 5'-GAGATCACAGCTATGACTGGTGATG-3';
Reverse primer: 5'-CCCGATTTCCGACTTCTTCA-3;
Probe: 5'-/56-FAM/TGTGAACGACGCGCCCGC/36-TAMRA/-3'.

Glyceraldehyde Phosphate Dehydrogenase (GAPDH), which is endogenously expressed in all cells was used as a housekeeping gene. GAPDH mRNA expression was analysed using Gene Expression Assay Hs99999905_m1 for human GAPDH (i.e. when analysing MM6 cell derived cDNA), or Gene Expression Assay Rn99999916_s1 for rat GAPDH (when analysing A7r5 cell derived cDNA).

Taqman gene expression assays contain two unlabelled primers for amplifying the sequence of interest as well as a TaqMan minor grove binding probe (MGB) which binds with and detects the sequence of interest. The TaqMan probe contains a reporter dye linked to the 5‟ end of the probe, a MGB which increases the melting temperature of the probe while retaining a relatively short length and a nonfluorescent quencher (NFQ) at the 3‟ end of the probe. When the quencher and reporter dye both remain intact fluorescence is quenched. During the PCR reaction, DNA Polymerase induced cleavage of the probe leads to separation of the reporter and quencher dyes resulting in increasing levels of fluorescence detection of the reporter dye which is recorded as the PCR reaction continues (see fig 3.2.1). It is important to note that DNA polymerase cleaves the probe between the reporter and quencher dye only if the probe has bound to its target – ie. only if bound to the sequence of the gene of interest (TaqMan Gene Expression Assays Protocol Booklet, Applied Biosystems, 2005). Thus, the magnitude of fluorescence generated is a reflection of the extent to which PCR amplification is occurring in each case. Results were then analysed using the $2^{\Delta\Delta CT}$ method where the cycle threshold (CT) values (the number of PCR cycles required to reach a predetermined threshold level of fluorescence) for SERCA2b and GAPDH were compared to give a semi-quantitative estimate of how SERCA2b mRNA expression varies compared with the expression of the endogenous house keeper gene GAPDH.

3.2.8.1 PCR amplification efficiency – optimisation of primers

Real time RT-PCR efficiency is reliant of a number of factors such as sample quality and integrity, experimental design and PCR reagents used (including the choice of primers). PCR amplification efficiency is the measurement of amplicon generation, with 100% efficiency denoting ideal amplicon replication for the gene of interest. To estimate the PCR amplification efficiency of a primer in a real time RT-PCR reaction, CT values were plotted against the logarithm of template dilution (ie. varying amounts in ng of cDNA). A slope of -3.32 gives a primer efficiency of 100% but any slope lying between -3.2 and -3.4 denotes a high PCR amplification (Applied Biosystems Application note: “Real Time PCR - Understanding C_T”).

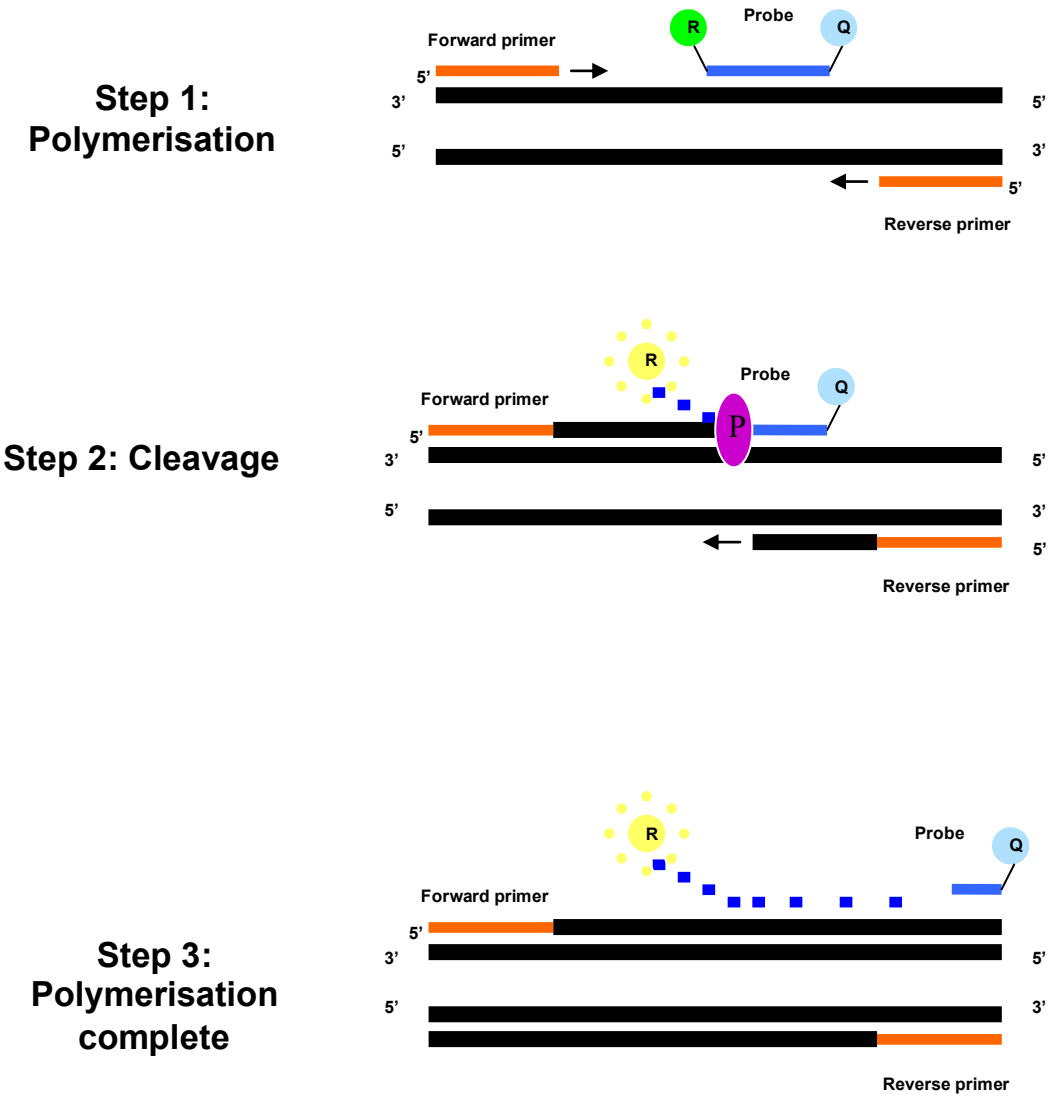

R = Reporter , Q = Quencher, P = DNA Polymerase

Fig 3.2.1: How 5'-3' nuclease activity of DNA polymerase is utilised in TaqMan gene expression assays during semi-quantitative real time RT-PCR analysis (Adapted from TaqMan Gene Expression Assays Protocol Booklet, Applied Biosystems, 2005)

As can be seen in fig 3.2.2, the slopes for GAPDH and SERCA2b in MM6 cells were -3.252 and -3.4056 respectively, giving PCR amplification efficiencies of 96.6% for GAPDH and 103% for SERCA2b. Both values fall comfortably within the recommended acceptable limits for PCR efficiency, and therefore these assays systems were deemed suitable for use in measuring SERCA2b and GAPDH mRNA expression in MM6 cells. In a7r5 cell derived cDNA, the slopes were -2.9424 and -2.97088 giving PCR amplification efficiencies of 118.8% for rat GAPDH and 117.1% for SERCA2b (figs 3.2.3).

(a)

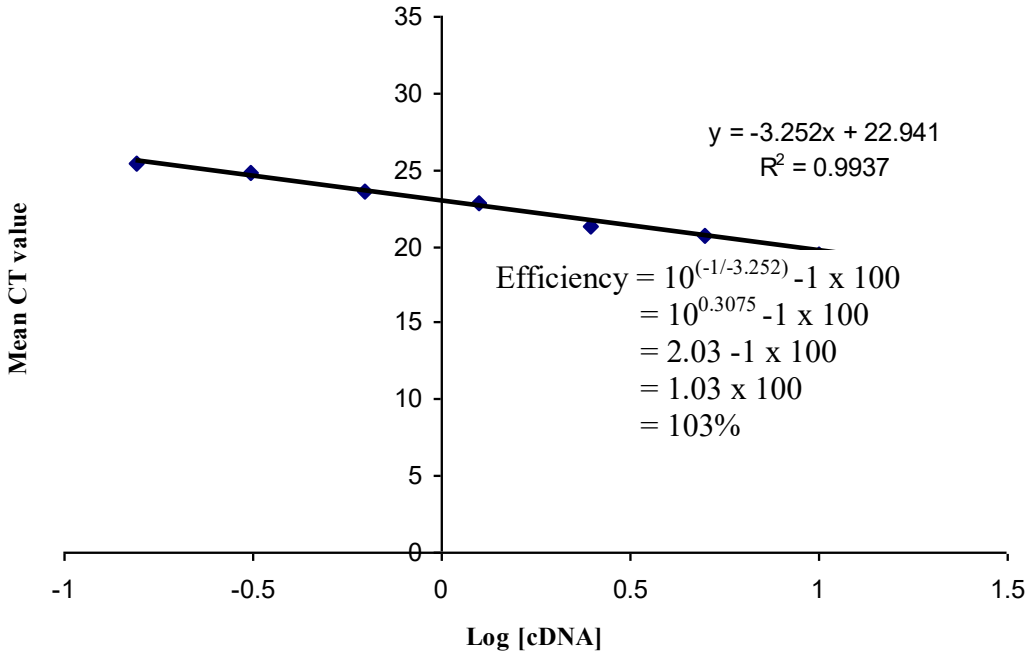

(b)

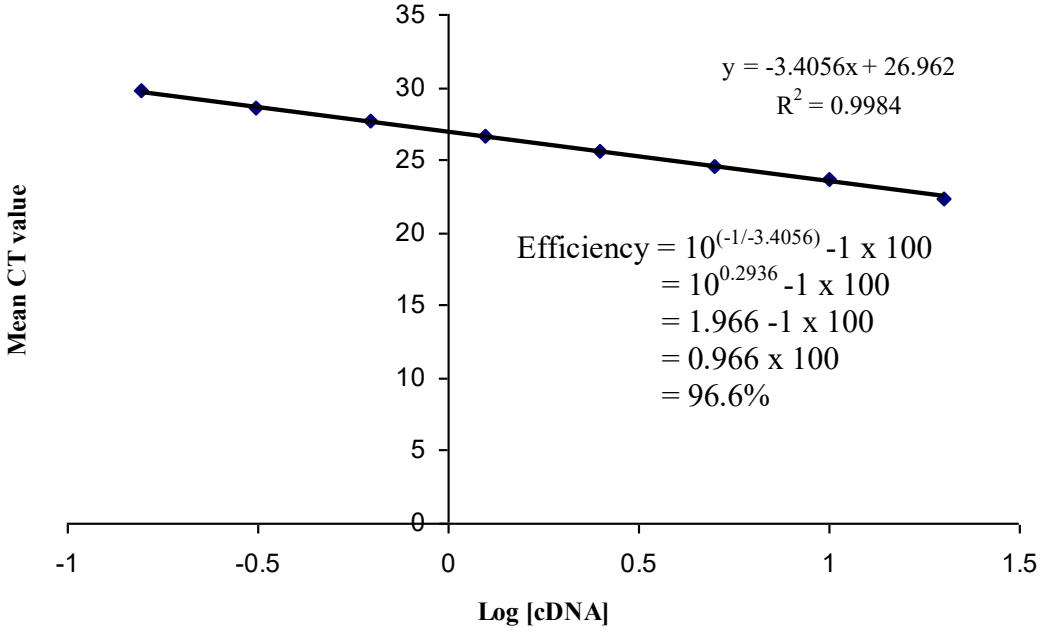

Fig 3.2.2: (a) human GAPDH and (b) SERCA2b primer efficiency in semi-quantitative real time RT-PCR analysis of mRNA expression in MM6 cells.

(a)

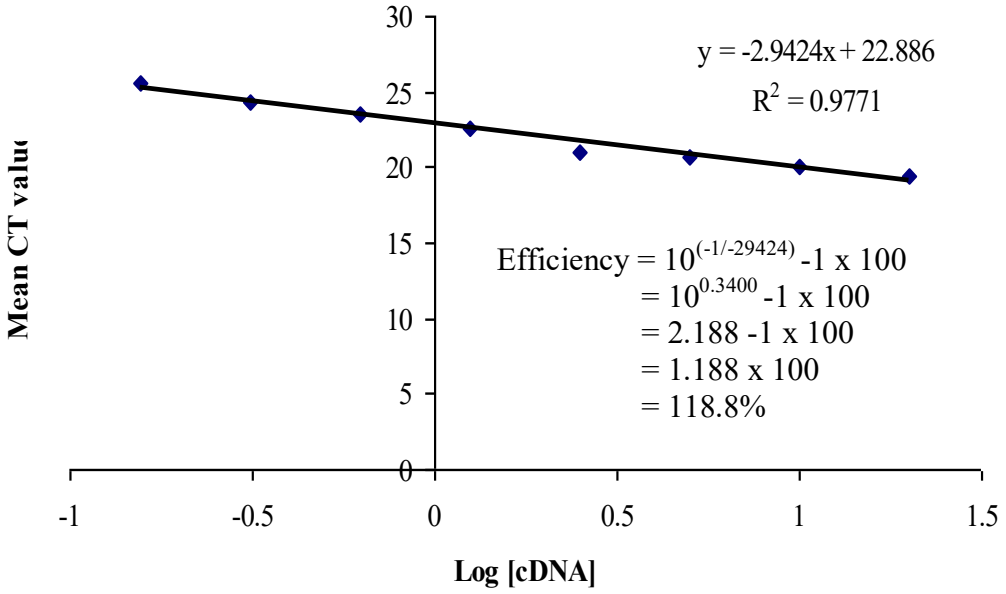

(b)

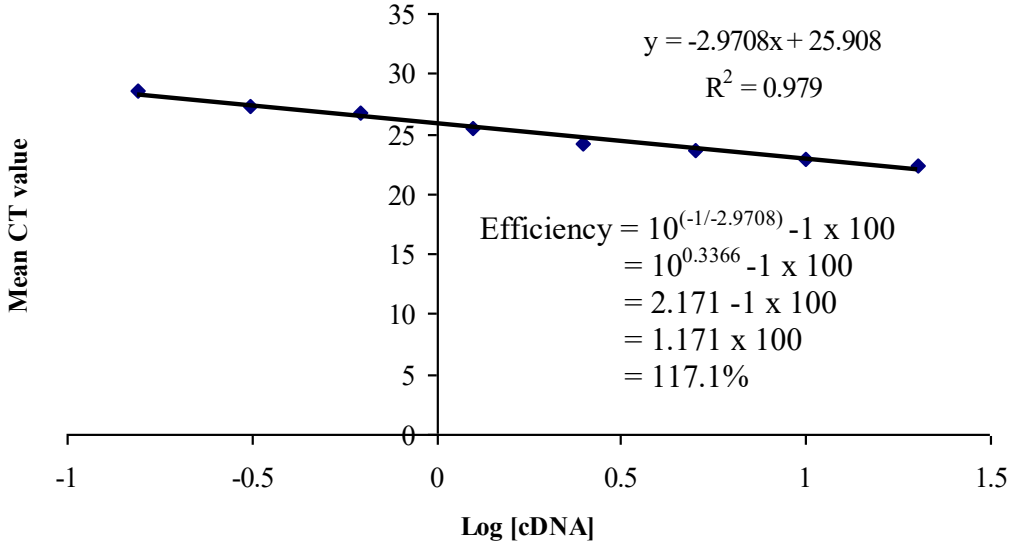

Fig 3.2.3: (a) rat GAPDH and (b) SERCA2b primer efficiency in semi-quantitative real time RT-PCR analysis of mRNA expression in A7r5 cells.

3.2.8.2 Validation of the semi-quantitative real time RT-PCR $2^{\Delta\Delta CT}$ method

In order for the $2^{\Delta\Delta CT}$ method to be used for quantification of mRNA amplification, it was necessary to perform a validation experiment to ensure that the amplification efficiency of the target (SERCA2) and housekeeping (GAPDH) genes used were approximately equal. ΔCT (the difference between the CT values for target and housekeeper) was plotted against the logarithm of template dilution (eg varying cDNA concentrations). It is required that both primers amplify independently of one another but retain similar amplification efficiencies, and ideally the slope of ΔCT versus log [cDNA] should be between -0.1 and +0.1. As can be seen below the slope was -0.0989 for SERCA2 versus GAPDH in MM6 cells, and -0.0284 for SERCA2 versus rat GAPDH in A7r5 cells, indicating that primer efficiencies were approximately equal in both instances and that therefore these assays systems were suitable for use in comparing SERCA2b and GAPDH mRNA expression in MM6 and A7r5 cells.

(a)

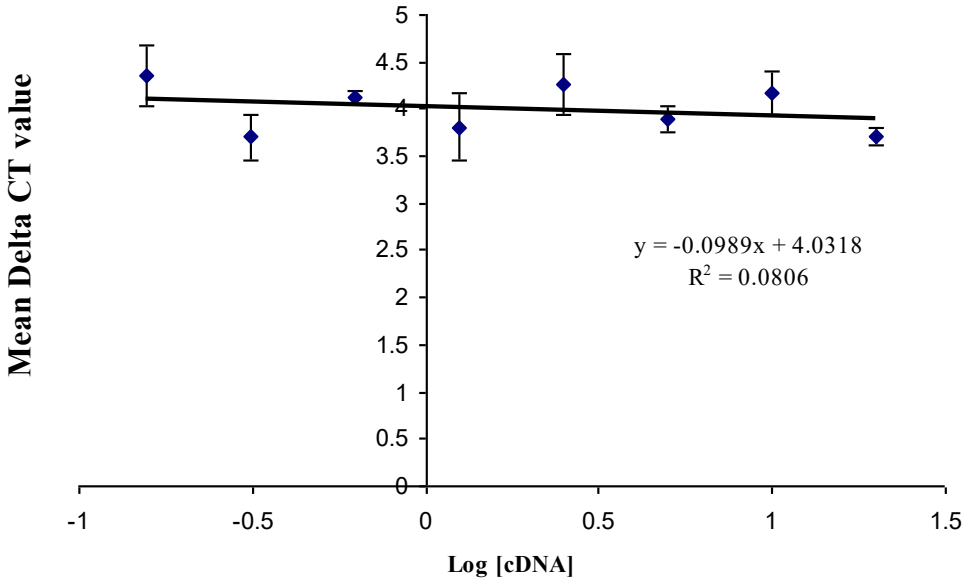

(b)

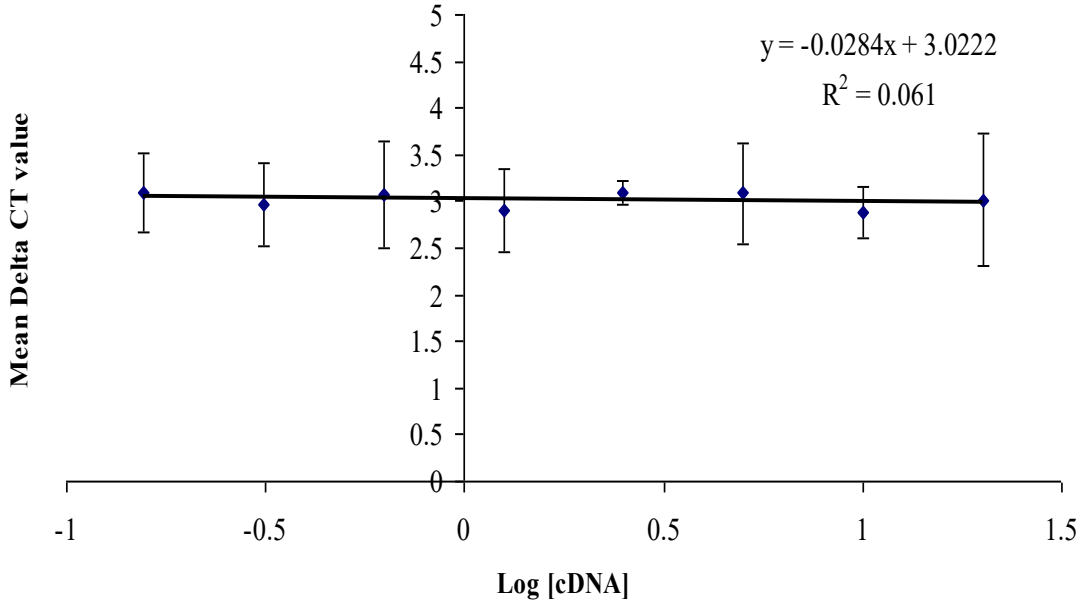

Fig 3.2.4: Validation of $2^{\Delta\Delta CT}$ method. Relative efficiency plot of (a) human GAPDH versus SERCA2b in MM6 cells and (b) rat GAPDH versus SERCA2b in A7r5 cells using semi-quantitative real time RT-PCR analysis of mRNA expression

3.2.9 Extraction of protein from MM6 monocytic cells

Total protein extracts were obtained by a solubilisation protocol as follows. MM6 cells were treated with either DMSO (0.1%) or Rosiglitazone (1 or 10µM) for 0-72 hrs. 5 x 10^6 cells were pipetted into a sterile centrifuge tube and spun at 300 RCF for 10 minutes. The supernatant was discarded and the pellet washed twice in 10ml ice cold PBS and spun at 300 RCF for 10 mins. 100µl RIPA buffer (100mM NaCl; 10mM Tris HCl, pH 7.2; 2mM EDTA; 0.5% *(w/v)* sodium deoxycolate; 1% *(v/v)* Nonidet P40) and 10µl protease inhibitor cocktail were added to lyse cells on ice for 30 mins; cells were vortexed 3 times during this incubation. The supernatant was transferred to a sterile microcentrifuge tube and lysate sonicated for 10-20s, on ice, to shear DNA and reduce sample viscosity. The lysate was then spun in pre-cooled micro-centrifuge at 12000RPM for 5 mins at 4°C. The supernatant was transferred in 25-50µl aliquots into sterile microcentrifuge tubes prior to storage at -80°C.

3.2.10 Western Blotting analysis of SERCA2b protein expression

SERCA2b protein expression was analysed by western blotting as described in 2.2.8. 50µg total protein extract was analysed in each case.

3.2.11 Analysis of Ca^{2+}ATPase activity in microsomal samples

Microsomes were prepared and Ca^{2+}ATPase activity measured using the subcellular fractionation and coupled-enzyme assay methodologies described in sections 2.2.6.3, 2.2.6.5 and 2.2.9 following treatment of MM6 cells for 72 hours with DMSO (0.1% v/v), Rosiglitazone (10µM) or thapsigargin (100nM).

3.2.12 Statistical analysis

All data are expressed as mean ± SEM unless otherwise stated. The students t-test was used to compare the differences between means of two samples and one-way analysis of variance (ANOVA) was used to compare group data. Statistical analysis was performed using Minitab version 14 (Minitab Inc, PA, USA) software. In all cases, statistical significance was set at $p<0.05$

3.3 Results

3.3.1 Bioinformatics analysis of the SERCA2 promoter

Bioinformatics screens of the SERCA2 promoter (Accession No:NC_000012.10) were carried out for the PPRE sequence AGGTCAnAGGTCA (Murphy & Holder, 2000) and for response elements for the UPR transcription factor XBP-1 (UPRE: GACAGCGTGTC (Ma *et al*, 2001); ERSE: **CCAAT**n9**CCACA** (Yoshida *et al*, 1998).

While no PPREs could be detected in this promoter, UPRE-like sequences were present at $^{-163}$[GGCAGCGTGGG] and $^{-335}$[AGCAGCGTGCC], and ERSE-like sequences at $^{-78}$[CCAATGAGCGGCGTCCACA],$^{-328}$[CCACTGTGAGCGCCCCACC] and $^{-973}$[GTAGCTTCTTTATATTGG] of the human SERCA2b promoter. *(NB. The final ERSE-like sequence is actually complementary to an ERSE, indicating that the ERSE itself is present on the antisense strand)*.

Therefore, this analysis supports the suggestion that SERCA2b is likely to be an ER stress-responsive UPR target gene, but is not a PPARγ target gene.

SERCA2 promoter with 2 UPREs and 3 ERSEs (Accession No:NC_000012.11)

GAGAATATGTTCATGTTTTGTTCATGAATTCCATGCAATTTCCCATCCCCT
TGTTAAGTAAT**GTAGC**TTCTTTAT**ATTGG**CAAAATTCCCTTTATCTTGCTT
GACCTGCGCTTTGTCCTCCCGAGCAGAGCAAATCATCTGTGGTTTAAGAG
AGCTTTGGATTCAAGTCCCCTTTTCTCCTGTCGAGGGAAGTGAGTCTATG
AAATGGCCTTCATCTGAAAGCCACAGCGAAGCACCTCCTAGCCCAAGTCT
AGCTGCTGTGTGGCAGCTCCAGCGGCGTGAACTGTGACTGCCCTGCAGAC
ACCTATCAAGCGCTGCGTCAGCTATTAATAATAAAATCAACTCTTCTCCC
TCCCCCCCGCGAGGGGGGTTCCCTCGTCAGGGCCCAGAACCCGCTGGGG
AAGAATCGGGGCTGGCGTGCGAAGGAGCTGGCGGCAGGGGGTGTAGGAT
GCGGTGTTCCCGAGGCGACAGATGAAGGATTTGGGTTGTGTGGGAAGTG
AACTGCGGAATTCCTCCCCTTGGTTTCTGAGGGGGGCTCTGAAGGAGCCA
GATTAGGATGCAGAGCGCAGCCCGGGCGACCGAGGGCGAGGAGGCGAG
CCAAGGACATCAGCCCGAGGGCGCCTCGAGACGCCCCGCGTGGACCGCG
CTCCCAGCTCCTCGGCCTCGCCTTCCAACCATCCGCCCACCGGCCCCAG**A**
GCAGCGTGCC**CACT**GTGAGCGCC**CCACC**CTGCGTCTGCAGGTGGGTGG
GTCAGAGAACCGCAGGCACAGAAGAGGGTACCCAGCTTCCCCTCCGCCA
GCCCCGCGACCGCGGCGCGCGGCCTCGATCCGGGTTCCTAGGGGCGG
CGCGCGGGAGGGGGCGGGGCCTGCGC**GGCAGCGTGGG**CGCCAGGCGCG
CGGGAGGAGGGAGCCGGGAGGAGGGGGCGGGGCCGCGCCGCCCGCGCC
GCGCTGGGCGCTCTCGG**CCAAT**GAGCGGCGT**CCACA**TGCCGCGGCGGCG
GCGAAAGGGGAGGCAGCGGCCGATAAATGCTATTAGAGCAGCCGCC

Transcription START SITE:
GCGGAGCCGTCCCCGACGCCACCTCCTTTTCCTTCGCCGCAGTTTCCTCCG
CCGCTGTCGGGCGTGCGGCGCTGAGGGACCCGGGCGAGCGCGCCGCGCA
CCGCCCCGCCGGCTCGCCTCCCTCGCCGCGTTCCGCCCTCAGTGGTCTGC
CGGGCGCCCCCTCCTCCGGCCCGGGCGGGGCCTCTGATCGCCTCAAGAGA
GCGGGGAGGGGGCTCGGGGGCCGCGGCCTGCCCTCCCGGCGGGCGGCTG
AGGGCGAGGGAGGCCCTCCCTTCTGGCGAGGGGAGGGAGGGTGGGTCAG
GAGCCCCCAACCCGCCCTGCGGAGCTCGGGGCCGCGCGAGGGGCGGTTG
TCTGGGGGAGGGGGCGCGGGGTGATTCAGCGCCCGGCGAGGCGGAAGCG
GCCGCAAGAGGAGGAGGGGAGAGCCCGTCCGCGCCTGGGCTCCCGGGGT
GGCACGAGCCCGCGGCCGGAGTGCGAGGCGGAGGCGAGGAGGCCGCGG
GGACGGGAGGCGAGGCCGGCCGGGCCCCCGAAGCC

Translation START SITE:
ATG……

Fig 3.3.0: The SERCA2 promoter region.
UPRE-like sequences are shown in red; ERSE-like sequences are underlined in black. All sequences were obtained from the NCBI database (http://www.ncbi.nlm.nih.gov/sites/entrez)

3.3.2 The effects of tunicamycin, rosiglitazone and thapsigargin on activation of XBP-1 in MM6 monocytic and A7r5 smooth muscle cells

To determine the effect of the following reagents on XBP-1 activation, MM6 cells were left untreated or treated with rosiglitazone (1 or 10μM), DMSO (0.1% v/v), tunicamycin (10μg/ml), or thapsigargin (100nM) for 1, 4, 24, 48 or 72 hours. mRNA obtained from these cells underwent reverse-transcriptase PCR with XBP-1 primers (see 3.2.4), and the resulting PCR products were run on 2% agarose gels.

Figs 3.3.1 and 3.3.2 show that 1μM rosiglitazone induced a small non-significant increase in XBP-1 activation at all time points (eg. XBP-1 activation after 72hrs 0.26±0.11 compared with a basal reading of 0.14±0.02, $P>0.05$ t-test), while 10μM rosiglitazone induced a statistically significant increase in XBP-1 activity again at all time points with a maximal 3-fold activation of XBP after 72 hours (XBP-1 activation after 72 hrs 0.42±0.09, $P<0.05$ t-test) .

Fig 3.3.2 shows that treatment with vehicle alone (DMSO) for 72hrs did not induce XBP-1 activation; results were comparable with the untreated control cells. Treatment with tunicamycin in contrast did not activate XBP-1 after 1hr but did induce ≥3 fold increase in XBP-1 activation after 4 and 24 hours (XBP-1 activations 0.52±0.08 and 0.46±0.08 respectively, $P<0.05$ t-test), before rapidly decreasing following extended incubation (XBP-1 activations 0.23±0.05 after 48 hrs and 0.18±0.04 after 72 hrs, $P>0.05$ t-test). (NB. Treatment with thapsigargin (24h) induced comparable XBP-1 activation to that seen with tunicamycin (data not shown)).

Fig 3.3.3 shows that 10μM rosiglitazone induced upregulation of XBP-1(s) in A7r5 cells (eg. from 10572±61 (0h) to 112594±16670 (48h) densitometric units; $p<0.05$; NB. due to the low „n" number (n=3), statistical significance was not achieved in all cases. Had time allowed, this experiment would have been repeated in order to attain statistical significance).

(a)

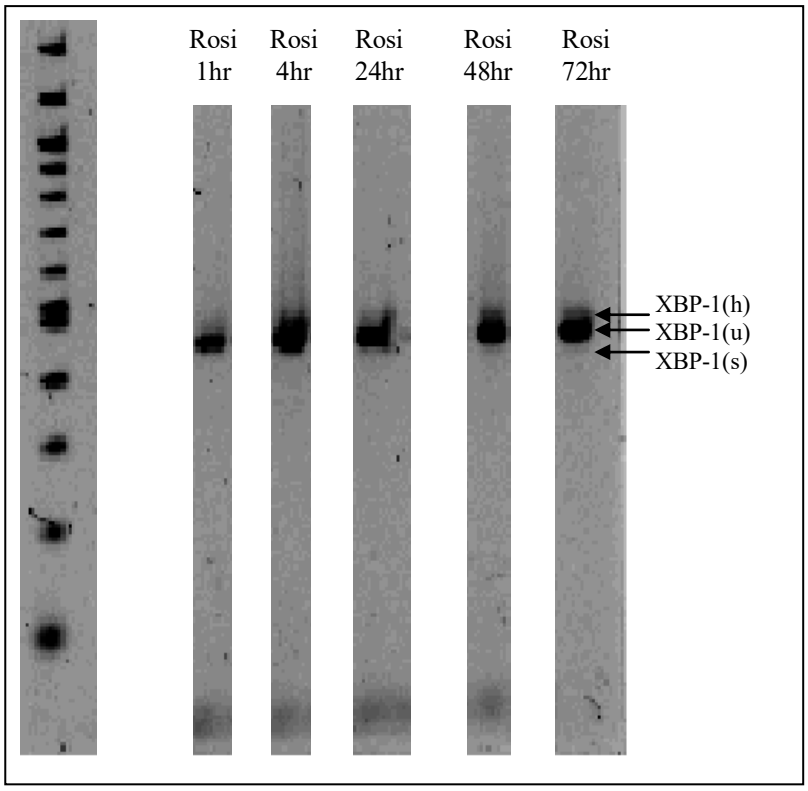

(b)

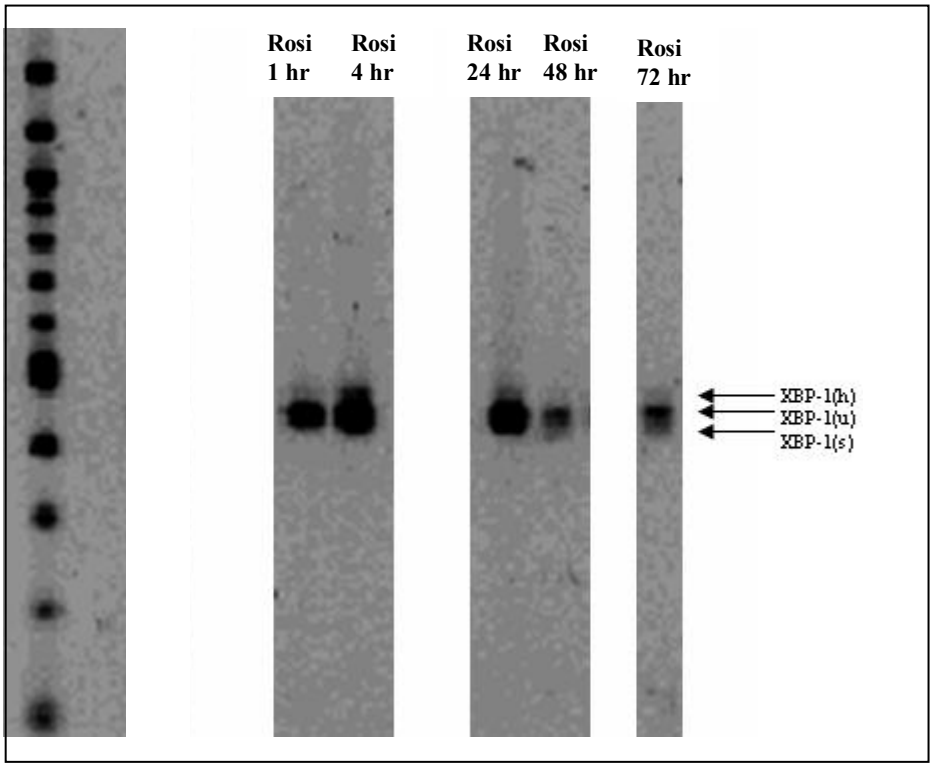

Fig 3.3.1: The effect of rosiglitazone on activation of XBP-1
Representative PCR gels showing activation of XBP-1 with rosiglitazone (a) 1µM (b) 10µM. MM6 cells were treated with 1µM or 10µM rosiglitazone for the indicated durations (n=4).

(a)

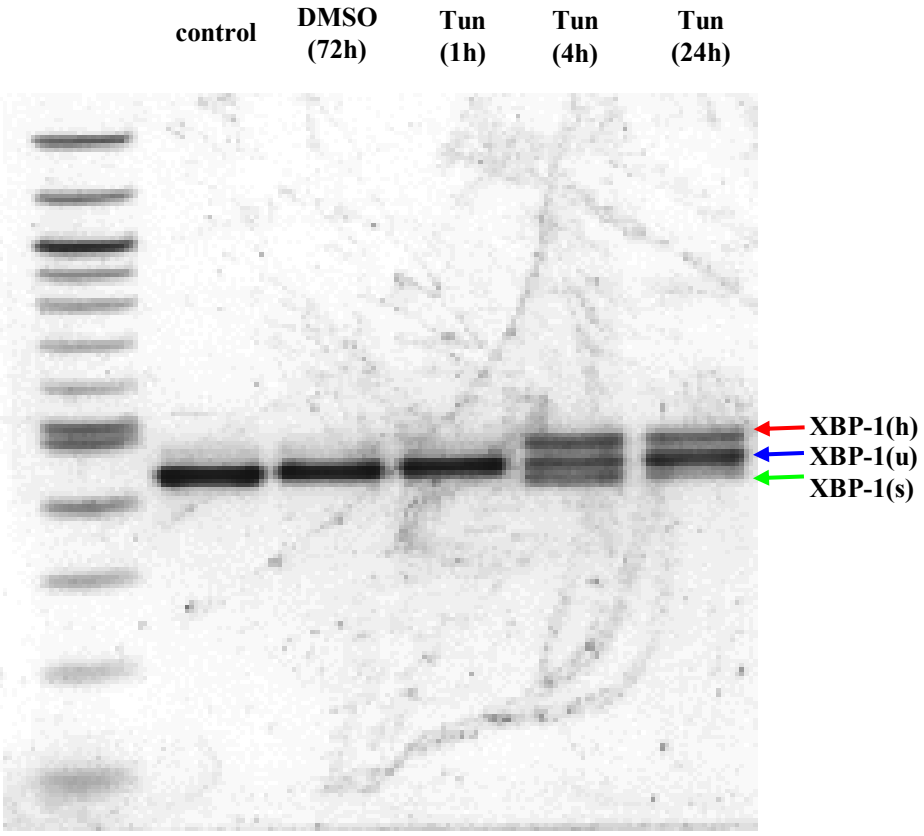

(b)

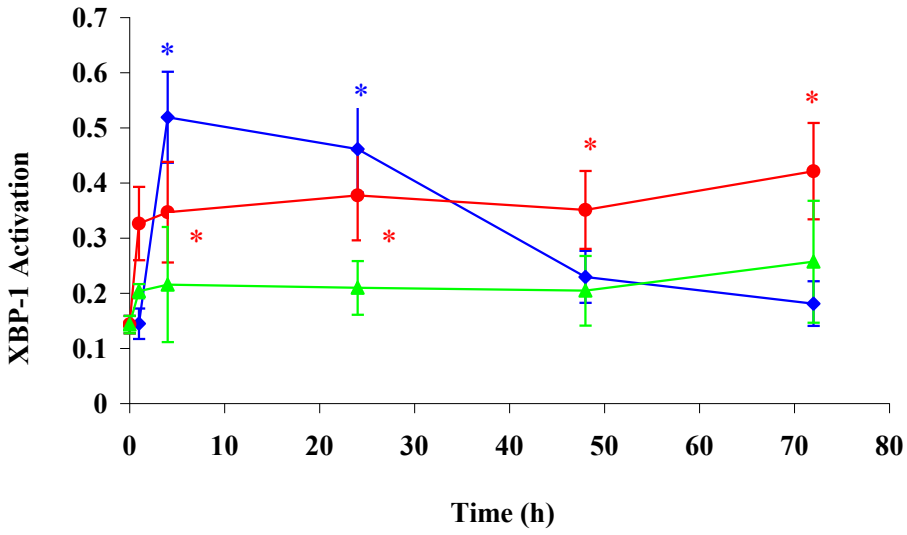

Fig 3.3.2: The effect of tunicamycin or rosiglitazone on activation of XBP-1 in mMM6 cells

(a) Representative PCR gel showing activation of XBP-1 with tunicamycin (b) Densitometry data showing activation of XBP-1 with tunicamycin or rosiglitazone. MM6 cells were treated with a positive control tunicamycin (10µg/ml – blue line), or with 1µM rosiglitazone (green line) or 10µM rosiglitazone (red line). Values are expressed as mean±SEM (tunicamycin n=3, rosiglitazone n=4). * highlights statistically significant result.

a)

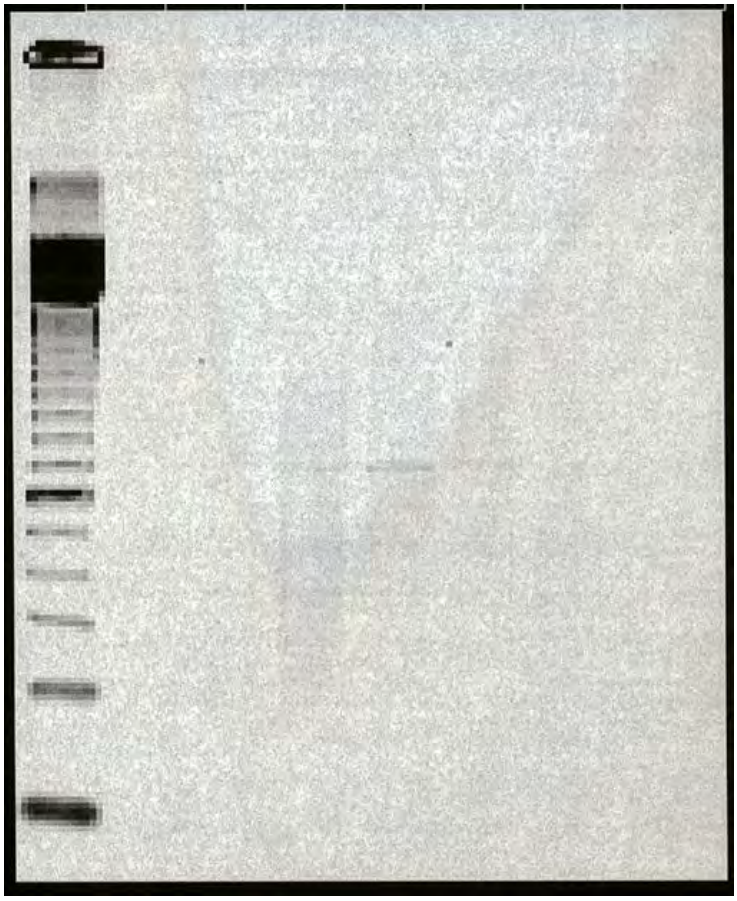

b)

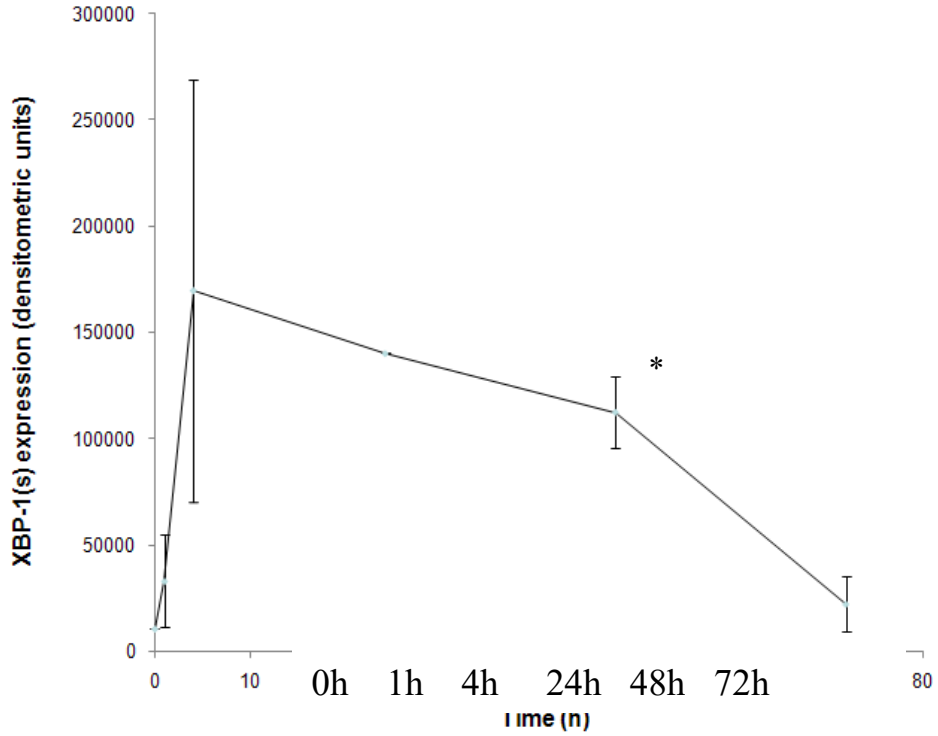

Fig 3.3.3: The effect of rosiglitazone on activation of XBP-1 in A7r5 cells
(a) Representative PCR gel showing activation of XBP-1 with rosiglitazone (b) Densitometry data showing activation of XBP-1 after A7r5 cells were treated with 10µM rosiglitazone for the indicated times. Values are expressed as mean±SEM. (Data was obtained with the help of Luke Richard, BSc BMS 2008)

3.3.3 The effects of rosiglitazone and thapsigargin on SERCA2b mRNA expression in MM6 monocytic cells

MM6 cells were treated with DMSO (0.1%), rosiglitazone (1 or 10μM) or thapsigargin (100nm) for 1-72 hours. mRNA from these cells was analysed semi-quantitatively by real-time RT-PCR. As shown in fig 3.3.4, levels of SERCA2b mRNA expression were increased following pre-incubation with 1 or 10μM rosiglitazone for 24 hours or more ($P<0.05$ t-test) but not for shorter time points or with DMSO. The effect did appear to be dose-dependent; 72 hour incubation with 10μM rosiglitazone induced a greater SERCA2b upregulation than 1μM (215.0 ± 30.9% vs. 138.7 ± 5.7% basal; $n \geq 3$; $p < 0.05$ t-test). Incubation with thapsigargin for short time periods (1-4hrs) saw no change, however upregulation of SERCA2b gene expression was seen at 24 hrs with a 3-fold increase seen after 48hrs (310.0±18.2% basal; n=3; $p<0.05$ t-test). SERCA2b mRNA expression decreased greatly after 72 hour incubation; however, it should be noted that after this duration, thapsigargin treatment has caused many if not most of the cells to have undergone apoptosis (see chapter 2).

3.3.4 The effect of rosiglitazone on SERCA2b gene expression in vascular smooth muscle cells

A7r5 cells were treated with DMSO (0.1%) or rosiglitazone (1 or 10μM) for 0-72 hours. cDNA from these cells was analysed semi-quantitatively by real-time PCR. As shown in fig 3.3.5, while incubation with DMSO had no effect at any time point, incubation with 1μM rosiglitazone correlated with an increase in SERCA2b gene expression after 48 hrs but not at shorter time intervals (48hrs = 131.3±20.3%; 72hrs = 147.8±11.7% basal, $P<0.05$ for 72hrs t-test). Pre-incubation with 10μM rosiglitazone showed SERCA2b upregulation after ≥24hrs with a peak at 72 hours (161.7±11.0% basal, $p<0.05$ t-test).

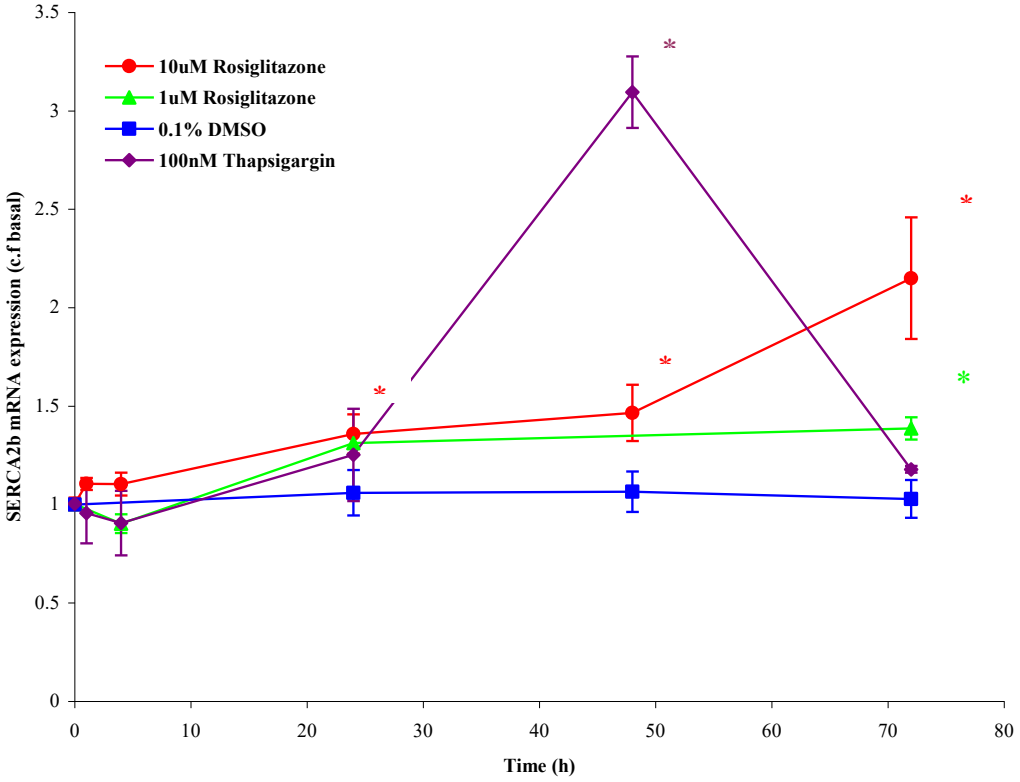

Fig 3.3.4: The effect of rosiglitazone and thapsigargin on SERCA2b mRNA expression in monocytes

MM6 cells were treated for 0-72hrs with either 0.1% DMSO (blue line), 1µM rosiglitazone (green line), 10µM rosiglitazone (red line) or 100nM thapsigargin (purple line). RNA was extracted and converted to cDNA before undergoing semi-quantitative analysis by real time PCR (Expression of SERCA2b was compared with the housekeeping gene GAPDH). Values are expressed as the mean± SEM (n= 3-6).

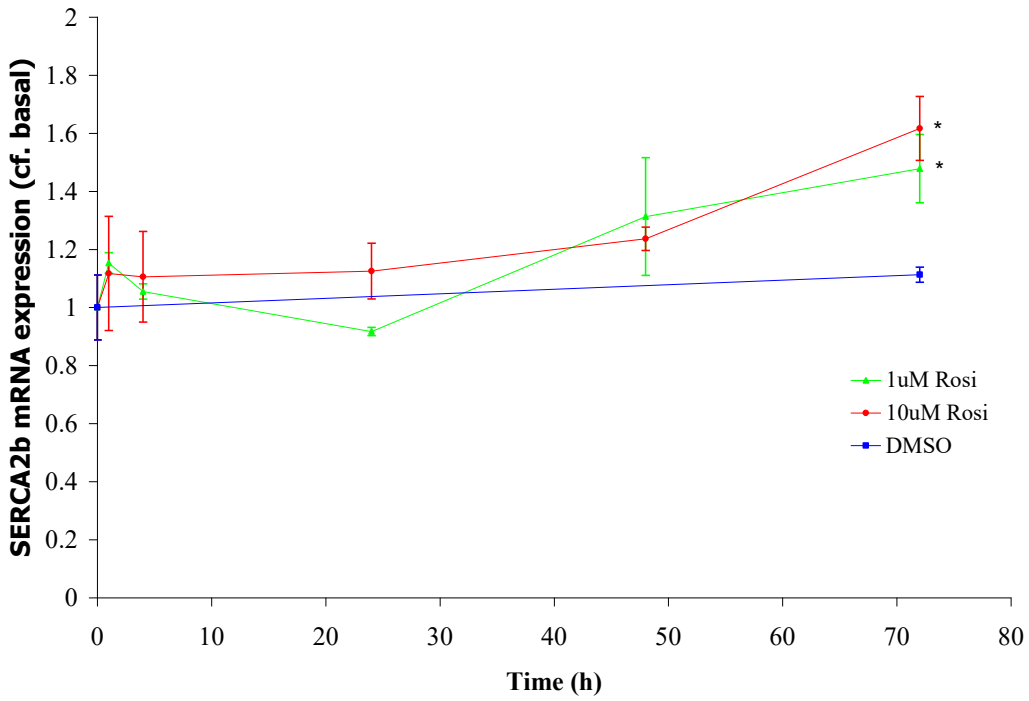

Fig 3.3.5: The effect of rosiglitazone on SERCA2b mRNA expression in vascular smooth muscle cells

A7r5 cells were treated for 0-72hrs with either 0.1% DMSO (blue line), 1µM rosiglitazone (green line) or 10µM rosiglitazone (red line). RNA was extracted and converted to cDNA before undergoing semi-quantitative analysis by real time PCR (Expression of SERCA2b was compared with the housekeeping gene rat GAPDH). Values are expressed as the mean± SEM (n= ≥2). * highlights statistically significant results.

3.3.5 The effect of rosiglitazone on SERCA2b protein expression in MM6 monocytic cells

To confirm that rosiglitazone-induced changes in mRNA expression were translated to the protein level, total protein extracts were prepared from MM6 cells(see method 3.2.7), and were treated with DMSO (0.1%) or rosiglitazone (1 or 10μM) for 0-48 hours. Western blotting was conducted using antiSERCA2b antibody to detect the expression of SERCA2b protein followed by subsequent densitometrical analysis of the immunogenic bands. As shown in fig 3.3.6, while incubation with DMSO had no effect at any time point (data not shown), treatment with 10μM rosiglitazone was associated with a statistically significant increase in SERCA2b protein expression at 24h (2.36±0.50 x basal; $p<0.05$) and 72h (2.70±0.61 x basal; $p<0.05$), but not after shorter durations of treatment.

3.3.6 The effect of extended incubation (72 hrs) with rosiglitazone on calcium-ATPase activity in microsomes prepared from MM6 monocytic cells

To investigate whether rosiglitazone-induced increases in mRNA and protein expression were associated with increased SERCA2b enzymatic activity, microsomes were prepared from MM6 cells)see method 2.2.7) that had been treated with DMSO (0.1%), rosiglitazone (1 or 10μM) or thapsigargin (100nM) for 72 hours before analysis with the coupled enzyme Ca^{2+}ATPase assay employed in chapter 2. As figure 3.3.7 shows, extended treatment with 1μM rosiglitazone caused a non-significant 2-fold increase in microsomal Ca^{2+}ATPase activity (0.039μmoles/mg/min compared with 0.018 μmoles/mg/min for control, n=8, $p>0.05$ t-test). However, treatment with 10μM rosiglitazone caused a statistically significant ~6-fold increase in activity (0.043μmoles/mg/min compared with 0.018 μmoles/mg/min for control, n= 7, $p<0.05$ t-test).

(a)

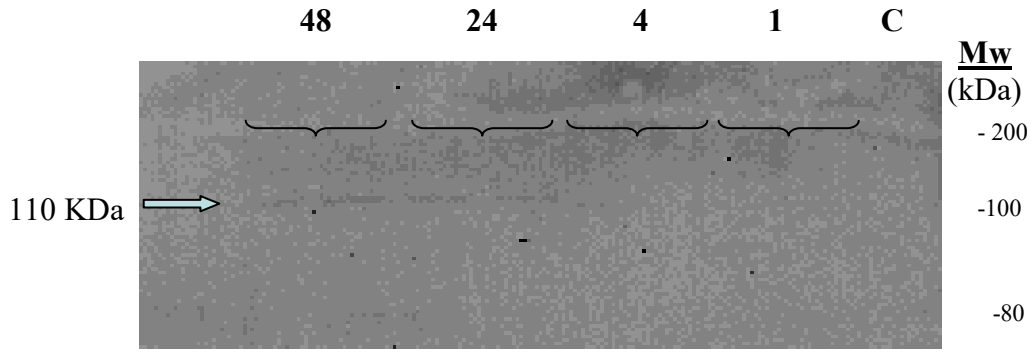

(b)

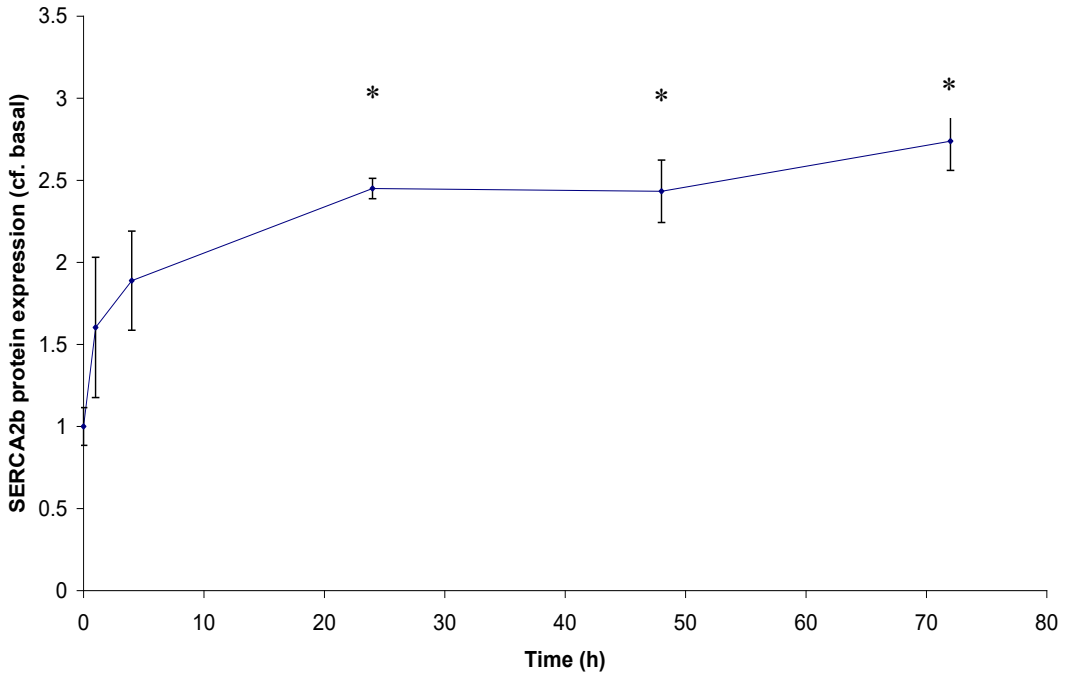

Fig 3.3.6: Effect of rosiglitazone on SERCA2b protein expression
(a): Representative blot of SERCA2b protein expression (gel is representative of 4 separate experiments). (b): Summary of densitometric data from all 4 experiments. MM6 cells were treated with rosiglitazone (10µM) or with DMSO (0.1% v/v – band labelled C on blot) for 0-72hrs (48 hrs only shown for DMSO). Values are expressed as mean±SEM (n=4). * highlights statistically significant result.

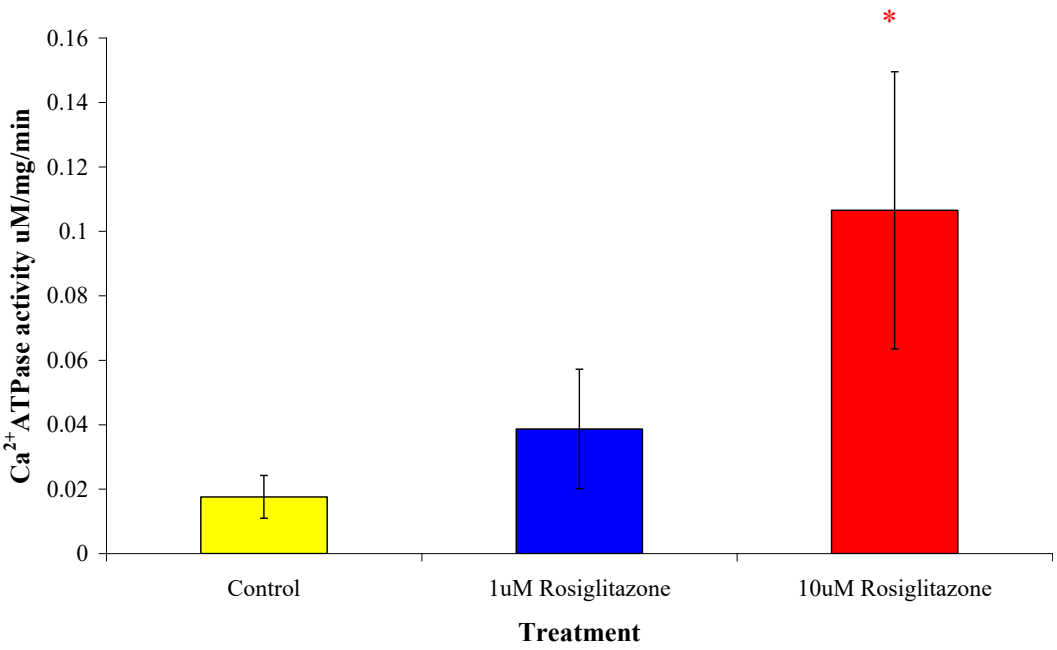

Fig 3.3.7: The effect of extended incubation with rosiglitazone (72hrs) on calcium-ATPase activity

MM6 cells were left untreated (yellow bar) or were treated for 72hrs with 1µM rosiglitazone (blue bar) or 10µM rosiglitazone (red bar). Microsomes were then prepared from these treated cells and Ca^{2+}ATPase assays conducted. Values are expressed as the mean± SEM (n= 7-8). (Data was obtained with the help of Jose Ruffino, BSc BMS 2008).

3.4 Discussion

As discussed in Chapter 1, $[Ca^{2+}]_{cyto}$ is routinely kept at very low levels ($[Ca^{2+}]_{cyto}$ <0.1μM), due to the cytotoxic nature of the cation if elevated levels persist. Stimulation of the cell by a specific agonist ensures Ca^{2+} is released into the cytoplasm from internal stores such as the ER, or from external sources, but homeostatic agents such as Ca^{2+} sequestrating „pump" enzymes from the SERCA subgroup of the P-type ATPase phylogenetic family ensure that any increase in $[Ca^{2+}]$cyto is seen only transiently. SERCA2b, the protein of interest to the current study, has subtly different functional characteristics to other SERCA enzymes (Lytton *et al*, 1992). The extra M11 transmembrane domain of SERCA2b ensures that this enzyme"s activity is controlled by Ca^{2+} homeostatic agents such as calreticulin in the ER lumen, so that it acts not only to terminate agonist-induced Ca^{2+} transients in the cytoplasm, but also as a constant „housekeeping" agent counteracting low-level non-specific Ca^{2+} leakage from the ER (John *et al*, 1998)..

Thus, given that SERCA2b is the SERCA isoform expressed in non-muscle ER (Gunteski-Hamblin *et al*, 1989), the short term incubation (5-30mins) of monocytic cells with rosiglitazone that has previously been shown to cause increases in $[Ca^{2+}]_{cyto}$ (Singh *et al*, 2005) may tentatively be linked to rosiglitazone-induced inhibition of SERCA2b. This study corroborates this, and data has been presented to suggest that this increase in $[Ca^{2+}]_{cyto}$ is due to dose-dependent inhibition of the Ca^{2+}ATPase SERCA2b (chapter 2). It has also been shown in chapter 2 of the current study that extended incubation (72hrs) with rosiglitazone leads to a restoration of normal calcium homeostasis. The current chapter provides evidence for the supposition that the monocytic cell and the vascular smooth muscle cell have the ability to respond over time to ER stress, as caused by inhibition of Ca^{2+} sequestration, via triggering of an UPR.

The consequences of the UPR can be two-fold: either upregulation of UPR target genes leads to a restoration of cellular function and the cell survives; or the response is not sufficient to restore normal cellular function and cell death is triggered. This effect is evident in the actions of the natural PPARγ ligand PGJ_2 on pancreatic β-cells. PGJ_2 induces UPR in pancreatic β-cells resulting in the inhibition of inflammatory cytokine production, and ultimately providing a cytoprotective anti-inflammatory effect (Weber *et al*, 2004b). However, when UPR activation is

prolonged, cytoprotective effects cease to work and β-cell apoptosis is initiated (Chambers *et al*, 2006).

There is a wealth of literature available showing the induction of UPR by two of the reagents used as positive controls in this study, namely tunicamycin and thapsigargin. As figure 3.1.1 illustrates, there are numerous „arms" of the unfolded protein response and any one of these can and have been used as markers for the induction of ER stress. In this study, the marker of choice was alternative splicing (and therefore activation) of the transcription factor XBP-1 (Shang, 2005). As expected, incubation of monocytic cells with tunicamycin and thapsigargin led to initiation of ER stress as attested by elevated levels of spliced XBP-1 (figs 3.3.2 and 3.3.3).

As discussed earlier, the contradictory nature of recent literature on the subject has not permitted definitive establishment of whether rosiglitazone triggers the UPR. Therefore, it is very important to note that the current study has shown incubation with 10μM rosiglitazone for 1 hour or more is associated with a three-fold increase in XBP-1 activation ($p<0.05$), indicating that the disruptive effect the drug has on the ER – an inhibition of SERCA2b's „housekeeping" role, which leads to unchecked leakage of Ca^{2+} from the ER lumen into the cytoplasm, and therefore disturbance of cellular Ca^{2+} homeostasis – **does** induce a cellular UPR. Comparable incubation with 1μM rosiglitazone produced only a very minor, non-significant increase in this UPR marker. Therefore this study may be the first to show that extended incubation with Rosiglitazone induces the ER stress response in monocytic cells.

Through bioinformatics analysis, SERCA2b has been shown in the current study to be a UPR-inducible protein via the identification of 2 UPRE-like and 3 ERSE-like sequences in the SERCA2 promoter (see Fig 3.3.0). This is in accord with previous studies where treatment of PC12 cells with thapsigargin and with tunicamycin, two agents known to initiate a stress response, have been shown to cause an increased SERCA2b mRNA expression of approximately 3-4 fold (Caspersen *et al*, 2000), which corresponded with increases in BiP and CHOP expression. Thapsigargin has also been seen to increase SERCA2 mRNA expression (~4-5 fold) in vascular smooth muscle cells, again with a corresponding increase in BiP expression (Wu *et al*, 2000). The current study has shown thapsigargin to rapidly increase SERCA2b

gene expression within 24 hours, peaking at 48 hours. Incubation for longer time periods (72 hrs) sees a dramatic drop in SERCA2b mRNA expression which may be due to the cytotoxicity of the reagent causing cellular apoptosis - as shown previously (see chapter 2).

A few recent studies have looked at the effect of rosiglitazone on SERCA2b gene expression. Rosiglitazone treatment (10μM) of ventricular myocytes was seen to induce an approx 1.5 fold increase in SERCA2 mRNA levels (Shah *et al*, 2004). However, Shah *et al* did not identify the mechanism by which this effect was brought about. Another recent study has shown that rosiglitazone increases SERCA2 mRNA expression ~10 fold in platelets. Interestingly this effect was only seen when the drug was used to treat bone marrow-derived CD34+ stem cells which were then stimulated to differentiate into megakaryocytes, and not when treating platelets directly (Randriamboavonjy *et al*, 2008). In the same study, 12 weeks rosiglitazone therapy of diabetic individuals also led to an increase in SERCA2 activity (Randriamboavonjy *et al*, 2008). In support of this data, it has been shown in the current study that pre-incubation with 10μM rosiglitazone for extended time periods (≥24 hours) caused significant increases in SERCA2b mRNA upregulation in both monocytes and vascular smooth muscle cells. This effect was dose-responsive: 1μM also induced statistically significant increases in SERCA2b expression in both cell types, but to a lesser degree than the higher drug concentration. It should be stressed, however, that while the above literature discuss the effects of rosiglitazone on SERCA2 (Shah *et al*, 2004; Randriamboavonjy *et al*, 2007), neither of these studies investigated - or considered their findings to be linked to - effects of the drug on the UPR. Therefore, this study appears to be the first to highlight the link between rosiglitazone‟s initiation of ER stress **and** its subsequent upregulation of the UPR-inducible gene SERCA2b.

Increased mRNA expression, while indicative of an increased production of the protein by the gene of interest, may not always correspond with such an increase. Treatment of ventricular myocytes with rosiglitazone, seen above to induce increased SERCA2 mRNA, however, was indeed found to be associated with a ~3-fold increase in SERCA2 protein (Shah *et al* 2004). Here, we show that comparative treatment (10μM rosiglitazone) in monocytic cells also leads to ~2.5-fold increases in SERCA2b protein expression following incubation for 24 hours or more.

Just as increased mRNA expression may not always lead to increased protein translation, the newly acquired protein does not necessarily lead to an improvement in cell function. In the case of SERCA2b, any increase in SERCA2b protein must be accompanied by an increase in SERCA2b pump activity for any improvement in cell function to be established. Larsen *et al* have shown that ER stress imposed by three distinct mechanisms (by the agents EGTA, tunicamycin and dithiothreitol) caused a 2 to 3-fold increase in the Ca^{2+} uptake of microsomes prepared from PC12 cells treated with the above agents (Larsen *et al*, 2001), while Shah *et al* reported that increased SERCA2 expression was associated with accelerated Ca^{2+} sequestration within the cardiomyocytes that were of the cells of interest to their study (Shah *et al*, 2004). Randriamboavonjy *et al* have also shown in an extended patient study that 12 week treatment of diabetic patients with rosiglitazone led to an increased platelet SERCA2 Ca^{2+}ATPase activity (Randriamboavonjy *et al*, 2008).

In line with these observations, the current study initially established a dose-dependent inhibition of SERCA2b following incubation with rosiglitazone for up to 30 minutes (chapter 2), but when monocytic cells were subsequently treated for an extended time period (72hrs) and the ATPase activity of the subsequently produced microsomes was established via the same enzymatic assay, treatment with 1μM rosiglitazone for 72 hours led to a 2-fold increase in ATPase activity (non-significant), while treatment with 10μM rosiglitazone initiated a statistically significant 6-fold increase in ATPase activity. This strongly suggested that extended incubation with the drug leads to an improved SERCA2b activity and subsequently in the calcium sequestration activity of the cell.

Finally, as discussed previously, tunicamycin and thapsigargin both impose severe stresses on the cell which leads to initiation of the unfolded protein response. However, unlike rosiglitazone, which has also been shown to promote ER stress responses, the stress is more severe or prolonged, cell survival mechanisms fail and the cell undergoes apoptosis (Carlberg *et al*, 1996). This study has shown via apoptosis assays that thapsigargin induces apoptosis within 24hrs (chapter 2). This cytotoxic effect is also seen following semi-quantitative analysis of SERCA2b mRNA where increased SERCA2b mRNA expression ceases dramatically at 72 hours, presumably due to cell apoptosis following prolonged incubation with

thapsigargin. Work conducted in our laboratory also shows tunicamycin to have the same effect – data not shown (L. Atkin-personal correspondence). However, it is not yet clear why rosiglitazone-induced UPRs result in restoration of normal cell physiology, while thapsigargin/tunicamycin-induced UPRs result in cell death. This issue will be explored further in the General Discussion chapter

3.4.1 Summary

Rosiglitazone has been shown here to induce alternate splicing of XBP-1, which is indicative of activation of the ER stress pathway. Further, through bioinformatics analysis, the presence of UPREs and ERSEs in the SERCA2 promoter was determined, suggesting the likelihood that the SERCA2 gene is a target for UPR transcription factors such as XBP-1. In this chapter, it was also documented that extended incubation with rosiglitazone (≥24 hrs) led to an increased SERCA2b mRNA expression in two cell types important in the pathogenesis of diabetes, namely monocytes and vascular smooth muscle cells. This increase in SERCA2b mRNA corresponded with evidence of increased translation into SERCA2b protein and an increased Ca^{2+}-ATPase activity in microsomes of cells treated for 72h with 10μM rosiglitazone. As SERCA2b is the predominant ER Ca^{2+} pump isoform in non-muscle and smooth muscle cells, this increased activity is likely to correspond to increased expression of active SERCA2b protein, and to a greater capacity for Ca^{2+} sequestration, and thence restoration of normal Ca^{2+} homeostasis.

In summary, the above data suggest that rosiglitazone does induce ER stress and the resultant activation of the unfolded protein response leads to upregulation of UPR inducible genes and a resultant increase in the ability of the cells to sequester Ca^{2+} in their ER lumen. This therefore is suggested to be the mechanism behind the restoration of calcium homeostasis seen in chapter 2 and provides further evidence, alongside the lack of apoptosis, that rosiglitazone may have a cytoprotective rather than cytotoxic effect in the cell lines studied here.

Chapter 4

The effects of rosiglitazone on vascular contractility and endothelial function in rabbit aortic rings

4.1.1 Introduction

As previously discussed, Ca^{2+} has a very important role in maintaining the normal functioning of the cell, and pertubations in cellular Ca^{2+} homeostasis are at the forefront of many disease processes including T2D. The current study has shown that rosiglitazone plays a role in correcting and maintaining such Ca^{2+} homeostasis under conditions of cellular stress in the two cell types investigated in this study. As these particular cell types and consequences of their impaired functionality are of particular importance with regards to T2D, in this chapter this work will be extended into investigation of the disruption rosiglitazone exerts on a relevant tissue, namely the arterial wall. The arterial wall is thought to be a suitable candidate for these experiments as it is a tissue whose intima/media consists almost entirely of vascular smooth muscle cells.

As described in Chapter 1, T2D is a condition intrinsically linked with cardiovascular disease and in particular atherosclerosis, leading to an increased morbidity rate in diabetic patients (Bagi *et al*, 2004). In fact, diabetes is associated with an elevated risk of atherosclerosis; with over 75% of individuals with T2D dying as a result of this disease compared to 40% in the general population (Aronson & Rayfield 2002).

While the development of atherosclerosis in diabetic patients is dependent on a multitude of factors, an important causative factor linking T2D with atherosclerosis is endothelial dysfunction-associated hypertension. The endothelium is vital in regulating vascular tone, and controls the balance between vasoconstriction and vasorelaxation via production of various vasoactive substances (Fig 4.1.1 and 4.1.2). Briefly, ligands that have traversed the endothelium induce generation of IP_3 at the plasma membrane of vascular smooth muscle cells, and induce subsequent release of Ca^{2+} from their SR. Activation of the Ca^{2+}/calmodulin complex ultimately leads to the phosphorylation of myosin light-chains, a process that mediates smooth muscle cell contraction and vasoconstriction. In contrast, diffusion of NO (which is generated by adjacent endothelial cells) to vascular smooth muscle cells leads ultimately to sequestration of Ca^{2+} back into the SR, dephosphorylation of myosin light-chains and thus to muscle cell relaxation and vasodilation.

Endothelial dysfunction occurs when this balance is lost, and the impaired endothelium-dependent vasorelaxation which results is one of the first steps in the

development of atherosclerosis. Many cardiovascular risk factors, including hypertension, arterial stiffness and increased LDL cholesterol, are associated with impaired endothelial function suggesting that such endothelial damage is contributory to the development of atherosclerosis (Cohen *et al*, 1995). In a progressively detrimental cycle, advancement of atherosclerosis then exacerbates hypertension in diabetic individuals as the larger blood vessels in the body become rigid and less able to expand in response to demands for increased blood flow, causing elevated systolic blood pressure (McFarlane *et al*, 2005; McEniery *et al*, 2008).

In order to maintain normal endothelial function, the endothelium produces nitric oxide (NO), a very potent vasodilator (Ignarro *et al*, 2002). Endothelial nitric oxide synthase (eNOS) catalyses the conversion of the amino acid L-arginine into NO and L-citrulline. The NO that is produced in the endothelial cell diffuses into the vascular smooth muscle cell where it activates the enzyme soluble guanylate cyclase, which catalyses the formation of the second messenger cyclic guanosine 3,5-monophosphate (cGMP; Ignarro *et al*, 2002). This activates cGMP-dependent protein kinase PKG, which initiates numerous events such as decreasing VSMC $[Ca^{2+}]_{cyto}$ via phosphorylation of the SERCA2b accessory protein phospholamban (Koller *et al*, 2003), and hence enhanced sequestration into the SR by SERCA2b (Cohen *et al*, 1999), and dephosphorylation of myosin light chains - both of which ultimately result in VSMC relaxation. Aside from its role in endothelium-dependent vasodilation, NO has numerous other anti-inflammatory functions such as inhibition of vascular smooth muscle cell proliferation, platelet aggregation and thrombosis, leukocyte adhesion and inflammation (Landmesser *et al*, 2004).

In addition to NO, the endothelium produces certain vaso-relaxatory prostaglandins (e.g. prostaglandin I_2 - PGI_2) as well as vasoconstricting factors including vasoconstricting prostaglandins (eg the arachidonic acid metabolite prostaglandin enderoperoxide - PGH_2) (Camacho *et al*, 1998).

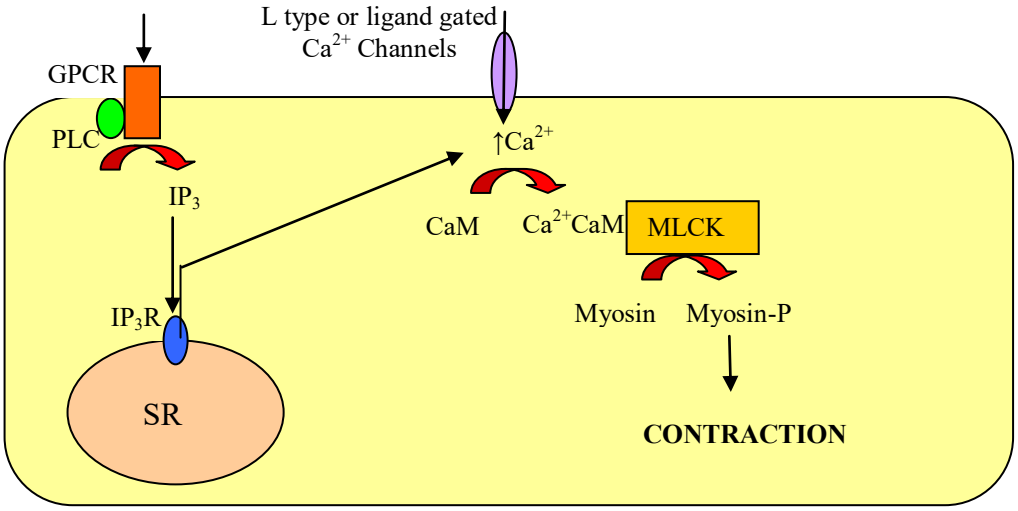

Key
GPCR – G-protein cell receptor
PLC- Phosphokinase C
IP_3 - Inositol 1,4,5-triphosphate
IP_3R - Inositol 1,4,5-triphosphate receptor
CaM -Calmodulin
$Ca^{2+}CaM$ - Calcium calmodulin complex
MLCK - myosin light chain kinase
SR - sarcoplasmic reticulum

Fig. 4.1.1 Vascular smooth muscle contraction is initiated by agonist-induced G-protein activation

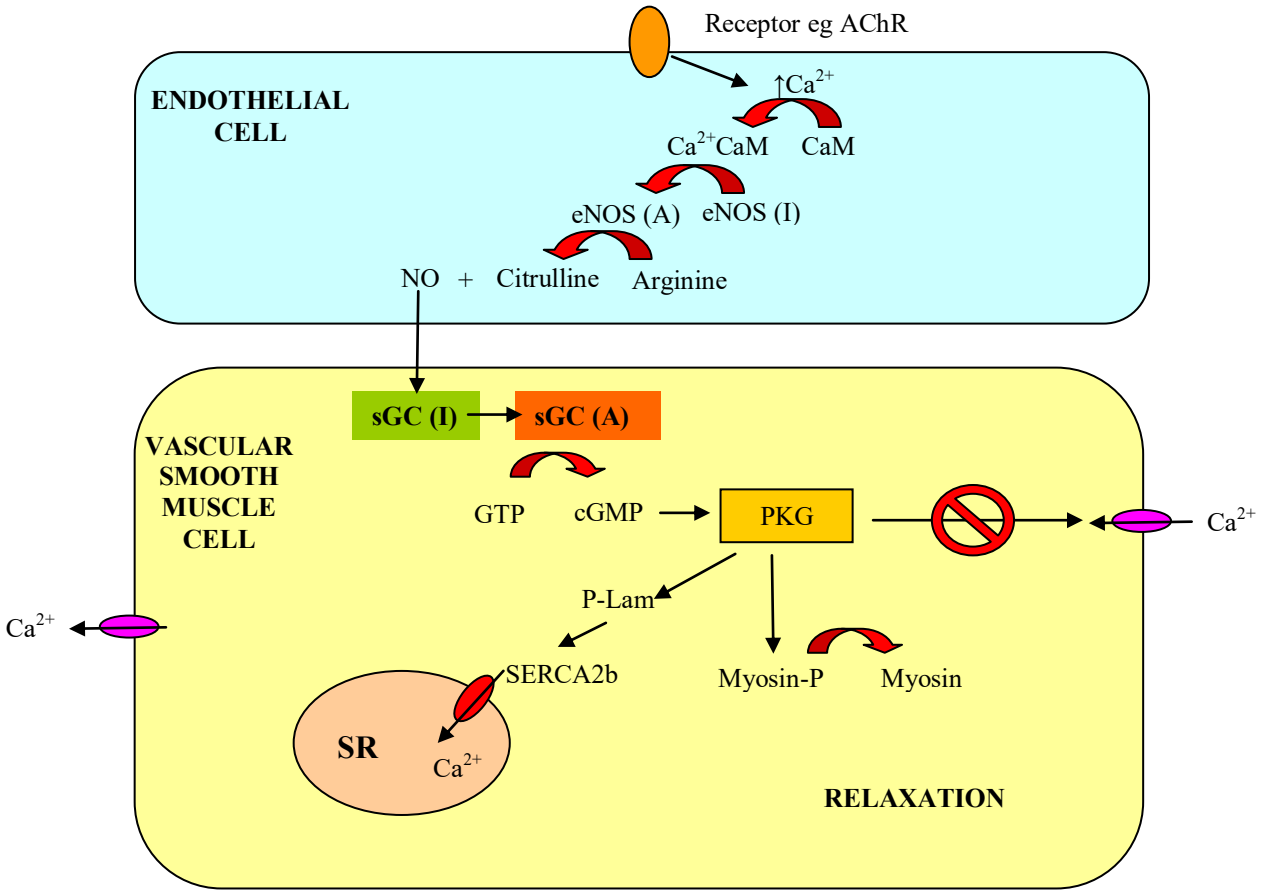

Key
AChR - acetylcholine receptor
CaM -Calmodulin
Ca^{2+}CaM - Calcium calmodulin complex
eNOS - endothelial nitric oxide synthase
(I) – inactive (A) - active
NO - nitric oxide
sGC - soluble guanylate cyclase
GTP - guanosine 5-triphosphate
cGMP - cyclic guanosine 3,5-mono-phosphate
PKG - phosphokinase G
SR - sarcoplasmic reticulum
SERCA2b - sarcoendoplasmic reticulum calcium ATPase isoform 2b
P-Lam - Phospholamban

Fig 4.1.2 Endothelial nitric oxide generation and subsequent vascular smooth muscle relaxation.

Endothelial function and PPARγ agonists

As described in Chapter 1, T2D is a complex metabolic disorder, and treatment of its metabolic complications has recently involved the oral anti-hyperglycaemic agents, the Thiazolidinediones (TZDs). These drugs act to increase insulin sensitisation by binding to and activating the transcription factor peroxisome proliferators-activated receptor-γ (PPAR-γ). PPAR-γ has been shown to be expressed in both vascular smooth muscle and endothelial cells (Bagi *et al*. 2004). TZDs have been associated with numerous improvements in vascular function in both animal models and human trials, but the exact mechanism by which these improvements occurred, and the extent of involvement of PPARγ, remain unclear.

In clinical studies, the TZDs, including pioglitazone and rosiglitazone, have been seen to be associated with decreases in blood pressure (Buchanan. 1995; Ryan *et al,* 2004; Majithiya *et al,* 2005; Diep *et al*, 2002), and with increases in flow-mediated dilation (Caballero *et al*, 2003; Hetzel *et al*, 2005). Rosiglitazone has also been shown to increase flow-mediated endothelium-dependent vasodilation in healthy humans within 24 hours (Hetzel *et al*. 2005). In another study, rosiglitazone was also shown to increase the vasodilatory response to acetylcholine (ACh) and improve endothelial function in diabetic individuals (Pitrosch *et al*, 2004). In animal studies, rosiglitazone treatment has been shown to decrease blood pressure and increase vasorelaxative responses to ACh and NO in carotid arteries in transgenic hypertensive mice (Ryan *et al*. 2004). Pioglitazone and rosigltazone have been shown to decrease blood pressure and normalise Ach-induced relaxation in angiotensin II (Ang II-infused hypertensive rats (however rosiglitazone alone slightly increased blood pressure in normal animals) (Diep *et al*, 2002). Rosiglitazone was also seen to improve endothelium-dependent vasodilation in hypercholesterolemic rabbits (Tao *et al,* 2003). All of the above studies show an improvement in endothelial function and thus anti-hypertensive improvements, though possibly via different mechanisms.

Importantly, it was postulated in the present study that the anti-hypertensive effects observed with TZD (and in particular rosiglitazone) treatment in previous literature (Buchanan. 1995; Ryan *et al,* 2004; Majithiya *et al,* 2005; Diep *et al*, 2002; Caballero *et al,* 2003; Hetzel *et al*, 2005) may be at least partly due to a novel mechanism: improvements in Ca^{2+} homeostasis via rosiglitazone-triggered upregulation of the UPR-inducible protein SERCA2b, as already seen on a cellular

basis in this study. Rosiglitazone-induced SERCA2b upregulation could play a vasorelaxatory role, because an enlarged pool of SERCA2b molecules may provide a mechanism for increased Ca^{2+}sequestration and therefore enhanced vasorelaxation in the blood vessels of patients undergoing rosiglitazone therapy.

This study has shown that, on a cellular level, rosiglitazone may initiate numerous beneficial effects independent of the action of PPARγ. This chapter aims to extend these observations to the tissue level, by investigating the effect of rosiglitazone on vascular reactivity, in order to determine the mechanism by which rosiglitazone may act on the endothelium and smooth muscle cell to influence changes in vascular tone

4.1.2 Aims

In Chapter 2, we saw that rosiglitazone treatment of monocytic and vascular smooth muscle cells caused initial disruption to Ca^{2+} sequestration into the ER via SERCA2b inhibition. We also saw however that this effect was reversed, and indeed cellular calcium homeostasis was restored in these cell types upon extended treatment with the drug. This was found to be due to subsequent upregulation of the SERCA2b mRNA, SERCA2b protein and hence increased SERCA2b activity. In Chapter 3, the mechanism behind this altered calcium homeostasis was determined to be via rosiglitazone‟s induction of ER stress, and resultant activation of the unfolded protein response. The subsequent upregulation of UPR inducible genes, including SERCA2b, led to a resultant functional increase in the ability of the cells to sequester Ca^{2+} in their ER lumen. In this chapter we aimed to discover whether the effects seen in the two cell types studied previously, can be mirrored/observed in an intact tissue – the artery wall.

Therefore the specific aims of this chapter were;

- To investigate the effect of rosiglitazone on aortic vascular smooth muscle tissue by measurement of agonist-induced contractility and relaxation of endothelium-denuded aortic ring samples,

- To determine the effect of rosiglitazone on endothelium-dependent relaxation of aortic tissue by measurement of agonist-induced relaxation in endothelium-intact aortic ring tissue,

- To investigate the effect of rosiglitazone on endothelium-independent relaxation of aortic tissue by measurement of agonist-induced relaxation in endothelium-intact aortic ring tissue and following blockade of eNOS-catalysed generation of the endothelium-derived vasodilator NO.

4.2 Methods

4.2.1 Materials

The thoracic aorta of male New Zealand White rabbits (2-2.5kg) was removed on the morning of the experiment following the induction of terminal anaesthesia with an intravenous overdose of sodium pentobarbitone (3-5ml).

4.2.2 Tissue preparation and Isometric tension recordings

Fresh aortic tissue was placed into Kreb‟s buffer containing the following (in mmol/L) NaCl 109, KCl 2.68, KH_2PO_4 1.2, $MgSO_4.7H_2O$ 1.2, $NaHCO_3$ 25, Glucose 11 and $CaCl_2.2H_2O$ 1.5. The buffer was constantly gassed with a mixture of 95% O_2 and 5% CO_2 to maintain the pH at 7.4, and to prevent precipitation of calcium back into the buffer. All fat, blood and connective tissue was removed from the aorta before it was cut into ring segments (approx 3mm in length). For those experiments requiring denuded tissue, the endothelial was removed from each ring by rubbing the intimal surface gently with a wooden stick (Fig 4.2.1). Two stainless steel hooks were introduced through the lumen of the aortic rings, one securing the ring in place and the other was connected to a strain gauge transducer. The rings were then suspended in 8ml tissue baths containing gassed fresh Kreb‟s buffer, a resting tension of 2g set and the tissue allowed to equilibrate for 1 hour with fresh buffer being introduced at regular intervals. Analogue to digital conversion was provided by MacLab hardware/software and changes in isometric tension displayed on a computer.

To test the contractile viability of the tissue it was first exposed to Kreb‟s buffer containing a high concentration of K^+ (70mM). Following depolarisation and maximal contraction the tissue was again rinsed with fresh standard Kreb‟s buffer. Once a baseline tension was re-established the tissues were exposed to a series of phenylephrine (PE; 10^{-6}M) addition and wash steps to condition the tissue and to obtain a repeatable contractile response to PE. For all rings, subsequent to contraction with PE, acetylcholine (ACh; 10^{-6}M) was added to the bath to confirm the presence/absence of endothelium. Experiments were then conducted as detailed below. Contractile responses to PE were expressed as a percentage of the maximum

contraction induced by K^+ (70mM), while relaxation responses were expressed as a percentage of the PE-induced contraction.

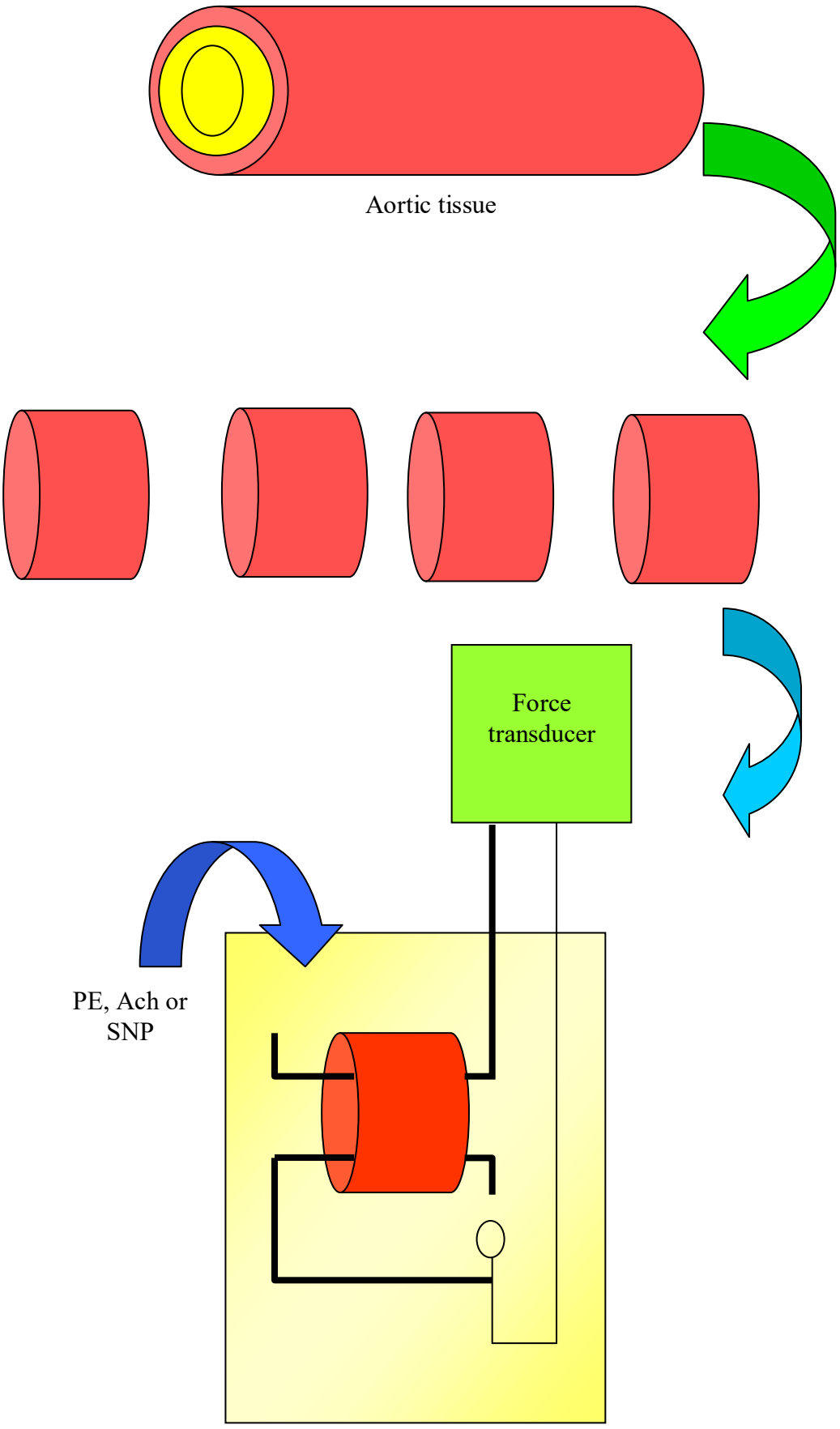

Fig 4.2.1 Measurement of Isometric Tension in Arterial Tissue. Aortic tissue was cut into rings, denuded or left intact then attached to a force transducer and suspended in Krebs buffer prior to addition of phenylephrine (PE), acetylcholine (Ach) or sodium nitroprusside (SNP)

4.2.3 Incubation of aortic ring tissue

For rings incubated for 4 or 24 hours, aortic tissue was cleaned and cut into rings, prior to being added to tissue culture media ±DMSO or rosiglitazone. The tissue culture medium used to incubate aortic tissue was DMEM (supplemented with 10% FCS, 10% newborn calf serum and penicillin-streptomycin-glutamine (PSG). Tissue was incubated overnight in vented falcon-cell culture flasks at 37°C in a humidified atmosphere with 5% CO_2. Isometric tension measurements were made the following day.

4.2.3.1 Contraction responses in endothelium-denuded aortic tissue

For shorter incubations (1 hour), aortic ring samples were endothelium-denuded prior to incubation with either vehicle (DMSO 0.1% v/v) or rosiglitazone (1 or 10μM) for 1 hour. For longer incubations, aortic ring samples were incubated with DMSO or rosiglitazone in DMEM for the required timescale (4 or 24 hours respectively) then endothelium-denuded prior to experiment. Following equilibration tissues were exposed to cumulative concentrations of PE (10^{-9}–10^{-5}M), and contractile responses measured.

4.2.3.2 Relaxation responses in endothelium-denuded aortic tissue

For shorter incubations (1 hour), aortic ring samples were endothelium-denuded prior to incubation with either vehicle (DMSO 0.1% v/v) or rosiglitazone (1 or 10μM) for 1 hour. For longer incubations, aortic ring samples were incubated with DMSO or rosiglitazone in DMEM for the required timescale (4 or 24 hours respectively) then endothelium-denuded prior to experiment. Following equilibration tissues were contracted to 70-80% of maximum with PE (10^{-6}M). Once a plateau was established the rings were exposed to cumulative concentrations of the NO donor sodium nitroprusside (SNP; 10^{-9}-10^{-5}M), and their relaxation responses measured.

4.2.3.3 Relaxation responses to acetylcholine in endothelium-intact aortic tissue

For shorter incubations (1 hour), aortic ring samples were endothelium-denuded prior to incubation with either vehicle (DMSO 0.1% v/v) or rosiglitazone (1 or 10μM) for 1 hour. For longer incubations, aortic ring samples were incubated with DMSO or rosiglitazone in DMEM for the required timescale (4 or 24 hours respectively) then endothelium-denuded prior to experiment. Following equilibration tissues were contracted to 70-80% of maximum with PE (10^{-6}M). Once a plateau was established the rings were exposed to cumulative concentrations of ACh (10^{-9}–10^{-5}M), and their relaxation responses measured.

4.2.3.4 Relaxation responses to sodium nitroprusside in endothelium-intact aortic tissue

For shorter incubations (1 hour), aortic ring samples were endothelium-denuded prior to incubation with either vehicle (DMSO 0.1% v/v) or rosiglitazone (1 or 10μM) for 1 hour. For longer incubations, aortic ring samples were incubated with DMSO or rosiglitazone in DMEM for the required timescale (4 or 24 hours respectively) then endothelium-denuded prior to experiment. They were consecutively incubated in the presence or absence of L-NAME (300μM), an inhibitor of eNOS, for 1 hour. Following equilibration tissues were contracted to 70-80% of maximum with PE (10^{-6}M). Once a plateau was established the rings were exposed to cumulative concentrations of SNP (10^{-9}–10^{-5}M), and their relaxation responses measured.

4.2.4 Statistical analysis

All data are shown as mean±SEM. Contraction and relaxation responses were subjected to non-linear regression analysis using Graph Pad Prism 5 (GraphPad Software, La Jolla, California, USA) to provide the concentration of vasoactive agent required to give half-maximal effects (EC_{50}). Individual EC_{50} values were compared using two-sample t-tests, while multiple comparisons were carried out via one-way ANOVA (Graph Pad Prism 5), and data were deemed to be significant when $p<0.05$. R_{max} values were also compared using the one-way ANOVA.

4.3 Results

4.3.1 The effect of rosiglitazone on phenylephrine-induced contraction in endothelium-denuded rabbit aortic rings

The aim of this part of the study was to determine the effects of the PPAR-γ agonist rosiglitazone on vascular reactivity in rabbit aortic rings. Aortic ring samples were incubated with various concentrations of the drug or DMSO for one hour or for extended periods of time (4 and 24 hours) and their subsequent responses to PE measured

4.3.1.1 - 1 hour incubation

It was observed (see Fig 4.3.1) that rosiglitazone treatment for 1 hour had no effect on the tissue‟s sensitivity to PE-induced contraction at either concentration (EC_{50}[DMSO]: 132.7±21.5nM; EC_{50}[1μM rosiglitazone]: 143.6±36.8nM; EC_{50}[10μM rosiglitazone]: 136.2±15.8nM; ($p>0.05$ *v.* DMSO in both cases).

Also, the maximal degree of contraction induced was similar in all cases (R_{max}[DMSO]: 191.6±4.8% max (ie. percentage of the contraction induced by 70mM K^+); R_{max} [1μM rosiglitazone]: 189.5±7.5% max; R_{max} [10μM rosiglitazone]: 193.1.2±3.9% max; ($p>0.05$ in all cases)).

4.3.1.2 - Extended incubation (4 and 24 hours)

It was observed (see Fig 4.3.2) that extended rosiglitazone treatment for either 4 or 24 hours had no effect on the tissue‟s sensitivity to PE-induced contraction at either concentration (4 hour treatments - EC_{50}[DMSO]: 309.9±57.4nM; EC_{50}[1μM rosiglitazone]: 277.0±38.5nM; EC_{50}[10μM rosiglitazone]: 355.8±49.3nM; 24 hour treatments - EC_{50}[DMSO]: 398.5±73.8nM,; EC_{50}[1μM rosiglitazone]: 312.7±50.6nM; EC_{50}[10μM rosiglitazone]: 381.0±70.6nM; ($p>0.05$ in all cases).

Also, the maximal degree of contraction induced was similar in all cases (4 hour treatments - R_{max}[DMSO]: 139.0±4.3% max (ie. percentage of the contraction

induced by 70mM K^+); R_{max} [1µM rosiglitazone]: 133.5±3.4% max; R_{max} [10µM rosiglitazone]: 132.5.2±3.5% max; 24 hour treatments - R_{max}[DMSO]: 137.6±4.6% max; R_{max} [1µM rosiglitazone]: 133.4±4.0% max; R_{max} [10µM rosiglitazone]: 130.1±4.2% max; ($p>0.05$ in all cases)).

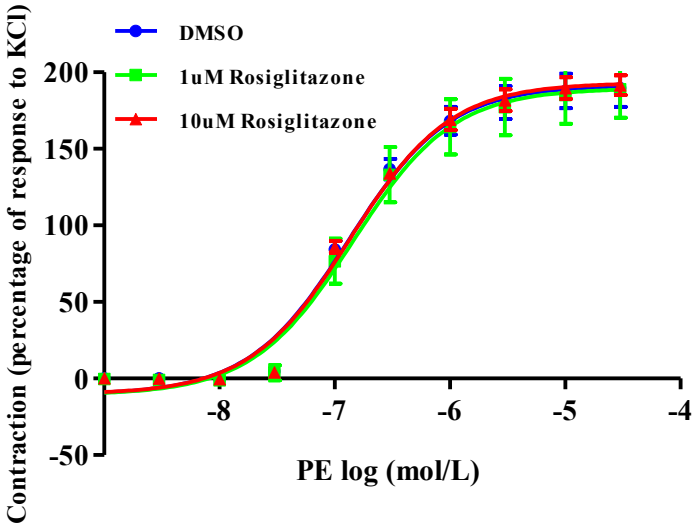

Fig 4.3.1: Short term effect of the PPAR-γ agonist, rosiglitazone on PE-induced contraction in endothelium-denuded rabbit aortic rings. Denuded aortic rings were incubated with 0.1% DMSO (blue circles), 1μM rosiglitazone (green squares) or 10μM rosiglitazone (red triangles) for 1 hour, prior to the addition of cumulative concentrations of PE. Values are expressed as a percentage of the contraction induced by K^+ (70mM) and as mean± SEM (n=3). (NB. % contraction is that compared with prior contraction with K^+ which was particularly poor in this set of experiments leading to high % contractions independent of treatment)

(a)

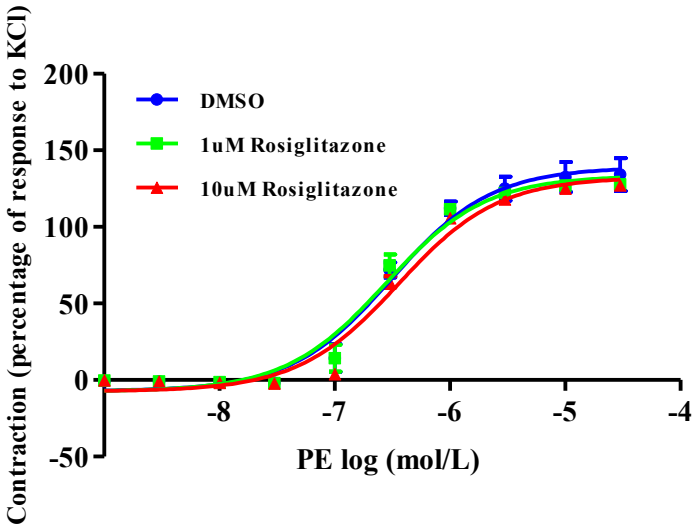

(b)

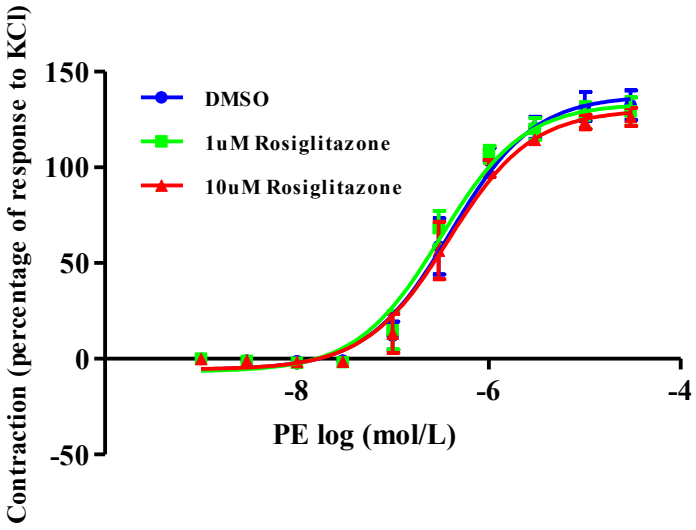

Fig 4.3.2: Long term effect of the PPAR-γ agonist, rosiglitazone on PE-induced contraction in endothelium-denuded rabbit aortic rings. Denuded aortic rings were incubated with 0.1% DMSO (blue circles) , 1μM rosiglitazone (green squares) or 10μM rosiglitazone (red triangles) for (a) 4 hours or (b) 24 hours, prior to the addition of cumulative concentrations of PE. Values are expressed as a percentage of the contraction induced by K^+ (70mM) and as the mean± SEM (**4 hour treatment** n= 4 for DMSO and 1μM rosiglitazone; n=3 for 10μM rosiglitazone ; **24 hour treatment** n= 4). (NB. % contraction is that compared with prior contraction with K^+ which was particularly poor in this set of experiments leading to high % contractions independent of treatment)

4.3.2 The effect of rosiglitazone on sodium nitroprusside-induced relaxation in PE-pre-constricted endothelium-denuded rabbit aortic rings

To investigate the relaxation response of the tissue following treatment with rosiglitazone, aortic ring samples were incubated with various concentrations of the drug or with DMSO (0.1%) for 1 hour or for extended periods (4 and 24 hours). They were then contracted with PE (10^{-6}M) followed by cumulative concentrations of SNP (10^{-9}-10^{-5}M), and their relaxation responses measured.

4.3.2.1 - 1 hour incubation

It was observed (see Fig 4.3.3) that incubation with either concentration of rosiglitazone for 1 hour slightly decreased the sensitivity of the relaxation response compared with control, although this response was not statistically significant (EC_{50}[DMSO]: 51.5±14.1nM; EC_{50}[1μM rosiglitazone]: 72.0±13.4nM; EC_{50}[10μM rosiglitazone]: 62.2±17.4nM; ($p>0.05$ *v.* DMSO in both cases). However, the maximal degree of relaxation induced was similar in all cases (R_{max}[DMSO]: 105.3±3.7% max (ie. percentage reversal of initial contraction induced by 10^{-6}M PE); R_{max} [1μM rosiglitazone]: 99.3±2.5nM% max; R_{max} [10μM rosiglitazone]: 100.8±3.7nM% max; ($p>0.05$ in all cases)).

4.3.2.2 – Extended incubation (4 and 24 hours)

It was observed that while extended treatment with 1μM rosiglitazone (4 and 24hrs) elicited no change compared to DMSO-treated samples, corresponding incubation with 10μM rosiglitazone did produce an increased relaxation response to SNP (with increases in both EC50 and Rmax values), although again these responses were not statistically significant. (<u>4hour treatments:</u> [DMSO]: EC_{50}=25.7±6.6nM/R_{max}= 107.9±3.3% max (ie. percentage reversal of initial contraction induced by 10^{-6}M PE); [1μM rosiglitazone]: EC_{50}=24.3±6.8nM/R_{max}=111.1±3.6% max; [10μM rosiglitazone] EC_{50}: 17.5±5.8nM/ R_{max}=119.0.2±4.2% max. <u>24 hour treatments:</u> [DMSO]: EC_{50}=39.8±7.4nM/R_{max}=116.1±3.0% max; [1μM rosiglitazone]: EC_{50}=43.4±10.1nM/R_{max}=117.8±3.6% max; [10μM rosiglitazone]: EC_{50}31.0±10.9nM/ R_{max}=130.1±5.7% max ($p>0.05$ *v.* DMSO in all cases)).

Interestingly, examination of the raw data for the experiments when samples were treated with 10μM rosiglitazone for 24hours revealed that one set of readings was substantially different from the remainder of the dataset (readings for the experiment carried out on 23rd April 2008 gave an EC_{50} values of >80nM). If the EC_{50} analysis was repeated after removal of this outlier, an EC_{50} of 21.6±0.7nM was obtained, which exhibited a statistically significant increase in sensitivity to SNP compared to the EC_{50} data obtained from DMSO-treated samples ($p<0.05$ v DMSO; t-test).

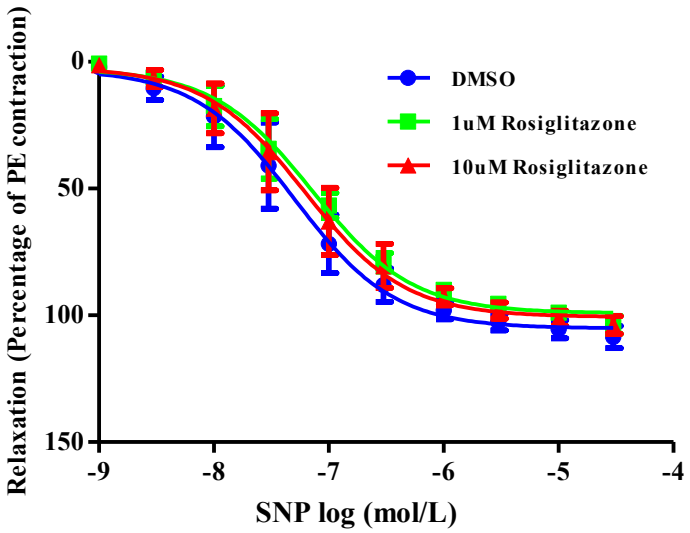

Fig 4.3.3: Short term effect of the PPAR-γ agonist, rosiglitazone on SNP-induced relaxation in endothelium-denuded rabbit aortic rings. Denuded aortic rings were incubated with DMSO (blue circles), 1µM rosiglitazone (green squares) or 10µM rosiglitazone (red triangles) for 1 hour, prior to the addition of cumulative concentrations of SNP. Values are expressed as a percentage of the contraction induced by PE (10^{-6}M) and as mean± SEM (n= 3).

(a)

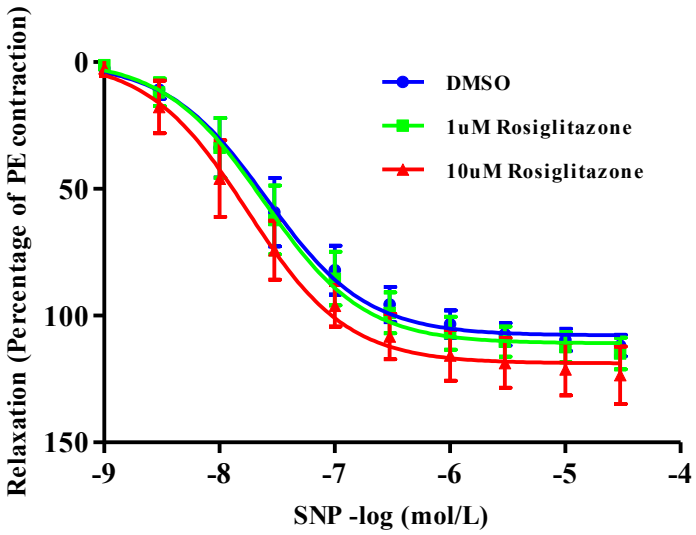

(b)

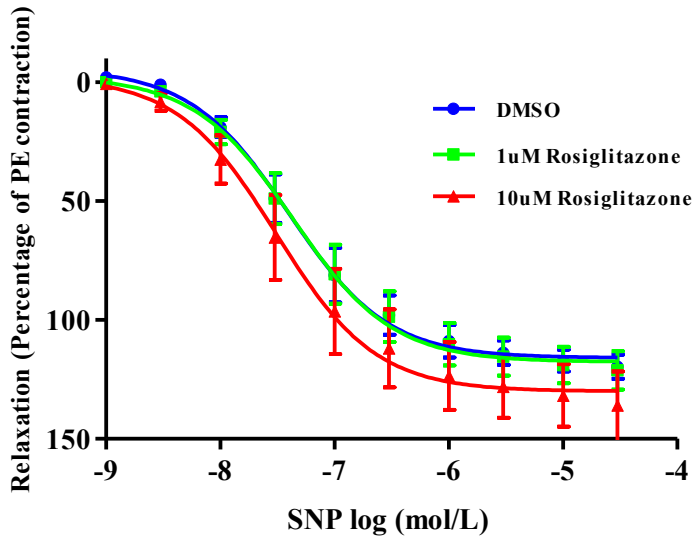

Fig 4.3.4: Long term effect of the PPAR-γ agonist, rosiglitazone on SNP-induced relaxation in endothelium-denuded rabbit aortic rings. Denuded aortic rings were incubated with 0.1% DMSO (blue circles), 1μM rosiglitazone (green squares) or 10μM rosiglitazone (red triangles) for (a) 4 hours or (b) 24 hours, prior to the addition of cumulative concentrations of SNP. Values are expressed as a percentage of the contraction induced by PE (10^{-6}M) and as mean± SEM; **4hour treatment** n= 4 for DMSO and 1μM rosiglitazone; n=3 for 10μM rosiglitazone; 24 hour treatment n= 3.

4.3.3 The effect of rosiglitazone on ACh-induced relaxation in endothelium-intact PE-pre-constricted rabbit aortic rings

To investigate the short-term effect of rosiglitazone on endothelium-dependent relaxation, aortic ring samples were incubated with various concentrations of rosiglitazone or DMSO for 1 hour or for extended periods (4 and 24 hours). They were then contracted with PE (10^{-6}M) followed by cumulative concentrations of ACh (which triggers endothelial generation of NO, and subsequent relaxation of the adjacent vascular smooth muscle – see Fig 4.1.2) and their responses measured.

4.3.3.1 – 1 hour incubation

It was observed (see Fig 4.3.5) that treatment for 1hour with either 1 or 10μM rosiglitazone caused a slight decrease in vascular relaxation compared with control, although this response was not statistically significant (EC_{50}[DMSO]: 77.2±10.7nM; EC_{50}[1μM rosiglitazone]: 84.2±13.7nM; EC_{50}[10μM rosiglitazone]: 92.6±21.5nM, $p>0.05$ *v.* DMSO in both cases).

In all cases, endothelium-intact samples did not maximally relax (ie. less than 100% reversal of the initial PE-induced contraction was seen). However, treatment with DMSO produced a statistically significant increase in maximal relaxation compared with rosiglitazone-treated tissue (R_{max}[DMSO]: 84.1±1.6% max (ie. percentage reversal of initial contraction induced by 10^{-6}M PE); R_{max} [1μM rosiglitazone]: 78.5±1.7% max; R_{max} [10μM rosiglitazone]: 78.5±2.5% max; ($p<0.05$ DMSO v. 1μM or 10μM rosiglitazone).

4.3.3.2 – Extended incubation (4 and 24 hours)

It was observed (see Fig 4.3.6) that treatment for either 4 or 24hours with either 1 or 10μM rosiglitazone caused a slight increase in the sensitivity of vascular relaxation compared with control although this response was not statistically significant (4hour treatment: EC_{50}[DMSO]: 71.5±11.6nM; EC_{50}[1μM rosiglitazone]: 66.0±7.6nM; EC_{50}[10μM rosiglitazone]: 68.6±12.7nM; 24hour treatment: EC_{50}[DMSO]:

72.7±8.4nM; EC_{50}[1μM rosiglitazone]: 63.3±7.3nM; EC_{50}[10μM rosiglitazone]: 67.4±4.7nM, p>0.05 *v.* DMSO in both cases).

Once again, in all cases, endothelium-intact samples did not maximally relax (ie. less than 100% reversal of the initial PE-induced contraction was seen). In this case, however, no overall change in maximal relaxation was seen with any treatment (4 hour treatments - R_{max}[DMSO]: 86.1±1.9% max (ie. percentage reversal of initial contraction induced by 10^{-6}M PE); R_{max} [1μM rosiglitazone]: 88.3±1.5% max; R_{max} [10μM rosiglitazone]: 86.1±2.3% max; 24 hour treatments - R_{max}[DMSO]: 81.8±1.4% max; R_{max} [1μM rosiglitazone]: 86.5±1.3% max; R_{max} [10μM rosiglitazone]: 86.7±0.9% max; (p>0.05in all cases).

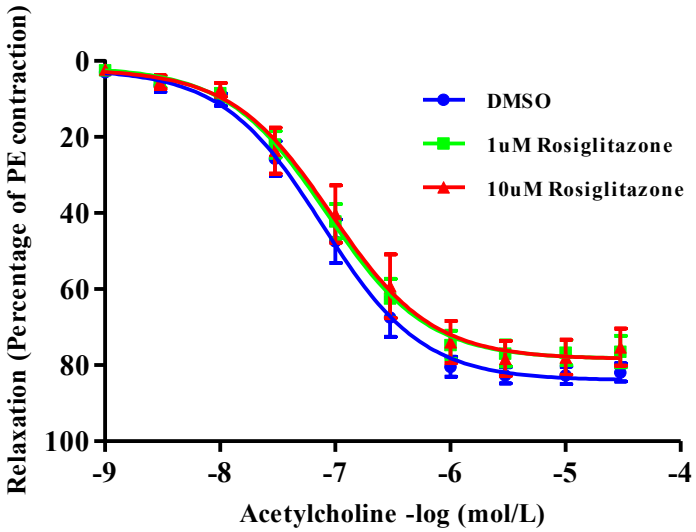

Fig 4.3.5: Short term effect of the PPAR-γ agonist, rosiglitazone on ACh-induced endothelium-dependent relaxation in intact rabbit aortic rings. Intact aortic rings were incubated with 0.1% DMSO (blue circles), 1μM rosiglitazone (green squares) or 10μM rosiglitazone (red triangles) for 1 hour, prior to the addition of cumulative concentrations of ACh. Values are expressed as a percentage of the contraction induced by PE (10^{-6}M) and as mean± SEM (n= 4 for DMSO and 1μM rosiglitazone; n=3 for 10μM rosiglitazone)

(a)

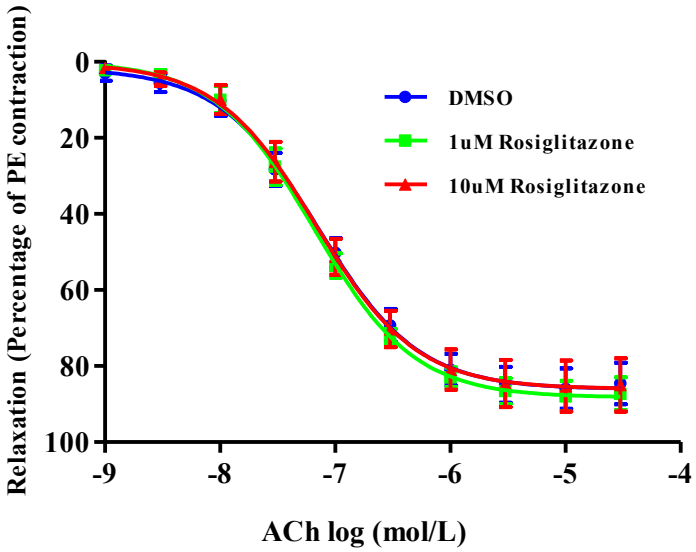

(b)

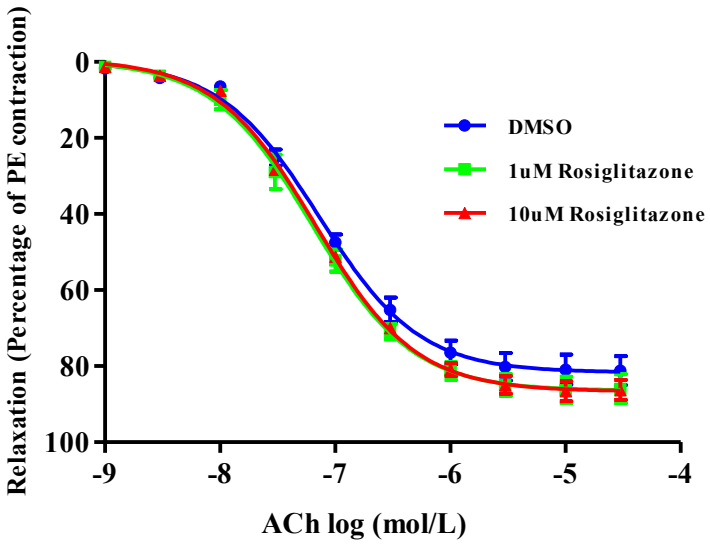

Fig 4.3.6: Long term effect of the PPAR-γ agonist, rosiglitazone on ACh-induced endothelium-dependent relaxation in intact rabbit aortic rings. Intact aortic rings were incubated with 0.1% DMSO (blue circles), 1μM rosiglitazone (green squares) or 10μM rosiglitazone (red triangles) for (a) 4 hours or (b) 24 hours, prior to the addition of cumulative concentrations of ACh. Values are expressed as a percentage of the contraction induced by PE (10^{-6}M) and as mean± SEM (4 hour treatment n=3; 24 hour treatment n=4 for DMSO and n=3 for 1μM and 10μM rosiglitazone).

4.3.4 The effect of rosiglitazone on SNP-induced relaxation in PE pre-constricted endothelium-intact rabbit aortic rings in the presence of L-NAME

Endothelium-intact aortic ring samples were incubated with various concentrations of rosiglitazone or DMSO (1, 4 or 24 hours), and then with L-NAME (300μM), an inhibitor of eNOS, for 1 hour. They were then contracted with PE (10^{-6}M) followed by cumulative concentrations of SNP (10^{-9}-10^{-5}M), and their responses measured.

4.3.4.1 – 1 hour incubation

It was observed (see fig 4.3.7) that treatment for 1hour with either 1 or 10μM rosiglitazone caused a slight decrease in vascular relaxation compared with control, although this response was not statistically significant. It should be noted that absolute relaxation values were lower in L-NAME-treated samples, but nevertheless a similar trend in terms of rosiglitazone-induced decreases in vascular relaxation was seen in either the presence or the absence of L-NAME. (1hour treatment [-L-NAME]: EC_{50}[DMSO]: 66.7±9.3nM; EC_{50}[1μM rosiglitazone]: 82.3±9.5nM; EC_{50}[10μM rosiglitazone]: 86.1±10.0nM; 1hour treatment [+L-NAME]: EC_{50}[DMSO]: 41.2±3.8nM; EC_{50}[1μM rosiglitazone]: 50.8±4.7nM; EC_{50}[10μM rosiglitazone]: 58.1±6.7nM, $p>0.05$ *v.* DMSO in both cases).

Full relaxation (ie. approximately 100% R_{max}) was achieved in all cases, but no overall change in maximal relaxation was seen with any treatment (1 hour treatment [-L-NAME]: R_{max}[DMSO]: 97.5±1.7% max (ie. percentage reversal of initial contraction induced by 10^{-6}M PE); R_{max}[1μM rosiglitazone]: 94.8±1.4% max; R_{max}[10μM rosiglitazone]: 94.2±1.3% max; 1hour treatment [+L-NAME]: R_{max}[DMSO]: 96.8±0.9% max; R_{max}[1μM rosiglitazone]: 96.2±1.2% max; R_{max}[10μM rosiglitazone]: 95.8±1.3% max; $p>0.05$ in all cases).

4.3.4.2 – Extended incubation (4 and 24 hours)

It was observed (see Fig 4.3.8) that treatment for either 4 or 24hours with either 1 or 10μM rosiglitazone in the presence of L-NAME caused vascular relaxation to return to approximately the same levels as were seen in control DMSO-treated samples (ie. abolition of the possible decreased vasorelaxation effect seen with 1hour (see Section

4.3.4.1 above)). (4 hours treatment [+L-NAME]: EC_{50}[DMSO]: 34.7±8.1nM; EC_{50}[1μM rosiglitazone]: 41.6±10.6nM; EC_{50}[10μM rosiglitazone]: 38.9±9.1nM; 24 hours treatment [+L-NAME]: EC_{50}[DMSO]: 28.4±5.9nM; EC_{50}[1μM rosiglitazone]: 32.5±8.4nM; EC_{50}[10μM rosiglitazone]: 30.6±5.7nM, $p>0.05$ *v.* DMSO in both cases).

Once again, full relaxation (ie. approximately 100% R_{max}) was achieved in all cases, but no overall change in maximal relaxation was seen with any treatment (4 hour treatment [+L-NAME]: R_{max}[DMSO]: 95.3±2.8% max (ie. percentage reversal of initial contraction induced by 10^{-6}M PE); R_{max}[1μM rosiglitazone]: 96.2±3.0% max; R_{max}[10μM rosiglitazone]: 96.8±2.7% max; 24 hour treatment [+L-NAME]: R_{max}[DMSO]: 96.9±2.8% max; R_{max}[1μM rosiglitazone]: 96.3±3.0% max; R_{max}[10μM rosiglitazone]: 98.6±2.2% max; $p>0.05$ in all cases).

(a)

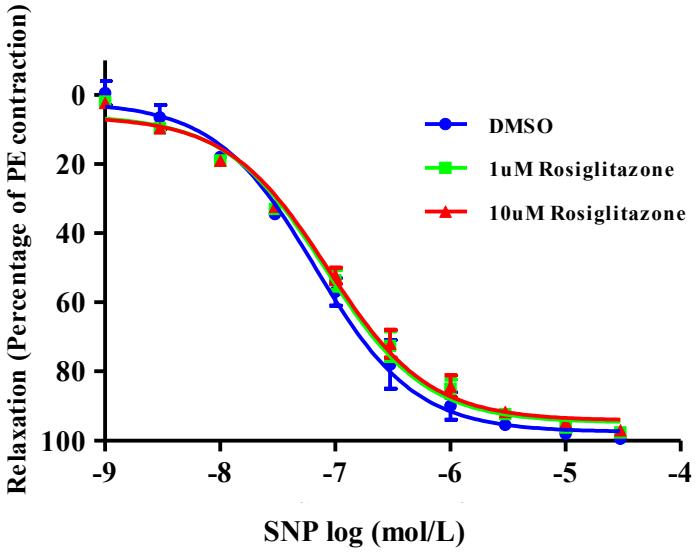

(b)

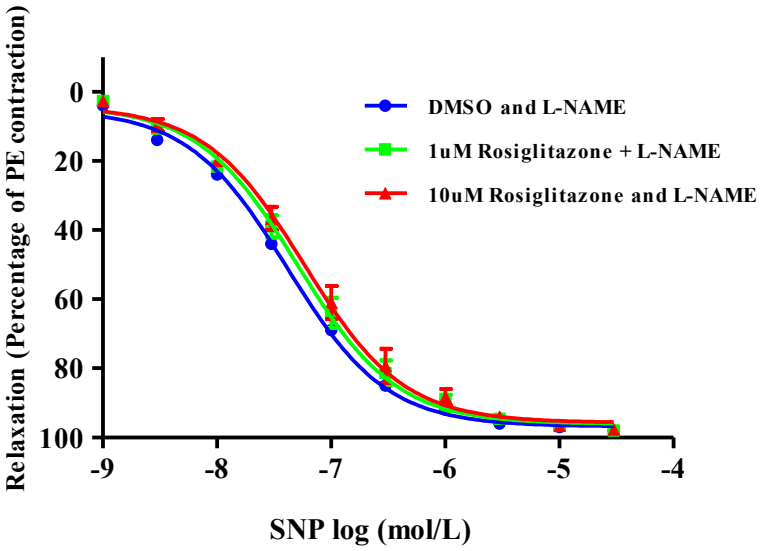

Fig 4.3.7: Short term effect of the PPAR-γ agonist, rosiglitazone on SNP-induced relaxation in endothelium-intact rabbit aortic rings. Intact aortic rings were incubated with 0.1% DMSO (blue circles), 1µM rosiglitazone (green squares) or 10µM rosiglitazone (red triangles) (a) alone or (b) consecutively with L-NAME (300µM) for 1 hour, prior to the addition of cumulative concentrations of SNP. Values are expressed as a percentage of the contraction induced by PE (10^{-6}M) and as mean± SEM (n=3).

(a)

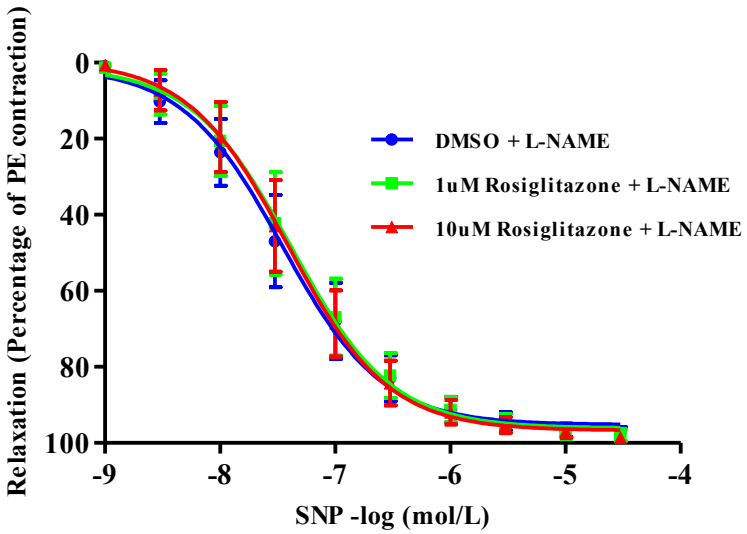

(b)

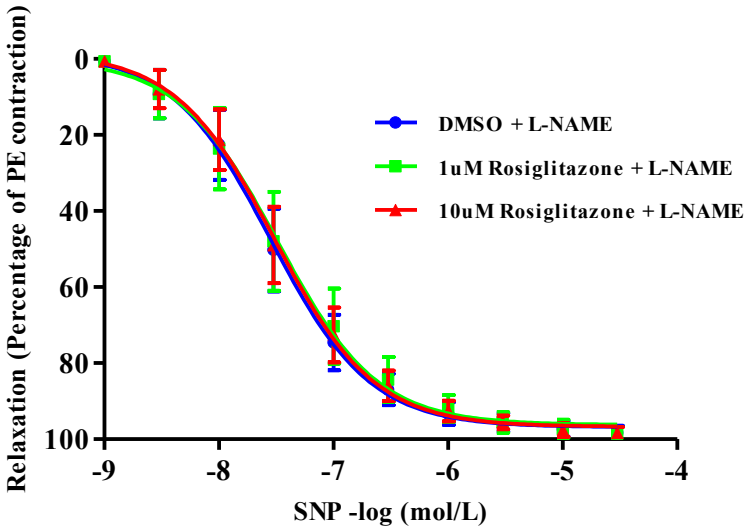

Fig 4.3.8: Long term effect of the PPAR-γ agonist, rosiglitazone on SNP-induced relaxation in endothelium-intact rabbit aortic rings. Intact aortic rings were incubated with 0.1% DMSO (blue circles), 1μM rosiglitazone (green squares) or 10μM rosiglitazone (red triangles) for (a) 4 hours or (b) 24 hours. They were then treated with L-NAME (300μM) for 1 hour prior to the addition of cumulative concentrations of SNP. Values are expressed as a percentage of the contraction induced by PE (10^{-6}M) and as mean± SEM (n= 3).

4.4 Discussion

Recent studies have shown that rosiglitazone and other TZDs are associated with improvements in vascular function in animal and human studies (e.g. Buchanan. 1995; Ryan *et al,* 2004, Diep *et al*, 2002). However, the proposed mechanism(s) behind these changes remain varied and yet to be fully elucidated.

It has been suggested that PPARγ ligands increase the bioavailability of the potent vasodilator NO via PPARγ-activation. Bagi *et al* suggested that PPARγ activation by rosiglitazone increases NO bioavailability via a reduction in oxidative stress (Bagi *et al*, 2004). Polikandriotis *et al* also showed that the PPARγ ligands 15d-PGJ2, ciglitazone and rosiglitazone enhanced NO release from human umbilical cord vein endothelial (HUVEC) cells and that this could be blocked by the addition of a PPARγ inhibitor GW9662 or by short-interfering RNA treatment of PPARγ, indicating that this increase was mediated via a PPAR-γ-dependent mechanism (Polikandriotis *et al*, 2005).

In contrast, the present study investigated a putative novel mechanism to underpin rosiglitazone-induced improvement in vascular function: UPR-triggered upregulation of SERCA2b and thus enhanced Ca^{2+} sequestration within VSMCs. This was achieved by measuring the isometric responses (contraction and relaxation) of ring segments of aortic tissue (±rosiglitazone) in the presence of various vasoconstricting and vasorelaxatory agents such as PE, ACh and SNP. Interestingly, previous similar research conducted in our laboratory showed that another PPARγ agonist GW7845 (>20μM) elicited slightly reduced contractile responses to PE and slightly increased relaxation responses to SNP in aortic tissue, but had no significant effect on eNOS expression or NO production in endothelial cells (Ahluwalia, M, 2005 - PhD thesis, University of Wales). However, no mechanism was put forward for this response at the time.

To determine the effect of rosiglitazone on vascular reactivity of the vascular smooth muscle cell alone, it was necessary to denude the tissue of endothelium prior to contraction/relaxation measurements. It was observed that when endothelium-denuded rabbit aortic rings were treated with rosiglitazone, there was no change in

the contraction response to PE - there was no change from basal following treatment with either drug concentration over any treatment duration (Figs 4.3.1 and 4.3.2). This data corresponds with data obtained by Llorens *et al* in rat aortic rings treated with rosiglitazone for 30 minutes (Llorens *et al*, 2007).

As there was no apparent effect on contraction, a second set of experiments were carried out in which endothelium-denuded aortic rings were treated as previously, but this time the relaxation response to the NO donor SNP was measured. While no significant differences in maximal relaxation (which was approximately 100% reversal of PE-induced contraction in all cases) could be seen between DMSO- and rosiglitazone-treated samples, differences in sensitivity to vasorelaxatory agents could be discerned between the different samples. Rosiglitazone incubation for 1 hour was seen to induce a slight decrease in vasorelaxatory sensitivity compared with control tissue (Fig 4.3.3). However, upon extended incubation with 10μM rosiglitazone only, this effect appears to reverse, with the drug inducing a slight non-significant increase in sensitivity to SNP at 4 hours (Fig 4.3.4a) and a greater statistically significant increase ($EC50_{(SNP)}$ values decreased from ~40nM to ~20nM) following 24 hour incubation (Fig 4.3.4b). One possible explanation for the decrease in sensitivity seen after 1 hour rosiglitazone treatment is that as we have shown in Chapter 2 of this study, short-term incubation with rosiglitazone leads to inhibition of SERCA2b (Fig 2.3.4), thereby causing cessation of Ca^{2+} sequestration into the SR and out of the cytoplasm, and preventing the smooth muscle cell from relaxing. The half-life of rosiglitazone is approximately 3.6 hours (Niemi *et al*, 2003), so upon extended incubation (4-24 hours) it is possible that this inhibition is beginning to be overcome due to degradation of the drug and also due to UPR-induced upregulation of SERCA2b gene and protein expression, as seen in Chapter 3. SERCA2b is activated by NO (via PKG-catalysed phosphorylation of the SERCA2b accessory protein phospholamban (Cohen et al, 1999)). As SERCA2b"s function is to reduce $[Ca^{2+}]_i$, this will lead to increased sequestration of Ca^{2+} into the SR, leading to vascular smooth muscle cell relaxation. We have shown in this study that 24hour incubation with 10μM rosiglitazone increases the upregulation of SERCA2b mRNA (Figs. 3.3.4 and 3.3.5) and SERCA2b protein (Fig. 3.3.6).

Thus, because there is more SERCA2b present in the SR membrane after prolonged rosiglitazone treatment, then rosiglitazone may induce increased sensitivity to NO.

At the same degree of NO-induced activation of each SERCA2b molecule, Ca^{2+} will be more rapidly and effectively returned to the internal stores by the enlarged pool of SERCA2b molecules in a rosiglitazone-treated sample. This may account for the apparent decrease in EC50 of approximately 50% from 39.8±7.4nM (DMSO) to 21.6±0.7nM (10µM rosiglitazone) seen in Fig 4.3.4b. As the tissue was endothelium-denuded, the vasorelaxative effect in this instance has occurred due to events in the smooth muscle cell alone (ie. in the absence of an endothelium), with the NO necessary to activate sGC being administered exogenously via the NO donor SNP.

To investigate whether rosiglitazone affects the endothelium-dependent relaxation of aortic tissue, endothelium-intact aortic rings were incubated as above and their response to ACh measured. As with the denuded samples (Fig 4.3.3), short-term treatment with rosiglitazone (1 hour) appeared to show a decrease in vasorelaxatory sensitivity compared with control for both concentrations of the drug (Fig 4.3.5). Moreover, the same effect was seen when exogenous NO was added via SNP to L-NAME-treated samples (Fig 4.3.7). These results are similar to those found in rat aortic rings (Llorens *et al*, 2007). These data suggests that rosiglitazone causes a similar decrease in sensitivity to NO generated by the endothelium in response to ACh, to the decrease in sensitivity to exogenously-added NO previously seen in denuded samples. Therefore, it seems that this effect is endothelium-independent.

After 4 hours treatment with rosiglitazone, the apparent rosiglitazone-induced desensitisation to ACh appears to be lost, as both DMSO and rosiglitazone-treated tissues responded to almost exactly the same extent (Fig 4.3.6a). This restoration of relaxation sensitivity to that of control tissue suggests that the tissue may be recovering from the initial rosiglitazone-induced desensitisation. Indeed, following 24 hour incubation, both 1 and 10µM rosiglitazone-treated samples display increased sensitivity to ACh (Fig 4.3.6b). However, the non-statistical significance of this positive vasorelaxatory effect after 24 hour rosiglitazone treatment of intact tissue should be contrasted with the significant increase in NO sensitivity seen after 4-24 hours in denuded tissue (Fig 4.3.4), and may be explained by a possible barrier effect of endothelium, with the drug unable to fully permeate into the smooth muscle.

Another possible explanation could be the presence of vasoconstrictor prostanoids generated by the endothelium (Llorens *et al*, 2007) cancelling out the increased NO

sensitivity described earlier, meaning that there appears to be no overall relaxation (as opposed to the denuded tissue where endothelial destruction negates any possible prostanoid interference). Thus, in the present study, the enhanced sensitivity to ACh-induced vasorelaxation seen at 24 hours (Fig 4.3.6b) suggests that eNOS is being activated by ACh, leading to the formation of NO, which eventually activates SERCA2b to reduce $[Ca^{2+}]_i$ and triggers relaxation. The decreased levels of maximal relaxation seen in endothelium-intact samples (approximately 80% reversal of PE-induced contraction (see Figs 4.3.5 and 4.3.6), rather than the total reversal seen in denuded samples (see Fig 4.3.3 and 4.3.4)) support this suggestion. In other words, the fact that the increase in relaxation generated in intact tissue compared with control tissue appears not to be as high as in denuded tissue may, in the light of Llorens‟ study, be explained by the potential presence of vasoconstrictor prostanoids (Llorens *et al*, 2007). Llorens *et al* showed that addition of indomethacin (a cyclooxygenase (COX) inhibitor) following pioglitazone treatment in aortic ring experiments caused a decrease in the PE-induced contractility seen in their study, suggesting that pioglitazone stimulates the endothelium to produce COX-dependent vasoconstricting agents, but that subsequent blockade of these by indomethacin allows vasodilators such as NO to exert their effect (Llorens *et al* 2007).

It is also possible that the amount of NO generated by ACh-induced eNOS activation may not be as plentiful/effective as that produced by the exogenous NO donor SNP. However, it should be noted that a similar previous study in our laboratory has shown that TZD treatment does not affect eNOS expression in endothelial cells (Ahluwalia, M, 2005 - PhD thesis, University of Wales), and so the effects of rosiglitazone in the present study are unlikely to involve changes in eNOS expression in aortic ring samples

To determine whether the responses observed above were due to changes in NO production or bioavailability as others suggest (Bagi *et al*, 2004; Polikandriotis *et al*, 2005), endothelium-intact aortic rings were incubated with drug or DMSO and also with L-NAME, which prevents NO production by blocking the actions of eNOS in the endothelium. Initial experiments were conducted to determine the effects on vascular reactivity in the absence or presence of L-NAME on short-term drug (1-10μM rosiglitazone) or vehicle only (DMSO)-treated intact aortic rings (1 hour). The data showed that 1 hour treatment with either concentration of rosiglitazone

induced a slight decrease in vasorelaxatory sensitivity compared with control rings in both L-NAME-treated and non-L-NAME-treated samples (Fig 4.3.7 – see above for explanation). The response to rosiglitazone was identical in these two samples, which suggests that the effect of rosiglitazone was not due to the actions of eNOS.

It should also be noted that incubation with L-NAME appeared to cause an increase in maximal levels of vasorelaxation (from approximately 80% reversal of PE-induced contraction (see Figs 4.3.5 and 4.3.6) to total reversal seen in denuded samples (see Fig 4.3.7 and 4.3.8) independent of drug/vehicle treatment. Previous research shows that incubation with L-NAME increases contractile responses to PE (Llorens *et al*, 2007). The data shown here seems to contradict this. One possible explanation for this could be that following incubation with L-NAME, the tissue is deprived of endothelial-derived NO so when NO is provided by SNP, the tissue may have a slight increased sensitivity for this NO and may relax to a greater extent. Alternatively, it may be the case that the 1 hour incubation employed in the present study did not provide adequate time for L-NAME to fully exert its effects.

As described above, the decreased sensitivity to SNP after 1 hour rosiglitazone treatment (Fig 4.3.7) is then overcome after 4 and 24 hours, when vasorelaxation occurs with the same sensitivity in rosiglitazone-treated samples as in controls (Fig 4.3.8). The lack of increased vasorelaxatory sensitivity (cf. control) in rosiglitazone (24 hours; 1-10μM)/L-NAME-treated tissue (Fig 4.3.8b) as compared with the enhanced sensitivity to ACh-induced vasorelaxation seen after 24hour treatment with rosiglitazone (Fig 4.3.6b) in intact aortic rings in the absence of L-NAME seems to suggest that the relaxation seen previously is endothelium-dependent, and not mediated solely by smooth muscle signaling. This appears to be in line with other studies that suggest rosiglitazone‟s effects on endothelial dysfunction to be endothelium-dependent (Pitrosch *et al* ; Hertzel *et al*).

Thus, it has been shown in this study that rosiglitazone may be linked to enhanced vasorelaxatory sensitivity in denuded tissues; for example, the 24 hour/10μM rosiglitazone data in Fig 4.3.4b shows statistically significant greatest increases in sensitivity to SNP-induced vasorelaxation cf. control. This provides further evidence to suggest that rosiglitazone causes effects in both the VSMC and the endothelium

(perhaps with the effects in smooth muscle predominating?), and that its effects cannot be deemed to be solely endothelium-dependent.

Furthermore, this data suggests that it may be the action of vasoconstrictor prostanoids such as PGH_2, produced by the endothelium (Camacho *et al*, 1998, Llorens *et al*, 2007) that is limiting enhanced vasorelaxation following extended rosiglitazone treatment in intact tissue (as opposed to the significantly enhanced vasorelaxation seen in denuded tissue). In their investigations, Llorens *et al* found that pioglitazone or rosiglitazone treatment of intact aortic tissue previously treated with indomethacin elicited a diminished contractile response to PE, but that this effect did not occur in comparative experiments with denuded aortic tissue. Llorens *et al* go further to suggest that this data provides evidence that TZD treatment in combination with non-steroidal anti-inflammatory drugs may be effective in the treatment of hypertensive individuals suffering from metabolic syndrome.

The data presented in this study builds upon previously published work in showing that rosiglitazone has a vasorelaxatory effect on aortic tissue, but goes further as to suggest that the mechanism behind this may possibly be initiation of the UPR and upregulation of the important Ca^{2+} regulatory/sequestrating protein SERCA2b in vascular smooth muscle cells. This potential anti-hypertensive „side effect" of TZD therapy may be added alongside its traditional anti-hyperglycaemic role, and so may potentially be of great importance in the clinical setting. Clearly, however, much more work would need to be conducted to validate the experimental findings described in this chapter before this work could be translated into a clinical setting.

4.4.1 Limitations

It is important to note that the experiments conducted in this chapter have been on a very small sample size only (have a low n number) due to time and laboratory constraints. As a result this may cause the lack of statistical significance in some aspects of the data presented here. There is a great deal of variability in animal tissue and therefore to gain a thorough insight into the effects of rosiglitazone on aortic tissue, ideally the sample size would need to be much larger and statistical significance would then be greater. Therefore, the data presented here can be described as preliminary findings and despite the low „n" number it may be worthy of note that the data does appear to show that rosiglitazone may be associated with some novel and potentially important effects.

4.4.2 Summary

Short term incubation with rosiglitazone (1 hour) has been shown here to cause a slight decrease in the vasorelaxatory sensitivity to both ACh and SNP (increased EC50s for both agonists) in both endothelium-denuded and intact aortic tissue. This endothelium-independent effect is thought to be due to rosiglitazone's inhibition of SERCA2b in the VSMC (highlighted in chapter 2), hindering the sequestration of Ca^{2+} back into the SR and hence preventing relxation in the presence of elevated $[Ca^{2+}]_{cyto}$. Longer incubation with rosiglitazone (24 hours and possibly 4 hours) in denuded tissue saw a significantly increased vasodilatory sensitivity to SNP (decreased EC50 for SNP) which can be explained by rosiglitazone's initiation of the UPR and subsequent increased SERCA2b expression and activity in the VSMC, as described in chapter 3. Also, as rosiglitazone has a half life of 3.6 hours, the effects of longer term rosiglitazone treatment could also be due to degradation of rosiglitazone so that the newly synthesised SERCA2b is no longer inhibited. Extended incubation of rosiglitazone in intact tissue saw a return to basal levels of sensitivity to ACh and SNP+L-NAME (ie. equal to [vehicle-only treated sample] levels). The reversion of the slight vasoconstrictor effect seen after 1 hour treatment to having no net effect on vascular tone suggests that initial SERCA2b inhibition has been reversed via the mechanisms stated above with regard to denuded tissue (induction of UPR and SERCA2b upregulation). This observed effect also highlights the possible presence and action of vasoconstrictor prostanoids produced by the intact endothelium which may counteract rosiglitazone's vasodilatory effects imposed on the VSCM. Also, the very presence of the endothelial layer may play a role in preventing adequate infusion of the drug into the vascular smooth muscle tissue.

In summary the data presented above suggests that the beneficial effects of rosiglitazone treatment observed on a cellular level in chapters 2 and 3, can indeed be observed in intact tissue and appear to facilitate an improvement in tissue function. This potential beneficial 'side effect' of rosiglitazone means that the data presented here may be of potential clinical importance in the field of T2D treatment by thiazolidinediones.

Chapter 5

General Discussion

5.0 General discussion

Following the introduction of the thiazolidinediones to T2D therapy over a decade ago, initially due to their insulin-sensitizing/anti-hyperglycaemic properties, there has been massive interest in these drugs, as it became apparent that they also appear to have additional potential benefits to the diabetic individual.

This study aimed to investigate rosiglitazone‟s apparent PPARγ-independent or „non-genomic‟ effects, in particular its effect on $[Ca^{2+}]_i$ in cell types involved in diabetic complications, and ultimately to establish the mechanism behind these actions. Secondly, the study aimed to show whether modulations seen on a cellular level led to improved function at tissue level by determining the effects of rosiglitazone on vascular smooth muscle contraction, and particularly relaxation via its potential actions on NO-induced vasodilatation.

5.1 General Resumé

Since disruptions in cellular Ca^{2+} handling have been found to be associated with many pathological conditions including T2D and its complications, maintenance of $[Ca^{2+}]_i$ and the mechanism(s) that control this is not only of the utmost importance in understanding T2D pathophysiology and progression, but also suggests a key point at which pharmacological intervention could provide potential clinical advantages to the diabetic patient. As described in Chapters 1 and 2, previous research conducted in our laboratory showed that the oral anti-hyperglycaemic drug rosiglitazone rapidly (<5 min) induced increases in $[Ca^{2+}]_i$ in non-muscle cells (Singh *et al*, 2005). The timescale involved suggested the involvement of the „housekeeping‟ ER-resident Ca^{2+} pump enzyme SERCA2b.

Two key cell types important to T2D, namely the monocyte and the VSMC, were chosen for use in the study. The first step was successful determination of the expression of SERCA2b in microsome preparations from these cell lines, and of an alternative Golgi-bound ER Ca^{2+} pump, PMR1 in microsomes from yeast cells (the inclusion of an alternate Ca^{2+} pump was chosen to serve as a control to elucidate

whether rosiglitazone exerted specific effects on SERCA2b, or more general effects on all Ca^{2+} pumps). Following identification of SERCA2b/PMR1 in these samples, functional activity assays determined that rosiglitazone inhibited the Ca^{2+}-ATPase activity of SERCA2b in a dose-dependent manner in monocyte and VSMC derived-microsomes, an effect which was not repeated in yeast cell microsomes, indicating that rosiglitazone"s inhibition seemed to be specific to SERCA2b and not to other Ca^{2+}-ATPase pumps such as PMR1.

Analysis of $[Ca^{2+}]_i$ in monocytes following incubation with rosiglitazone showed that 10μM rosiglitazone initiated a rapid increase in $[Ca^{2+}]_i$, peaking at 24 hrs before returning to basal after 72 hrs. Corresponding treatment of VSMCs showed a comparative rapid increase, which then decreased below basal levels after ~4hrs and remained low until being restored to basal levels after 72 hrs. This restoration of $[Ca^{2+}]_i$ to basal levels shows that extended rosiglitazone treatment in both cell types leads to a restoration of Ca^{2+} homeostasis, albeit by different mechanisms. The difference in how each cell responds is determined by its cell type. The monocyte being a non-contractile cell seems to be able to tolerate elevated background levels of cytoplasmic Ca^{2+} whilst homeostatic mechanisms kick in, possibly due to a buffering effect imposed by cytoplasmic proteins such as calbindin (Parmentier *et al*, 1989). In contrast, it may be speculated that the VSMC, being a contractile cell, is unable to allow elevated levels of $[Ca^{2+}]_i$ to persist for very long as Ca^{2+} induces contraction and without its rapid and complete expulsion from the cell, relaxation cannot occur - such prolonged cellular stimulation would no doubt be detrimental to the cell. Therefore, it may be tentatively concluded that the VSMC has to expel Ca^{2+} from the cell until the return of homeostatic normality, so as to allow relaxation to take place and to allow continued cell survival.

Cell viability following rosiglitazone treatment was determined via cell count and apoptosis assays. Apoptosis assays showed that 1μM rosiglitazone induced a non-significant mild apoptotic effect on the monocytic cell (~1.5-fold), with the higher concentration (10μM) inducing a slightly larger significant increase in apoptosis of the magnitude of ~3-fold over control. It appears from the data presented in Chapter 2 that VSMCs seem to be less sensitive to rosiglitazone-induced apoptosis than monocyes (however it is important to note that apoptosis assays were not carried out for as long a period as for monocytes due to differences in cell culture technique in

the adherent and non-adherent cell lines). Despite the slight increases in apoptosis described above, cell count data collected for up to 14 days post drug treatment (72 hrs only for VSMCs) show that neither cell line appeared to be detrimentally affected as far as cell growth was concerned. Every population of cells has a certain percentage actively dividing and replicating and some that are naturally apoptosing, so apoptosis assays alone should be judged carefully. The overall conclusion taking into account both the apoptosis data and cell count data is that the viability of the overall cell population does not appear to be affected by rosiglitazone treatment in either cell line over the time durations of the experiments in this study.

Having established in chapter 2 that extended rosiglitazone treatment brings about only a transient disruption of Ca^{2+} before restoration in Ca^{2+} homeostasis, and therefore no overall detrimental effect on the survival of the entire cell population, chapter 3 of the study aimed to elucidate the mechanism behind this restoration. The identification of the mechanism behind the rapid increase in Ca^{2+} observed upon incubation with rosiglitazone, as dose-dependent inhibition of a Ca^{2+}ATPase activity that is likely to be attributable to the enzymatic activity of SERCA2b, led to the postulation that the subsequent restoration of Ca^{2+} homeostasis seen upon extended rosiglitazone treatment may involve further changes in SERCA2b expression or activity.

Incorrect functioning of some aspect of a cell‟s physiology, such as aberrant Ca^{2+} homeostasis, causes cellular stress and can lead to activation of stress responses such as the UPR or ER Stress Response. In this study, it was found that incubation of monocytic cells with rosiglitazone causes alternate splicing and activation of the transcription factor XBP-1, indicative of initiation of a UPR. Indeed it appears that this study constitutes the first report of rosiglitazone‟s UPR-inducing ability.

In addition, the current study performed bioinformatics analysis, which found SERCA2b to be an UPR-inducible protein, and thus provided a rationale for the gene expression of SERCA2b to be studied in more detail. Whilst other studies in ventricular myocytes (Shah *et al*, 2004) and platelets (Randriamboavonjy *et al*, 2008) have described SERCA2b upregulation after prolonged treatment with rosiglitazone, the authors in these cases did not attempt to elucidate a mechanism for this increase. This study showed that extended incubation with rosiglitazone (>24 hrs) led to

increased SERCA2b mRNA expression in both monocytes and VSMCs; given the previous findings of UPR initiation via XBP-1 activation by rosiglitazone, it appears likely that the UPR is the mechanism behind increased SERCA2b gene expression. It was also shown using Western blot analysis and additional Ca^{2+}ATPase assays that this increased SERCA2b mRNA expression is translated into an increased SERCA2b protein production, and also to an increased SERCA2b Ca^{2+}ATPase activity in monocytic cell-derived microsomes.

The current literature and experimental evidence discussed in Chapters two and three allow the establishment of a tentative mechanism for how the monocytic cell (Fig. 5.1) and the smooth muscle cell (Fig. 5.2) respond to rosiglitazone treatment: activation of a UPR, upregulation of UPR target genes, and ultimately restoration of cellular Ca^{2+} homeostasis and cell survival. Chapter two provides evidence that rosiglitazone treatment causes a dose-dependent inhibition of the Ca^{2+}ATPase SERCA2b, leading to a disruption of both ER function and normal Ca^{2+} homeostasis, the result of this inhibition being an increase in $[Ca^{2+}]_i$. As a consequence, due either to a rise in $[Ca^{2+}]_i$ or the loss of Ca^{2+} from the ER (the ER continuously „leaks" calcium but this cannot be replenished if SERCA2b is inhibited (Roderick *et al,* 2000) the cell initiates a sequence of survival mechanisms to try to deal with the imposed stress. Step one is the initiation of the unfolded protein response, as epitomised by the activation of the transcription factor XBP-1 amongst others. This leads to upregulation of UPR target genes, genes which can help to bring about a response to the cellular stress - in this instance it has been shown that activation of XBP-1 leads to increased gene expression of the ER Ca^{2+} pump SERCA2b. Subsequent upregulation of SERCA2b protein and improvements in SERCA2b"s Ca^{2+} sequestering abilities lead to an increased ability of the cell to reduce its $[Ca^{2+}]_i$ and thus restoration of the cells normal Ca^{2+} homeostasis properties.

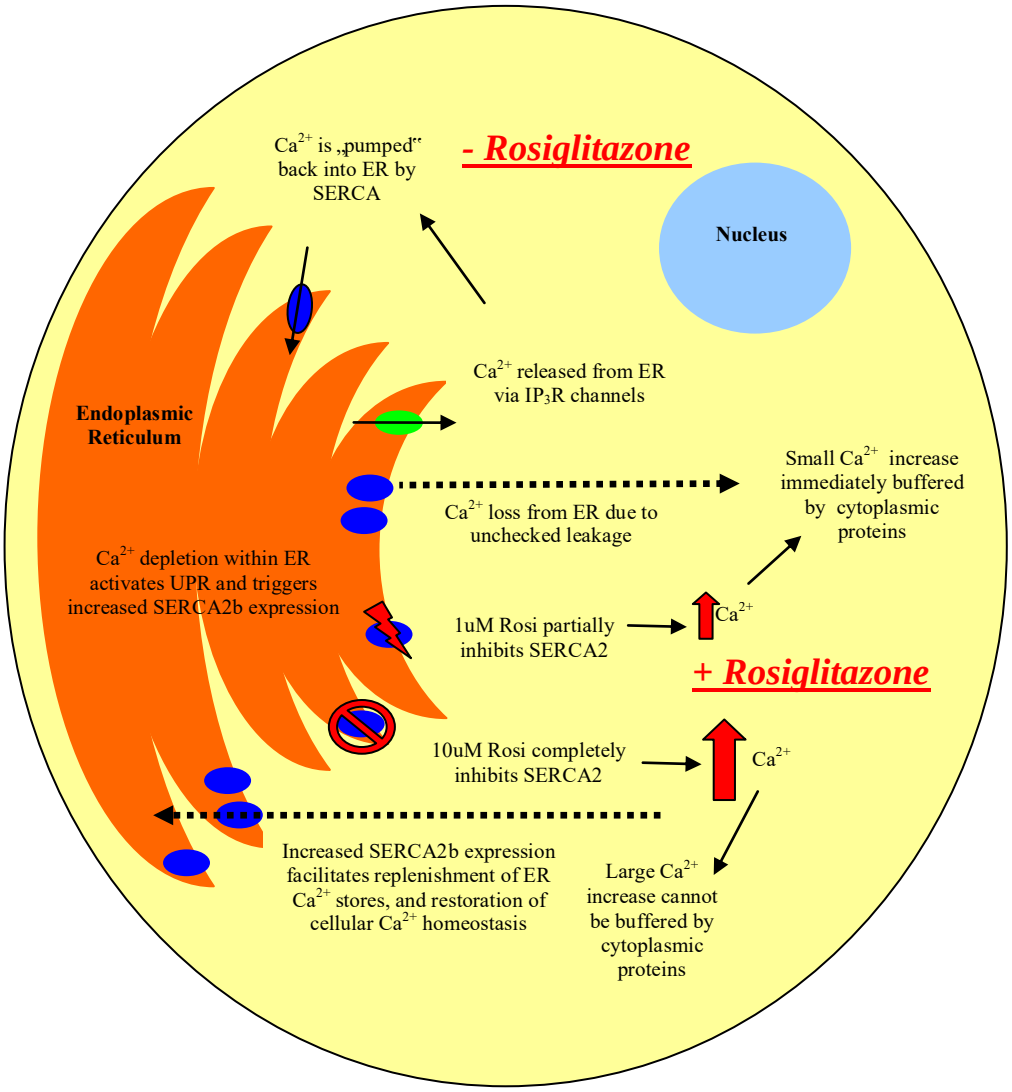

Fig. 5.1 Proposed Ca^{2+} homeostatic mechanism occuring in the monocytic cell in the presence and absence of rosiglitazone

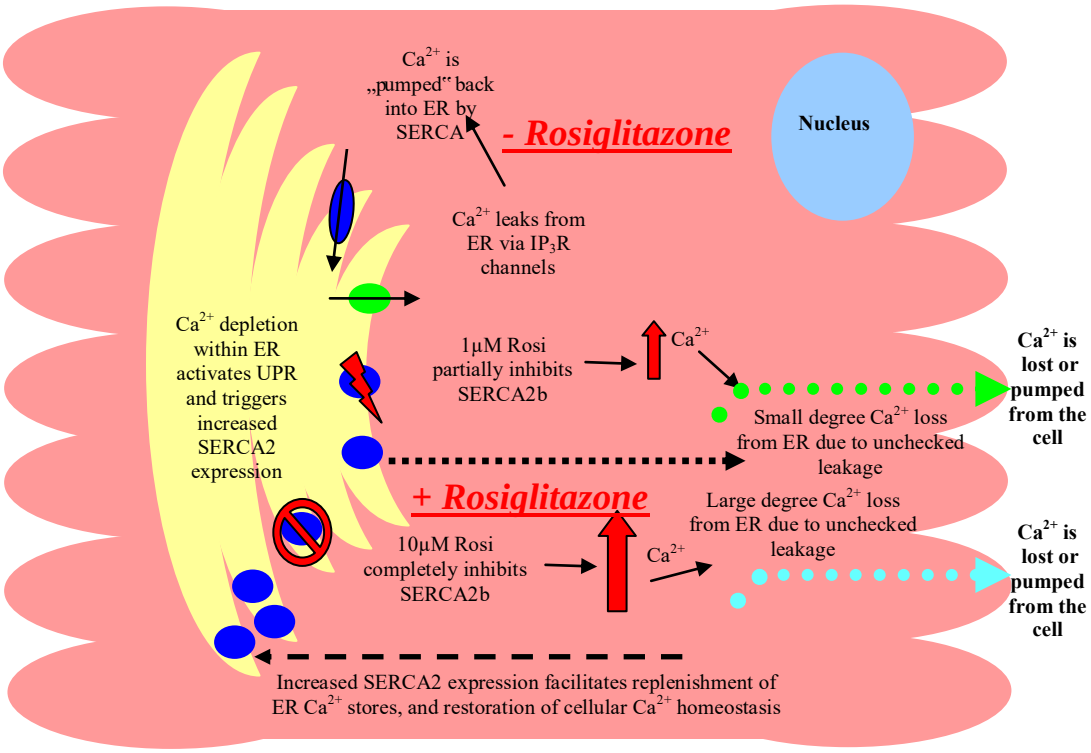

Fig. 5.2 Proposed Ca^{2+} homeostatic mechanism occuring in the vascular smooth muscle cell in the presence and absence of rosiglitazone

The experimental findings discussed in Chapters two and three provide substantial evidence to back up the proposal that 1) rosiglitazone causes initial disruption in Ca^{2+} re-sequestration into the ER via inhibition of SERCA2b and 2) extended incubation with rosiglitazone brings about a restoration in Ca^{2+} homeostasis via initiation of a UPR and upregulation of SERCA2b, a UPR target gene. However, the experiments were conducted in stand-alone cellular models only and it was deemed prudent to determine whether in fact rosiglitazone"s actions could be translated into a tissue model and thus provide further evidence for the hypothesis of a beneficial „side effect" of rosiglitazone therapy. A wealth of literature exists showing that TZDs including rosiglitazone exert beneficial effects on the vasculature in animal and human models, including improvements in blood pressure, flow-mediated dilation and endothelial-dependent vasodilation leading to improvements in endothelial function (Buchanan, 1995; Ryan *et al*, 2004; Majithiya *et al,* 2005; Diep *et al*, 2002; Pitrosch *et al*, 2004). However, the proposed mechanism(s) behind these studies remain varied and unsubstantiated. In light of the above literature, and the proposed mechanism of rosiglitazone-induced SERCA2b upregulation being responsible for improvement in Ca^{2+} homeostasis in VSMCs shown earlier in this study, it was decided that vascular tissue would be a good setting in which to test whether events mediated by rosiglitazone within cultured cells (as described above) could be transferred to a tissue system and hence provide further support for a plausible mechanism to explain both our current and the literature"s findings.

In order to investigate rosiglitazone"s effect on vascular tissue, experiments were conducted to measure the isometric responses (contraction and relaxation) of ring segments of aortic tissue (±rosiglitazone) in the presence of various vasoconstricting and vasorelaxatory agents such as PE, Ach and SNP. As there is some question in the literature regarding whether rosiglitazone"s vascular effects are mediated by the endothelium or via the smooth muscle itself, experiments were conducted on both endothelium-denuded and endothelium-intact aortic tissue. In denuded tissue, rosiglitazone was found to have no effect on PE-induced vasoconstriction at any concentration or for any incubation duration. However, incubation with 10µM rosiglitazone was seen to initially reduce SNP-induced vasodilation after incubation for 1hr, while incubation for extended time periods (4-24 hr) elicited an increase in vasodilation compared with control (with a statistically significant increase being achieved after 24hrs treatment). This time-dependent effect appears to be explained

by our findings in chapter 2, that initially rosiglitazone's inhibition of SERCA2b leads to elevated $[Ca^{2+}]_i$ and hence slight contraction in muscle cells, while extended incubation sees initiation of the UPR, up-regulation of SERCA2b mRNA and protein, and hence enhanced Ca^{2+}ATPase activity and restoration of SERCA2b's Ca^{2+} sequestration properties. This could be responsible for both greater NO-induced relaxation of each individual VSMC, and also greater vasorelaxation at the tissue level. The half-life of rosiglitazone being ~3.6 hours (Niemi *et al*, 2003) fits well with this explanation, as rosiglitazone appears to detrimentally affect vascular tissue function after 1 hour incubation but these effects seem to be lost and normalisation and/or improvements in vasodilatory capacity seen after 4-24hrs (when rosiglitazone is being rapidly broken down and therefore eliciting less effect on the tissue). Obviously as the experiments conducted in this study are stand-alone cellular or tissue models not patient studies, it is difficult to determine whether the half life of the drug is the same in these experimental situations as in the human body, but the results presented here suggest that the half-life of rosiglitazone in our cell/tissue experiments may be approximately comparable to that seen in vivo. The upregulation of SERCA2b and the subsequent improvements in Ca^{2+} re-sequestration lends itself to the explanation that rosiglitazone may exert its vasodilatory effects by increasing the sensitivity of the tissue to NO. The absence of the endothelium in the tissue also shows that this effect is endothelium-independent.

Comparative experiments on intact tissue measuring Ach-induced vasorelaxation, again showed a decreased vasodilatory response after 1h incubation with the drug, which was subsequently overcome and restored to that of control tissue after 4 hr incubation, followed by a slight non-significant increased vasodilatory response after 24 incubation. As discussed in chapter 4, the improvement to basal values after 4hr incubation suggests that the tissue is responding to the initial desensitisation to NO caused by SERCA2b inhibition, and that the improvement in vasodilation seen after 24 hours may be due to the UPR-induced increased NO sensitivity described above. That the magnitude of the vasodilatory response was not comparable in intact and denuded tissues leads us to agree with Llorens *et al*'s finding that rosiglitazone-induced production of endothelium-derived vasoconstrictor prostanoids may counteract rosiglitazone's vasodilatory effect on smooth muscle thus somewhat dampening the effect observed in samples lacking endothelia (ie denuded aortic rings) (Llorens *et al*, 2007).

To confirm whether the effects observed were in fact endothelium-dependent or independent, intact tissue was pre-treated with L-NAME, which blocks NO production via the endothelium, with exogeneous NO being provided by SNP. Once again, 1h incubation with rosiglitazone brought about a decreased propensity to tissue relaxation, which was subsequently reversed and reverted to that of control tissue following extended incubation (4-24 hrs). The lack of an overall increase in vasodilation after 24h treatment (as seen previously in intact tissue not treated with L-NAME), suggests that the effect may be endothelium-dependent and not purely an effect of changes in smooth muscle cells.

Taking the three different experiments together, it appears that both the endothelium and VSMC play a role in the increased vasodilatory response to rosiglitazone, and that the presence of vasoconstrictor prostanoids may be somewhat hindering the ability of the intact tissue to relax to the same degree as denuded tissue.

Thus, in conclusion, the experimental evidence presented in Chapters 2, 3 and 4 of this study go some way to adding to previously published literature regarding rosiglitazone‟s PPARγ-independent or „non-genomic‟ effects in monocytic and VSMCs, and that these effects may be responsible for potential improvements in vascular tissue function.

5.2 Interpretation of data

5.2.1 The importance of rosiglitazone on Ca^{2+} homeostasis and the UPR

While rosiglitazone and other TZDs were clinically marketed on the basis of their PPARγ-dependent modulation of glycaemic control, this study has highlighted the importance of rosiglitazone‟s PPARγ-independent „side-effects‟. Specifically, it has highlighted the importance of rosiglitazone‟s effects on Ca^{2+} homeostasis and the mechanism behind this, namely activation of the UPR in response to imposed ER stress.

As mentioned briefly previously with respect to the adverse cardiovascular outcomes seen with rosiglitazone administration, beneficial effects of a drug on one particular cell type do not necessarily confer the same positive effects on another cell type with a completely different function. One of the most widely studied cell types, with respect to T2D and its complications, is the pancreatic β-cell. As previously discussed, Type 1 Diabetes Mellitus is an autoimmune disorder in which

inflammatory cellular reactions lead to destruction of pancreatic β-cells, mediated by the production of pro-inflammatory cytokines. The natural PPARγ agonist 15d-PGJ_2, has been shown, in addition to its PPARγ-dependent anti-hyperglycaemic actions, to prevent such cytokine signalling in pancreatic β-cells (Weber *et al*, 2004a) and in human blood monocytes (Hinz *et al*, 2003) in a PPARγ-independent manner. Furthermore, Weber *et al* have confirmed that 15d-PGJ_2‟s actions occur via initiation of an ER stress response (Weber *et al*, 2004b), because as described in Chapter 3, one component of a UPR is a translational block on all gene products except those encoded by UPR-responsive genes (eg. BiP, SERCA2). Thus, no new cytokines would be manufactured in cells exposed to 15d-PGJ_2.. Indeed, previous research showed that another natural PPARγ-ligand 12d-PGJ_2 regulated BiP expression via UPR (Odani *et al*, 1996; Takahashi *et al*, 1998).

Therefore, in certain contexts, this „side-effect‟ of treatment with natural PPARγ-ligands such as15d-PGJ_2 - the initiation of the UPR - plays a very important role in mediating the improvement in diabetic complications. However, if the synthetic TZDs including rosiglitazone were designed to mimic the PPARγ-dependent effects of their natural counterparts, the cyclopentone prostaglandins including 15d-PGJ_2 (tentatively theorised purely due to their similarity in chemical structure), then it would follow that, alongside 15d-PGJ_2‟s anti-hyperglycaemic actions, may have been conferred the same or similar PPARγ-independent effects - such as the initiation of UPR events. While it appears from literature and from experimental evidence presented in this study, that in the monocytic cell and the VSMC, the initiation of the UPR by rosiglitazone appears to elicit potential positive „side-effects‟, this will not necessarily be the case for many other cell type in the body. Indeed, caution should be employed when speculating on the benefits of rosiglitazone-induced UPRs for many reasons, including rosiglitazone‟s longer half-life compared to 15d-PGJ_2, and its potential to have a wider tissue distribution throughout the body.

Initiation of the UPR in the examples cited above leads to positive effects by restoring the cell‟s correct functioning. However, continued initiation of the UPR, ultimately leading to cellular apoptosis, can in the right setting also constitute an advantage, for example in the use of PPARγ-ligands in cancer therapy. One such recent publication states that production of 15d-PGJ_2 by another natural compound

Fuligocandin B, causes leukaemia cells to become more sensitive to the apoptosis inducing ligand tumor necrosis factor-related apoptosis-inducing ligand (TRAIL) and thus more susceptible to apoptosis (Hasegawa *et al*, 2007), which is obviously in this cell type and situation, a positive clinical effect. Therefore, how different cells respond to rosiglitazone-induced UPR effects is dependent on their locality and function; this may be a potentially relevant point in situations where there have been reported adverse correlations with rosiglitazone therapy.

As discussed in Chapter 1, modern living with its increased life-expectancy, poor diet and lack of exercise have lead to increased cellular stress on cells such as pancreatic β-cells, leading to the development of insulin resistance and ultimately an increase in T2D in the general population. Evidence of this increased ER stress in pancreatic β-cells has been documented in numerous studies, with increased staining of ER stress proteins CHOP and BiP in pancreatic secretions from T2D patients as opposed to non-diabetics (Laybutt *et al*, 2007), and the observation of a 2-fold increase in ER size in β-cells form T2D patients as opposed with healthy controls (Marchetti *et al*, 2007). In this untreated state, constant triggering of the UPR by lifestyle induced ER stress markers leads to long term functional damage and eventually death of the pancreatic β-cell. However, the literature provides evidence that PPARγ-ligand-induced PPARγ-independent initiation of the UPR provides a beneficial effect on the cell (Weber *et al*, 2004a; Weber *et al*, 2004b; Odani *et al*, 1996; Takahashi *et al*, 1998); importantly, these occur distinct from, and in addition to, PPARγ-ligand-induced PPARγ-dependent anti-hyperglycaemic effects.

5.2.2 Rosiglitazone and cardiovascular safety

As discussed in Chapter 1, there has been much recent debate regarding the continued use of rosiglitazone in clinical practice, in the light of numerous studies indicating that the drug may be associated with a greater risk of adverse cardiovascular outcomes.

Numerous clinical studies have been undertaken to determine the effects of the TZDs including rosiglitazone, in comparison with or in combination with other forms of anti-hyperglycaemic medications, eg the sulphonylureas and metformin. These studies encompass not only their comparative abilities to improve glycaemic control

but also on independent factors such as cardiovascular risk. Some of the most notable, large-scale clinical trial include the „UK Prospective Diabetes Study" (UKPDS), „A Diabetes Outcome Progression Trial" (ADOPT), „the Diabetes Reduction Assessment with ramipril and rosiglitazone Medication" (DREAM) and „Rosiglitazone evaluated for cardiovascular outcomes in oral agent therapy for type 2 diabetes" (RECORD) – all of which were discussed in detail in Chapter 1 (Matthews *et al*, 1998; Kahn *et al*, 2006; The DREAM Trial Investigator, 2008; Home *et al*, 2007 and Home *et al*, 2009) . The publication of several meta-analyses (Nissen *et al*, 2007; Singh *et al*, 2007) covering some of these large scale trials along with several smaller trials caused controversy in the medical field when it was highlighted that rosiglitazone use appeared to be associated with an increased risk of adverse cardiovascular outcomes, including heart failure and myocardial infarction.

In the most recently published study, where Juurlink *et al* compare the TZDs rosiglitazone and pioglitazone, the author states that as rosiglitazone appears to be associated with a greater risk of adverse cardiovascular outcomes than pioglitazone, whilst at the same time conferring no additional clinical benefit, that there is no justification for its continued use (Juurlink *et al*, 2009). In the light of Juurlink *et al'*s comments, the findings of this PhD study highlight the importance of continued investigation into, amongst other areas, rosiglitazone"s PPARγ-independent or „non-genomic" effects, in order to more accurately assess the long-term impact, whether beneficial or detrimental, of rosiglitazone therapy in comparison with other medications. All medications have side effects including in some cases serious complications associated with their use, but the ultimate goal in choosing a particular drug or therapy regime is that the drug"s advantages outweigh any detrimental effect of the treatment regime, or indeed the consequences that would naturally occur if the drug were not prescribed. In this study, it has been shown that rosiglitazone-induced ER stress leads to UPR activation and subsequent restoration/improvements in cellular Ca^{2+} homeostasis in cellular models. This effect also appeared to be transferred to a tissue model due to the observation of improved agonist-induced vasorelaxation of arterial tissue following extended incubation with rosiglitazone. As Ca^{2+} homeostasis is disrupted in T2D leading to the pathogenesis of the disease and to the development of diabetic complications, rosiglitazone"s potential ability to mediate Ca^{2+} homeostatic improvements, which may lead to improved endothelial function, decreased hypertension and a reduction in atherosclerosis, could prove to

be clinically important when deciding on a course of therapy for a diabetic individual. In this light, in the opinion of the current author, it is of the utmost importance that research into rosiglitazone‟s PPARγ-dependent and independent effects are continued.

5.2.3 Mode of action of rosiglitazone on the ER

While this study goes some way to adding to the published literature in elucidating rosiglitazone‟s effects, and provides a tentative mechanism behind these effects, as yet rosiglitazone‟s exact mode of action on the ER remains elusive. We can however look at the mode of action of other natural and synthetic compounds on the ER to tentatively predict how rosiglitazone may exert its effects.

The sesquiterpene lactone thapsigargin is a terpenoid secondary metabolite produced by the plant *thapsia garganica* (Thastrup *et al*, 1989). Thapsigargin brings about complete and permanent inhibition of SERCA enzymes by binding to the stalk region of the transmembrane section, locking the enzyme in its E2 conformation and thus preventing cytosolic-bound Ca^{2+} from being released into the ER lumen (Thastrup *et al*, 1989). Depletion of ER Ca^{2+} stores (via continued non-specific leakage of Ca^{2+} into the cytoplasm and blocked re-sequestration of Ca^{2+} back into the ER by SERCA2b) triggers a UPR response including up-regulation of SERCA2b. However, due to the permanent nature of thapsigargin‟s inhibition of SERCA, and due to its extremely high potency (IC_{50} < 30nM; Thastrup *et al*, 1990)), any newly synthesised SERCA2b is immediately inhibited by surplus thapsigargin molecules. This ultimately prolongs stimulation of the UPR response, and thus causes a situation that leans towards the apoptosis scenario rather than facilitating restoration of normal cell physiology (see Fig 3.1.1, Chapter 3). It has been shown in the current study that incubation with rosiglitazone causes transient inhibition of SERCA2b and that newly synthesised SERCA2b protein, subsequently produced during the initiated UPR response, is not inhibited by rosiglitazone. This may be due to rosiglitazone having a shorter half life than thapsigargin, but may also be due to their conflicting mode of action.

Several lines of evidence suggest that rosiglitazone and its natural counterpart 15d-PGJ2, may behave in a manner similar to that of cholesterol. The ER membrane normally contains very little cholesterol but it has been shown that under lipotoxic

conditions within the vasculature of obese individuals, integration of large amounts of „free" or unesterified cholesterol (FC) into the ER membrane occurs (Tabas *et al*, 2004). This would be expected to lead to an increased rigidity of the ER membrane (Webb *et al*, 1997). Increased rigidity due to enrichment of the ER with FC in macrophages, such as in the case of foam cell development (the primary step in the development of atherosclerosis), leads to depletion of ER Ca^{2+} stores via inhibition of SERCA2b (Li *et al*, 2004). The ability of SERCA enzymes to transport Ca^{2+} depends on their ability to undergo conformational changes while situated within the ER membrane. Crystallographic studies have shown that the E1 and E2 conformations are distinct (Toyoshima *et al*, 2000: Toyoshima *et al*, 2002), and therefore, different domains of the enzyme (including its transmembrane domains) must move relative to each other, and relative to the phospholipid bilayer in which the enzyme is embedded, when the enzyme changes from E1 to E2 or vice versa. Conversely, embedding in a cholesterol-rich ER membrane of reduced flexibility that will not permit such movements, would be predicted to prevent SERCA enzymes from undergoing conformational changes, and thus from transporting Ca^{2+}. This has been previously demonstrated by studies in which SERCA enzymes were reconstituted within synthetic membranes whose physical characteristics could be controlled by manipulation of the nature of the phospholipid bilayers of which they were composed (Lee *et al*, 1995; Starling *et al*, 1995).

This has been suggested to have clinical consequences: in macrophages whose ER membranes are overwhelmed with cholesterol, SERCA2b inhibition causes initiation of the UPR, upregulation of the UPR-inducible gene CHOP and ultimately leads to macrophage apoptosis via an ER-stress dependent pathway (DeVries-Seimon *et al*, 2005). Such a chain of events in the macrophages present in atherosclerotic plaques can lead to a build-up of necrotic tissue (due to accumulation of apoptosed macrophages), and thus the destabilisation of advanced plaque lesions, causing vascular blockages and tissue infarction (Tabas, 2004).

Rather than binding specifically to SERCA as thapsigargin does, rosiglitazone and 15d-PGJ2 may potentially mediate their actions by affecting the fluidity of the ER membrane in which the SERCA enzyme is situated (as with cholesterol), and as such prevent conformational changes in SERCA2b configuration, leading to SERCA2b inhibition and initiation of the UPR. Unlike cholesterol, however (which does not

get degraded easily, leading to prolonged activation of the UPR, CHOP up-regulation and apoptosis), rosiglitazone and 15d-PGJ2 are broken down rapidly in the ER by the cytochrome P450 isoform 2C8 (Hruska and Frye, 2004). This may explain why treatment with rosiglitazone and 15d-PGJ2 results in the restoration of normal cell physiology and therefore cell-survival rather than cell-destructive UPR-triggered apoptosis (see fig 3.1.1. in chapter 3). Indeed, inhibition of cytochrome P450 2C8 by gemfibrozil increased rosiglitazone‟s elimination half-life (t(1/2)) from 3.6 to 7.6 hours (Niemi *et al*, 2003). In a later study, Niemi *et al* showed that another cytochrome P450 2C8 inhibitor trimethoprim increased rosiglitazone‟s peak plasma concentration (C max) by 14% and its t(1/2) from 3.8 to 4.8 hours, while rifampin, an inducer of cytochrome enzymes decreased rosiglitazone C max by 28% and decreased the t(1/2) from 3.8 to 1.9 hours (Niemi *et al*, 2004).

Thus, it may be tentatively concluded that Rosiglitazone may exert its effects on monocyte and VSMC Ca^{2+} homeostasis via modulation of ER membrane properties, SERCA2b inhibition, and induction of a UPR response. However, due to the presence of enzymes within the ER that can degrade rosiglitazone within only a few hours, this effect is only a transient one, and so it does not lead to widespread apoptosis or a decrease in cell viability in the cell population as a whole.

5.3 Evaluation of study and suggestions for further study

It is the author‟s belief that this study was, on the whole, a successful attempt to combine current literature findings with novel experimental evidence that has provided some new insights and explanations into the actions of a very controversial drug.

However, every study has its limitations and this is no different. The major limitation of this study is that experimental investigations were conducted purely on stand-alone cell-culture and isolated tissue models. This was due to many reasons, such as time constraints and available equipment amongst others, however it must be conceded that the lack of experimental evidence in live animal models or from patient studies does limit the scope of this study.

Yeast cells were initially included in this study as they express the alternate Ca^{2+}ATPase pump PMR1 in their Golgi; their inclusion in the study was deemed appropriate to distinguish general effects on Ca^{2+}ATPase from SERCA2b-specific effects. However, upon use of microsomes derived from these cells in Ca^{2+}ATPase activity assays in Chapter 2, it was discovered that the background signal prior to the addition of Ca^{2+} was very noisy and therefore an accurate background or „resting" reading could not be repeatedly established and may have adversely affected the experiment. This is why yeast cells were used only in the introductory experiments and their use was not continued.

Furthermore, the data presented in chapter 4 on aortic tissue reveals some very interesting data. However, again due to time constraints and tissue availability, the experiments were only conducted on a very small sample size and therefore the results can only be deemed to be preliminary findings.

Further study

In the light of the study's findings that rosiglitazone causes - in both monocytic cells and VSMCs - an initial distruption in Ca^{2+} re-sequestration into the ER followed by subsequent restoration of this Ca^{2+} homeostasis via initiation of UPR and upregulation of UPR target genes; and in the light of the current concern over rosiglitazone's potential to cause problems in cardiac tissue (Nissen *et al*, 2007; Horne *et al* 2009), it would be very interesting to repeat the investigations detailed in this study in cardiac cells. The cardiomyocyte-like cell line, HL-1 (Claycomb *et al*, 1998) would be a good candidate for these investigations, and may provide a valuable insight into 1) whether the effects seen in the current study occur in cardiac cells, and 2) whether this mechanism may be responsible for the adverse cardiovascular outcome reported with rosiglitazone therapy.

As previously highlighted, the initiation of the UPR response is clearly beneficial in certain cell types, such as the cell types studied here and in pancreatic β-cells (as seen with the natural PPARγ ligand 15d-PGJ2 (Weber *et al*, 2004)). This may not be the case in all cell types/tissues however, and as such the UPR may provide a plausible explanation for the apparent harmful effects potentially elicited by rosiglitazone in cardiac tissue, as opposed to the beneficial effects observed in other tissues, such as the vasculature.

As discussed, a major limitation in this study is that the effects were observed either in cellular models or in healthy animal tissue. In order to determine the full extent of rosiglitazone‟s actions, it would have been desirable to tailor the experiments more in line with a clinical setting rather than relying exclusively on stand-alone in-vitro experiments. One such relevant clinical factor is the manner of administration of rosiglitazone. The effects observed in this study followed a single dose administration of the drug with subsequent analytical investigations conducted over the following hours/days. In a clinical setting, the drug is obviously administered in a different regime with either daily or twice daily dosing (4mg or 8mg/day (GSK summaries of product characteristics factsheet: Avandia 4mg & 8mg film-coated tablets, 2009)), and it would be interesting to see whether such repeated dosing in our cellular/tissue models would have produced the same results as a one-off dosing.

For the same reason, it would be very insightful to look at the effects of rosiglitazone in animal models and in particular, in diabetic animal models for example diabetic Zucker rat models or streptozotocin-induced diabetic mice models. In these instances the pharmacokinetics of rosiglitazone therapy (i.e. absorption time, half life, tissue distribution and drug removal) could be more accurately reproduced/represented than in simple cellular models, and therefore this could be a positive first step in determining whether the effects observed in this study would also occur in a patient clinical setting. It is interesting to note that in patient studies it appears that while rosiglitazone treatment (in conjunction with insulin therapy) takes approximately 8-12 weeks to lead to improvements in glycaemic control (Raskin *et al*, 2001), that its anti-inflammatory effects seem to be mediated within only 2 weeks (Marx *et al*, 2003). Obviously, the best way to establish the effects of the drug in humans is to conduct patient studies and in the opinion of the author, there is a need to look at rosiglitazone‟s effects on Ca^{2+} homeostasis using the techniques previously conducted in the present study using extracted mononuclear cells from healthy donors, from diabetic individuals both undertaking and abstaining from rosiglitazone therapy.

Other techniques that could be employed to more closely examine rosiglitazone‟s effects in cellular models are the implementation of fluorescently-labelled rosiglitazone and the use of electron spin resonance (ESR). Addition of a fluorescent

tag to rosiglitazone would facilitate the visualisation of rosiglitazone‟s targets and distribution within the cell and allow more clear understanding of its actions. Use of ESR would also allow a more detailed analysis of the physical characteristics of the ER membrane before and after treatment with rosiglitazone. This could aid in investigation of the hypothesis that rosiglitazone induces its effects on SERCA2b via modulation of the physical characteristics of the ER membrane. Finally, another way of substantiating rosiglitazone‟s actions on SERCA2b would be to employ the use of siRNA techniques to effectively silence SERCA2b to further establish/consolidate the importance of this ER-bound protein in rosiglitazone‟s mode of action.

As previously discussed, there were numerous limitations in the work on aortic ring tissue described in Chapter 4, including time constraints, sample size/sample repetition and the number and range of experiments conducted. It is important to acknowledge that to effectively establish rosiglitazone‟s potential to increase Ach and SNP-induced-vasodilation and hence potentiate improvements in vascular function would require a much greater repetition of experiments to give a bigger „n‟ number and for this reason, the current study must be viewed as preliminary investigation into this topic.

It would also be beneficial to consider repeated drug dosing of aortic tissue, as discussed with regard to the cell culture setting above. Given that Ach-induced vasodilation of intact tissue appeared to produce a less substantial increase in aortic ring relaxation compared with SNP in denuded tissue (after 24hr rosiglitazone incubation) possibly due to the presence of endothelium-derived vasoconstrictor prostanoids and Llorens findings that blockage of such prostanoids with indomethacin reduced PE-induced contractility of pioglitazone treated aortic rings (Llorens *et al*, 2007), it would be beneficial to repeat the investigations described in Chapter 4 in the presence of the prostanoid inhibitor indomethacin. This would allow investigation of the hypothesis that prostanoid formation is indeed the reason for the reduction in Ach-induced endothelium-dependent vasodilation seen in intact aortic tissue as compared to the enhanced SNP-induced endothelium-independent vasodilation seen in denuded aortic tissue.

Finally, research is currently being conducted in our laboratory to determine whether natural PPARγ-ligands elicit the same Ca^{2+} homeostatic effects as rosiglitazone in the cell lines studied here. To date it has been determined that:

a) 15d-PGJ2 (3µM) inhibits Ca^{2+}ATPase activity in monocytic microsomes (30min), triggers the upregulation of UPR genes in cultured monocytes (4h), but does not induce widespread apoptosis in these cells (0-10days; Isa, S – personal communication). Thus, the earlier suggestion that rosiglitazone and 15d-PGJ2 act via similar mechanisms seems to be supported by these data.
b) Cholesterol (200µg/ml) inhibits Ca^{2+}ATPase activity in monocytic microsomes (30min), but does not exert any effects on XBP-1 splicing, UPR gene expression or apoptosis in intact cells (Isa, S. – personal communication), presumably because free cholesterol is not readily imported into monocytes.
c) Oxidised low density lipoprotein (oxLDL; 40µg/ml) – a cholesterol-containing lipoprotein particle taken up into cells by the scavenger receptor CD36, whereupon it is broken down within lysosomes into free cholesterol (Tabas, 2004) – did not inhibit Ca^{2+}ATPase activity in monocytic microsomes (30min). However, in intact cells that contain lysosomes, oxLDL did trigger XBP-1 splicing and thus UPR activation (Isa, S. – personal communication)

Given the importance of lipotoxicity in foam cell formation, and thus apoptotic cell death within atherosclerotic plaques (Tabas *et al*, 2004), this presents the intriguing possibility that, as rosiglitazone may be acting in a similar way to cholesterol/cholesterol-containing lipoprotein particles, rosiglitazone could be used as a „positive control" when monitoring the lipotoxic effects of various cholesterol levels within samples taken from obese subjects.

5.4 Conclusion

This study has added to the previously published literature and provided further evidence for the existence of PPARγ-independent „non-genomic" effects as exerted by the anti-hyperglycaemic agent rosiglitazone. This study has shown that initial incubation with the drug causes a rapid rise in $[Ca^{2+}]_i$ via dose-dependent inhibition of the ER-bound Ca^{2+}ATPase SERCA2b. This hindered re-sequestration of Ca^{2+} into the ER, combined with continued non-specific leakage of Ca^{2+} into the ER, causes ER Ca^{2+} levels to decrease which confers stress upon the organelle and the initiation of the unfolded protein response (via activation of transcription factors including XBP-1). UPR initiation leads to the up-regulation of UPR-inducible genes such as SERCA2b, which leads to production of new uninhibited SERCA2b protein, increased Ca^{2+} sequestration into the ER and ultimately a restoration of normal resting cellular $[Ca^{2+}]_i$.

The above sequence of events has been shown in this study to occur in two cell types important in the pathophysiology of T2D and the development of its associated complications. Such restorative improvements in cellular function led to the postulation that the drug may, via the proposed mechanism, confer functional improvement in tissues such as the vasculature. Thus, the current study has shown that extended incubation with rosiglitazone (24hrs) leads to increased SNP-induced vasodilation in denuded aortic tissue, and to (non-statistically significant) enhanced NO-mediated Ach-induced vasodilation in intact aortic tissue. This preliminary evidence leads to the conclusion that rosiglitazone may exert functional improvements on the vasculature via its actions on the VSMC (and possibly also the endothelial cell), potentially via the above postulated mechanism of improved Ca^{2+} homeostasis.

In the light of the current debate regarding the safety of TZDs - especially rosiglitazone - due to their increased potential to augment adverse cardiovascular outcomes, this study"s description of potential improvements in Ca^{2+} homeostasis as a result of rosiglitazone treatment, takes on extra importance. If, as several researchers highlight, rosiglitazone"s potential adverse cardiovascular „side-effects" outweigh its anti-hyperglycaemic properties then its continued use in clinical practice has to be questioned. However if, as the preliminary findings of this and other studies

suggest, rosiglitazone induces other potentially beneficial „side-effects" such as improvements in Ca^{2+} homeostasis, alongside improvements in glycaemic control, then the risk of adverse outcomes may be exceeded by the positive effects this therapy may induce in diabetic individuals. Clearly, the data presented in this *in vitro* cell model-based study has to be treated tentatively and much more research has to be conducted before the potentially beneficial „non-genomic" effects highlighted can be firmly identified as being of clinical significance. Nevertheless, in conclusion, it is the opinion of the author that the current study does support a continued potential therapeutic benefit of administration of this drug in a carefully controlled diabetic population.

Chapter Six

References

Chapter 6: References

Adachi, T., Matsui, R., Weisbrod, R.M., Najibi, S., & Cohen, R.A. 2001, "Reduced sarco/endoplasmic reticulum $Ca^{(2+)}$uptake can account for the reduced response to NO, but not sodium nitroprusside, in hypercholesterolemic rabbit aorta", *Circ*, vol. 104, pp. 1040-1045.

Advani, A., Marshall, S.M., & Thomas, T.H. 2004, "Impaired neutrophil store-mediated calcium entry in Type 2 diabetes", *Eur.J.Clin.Invest*, vol. 34, no. 1, pp. 43-49.

Ahluwalia, M. (2005). The effects of peroxisome proliferators-activated receptor-gamma (PPARγ) agonists on monocytic cell activation and endothelial function indiabetes. PhD thesis, University of Wales Institute, Cardiff, University of Wales.

Akhondi, 2008, BSc dissertation, University of Wales Institute, Cardiff, University of Wales.

Aronson, D., and Rayfield, E.J. 2002, "How hyperglycaemia promotes atherosclerosis:molecular mechanisms", *Cardiovasc Diabetol*, vol. 1, no. 1, pp. 1-10.

Arredouani, A., Guiot, Y., Jonas, J.C., Liu, L.H., Nenquin, M., Pertusa, J.A., Rahier, J., Rolland, J.F., Shull, G.E., Stevens, M., Wuytack, F., Henquin, J.C., & Gilon, P. 2002, "SERCA3 ablation does not impair insulin secretion but suggests distinct roles of different sarcoendoplasmic reticulum Ca^{2+} pumps for Ca^{2+} homeostasis in pancreatic beta-cells", *Diabetes*, vol. 51, pp. 3245-3253.

Asashi, M., Sugita, Y., Kurzydlowski, K., De Leon, S., Tada, M., Toyoshima, C and MacLennan, D.H. 2003, "Sarcolipin regulates sarco(endo)plasmic reticulum Ca2+-ATPase (SERCA) by binding to transmembrane helices alone or in association with phospholamban", *PNAS*, vol.100, no. 9, pp. 5040-5045.

Atkin, L. 2008, "Rosiglitazone-induced SERCA2b inhibition: implications for monocyte cytoskeletal remodelling and diabetic microangiopathy", Bioscience Horizons, vol. 1, no. 1, pp. 1-7.

Axelsen, K.B., & Palmgren, M.G. 1998, "Evolution of substrate specificities in the P-type ATPase superfamily", *J Mol Evol*., vol. 46, no. 1, pp. 84-101.

Bagi, Z., Koller, A., & Kaley, G. 2004, "PPARγ activation by reducing oxidative stress, increases NO bioavailability in coronary arterioles of mice with Type 2 diabetes", *Am J Physiol Heart Circ Physiol*, vol. 286, pp. H742-H748.

Bagley, K.C., Abdelwahab, S.F., Tuskan, R.G., & Lewis, G.K. 2004, "Calcium signalling through phospholipase C activates dendritic cells to mature and is necessary for the activation and maturation of dendritic cells induced by diverse agonists", *Clin.Diagn.Lab.Immunol*, vol. 11, no. 1, pp. 77-82.

Balasubramanyam, M., Balaji, R.A., Subashini, B., & Mohan, V. 2001, "Evidence for mechanistic alterations of Ca^{2+} homeostasis in Type 2 Diabetes Mellitus", *Int.Jnl.Experimental.Diab.Res*, vol. 1, pp. 275-287.

Baylor College of Medicine, Houston, Texas website: Henry.J.Pownall PhD (http://www.bcm.edu/cmb/?pmid=2382) - Accessed 22-10-09.

Belke, D.D., Swanson, E.A., & Dilmann, W.H. 2004, "Decreased sarcoplasmic reticulum activity in diabeticdb/db mouse heart" *Diabetes*, vol. 53, no. 12, pp.3201-3208.

Bell, D.H.S. 2003, "Heart failure. The frequent, forgotten, and often fatal complication of diabetes", *Diabetes Care*, vol. 26, pp. 2433–2441.

Berger, J., Leibowitz, M.D., Doebber, T.W., Elbreecht, A., Zhang, B., Zhou, G., Biswas, C., Cullinan, C.A., Hayes, N.S., Li, Y., Tanen, M., Ventre, J., Wu, M.S., Berger, G.D., Mosley, R., Marquis, R., Santini, C., Sahoo, S.P., Tolman, R.L., Smith, R.G., & Moller, D.E. 1999, "Novel peroxisome proliferators-activated receptor (PPAR) gamma and PPARdelta ligands produce distinct biological effects", *J.Biol.Chem*., vol. 274, no. 10, pp. 6718-6725.

Berridge, M.J. 1997, "Elementary and global aspects of calcium signalling", *J Physiol*, vol. 499, no. 2, pp. 291-306.

Berridge, M.J. 2002, "The endoplasmic reticulum: a multifunctional signalling organelle", *Cell Calcium*, vol. 32, no. 5, pp. 235-249.

Bierhaus, A., Hofmann, M.A., Ziegler, R., & Nowrith, P.P. et al .1998, "AGEs and their interactions with AGE receptors in vascular disease and diabetes. The AGE concept", *Cardiovasc. Res,* vol. 37, no. 3 ,pp. 586-600.

Bisadee, K.R., Zhang, Y., Shao, C.H., Wang, M., Patel, K.P., Dincer, U.D., & Besch, H.R Jn. 2004, "Diabetes increases formation of advanced glycation end products on Sarco(endo)plasmic reticulum Ca2+-ATPase", *Diabetes*, vol. 53, no. 2, pp. 463-473.

Borge, P.D., & Wolf, B.A. 2003, "Insulin receptor substrate 1 regulation of sarco-endoplasmic reticulum calcium ATPase 3 in insulin-secreting β-cells", *J Biol Chem*, vol. 278, no. 13, pp. 11359-11368.

Brandl, C.J., deLeon, S., Martin, D.R., and MacLennan, D.H. 1987, "Adult forms of the Ca^{2+}ATPase of sarcoplasmic reticulum. Expression in developing skeletal muscle" *J Chem Biol*, vol. 262, no. 8, pp. 3766-3774.

Bray, J.J. (1986). Lecture Notes on Human Physiology, Blackwell Publishers, Oxford.

British Heart Foundation Statistics Website (http://www.heartstats.org/temp/ESspweb08sppages1to10%281%29.pdf) – accessed via www.bhf.org.uk, 21/10/2009.

Brownlee, M. 1995, "Advanced protein glycosylation in diabetes and aging", *Ann Rev Med*, vol. 46, pp. 224-234.

Brownlee, M. 2001, "Biochemistry and molecular cell biology of diabetic complications", *Nature*, vol. 414, no. 6865 , pp. 813-820.

Buchanan, T.A., Meehan, W.P., Jeng, Y.Y., Yang, D., Chan, T.M., Nadler, J.L., Scott, S., Rude, R.K., & Hsueh, W.A. 1995, "Blood pressure lowering by pioglitazone", *J.Clin.Invest*, vol. 96, no. 1, pp. 354-360.

Burk, S.E., Lytton, J., MacLennan, D.H., & Shull, G.E. 1989, "cDNA cloning, functional expression and mRNA tissue distribution of a third organellar Ca2+ pump", *J Biol Chem*, vol. 264, no. 31, pp. 18561-18568.

Caballero, A.E., Saouaf, R., Lim, S.C., Hamdy, O., Abou-Elenin, K., O'Connor, C., Logerfo, F.W., Horton, E.S., & Veves, A. 2003, "The early effects of troglitazone, an insulin-sensitizing agent, on the endotheliual function in early and late type 2 diabetes: a placebo-controlled randomiszed clinical trial", *Metabolism,* vol. 52, no. 2, pp. 173-180.

Camacho, M., Lopez-Belmonte, J., & Vila Luis. 1998, "Rate of Vasoconstrictor Prostanoids Released by Endothelial Cells Depends on Cyclooxygenase-2 Expression and Prostaglandin I Synthase Activity", *Circ.Res*, vol. 83, pp. 353-365.

Camp, H.S. 2003, "Thiazolidinediones in diabetes: current status and future outlook", *Curr Opin Investig Drugs*, vol. 4, no. 4 ,pp. 406-11.

Campbell, A.M., Kessler, P.D., & Fambrough, D.M. 1992, "The alternative carboxyl termini of avian cardiac and brain sarcoplasmic reticulum/endoplasmic reticulum Ca^{2+}-ATPases are on the opposite side of the membrane", *J.Biol.Chem*, vol. 267, no. 13 , pp. 9321-9325.

Campbell, I., & Duffus, J.H. 1988, "Yeast: A Practical Approach", Oxford University Press.

Carlberg, M., Dricul, A., Blegenl, H., Kass, G.E.N., Orrenius, S., & Larsson, O. 1996, "Short exposures to tunicamycin induce apoptosis in SV40-transformed but not in normal human fibroblasts", *Cardnogenesis***,** vol.17, no.12, pp.2589-2596.

Caspersen, C., Pedersen, P.S., & Treiman, M. 2000, "The sarco/endoplasmic reticulum calcium-ATPase 2b is an endoplasmic reticulum stress-inducible protein", *J Biol Chem*, vol. 275, no. 29, pp. 22363-22372.

Chambers, K.T., Weber, S.M., & Corbett, J.A. 2006, "PGJ2-stimulated β-cell apoptosis is associated with prolonged UPR activation", *Am J Physiol Endocrinol Metab*, vol. 292, pp. E1052-E1061.

Chappey, O, Dosquet, C., Wautier, M.P., & Wautier, J.L. 1997, "Advanced glycation end products, oxidant stress and vascular lesions", *Eur J Clin Invest*, vol. 27, no. 2, pp. 97-108.

Chawla, A., Barak, Y., Nagy, L., Tontonoz, P., & Evans, R.M. 2001, "PPARγ dependent and independent effects on macrophage-gene expression in lipid metabolism and inflammation". *Nature Medicine*, vol. 7, no. 1 , pp. 48-52.

Chawla, A., & Niwa, M. 2005, "The unfolded protein response", Curr Biol. Vol.15, no. 22, p. R907.

Chen, L.H., Jiangy, C.C., Kiejda, K.A., Wang, Y.F., Thorne, R.F., Zhang, X.D., & Hersey, P. 2007, "Thapsigargin sensitizes human melanoma cells to TRAIL-induced apoptosis by up-regulation of TRAIL-R2 through the unfolded protein response", *Carcinogenesis*, vol.28, no.11, pp.2328–2336.

Chiarelli, F. and Di Marzio, D. 2008, "Peroxisome proliferators-activated receptor-γ agonists and diabetes: Current evidence and future perspectives", *Vascular Health and Risk Management*, vol. 4, no. 2, pp. 297-304.

Clapham, D.E. 1995, "Intracellular calcium. Replenishing the stores", *Nature*, vol. 375, no. 6533, pp. 634-635.

Clark, R.J., McDonough, P.M., Swanson, E., Trost, S.U., Suzuki, M., Fukuda, M., & Dilmann, W.H. 2003, "Diabetes and the accompanying hyperglycaemia impairs cardiomyocyte calcium cycling through increased nuclear O-GlcNAcylation", *J Biol Chem*, vol. 278, no. 45, pp. 44230-44237.

Claycomb, W.C., Lanson, N.A. jr., Stallworth, B.S., Egeland, D.B., Delcarpio, J.B., Bahinski, A., & Izzo, N.J. Jr. 1998, "HL-1 cells: a cardiac muscle cell line that contracts and retains phenotypic characteristics of the adult cardiomyocyte", *PNAS*, vol. 95, no. 6, pp. 2979-2984.

Cohen, R.A. 1995," The role of nitric oxide and other endothelium-derived vasoactive substances in vascular disease", *Prog Cardiovasc Dis*., vol. 38, no. 2, pp. 105-128.

Cohen, R.A., Weisbrod, R.M., Gericke, M., Yaghoubi, M., Bieri, C., & Bolotina, V.M. 1999, "Mechansim of nitric oxide-induced vasodilation. Refilling of intracellular stores by sarcoplasmic reticulum Ca^{2+} ATPase and inhibition of store-operated Ca^{2+} influx", *Circ Res*, vol. 84, no. 210-219.

Dally, S., Bredoux, R., Corvazier, E., Andersen, J.P., Clausen, J.D., Dode, L., Fanchaouy, M., Gelebart, P., Monceau, V., Del Monte, F., Gwathmey, J.K., Hailjar, R., Chaabane, C., Bobe, R., Raies, A., & Enouf, J. 2006, "Ca^{2+}-ATPases in non-failing and failing heart: evidence for a novel cardiac sarco/endoplasmic reticulum Ca^{2+}-ATPase 2 isoform (SERCA2c)", *Biochem.J*, vol. 395, no. 2, pp. 249-258.

Deng, T., Yu, L., Ge, Y., Zhang, L., & Zheng, X. 2005, "Intracellular-free calcium dynamics and F-actin alteration in the formation of macrophage foam cells", *BBRC*, vol. 338, pp. 748-756.

Desvergne, B., & Wahli, W. 1999, "Peroxisome proliferator-activated receptors: nuclear control of metabolism", *Endocr Rev*, vol. 20, no. 5, pp. 649-688.

DeVries-Siimon, T., Li, Y., Yao, P.M., Stone, E., Wang, Y., Davis, R.J., Flavell, R., & Tabas, I. 2005, "Cholesterol-induced macrophage apoptosis requires ER stress pathways and engagement of the type A scavenger receptor", *Journal of Cell Biology*, vol. 171, no. 1, pp. 61-73.

Diep, Q.N., Mabrouk, M.E., Cohn, J.S., Endemann, D., Amiri, F., Virdis, A., Neves, M.F., & Schrifiin, E.L. 2002, "Structure, endothelial function, cell growth, and

inflammation in blood vessels of angiotensin II-infused rats. Role of peroxisome proliferators-activated receptor-γ", *Circ*, vol. 105, pp. 2296-2302.

Diradourian, C., Girard, J., & Pégorier, J. 2005, "Phosphorylation of PPARs:from molecular characterization to physiological relevance", *Biochimie*, vol. 87, pp. 33-38.

Dogra, G.K., Herrmann, S., Irish, A.B., Thomas, M.A., & Watts, G.F. 2002, " Insulin resistance, dyslipidemia, inflammation and endothelial function in nephrotic syndrome", Nephrol Dial Transplant, vol. 17, no. 12, pp. 2220-2225.

Dorlands Online Dictionary (http://www.dorlands.com) - Accessed 22-10-09

Dyck, P.J., Kratz, K.M., Larnes, J.L., Litchy, W.J., Klein, R., Pach, J.M., Wilson, D.M., O'Brien, P.C., Melton L.J. 3rd, & Service, F.J. 1993, "The prevalence by staged severity of various types of diabetic neuropathy, retinopathy and nephropathy in a population-based cohort: the Rochester Diabetic Neuropathy Study", *Neurology*, vol. 43, no. 4, pp. 817-824.

Dyck, P.J., & Giannini, C. 1996, "Pathologic alterations in the diabetic neuropathies of humans: a review", *J Neuropathol Exp Neurol*, vol. 55, no. 12, pp. 1181-1193.

East, J.M. 2000, "Sarco(endo)plasmic reticulum calcium pumps:recent advances in our understanding of structure/function and biology (Review)", *Mol Memb Biol*, vol. 17, no. 4, pp. 189-200.

Eckstein-Ludwig, U., Webb, R.J., Van Goethem, I.D., East, J.M., Lee, A.G., Kimura, M., O'Neill, P.M., Bray, P.G., Ward, S.A.. & Krishna, S. 2003, "Artemisinins target the SERCA of Plasmdium falciparum", *Nature*, vol. 424, no. 6951, pp. 957–961.

Eizirik, D.L., Cardozo, A.K., & Cnop, M. 2008, "The role for endoplasmic reticulum stress in diabetes mellitus", *EndocrineReviews*, vol. 29, no. 1, pp. 42-61.

Elsner, J., Norgauer, J., Dobos, G.J., Emmendorffer, A., Schopf, E., Kapp, A., & Roesler, J. 1993, "Flow cytometry reveals different lag times in rapid cytoplasmic calcium elevations in human neutrophils in response to N-formyl peptide*", J Cell Physiol,* vol. 157, no. 3, pp. 637-643.

Endo, M., Mori, M., Akira, S., & Gotoh, T. 2006, "C/EBP homologous protein (CHOP) is crucial for the induction of caspase-11 and the pathogenesisi of lipopolysaccharide-induced inflammation", *J Immunol*, vol. 176, no. 10, pp. 6245-6253.

Farah, R, Shurt-Swirski, R., & Lapin, O. 2008, "Intensification of oxidative stress and inflammation in type 2 diabetes despite antihyperglycaemic treatment", *Cardiovasc Diabetol*, vol. 22, pp. 7-20.

Feinstein, D.L., Spagnolo, A., Akar, C., Weinberg, G., Murphy, P., Gavrilyuk, V., & Dello Russo, G. 2005, "Receptor-independent actions of PPAR thiazolidinedione agonists: Is mitochondrial function the key?", *Biochemical Pharmacology*, vol. 70, no. 2 , pp. 177-188.

Ferré, P. 2004, "The Biology of Peroxisome Proliferator-Activated Receptors. Relationship with lipid metabolism and insulin sensitivity", *Diabetes*, vol. 53, no. s1 , pp. s43s50.

Ferrington, D.A., Kraine, A.G., & Bigelow, D.J. 1998, "Altered turnover of calcium regulatory proteins of the sarcoplasmic reticulum in aged skeletal muscle", *J Biol Chem*, vol. 273, no. 10, pp. 5885-5891.

Ferris, C.D., Huganir, R.L., Supattapone, S., & Snyder, S.H. 1989, "Purified inositol 1,4,5-trisphosphate receptor mediates calcium flux in reconstituted lipid vesicles", *Nature,* vol. 342, no. 6245, pp. 87-89.

Frischauf, I., Schindl, R., Derler, I., Bergsmann, J., Fahrner, M., and Romanin, C. 2008, "The STIM/Orai coupling machinery", *Channels*, vol. 2, no. 4, pp. 261-268.

Fuenzalida K., Quintanilla, R., Ramos, P., Piderit, D., Fuentealba, R.A., Martinez, G., Inestrosa, N.C., & Bronfman, M. 2007, "Peroxisome proliferator-activated receptor gamma up regulates the Bcl-2 anti-apoptotic protein in neurons and induces mitochondrial stabilization and protection against oxidative stress and apoptosis", *J Biol Chem*, vol. 282, no. 51, pp. 37006-37015.

Gardner, O.S., Shiau, C.W., Chen, C.S., & Graves, L.M. 2005, "Peroxisome proliferator-activated receptor gamma-independent activation of p38 MAPK by thiazolidinediones involves calcium/calmodulin-dependent protein kinase II and protein kinase R: correlation with endoplasmic reticulum stress", *J Biol Chem*, vol. 280, no. 11, pp. 10109-10118.

Genolet, R., Wahli, W., & Michalik, L. 2004, "PPARs as drug targets to modulate inflammatory responses?", *Curr Drug Targets Inflamm Allergy*., vol. 3, no. 4, pp. 361-375.

GlaxoSmithKline factsheet – Avandia 4mg and 8mg film-coated tablets, Revised edition (http://emc.medicines.org.uk/medicine/3200/SPC/Avandia4mg&8mgfilm-coatedTablets/.) – Accessed 18/09/09.

Goetze, S., Eilers, F., Bungenstock, A., Kintscher, U., Stawowy, P., Blaschke, F., Graf, K., Law, R.E., Fleck, E., & Grafe, M. 2002, "PPAR activators inhibit endothelial cell migration by targeting Akt", *Biochem Biophys Res Commun*., vol. 293, no. 5, pp. 1431-1437.

Greene, M.E., Blumberg, B., McBride, O.W., Yi, H.F., Kwan, K., Hsieh, L., Greene, G., & Nimer, S.D. 1995, "Isolation of the human peroxisome proliferators activated receptor gamma cDNA: expression in hematopoietic cells and chromosomal mapping", *Gene Exp*, vol. 4, no. 4-5, pp. 281-299.

Groenendyk, J., Lynch, J., & Michalak, M. 2004, "Calreticulin, Ca^{2+} and Calcineurin – Signalling from the endoplasmic reticulum", *Mol. Cells*, vol. 17, no. 3 , pp. 383-389.

Gruber, A., Nasser, K., Smith, R., Sharma, J.C., & Thomson, G.A. 2006, "Diabetes prevention:is there more to it than lifestyle changes?", *Int.J.Clin.Pract*., vol. 60, no. 5, pp. 590-594.

Gunteski-Hamblin, A, Greeb, J., & Shull, G.E. 1988, "A novel Ca2+ pump expressed in brain, kidney and stomach is encoded by an alternate transcript of the slow-twitch muscle sarcoplasmic reticulum Ca-ATPase gene", *J Biol Chem*, vol. 263, no. 29, pp. 15032-15040 *et al*, 1989

Gustafsson, I., Brendorp, B., Seibaek, M., Burchardt, H., Hildebrant, P., Kober, L., & Torp-Pedersen, C. 2004, "Influence of diabetes and diabetes-gender interaction on the risk of death in patients hospitalised with congestive heart failure", JACC, vol. 43, no. 5, pp. 771-777.

Hasegawa, H., Yamada, Y., Komiyama, K., Hayashi, M., Ishibashi, M,., Sunazuka, T., Izuhara, T., Sugahara, K., Tsuruda, K., Masuda, M., Takasu, N., Tsukasaki, K., Tomonaga, M., & Kamihira, S. 2007, "A novel natural compound, a cycloanthranilylproline derivative (Fuligocandin B), sensitizes leukaemia cells to apoptosis induced by tumor necrosis factor related apoptosis-inducing ligand (TRAIL) through 15-deoxy-{Delta}12,14 prostaglandin J2 production", *Blood*, vol. 110, no. 5, pp. 1664-1674.

He, Q., Pang, R., Song, X., Chen, J., Chen, H., Chen, B., Hu, P., & Chen, M. 2008, "Rosiglitazone suppresses the growth and invasiveness of SGC-7901 gastric cancer cells and angiogenesisi in vitro via PPARgamma dependent and independent mechanisms", *PPAR Res*, vol. 2008.

Heine, R.J., Diamant, M., Mbanya, J.C., & Nathan, D.M. 2006, "Management of hyperglycaemia in type 2 diabetes: the end of recurrent failure?", *BMJ*, vol. 333, no. 7580, pp. 1200-1204.

Hetzel, J., Balletshofer, B., Rittig, K., Walcher, D., Kratzer, W., Hombach, V., Haring, H., Koenig, W., & Marx, N. 2005, "Rapid effects of rosiglitazone treatment on endothelial function and inflammatory biomarkers", *Arterioscler. Thromb. Vasc. Biol.* vol. 25, pp. 1804-1809.

Hinz, B., Brune, K., & Pahl, A. 2003, "15-Deoxy-Δ12,14-prostaglandin J2 inhibits the expression of proinflammatory genes in human blood monocytes via a PPARγ-independent mechanism", *Biochem Biophys Res Comm*, vol. 302, pp. 415-420.

Hirota, M., Kitagaki, M., Itagaki, H., and Aiba, S. 2006, "Quantitative measurement of spliced XBP1 mRNA as an indicator of endoplasmic reticulum stress", *The Journal of Toxicological Sciences*, vol.31, pp. 149-156.

Home, P.D., Pocock, S.J., Beck-Nielsen, H., Gomis, R., Hanefeld, M., Jones, N.P., Komajda, M., & McMurray, J.J.V for the RECORD Study Group. 2007, "Rosiglitazone Evaluated for Cardiovascular Outcomes – An Interim Analysis", *N Engl J Med*, vol. 357, no. 1 , pp. 28-38.

Home, P.D., Pocock, S.J., Beck-Nielsen, H., Curtis, P.S., Gomis, R., Hanefeld, M., Jones, N.P., Komajda, M., & McMurray, J.J.V for the RECORD Study Group. 2009, "Rosiglitazone Evaluated for Cardiovascular Outcomes in oral agent combination therapy for type 2 diabetes (RECORD): a multicentre, randomised, open-label trial", *Lancet*, vol. 373, no. 9681, pp. 2125-2135.

Hruska, M.W., & Frye, R.F. 2004, "A simplified method for determinination of rosiglitazone in human plasma", *J Chromatogr B Analyt Technol Biomed Life Sci*, vol. 803, no. 2, pp. 317-320.

Hu, Z., Bonifas, J.M., Beech, J., Bench, G., Shigihara, T., Ogawa, H., Ikeda, S., Mauro, T., & Epstein E.H. Jr, 2000, "Mutations in ATP2C1, encoding a calcium pump, cause Hailey-Hailey disease", *Nat Genet*, vol. 24, no. 1, pp. 61-65.

Ignarro, L.J., Napoili, C., & Loscalzo, J. 2002, "Nitric oxide donors and cardiovascular agents modulating the bioavailability of nitric acid: an overview", *Circ Res*, vol. 90, no. 1, pp. 21-28.

Jaiswal, J.K. 2001, "Calcium - how and why?", *J Biosci*., vol. 26, no. 3, pp. 357-363.

Jiang, G., Ting, A.T., & Seed, B. 1998, "PPAR-gamma agonists inhibit production of monocyte inflammatory cytokines", *Nature,* vol. 391, no. 6662, pp. 82-86.

John, L.M., Lechleiter, J.D., & Camacho, P. 1998, "Differential modulation of SERCA2 isoforms by caltreticulin", *J Cell Biol*, vol. 142, no. 4, pp. 963-973.

Juurlink, D.N., Gomes, T., Lipscombe, L.L., Austin, P.C., Hux, J.E., & Mamdani, M.M. 2009, "Adverse cardiovascular events during treatment with pioglitazone and rosiglitazone: population based cohort study", *BMJ*, vol. 339, pp. b2942.

Kahn, H.A., & Moorhead, H.B. 1973, "Statistics on blindness in the model reporting area 1969-1970 US. Department of Health, Education and Welfare Publication No. (MIH) US. Government Printing Office, Washington, pp. 73-427.

Kahn, S.E., Haffner, S.M., Heise, M.A., Herman, W.H., Holman, R.R., Jones, N.P., Kravitz, B.G., Lachin, J.M., O'Neill, M., Zinman, B., &Viberti, G. 2006, "Glycaemic durability of rosiglitazone, metformin or glyburide monotherapy", *N Eng J Med*, vol. 355, no. 23, pp. 2427-2443.

Kass, G.E.N., & Orrenius,.S. 1999, Calcium signalling and cytotoxicity", Environmental Health Perspectives, vol. 107, no. 1, pp. 25-35.

Kim, K.Y., Ahn, J.H., & Cheon, H.G. 2007, "Apoptotic action of peroxisome proliferator-activated receptor-gamma activation in human non small-cell lung cancer is mediated via proline oxidase-induced reactive oxygen speciesd formation", *Mol Pharmacol*, vol. 72, no. 3, pp. 674-685.

Kim, Y.H., Jung, E.M., Lee, T.J., Kim, S.H., Choi, Y.H., Park, J.W., Park, J.W, Choi, K.S., & Kwon, T.K. 2008, "Rosiglitazone promotes tumor necrosis factor-related apoptosis-inducing ligand-induced apoptosis by reactive oxygen species up-regulation of death receptor 5 and down-regulation of c-FLIP", *Free Radic Biol Med,* vol. 44, no. 6, pp. 1055-1068.

Kimes, B.W, & Brandt, B.L. 1976, "Characterization of two putative smooth muscle cell lines from rat thoracic aorta", *Exp Cell Res*, vol. 98, no. 2, pp. 349-366.

Koh, E.H., Park, J.Y., Park, H.S., Jeon, M.J., Ryu, J.W., Kim, M., Kim, S.Y., Kim, M.S., Kim, S,W., Park, I.S., Youn, J.H., & Lee, K.U. 2007, "Essential role of

mitochondrial function in adiponectin synthesis in adipocytes“, *Diabetes*, vol. 56, no. 12, pp. 2973-2981.

Kohlroser, J., Mathai, J., Reichheld, J., Banner, B.F., & Bonkovsky, H.L. 2000, “Hepatoxicity due to troglitazone: report of two cases and review of adverse events reported to the United States Food and Drug Administration”, *Am J Gastroenterol*, vol. 95, pp. 272-276.

Koller, A., Schlossmann, J., Ashman, K., Uttenweiler-Joseph, S., Ruth, P., & Hofmann, F. 2003, „Association of phospholamban with a cGMP linase signalling complex“, *BBRC*, vol. 300, pp.155-160.

Koro, C.E., Bowlin, S.J., & Weiss, S.R. 2005, “Antidiabetic therapy and the risk of heart failure in type 2 diabetic patients: an independent effect or confounding by indication”, *Pharmacoepidemiology and drug safety*, vol. 14, pp. 697–703.

Kozel, P.J., Friedman, R.A., Erway, L.C., Yamoah, E.N., Liu, L.H., Riddle, T., Duffy, J.J., Doetschman, T., Miller, M.L., Cardell, E.L., & Shull, G.E, 1998, “Balance and hearing deficits in mice with a null mutation in the gene encoding plasma membrane Ca2+-ATPase isoform 2“, *J Biol Chem*, vol. 273, no. 30, pp. 18693-18696.

Krishna, S., Woodrow, C.,, Webb, R., Penny, J., Takeyasu, K., Kimura, M., & East, J.M. 2001, “Expression and functional characterization of a Plasmodium falciparum Ca2+-ATPase (PfATP4) belonging to a subclass unique to apicomplexan organisms”, *J Biol Chem*, vol. 276, no. 14, pp. 10782-10787.

Kubisch, C.H., Sans, M.D., Arumugam, T., Ernst, S.A., Williams, J,A. & Logsdon, C.D. 2006, “Early activation of endoplasmic reticulum stress is associated with arginine-induced acute pancreatitus”, *Am J Physiol Gastrointest Liver Physiol*, vol. 291, no. 2, pp.G238-245.

Kumar, V. (1997). Basic Pathology (6th edn). WB Saunders Publishers, Pennsylvania; ISBN 0721651224

Landmesser, U., Hornig, B., & Drexler, H. 2004, „Vascular effects of statins. Endothelial Functiom. A critical determinant in atherosclerosis?”, *Circ*, vol. 109, pp. II27-II33.

Larsen, A.H., Frandsen, A., & Treiman, M. 2001, “Upregulation of the SERCA-type Ca2+ pump activity in response to endoplasmic reticulum stress in PC!” cells”, *BMC Biochemistry*, vol. 2, no. 4.

Launay, S., Giannı`, M., Diomede, L., Machesky, L.M., Enouf, J., & Pap, B. 2003, “Enhancement ofATRA-induced cell differentiation by inhibition of calcium accumulation into the endoplasmic reticulum: cross-talk between RAR_ and calcium-dependent signaling”, *Blood*, vol. 101, pp. 3220-3228.

Lakhani, S.R. (2003). Basic Pathology: An Introduction to the Mechanisms of Disease (3rd edn), Arnold Publishers, London.

Law, R.E., Goetze, S., Xi, X.P., Jackson, S., Kawano, Y., Demer, L., Fishbein, M.C., Meehan, W.P., & Hsueh, W.A. 2000, "Expression and function of PPARgamma in rat and human vascular smooth muscle cells", *Circ*, vol. 101, no. 11, pp. 1311-1318.

Laybutt, D.R., Preston, A.M., Akerfeldt, M.C., Kench, J.G., Busch, A.K., Biankin, A.V., & Biden, T.J. 2007, "Endoplasmic reticulum stress contributes to beta cell apoptosis in type 2 diabetes", *Diabetologia*, vol. 50, no. 4, pp. 752-763.

Lee, A.G., Dalton, K.A., Duggleby, R.C., East, J,M., & Starling, A.P. 1995, "Lipid structure and Ca($^{2+}$)-ATPase function", *Biosci Rep*. vol. 15, no. 5, pp. 289-298.

Lee, A.H., Iwakoshi, N.N., & Glimcher, L.H. 2003, "XBP-1 regulates a subset of endoplasmic reticulum resident chaperone genes in the unfolded protein response", *Mol Cell Biol*, vol. 23, no. 1, pp. 7448-7459.

Levy, J., Zhu, Z., & Dunbar, J.C. 1998, "The effect of glucose and calcium on Ca2+-adenosine triphosphate in pancreatic islets isolated from normal and non-insulin-dependent diabetes mellitus rat model", *Metabolism*, vol. 47, no. 185-189.

Li, Y., Ge, M., Ciani, L., Kuriakose, G., Westover, E.J., Dura, M., Covey, D.F., Freed, J.H., Maxfield, F.R., Lytton, J., & Tabas, I. 2004, "Enrichment of Endoplasmic Reticulum with cholesterol inhibits sarcoplasmic-endoplasmic reticulum calcium ATPase-2b activity in parallel with increased order of membrane lipids", *J Biol Chem*, vol. 279, no. 35, pp. 37030-37039.

Lipskaia, L., Hulot, J.S., & Lompre, A.M. 2007, "Role of sarcoendoplasmic reticulum calcium content and calcium ATPase activity in the control of cell growth and proliferation", Pflugers Arch, vol. 457, no. 3, pp/ 673-685.

Lin, M.S., Chen, W.C., Bai, X., & Wang, Y.D. 2007, "Activation of peroxisome proliferator-activated receptor gamma inhibits cell growth via apoptosis and arrest of the cell cycle in human colorectal cancer", *J Dig Dis*, vol. 8, no. 2, pp. 82-88.

Liu, L.H, Paul, R.J., Sutliff, R.L., Miller, M.L., Lorenz, J.N. Pun, R.Y., Duffy, J.J. Doetschman, T., Kimura, Y., MacLennan, D.H, Hoying, J.B., & Shull, G.E. 1997, "Defective endothelium-dependent relaxation of vascular smooth muscle and endothelial cell Ca2+ signalling in mice lacking sarco(endo)plasmic reticulum Ca^{2+}-ATPase isoform 3", *J Biol Chem*, vol. 272, no. 48, pp. 30538-30545.

Llorens. S., Mendizaball, Y., & Nava, E. 2007, "Effects of rosiglitazone on aortic vascular function in rat genetic hypertension", *Eur J Pharmacol*, vol. 575, pp. 105-112.

Lodish, H. (2004). Molecular Cell Biology (5th edn), W.H. Freeman and Company Publishers, New York.

Luscinskas, F.W., Kansas, G.S., Ding, H., Pizcueta, P., Schleiffenbaum, B.E., Tedder, T. F., & Gimbrone, M.A., Jr. 1994, "Monocyte rolling, arrest and spreading on IL-4-activated vascular endothelium under flow is mediated via sequential action of L-selectin, beta 1-integrins, and beta 2-integrins"., *J. Cell Biol.,* vol. 125, no. 6, pp. 1417-1427

Lytton, J., & MacLennan, D.H. 1988, “Molecular cloning of cDNAs from human kidney coding for two alternatively spliced products of the cardiac Ca2+-ATPase gene, *J Biol Chem*, vol. 263, no. 29, pp. 15024-15031.

Lytton, J., Westlin, M., Burk, S.E., Shull, G.E., & MacLennan, D.H. 1992, “Functional comparisons between isoforms of the sarcoplasmic or endoplasmic reticulum family of calcium pumps”, *J Biol Chem*, vol. 267, no. 20, pp. 14483-14489.

Ma, Y., & Hendershot, L.M. 2001, “ The unfolding tale of the unfolding protein response“, *Cell*, vol. 107, no. 7, pp. 827-830.

MacLennan, D.H. 1970, “Purification and properties of an adenosine triphosphatase from saarcoplasmic reticulum”, *J Biol Chem*, vol. 245, pp. 4508-4518.

Majithiya, J.B., Paramar, A.N., and Balaraman, R. 2005, “Pioglitazone, a PPARgamma agonist, restores endothelial function in aorta of streptozotocin-induced diabetic rats”, *Cardiovasc Res*, vol. 66, no. 1, pp. 150-161.

Maru, S., Koch, G.G., Stender, M., Clark, D., Gibowski, L., Petri, H., White, A.D., & Simpson Jnr, R.J. 2005, “Antidiabetic drugs and heart failure risk in patients with type 2 diabetes in the U.K. primary care setting”, *Diabetes Care*, *vol.* 28, no. 1, pp, 20–26.

Maruyama, K., & MacLennan, D.H. 1988. “Mutation of aspartic acid-351, lysine-352, and lysine-515 alters the Ca2+ activity of the Ca2+-ATPase expressed in COS-1 cells”, *Proc. NAtl. Acad. Sci*., vol. 85, pp. 3314-3318.

Marx, N., Schonbeck, U., Lazar, M.A., Libby, P., & Plutzky, J. 1998, “Peroxisome proliferator-activated receptor gamma activators inhibit gene expression and migration in human vascular smooth muscle cells”, *Circ.Res*., vol. 83, no. 11, pp. 1097-1103.

Marx, N. 2002, “Peroxisome Proliferator-activated receptoy-γ and Atherosclerosis”, *Current Hypertension Reports*, vol. 4, no. 1, pp. 71-77.

Marx, N., Froehlich, J., Siam, L., Ittner, J., Wierse, G., Schmidt, A., Scharnagl, H., Hombach, V., & Koenig, W. 2003, “Antidiabetic PPARγ-activator rosiglitazone reduces MMP-9 serum levels in type 2 diabetic patients with coronary artery disease”, *Thromb Vasc Biol*., vol. 23, pp. 283-288.

Matthews, D.R., Cull, C.A., Stratton, I.M., Holman, R.R., & Turner, R.C. 1998. “UKPDS 26: Sulphonylurea failure in non-insulin-dependent diabetic patients over six years. UK Prospective Diabetes Study (UKPDS) Group”, Diabet Med, vol. 15, no. 4, pp. 297-303.

Mazzoni, M.C. & Schmid-Schonbein, G.W. 1996, "Mechanisms and consequences of cell activation in the microcirculation", *Cardiovasc. Res,* v*ol.* ***32,*** no. 4, pp. 709-719).

McCullough, K.D., Martindale, J.L., Klotz, L.O., Aw, T.Y., & Holbrook, N.J. 2001, "Gadd153 sensitizes cells to endoplasmic reticulum stress by down-regulating Bc12 and perturbing the cellular redox state", *Mol Cell Biol,* vol. 21, no. 4, pp.1249-1259.

McEniery CM, Yasmin, *McDonnell B*, Munnery M, Wallace SM, Rowe CV, Cockcroft JR, Wilkinson IB; Anglo-Cardiff Collaborative Trial Investigators. 2008, "Central pressure: variability and impact of cardiovascular risk factors: the Anglo-Cardiff Collaborative Trial II", *Hypertension*, vol. 51, no. 6, pp. 1476-1482.

McFarlane, C., Young, I.S., Hare, L., Mahon, G., & McEneny, J. 2005, "A rapid methodology for the isolation of intermediate-density lipoprotein: characterization of lipid composition and apoprotein content", *Clin Chim Acta*, vol. 353, no. 1-2, pp. 117-125.

Mesaeli, N., Nakamura, K., Zvaritch, E., Dickie, P., Dziak, E., Krause, K.H., Opas, M., MacLennan, D.H., & Michalak, M. 1999, "Calreticulin is essential for cardiac development", *J Cell Biol*, vol. 144, no. 5, pp. 857-868.

Miller, J.C., & Colagiuri, S. 1994, "The carnivore connection: dietary carbohydrate in the evolution of NIDDM", Diabetologia, vol. 37, no. 12, pp. 1280-1286.

Miller, Y.I., Worrall, D.S., Funk, C.D., Feramisco, J.R., & Witztum, J.L. 2003, "Actin polymerisation in macrophages in response to oxidised LDL and apoptotic cells: role of 12/15 lipoxygenase and phosphoinositide 3-kinase", *Mol. Biol. Cell*, vol. 14, no. 10, pp. 4196-4206.

Missaen, L., Vanoevelen, J., Parys, J.B., Raeymaekers, L., De Smedt, H., Callewarert, G., Erneux, C., & Wuytack, F. 2001, "Ca2+ uptake and release properties of a thapsigargin-insensitive nonmitochondrial Ca2+ store in A7r5 and 16HBE14o- cells", *J Biol Chem*, vol. 277, no. 9, pp. 6898-6902.

Miyamoto, K., Ogura, Y., Kenmochi, S., & Honda, Y. 1997, "Role of leukocytes in diabetic microcirculatory disturbances", Microvas.Res., vol. 54, no. 1, pp. 43-48.

Murphy, G.J. & Holder, J.C. 2000, "PPAR-gamma agonists: therapeutic role in diabetes, inflammation and cancer", TiPS, vol. 21,no. 12, pp. 469-474.

National Heart Forum: Economic cost of Heart Disease (http://www.heartforum.org.uk/AboutCHD_Economicburden.aspx) – accessed 22/10/09.

National Heart Forum: Type 2 Diabetes (http://www.heartforum.org.uk/AboutCHD_riskfac_type2diab.aspx) – accessed 21-10-09].

Neel, J.V. 1962, "Diabetes mellitus: a "thrifty" genotype rendered detrimental by "progress"?", *Am J Hum Genet.,* vol. 14, pp. 353-362.

NHS document - Designed for Life: Creating World Class Health ans Social care for Wales in the 21st Century (http://www.wales.nhs.uk/documents/designed-for-life-e.pdf) - Accessed 21/08/2009.

Nichols, G.A., Gullion, C.M., Koro, C.E., Ephross, S.A., & Brown, J.B. 2004, "The incidence of congestive heart failure in type 2 diabetes", *Diabetes Care*, vol. 27, pp. 1879-1884.

Nichols, G.A., Koro, C.E., Gullion, C.M., Ephross, S.A., & Brown, J.B. 2005, "The incidence of congestive heart failure associated with antidiabetic therapies", *Diabetes Metab Res Rev*, vol. 21, pp. 51-57.

Niemi, M., Backman, J.T., Granfors, M., Laitila, J., Neuvonen, M., & Neuvonen, P.J. 2003, "Gemfibrozil considerably increases the plasma concentrations of rosiglitazone", *Diabetologia*, vol. 46, pp. 1319-1323.

Niemi, M., Backman, J.T., & Neoven, P.J. 2004, "Effects of trimethoprim and rafampin on the pharmacokinetics of the cytochrome P450 2C8 substrate rosiglitazone", *Clin Pharmacol Ther*, vol. 76, no. 3, pp. 239-249.

Nissen, S.E., & Wolski, K. 2007, "Effect of Rosiglitazone on the Risk of Myocardial Infarction and Death from Cardiovascular Causes". *N Engl J Med*, vol. 356, no. 24, pp. 2457-2471.

Odani, N., Negishi, M., Takahashi, S., Kitano, Y., and Kozutsumi, Y. 1996, "Regulation of BiP gene expression by cyclopenetone prostaglandins through unfolded protein response element", *J Biol Chem*, vol. 271, no. 28, pp. 16609-16613.

Okunade, G.W., Miller, M.L., Pyne, G.J. Sutliff, R.L., O'Connor, K.T., Neumann, J.C., Andringa, A., Miller, D.A., Prasad, V., Doetschman, T., Paul, R.J., & Shull, G.E. 2004, "Targeted ablation of plasma membrane Ca^{2+}ATPase isoforms 1 and 4 indicates a major housekeeping function for PMCA1 and a critical role in hyperactivated sperm motility and male fertility for PMCA4". *J Biol Chem*, vol. 279, pp. 33742-33750.

Oshitari, T., Hata, N., & Yamamoto, S. 2008, "Endoplasmic reticulum stress and diabetic retinopathy", *Vascular Health and Risk Management*, vol. 4, no. 1, pp. 115–122.

Pan, Y., Zvaritch, E., Tupling, A.R., Rice, W.J., de Leon, S., Rudnicki, M., McKerlie, C., Banwell, B.L., & MacLennan, D.H. 2003, "Targeted Disruption of the *ATP2A1* Gene Encoding the Sarco(endo)plasmic Reticulum Ca^{2+}- ATPase Isoform 1 SERCA1) Impairs Diaphragm Function and Is Lethal in Neonatal Mice". *J Biol Chem*, vol. 278, no. 15, pp. 13367-13375.

Papp, B., Enyedi, A., Paszty, K., Kovacs, T., Sarkadi, B., Gardos, G., Magnier, C., Wuytack, F., & Enouf, J. 1992. "Simultaneous presence of two distinct endoplasmic-reticulum-type calcium-pump isoforms in human cells". *Biochem J*, vol. 288, pp. 297-302.

Parmentier, M., Szpirer, J., Levan, G., & Vassart, G. 1989, "The human genes for calbindin 27 and 29 kDa proteins are located on chromosomes 8 and 16 respectively", *Cytogenet Cell Genet*, vol. 52, no. 1-2, pp. 85-87.

Periasamy, M., Reed, TD., Liu, L.H., Loukianov, E., Paul, R.J., Nieman, M.L., Riddle, T., Duffy, JJ., Doetschman, T., Lorenz, J.N., & Shull, G.E. 1999, "Impaired cardiac performance in heterozygous mice with a null mutation in the sarco(endo)plasmic reticulum Ca2+-ATPase isoform 2 (SERCA2) gene". *J Biol Chem*, vol .274, no. 4, pp. 2556-2562.

Periasamy, M., & Kalyanasundaram, M.S. 2007, "SERCA pump isoforms: Their role in calcium transport and disease". *Muscle Nerve*, vol. 35, no. 4, pp. 430-442.

Pitrosch, F., Passauer, J., Fuecker, K., Hanefeld, M., & Gross, P. 2004, "In type 2 diabetes, rosiglitazone therapy for insulin resistance ameliorates endothelial dysfunction independent of glucose control", *Diabetes Care*, vol. 27, no. 2, pp. 484–490.

Polikandriotis, J.A., Mazzell, L.J., Rupnow, H.L., & Hart, C.M. 2005, "Peroxisome proliferators-activated receptor [gamma] ligamds stimulate endothelial nitric oxide production through distinct peroxis*ome proliferators-activated receptor [gamma]-dependent mechanisms",* Arterioscler *Thromb Vasc Biol*, vol. 25, no. 9, pp. 1810-1816.

Prasad, V., Okunade, G.W., Miller, M.L., & Shull, G. 2004, "Phenotypes of SERCA and PMCA knockout mice". *Biochem Biophys Res Comm*, vol. 322, no. 4, pp. 1192-1203.

Psaty, B.M., & Furberg, C.D. 2007, "The Record on Rosiglitazone and the Risk of Myocardial Infacrction". *N Engl J Med*, vol. 357, no. 1, pp. 67-69.

Rabe, K., Lehrke, M., Parhofer, K.G., & Broedl, .UC. 2008, "Adipokines and insulin resistance", *Mol Med.* Vol. 14, no. 11-12, pp. 741-51.

Randriamboavonjy, V., Pitrosch, F., Bolck, B., Schwinger, R.H., Dixit, M., Badenhoop, K., Cohen, R.A., Busse, R., & Fleming, I. 2008, "Platelet sarcoplasmic endoplasmic reticulum Ca2+Atpase and mu-caplain activity are altered in type 2 diabetes and restored by rosiglitazone", *Circ*, vol. 117, no. 1, pp. 52-60.

Raskin, P., Rendell, M., Riddle, M.C., Dole, J.F., Freed, M.I., & Rosenstock, J. 2001, "A randomized trial of rosiglitazone therapy in patients with inadequately controlled insulin-treated type 2 diabetes", *Diabetes Care,* vol. 24, no. 7, pp. 1226–1232.

Ricote, M., Li, A.C., Willson, T.M., Kelly, C.J., & Glass, C.K. 1998, "The peroxisome proliferator-activated receptor-gamma is a negative regulator of macrophage activation", *Nature*, vol. 391, no. 6662, pp. 79-82.

Ritz, E., Rychlik, I., Locatelli, F., & Halimi, S. 1999, "End-stage renal failure in type 2 diabetes: A medical catastrophe of wordwide dimensions". *Am J Kidney Dis*, vol, 34, no. 5 , pp. 795-808.

Roderick, H.L., Lechleiter, J.D., & Camacho, P. 2000, "Cytosolic phosphorylation of calnexin controls intracellular Ca2+ oscillations via an interaction with SERCA2b", *J Cell Biol*, vol. 149, no. 6, pp.1235-47.

Rudolph, H.K., Antebi, A., Fink, G.R., Buckley, C.M., Dorman, T.E., LeVitre,

J., Davidow, L.S., Mao, J.I., & Moir, D.T. 1989, "The yeast secretory pathway is perturbed by mutations in PMR1, a member of a Ca^{2+} ATPase family", *Cell*, vol. 58, no. 1, pp. 133–145.

Ryan, M.J., Didion, S.P., Mathur, S., Faraci, F.M., & Sigmund, C.D. 2004, "PPARγ agonist rosiglitazone improves vascular function and lowers blood pressure in hypertensive transgenic mice", *Hypertension*, vol. 43, pp. 661-666.

Sagara, Y., & Inesi, G. 1991, "Inhibition of the sarcoplasmic reticulum Ca^{2+} transport ATPase by thapsigargin at subnanomolar concentrations". *J Biol Chem*., vol. 266, no. 21, pp. 13503-13506.

Saltiel, A.R. 2001, "New perspectives into the molecular pathogenesis and treatment of type 2 diabetes". *Cell*, vol. 104, no. 4, pp. 517-529.

Scapagnini, G., Nelson, T.J., & Alkon, D.L. 2004 "Regulation of Ca2+ stores in glial cells", *Advances in Molecular and Cell biology*, vol. 31, no. 5, pp. 635-660.

Scheen, A.J. 2001, "Thiazolidinediones and liver toxicity", *Diabetes Metab (Paris)*, vol. 27, no. 3, pp. 305-313.

Schroder, S., Palinski, W., & Schmid-Schonbein, G. W. 1991, "Activated monocytes and granulocytes, capillary nonperfusion, and neovascularization in diabetic retinopathy", *Am. J. Pathol.,* vol. **139,** no. 1, pp. 81-100.

Seidler, N.W., Jona, I., Vegh, M., & Martonosi, A. 1989, "Cyclopiazonic acid is a specific inhibitor of the Ca2+Atpase of sarcoplasmic reticulum", *J Biol Chem*, vol. 264, no. 30, pp. 17819-17823.

Shah, R.D., Gonzales, F., Golez, E., Augustin, D., Caudillo, S., Abbott, A, Morello, J., McDonough, P.M., Paolini, P.J., & Shubeita, H.E. 2004, "The antidiabetic agent rosiglitazone upregulates SERCA2 and enhances TNF-α- and LPS-induced NF-κB-dependent transcription and TNF-α-induced IL-6 secretion in ventricular myocytes", *Cell Physiol Biochem*, vol. 15, pp. 41-50.

Shang, J. 2005, "Quantitative measurement of events in the mammalian unfolded protein response". *Methods*, vol. 35, pp. 390-394.

Shull, G. 2000, "Gene knockout studies of Ca^{2+}-transporting ATPases", *Eur J Biochem*, vol. 267, no. 17, pp. 5284-5290.

Sidrauski, C., Chapman, R., & Walter, P. 1998, "The unfolded protein response: an intracellular signalling pathway with many surprising features". *Trends Cell Biol*, vol. 8, pp. 245-249.

Simmerman, H.K., Kobayashi, Y.M., Autry, J.M., & Jones, L.R. 1996, "A leucine zipper stabilizes the pentameric membrane domain of phospholamban and forms a coiled-coil pore structure", *J Biol Chem*, vol. 271, no. 10, pp. 5941-5946.

Singh, N., Webb, R., Adams, R., Evans, S., Al-Mosawi, A., Evans, M., Roberts, A.W., & Thomas, A.W. 2005, "The PPAR-γ activator, Rosiglitazone, inhibits actin

polymerisation in monocytes: Involvement of Akt and intracellular calcium". *Biochem Biophys Res Comm*, vol. 333, no. 2, pp. 455-462.

Singh, R., Barden, T., & Beilen, L. 2001, "Advanced glycation end-products: a review", *Diabetologia*, vol. 44, no. 2, pp. 129-146.

Singh, S., Loke, Y.K., & Furberg, C.D. 2007, "Long-term risk of cardiovascular events with rosiglitazon: A meta analysis", JAMA, vol. 298, no. 10, pp. 1189-1195.

Smith, S.A. 2003, "Central role of the adipocyte in the insulin-sensitising and cardiovascular risk modifying actions of the thiazolidinediones", *Biochimie*, vol. 85, pp. 1219-1230.

Song, B., Scheuner, D., Ron, D., Pennathur, S., & Kaufman, R.J. 2008, "*Chop* deletion reduces oxidative stress, improves β cell function, and promotes cell survival in multiple mouse models of diabetes", *J. Clin. Invest*, vol. 118, no. 10, pp. 3378-3389.

Sorin, A., Rosas, G., & Rao, R. 1997, "PMR1, a Ca^{2+}-ATPase in yeast Golgi, has properties distinct from sarco/endoplasmic reticulum and plasma membrane calcium pumps" , *J Biol Chem*, vol. 272, no. 15, pp. 9895–9901.

Starling, A.P., East, J.M., & Lee, A.G. 1995, "Effects of phospholipid fatty acyl chain length on phosphorylation and dephosphorylation of the $Ca(^{2+})$-ATPase", Biochem J, vol. 310, no. 3, pp. 875-879.

Stern, M.P. 1995, "Diabetes and cardiovascular disease. The "common soil" hypothesis", *Diabetes.* vol. 44, no. 4, pp. 369-74.

Strehler, E.E., & Zacharias, D.A. 2001, "Role of alternative splicing in generating isoform diversity among plasma membrane calcium pumps", *Physiological Reviews*, vol. 81, no. 1, pp. 21-50.

Sudbrak, R., Brown, J., Dobson-Stone, C., Carter, S., Ramser, J., White, J., Healy, E., Dissanayake, M., Larregue, M., Perrussel, M., Lehrach, H., Munro, C.S., Strachan, T., Burge, S., Hovnanian, A., & Monaco, M.P. 2000, "Hailey-Hailey disease is caused by mutations in ATP2C1 encoding a novel Ca^{2+} pump". *Human Molecular Genetics*, vol. 9, no. 7, pp. 1131-1140.

Tabas, I. 2004, "Apoptosis and plaque destabilistation in atherosclerosis:the role of macrophage apoptosis induced by cholesterol", *Cell Death and Differentiation*, vol. 11, pp. S12-S16.

Tada, M., & Kadoma, M. 1989, "Regulation of the Ca^{2+} pump ATPase by cAMP-dependent phosphorylation of phospholamban". *Bioessays*, vol. 10, no. 5, pp. 157-163.

Takahashi, S., Odani, N., Tomokiyo, K., Futura, K., Suzuki, M., Ichikawa, A., & Negishi, M. 1998, "Localization of a cyclopentenone prostaglandin to the endoplasmic reticulum and induction of BiP mRNA", *Biochem J*, vol. 335, no. 1, pp/ 35-42.

Takeda, K., Ichiki, T., Tokunou, T., Iino, N., & Takeshita, A. 2001, "15-Deoxy-delta 12,14-prostaglandin J2 and thiazolidinediones activate the MEK/ERK pathway through phosphatidylinositol 3-kinase in vascular smooth muscle cells", *J.Biol.Chem*. vol. 276, no. 52, pp. 48950-48955.

Tao, L., Liu, H., Gao, E., Teng, Z., Lopez, B.L., Christopher, T.A., Ma, X., Batinic-Haberle, I., Willette, R.N., Ohlstein, E.H. & Yue T. 2003, "Antioxidative, antinitrative and vasculoprotective effects of a peroxisome proliferator-activated receptor-γ agonist in hypercholesterolemia", *Circ*, vol. 108, pp. 2805-2811.

TaqMan Gene Expression Assays Protocol Booklet, Applied Biosystems, 2005).. (Applied Biosystems Application note: "Real Time PCR - Understanding C_T").

Thastrup, O., Dawson, A.P., Scharff, O., Foder, B., Cullen, P.J., Drobak, B.K., Bjerrum, P.J., Christensen, S.B. & Hanley, M.R. 1989, "Thapsigargin, a novel molecular probe for studying intracellular calcium release and storage", *Agents Actions*, vol. 27, no. 1-2, pp. 17-23.

Thastrup, O, Cullen, P.J., Drobek, B.K, Hanley, M.R., & Dawson, A.P. 1990, "Thapsigargin, a tumor promoter, discharges intracellular Ca2+ stores by specific inhibition of the endoplasmic reticulum Ca2(+)-ATPase",*PNAS*, vol. 87, no. 7, pp. 2466-2470.

The DREAM Trial Investigators. 2008, "Effects of ramipril and rosiglitazone on cardiovascular and renal outcomes in people with impaired glucose tolerance or impaired fasting glucose". *Diabetes Care*, vol. 31, no. 5, pp. 1007-1014.

Thornberry, N.A., Rano, T.A., Peterson, E.P., Rasper, D.M., Timkey, T., Garcia-Calvo, M., Houtzager, V.M., Nordstrom, P.A., Roy, S., Vaillancourt, J.P., Chapman, K.T., & Nicholson, D.W. 1997, "A combinatorial approach defines specificities of members of the caspase family and granzyme B", *J Biol Chem*, vol. 272, no. 29, pp. 17907-17911.

Thornally, P.J. 1998, "Cell Activation by glycated proteins: AGE receptors recognition factors and functional classification of AGEs". *Cellular and Molecular Biology*, vol. 44, no. 7, pp. 1013-1023.

Thrainsdottir, I.S., Aspelund, T., Thorgeirsson, G., Gudnason, V., Hardarson, T., Malmberg, K., Sigurdsson, G., & Ryd‟en, L. 2005, "The association between glucose abnormalities and heart failure in the population-based Reykjavı´k study", *Diabetes Care,* vol. 28, no. 3, pp. 612-616.

Thuerauf, D.J., Hoover, H., Meller, J., Hernandez, J., Su, L., Andrews, C., Dillmann, W.H., McDonough, P.M. & Glembotski, C.C. 2001, "Sarco/endoplasmic reticulum calcium ATPase-2 expression is regulated by ATF6 during the endoplasmic reticulum stress response", *J Biol Chem*, vol. 276, no. 51, pp. 48309-17.

Touyz, R.M., & Schriffin, E.L., 2006, "Peroxisome proliferators-activated receptors in vascular biology-molecular mechanisms and clinical implications". *Vascular Pharmacology*, vol. 45, pp. 19-28.

Toyoshima, C., Nakasako, M., Nomura, H., & Ogawa, H. 2000, "Crystal structure of the calcium pump of sarcoplasmic reticulum at 2.6Å resolution", *Nature,* vol. 405, pp.647-655.

Toyoshima, C., & Nomura, H. 2002, "Structural changes in the calcium pump accompanying the dissociation of calcium", *Nature*, vol. 418, pp. 605-611.

Toyoshima, C., Asahi, M., Sugita, Y., Khanna, R., Tsuda, T., & MacLennan, D,H. 2003, "Modeling of the inhibitory interaction of phospholamban with the Ca2+ ATPase", *PNAS*, vol. 100, no. 2, pp. 467-472.

Treiman, M., Caspersen, C., & Christensen, S.B. 1998, "A tool of coming of age: thapsigargin as an inhibitor of sarco-endoplasmic reticulum Ca(2+)-ATPases", *Trends Pharmacol Sci*, vol. 19, no. 4, pp. 131-135.

Ulug, P. (2004). MSc dissertation, University of Wales Institute, University of Wales.

Vanoevelen, J., Dode, L., Van Baelen, K., Fairclough, R.J., Missiaen, L., Raeymaekers, L., & Wuytack, F. 2005, "The secretory pathway Ca2+/Mn2+-ATPase 2 is a Golgi-localized pump with high affinity for Ca^{2+} ions". *J Biol Chem*, vol. 280, no. 24, pp. 22800-22808.

Varela-Roman, A., GShamagian, L.G., Caballero, E.B., Ramos, P.M., Veloso, P.R., & Gonzalez-Juanatey, J.R. 2005, "Influence of diabetes on the survival of patients hospitalized with heart failure", *The European Journal of Heart Failure*, vol. 7, pp. 859-864.

Xiang, M., Mohamalawari, D., & Rao, R. 2005, "A novel isoform of the secretory pathway Ca2+,Mn(2+)-ATPase, hSPCA2, has unusual properties and is expressed in the brain". *J Biol Chem*. vol. 280, no. 12, pp. 11608-11614.

Xu, C., Baily-Maitre, B., & Reed, J.C. 2005, "Endoplasmic reticulum Stress:cell life and death decisions". *J. Clin. Invest*, vol. 115, pp. 2656-2664

Wang, Y., Mattson, M.P., & Furukawa, K. 2002, "Endoplasmic reticulum calcium release is modulated by actin polymerisation", *J. Neurochem*.,vol. 82, pp. 945–952.

Webb *et al*, 1997

Webb, R.J., East, M.J., Sharna, R.P., & Lee, A.G. 1998, "Hydrophobic mismatch and the incorporation of peptides into lipid bilayers: A possible mechanism for retention in the Golgi", Biochemistry, vol. 37, no. 673-679.

Weber, S.M., Chambers, K.T., Bensch, K.G., Scarim, A.L., and Corbett, J.A. 2004, "PPARγ ligands induce ER stress in pancreatic β-cells: ER stress activation results in attenuation of cytokine signalling", *Am J Physiol Endocrinol Metab*, vol. 287, pp. E1171-E1177.

Weber, S.M., Scarim, A.L., & Corbett, J.A. 2004, "PPARγ is not required for the inhibitory actions of PGJ_2 on cytokine signalling in pancreatic β-cells", *Am J Physiol Endocrinol Metab*, vol. 286, pp. E329–E336.

Willson, T.M., Brown, P.J., Sternbach, D.D., & Henke, B.R. 2000, "The PPARs: from orphan receptors to drug discovery", *J Med Chem*, vol. 43, no. 4, pp. 527-44.

Wise, J. 1997, "Diabetes drug withdrawn after reports of hepatic events". *BMJ,* vol. 315, no. 7122, p 1564.

Wu, K., Bungard, D., & Lytton, J. 2001, "Regulation of SERCA Ca2+ pump expression by cytoplasmic [Ca2+] in vascular smooth muscle cells", *Am J Cell Physiol*, vol. 280, pp. 843-851.

Wuytack, F., Raeymaekers, L., De Smedt, H., Eggermont, J.A., Missiaen, L., Van Den Bosch, L., De Jaegere, S., Verboomen, H., Plessers, L., & Casteels, R.C. 1992, "Ca($^{2+}$)-transport ATPases and their regulation in muscle and brain". *Ann N Y Acad Sci.*.vol. 671, pp. 82-91.

Yamaguchi, H., & Wang, H. 2004, "CHOP Is involved in endoplasmic reticulum stress-induced apoptosis by enhancing DR5 expression in human carcinoma cells", *J Biol Chem*, vol. 279, no. 44, pp. 45495-45502.

Yoshida, H., Haze, K., Yanagi, H., Yura, T., & Mori, K. 1998, "Identification of the cis-acting endoplasmic reticulum stress response element responsible for transcriptional induction of mammalian glucose-regulated proteins. Involvement of basic leucine zipper transcription factors" *J Biol Chem*, vol. 273, no. 50, pp. 33741-33749.

Zhang, S.L., Yu, Y., Kozak, A., Deerinck, T.J., Ellismann, M.H., Stauderman, K.A. & Cahalan, M.D. 1995, "STIM1 is a Ca^{2+} sensor that activates CRAC channesl and migrates from the Ca^{2+} store to the plasma membrane", *Nature*, vol. 437, pp. 902-905.

Zhang, K., & Kaufman, R. 2004, "Signalling the unfolded protein response from the endoplasmic reticulum", *J Biol Chem*, vol. 279, no. 25, pp. 25935-25938.

Zhong, Y., Ahmed, S., Grupp, I.L., & Matlib, M. 2001, "Altered SR protein expression associated with contractile dysfunction in diabetic rat hearts", *Am J Physiol Heart Circ Physiol*, vol. 281, pp. H1137–H1147.

Ziegler, D. 2005, "Type 2 diabetes as an inflammatory cardiovascular disorder", *Curr Mol Med*., vol. 5, no. 3, pp. 309-322.

Ziegler-Heitbrock, H.W., Thiel, E., Futterer, A., Herzog, V., & Wirtz, A. 1988, "Establishment of a human cell line (Mono Mac 6) with characteristics of mature monocytes", *Cancer*, vol. 41, pp 456-461.

Chapter Seven

Appendices

Appendices

Appendix A: Certificates of Ethical approval

Appendix B: **J. Caddy**, N. Singh, L. Atkin, M. Ahluwalia, A. Roberts, D.Lang, A.W. Thomas, R. Webb (2008). Rosiglitazone transiently disturbs calcium homeostasis in monocytic cells. *BBRC*, vol. 366, pp. 149-155.

Appendix A

cshs/als/ ethics/check

Caddy, Jo
PhD
Cardiff School of Health Sciences
Llandaf Campus
Western Avenue
Cardiff CF5 2YB

Dear Applicant

Re: Application for Ethical Approval : The effect of PPAR-Gamma Agonists in inducing E.R. Stress Responses in Mammalian Cells

Your Ethics Review Checklist, was presented at the Applied Life Sciences Ethics Panel on 12/5/2007

The Panel confirms that you do not need to apply for formal ethical approval and you may proceed with your research project.

Please ensure you complete a full Risk Assessment where applicable.

Prof K Jones
Chair of Department of Applied Life Sciences Ethics Panel
Cardiff School of Health Sciences
Llandaf Campus
Western Avenue
Cardiff CF5 2YB

Tel : 029 20416896
E-mail : kpjones@uwic.ac.uk

Cc: Webb, Richard

cshs/als/ethics/app

Jo Caddy
PhD Student
Cardiff School of Health Sciences
Llandaf Campus
Western Avenue
Cardiff CF5 2YB

Dear Applicant

The effects of the PPAR-γ ligand on [Ca2+]i in monocytic and smooth muscle cells

Your research project proposal, as shown above, was amongst those considered at the meeting of the 3rd February 2006

I am pleased to inform you that your application for ethical approval was **APPROVED** subject to the conditions listed below – please read carefully.

Conditions of approval

That any changes in connection to the proposal as approved, are referred to the Panel.

That any untoward incident which occurs in connection with this proposal should be reported back to the Panel **without delay**.

Yours sincerely

Professor K Jones
Chair of Department of Applied Life Sciences Ethics Panel
Cardiff School of Health Sciences
Llandaf Campus
Western Avenue
Cardiff CF5 2YB

Tel : 029 20416896
E-mail : kpjones@uwic.ac.uk

PLEASE RETAIN THIS LETTER FOR REFERENCE

Appendix B

Available online at www.sciencedirect.com
ScienceDirect
Biochemical and Biophysical Research Communications 366 (2008) 149–155
BBRC
www.elsevier.com/locate/ybbrc

Rosiglitazone transiently disturbs calcium homeostasis in monocytic cells

J. Caddy [a], N. Singh [a], L. Atkin [a], M. Ahluwalia [a], A. Roberts [b], D. Lang [b], A.W. Thomas [a], R. Webb [a,*]

[a] Centre for Biomedical Sciences, Cardiff School of Health Sciences, University of Wales Institute Cardiff, Cardiff CF5 2YB, UK
[b] School of Medicine, Cardiff University, Heath Park Campus, Cardiff CF14 4XN, UK

Received 9 November 2007
Available online 4 December 2007

Abstract

The PPARγ agonist Rosiglitazone exerts anti-hyperglycaemic effects by regulating the long-term expression of genes involved in metabolism, differentiation and inflammation. In the present study, Rosiglitazone treatment rapidly inhibited (5–30 min) the ER Ca^{2+} ATPase SERCA2b in monocytic cells ($IC_{50} = 1.88\ \mu M$; $p < 0.05$), thereby disrupting short-term Ca^{2+} homeostasis (resting $[Ca^{2+}]_{cyto} = 121.2 \pm 2.9\%$ basal within 1 h; $p < 0.05$). However, extended Rosiglitazone treatment (72 h) induced dose-dependent SERCA2b up-regulation, and restored calcium homeostasis, in monocytic cells (SERCA2b mRNA: $138.7 \pm 5.7\%$ basal (1 μM)/ $215.0 \pm 30.9\%$ basal (10 μM); resting $[Ca^{2+}]_{cyto} = 97.3 \pm 8.3\%$ basal (10 μM)). As unfavourable cardiovascular outcomes, possibly related to disrupted cellular Ca^{2+} homeostasis, have been linked to Rosiglitazone, this effect may be of clinical interest. In contrast, in PPRE-luciferase reporter-gene assays, Rosiglitazone induced non-dose-dependent PPARγ-dependent effects (1 μM: $152.5 \pm 4.9\%$ basal; 10 μM: $136.1 \pm 5.1\%$ basal ($p < 0.05$ for 1 μM *vs.* 10 μM)). Thus, we conclude that Rosiglitazone can exert PPARγ-independent non-genomic effects, such as the SERCA2b inhibition seen here, but that long-term Rosiglitazone treatment did not perturb resting $[Ca]_{cyto}$ in this study.

Keywords: Rosiglitazone; Monocyte; PPARγ; Intracellular Ca^{2+}; SERCA2b; Anti-hyperglycaemic effects

It has been widely reported that increased cytoplasmic free calcium concentrations ($[Ca^{2+}]_{cyto}$) are involved in the pathophysiology of diabetes and its complications in a variety of cell types, including monocytes [1]. Disrupted Ca^{2+} homeostasis may—depending on cell type—contribute to hypertension, cardiac dysfunction and other diabetic complications [1–3]. For example, monocyte dysfunction has been linked to increased cytoskeletal rigidity and reduced cell deformability, leading to microchannel occlusions and microvascular diabetic complications [4].

Of direct interest in this regard is SERCA2b, the predominant 'Ca^{2+} pump' enzyme of non-muscle and smooth muscle cells, which is responsible for sequestration of Ca^{2+} into the endoplasmic reticulum after Ca^{2+} signalling events, and compensatory to non-specific leakage into the cytoplasm [5]. Many studies have reported decreased SERCA2b expression/activity in diabetes [3,6,7]. Indeed, it has been reported that decreased SERCA2b expression/activity correlates with both increased resting $[Ca^{2+}]_{cyto}$ and progression of diabetes [7].

Thiazolidinedione (TZD) drugs exert anti-hyperglycaemic effects by acting as ligands for the nuclear receptor PPARγ, which regulates the expression of a plethora of genes involved in metabolism, cell differentiation and inflammation [8]. However, it has been questioned whether all effects of TZDs depend on their metabolic action, or whether some effects may occur via distinct mechanism(s) [9]. We have previously shown [4] that short-term treatment with Rosiglitazone, at doses not toxic to cells (1 h; $IC_{50} = 3.72\ \mu M$), significantly reduces monocyte f-MLP-induced actin polymerisation, and that this change involves modulations in Ca^{2+}signalling. We suggested that this constituted a 'non-genomic PPARγ-independent' effect

* Corresponding author. Fax: +44 2920 416982.
E-mail address: rwebb@uwic.ac.uk (R. Webb).

0006-291X/$ - see front matter © 2007 Elsevier Inc. All rights reserved.
doi:10.1016/j.bbrc.2007.11.095

involving modulation of pre-existing intracellular signalling pathways by Rosiglitazone [4]. Thus, to bring about non-genomic effects, Rosiglitazone may interact with as-yet-undefined cellular component(s) to influence signalling events downstream of surface receptors to modulate cell signalling processes in a PPARγ-independent manner. Consequently, the net effects of TZD therapy may be due to a combination of PPARγ-dependent and -independent events [4].

Given that Ca^{2+} signalling is a fundamental component of cellular function, particularly within the cardiovascular (CV) system, and in the light of recent literature associating Rosiglitazone with negative CV outcomes [10,11], the investigation of links between the TZDs and modulations in $[Ca]_{cyto}$ assumes great importance. However, to our knowledge few studies have explored this topic. One study reported that long-term treatment with high doses of Rosiglitazone (10 μM; 72 h) induces ~1.5-fold increases in SERCA2 promoter activity and mRNA levels in cardiomyocytes, and consequent improvements in Ca^{2+} handling in Rosiglitazone-treated cells [12]. However, no evidence of a PPARγ response element (PPRE) in the SERCA2 promoter was found, and so the mechanism by which Rosiglitazone upregulated SERCA2 is not yet known.

Here, we report that incubation with Rosiglitazone rapidly (within 5 min) induces minor but statistically significant increases in resting $[Ca^{2+}]_{cyto}$ via a non-genomic mechanism of action in monocytic cells. We also identify the mechanism underpinning this effect as dose-dependent inhibition of SERCA2b. We further show that, after extended incubation with Rosiglitazone (>24 h), cells compensate for consequent increases in $[Ca^{2+}]_i$ by upregulating SERCA2b, and thereby provide a mechanism for restoring Ca^{2+} homeostasis, suggesting—at least at the level of the individual monocytic cell—that long-term Rosiglitazone therapy may not bring about adverse calcium-related effects in the monocytes of patients with diabetes.

Materials and methods

Materials. All reagents were purchased from Sigma Aldrich (Poole, UK) unless stated otherwise. Cell permeabilisation reagents, Fluo 3/AM and Rosightazone were obtained from Harlan SERA-LAB Ltd. (Loughborough, UK), Molecular Probes, Inc. (Eugene, OR), and GlaxoSmithKline (Uxbridge, UK), respectively. Cultured MM6 monocytic cells were obtained from the German Collection of Micro-Organisms and Cell Culture (Braunschweig, Germany). PPARγ-responsive luciferase reporter (PPRE-luc) constructs and rabbit sarcoplasmic reticulum (SR) preparations were kindly provided by Professor W. Wahli (Lausanne University, Switzerland) and Professor A.G. Lee (Southampton University, UK).

Maintenance of cells in culture. Monocytic MM6 cells were utilised as an *in vitro* model for peripheral monocytes. Cells were cultured (37 °C; 5% CO_2) in RPMI medium plus 10% foetal calf serum and 1% penicillin (50 IU/ml)/streptomycin (100 μg/ml), and were sub-cultured when a cell density of $0.85–1.00 \times 10^6$ was attained; cells of passage number < 25 were used in all cases.

Subcellular fractionation and Western blot analysis. To confirm the expression and subcellular localisation of SERCA2b in MM6 cells, whole-cell homogenates, total protein extracts, cytoplasmic, mitochondrial and microsomal subcellular fractions (prepared using the method of Maruyama & MacLennan [13]) were subjected to Western blotting analysis. To immunologically characterise PPARγ expression, total cell protein lysates were subjected to Western blotting analysis.

In all cases, Western blot analyses were performed using 32.5 μg protein/sample, and anti-SERCA2b, anti-PPARγ or anti-phospho-MAPK primary (1:500 dilution in TBST (16 h)), followed by HRP-labelled anti-goat IgG/anti-rabbit IgG secondary antibody (1:2000 dilution in TBST (2 h); all from Cell Signalling Technology, Beverley, MA). Immunogenic proteins were detected by ECL-enhanced chemiluminescence, and band intensities determined and quantitated using AC-1 BioImaging and VisionWorksLS Software systems (UltraVioletProducts Ltd, Cambridge, UK).

Measurement of intracellular Ca^{2+} concentrations. $[Ca^{2+}]_{cyto}$ was measured by the method of Elsner et al. [14], in which fluo-3 fluorescence as detected via flow cytometry was used as an indicator of resting $[Ca^{2+}]_{cyto}$. Monocytic cells were pre-incubated ± 1–10 μM Rosiglitazone (or 0.1% v/v dimethylsulfoxide (DMSO) vehicle) for up to 72 h at 37 °C, and then incubated with 3 μM fluo-3/AM for 40 min at 37 °C, harvested by centrifugation, and the cell pellet resuspended in 0.5 ml PBS before analysis using a Cytomics FC500MPL flow cytometer ($\lambda_{ex} = 488$ nm; $\lambda_{em} = 530$ nm; Beckman Coulter, Buckinghamshire, UK). Data were expressed as percentages of fluorescence due to resting $[Ca^{2+}]_{cyto}$ in untreated cells.

Ca^{2+}-ATPase assays. Ca^{2+}-dependent ATP hydrolysis was measured using a coupled enzyme assay, and free Ca^{2+} concentrations calculated, as described previously [15,16]. Briefly, samples (2–50 μg protein) were incubated at 25 °C in 2.5 ml buffer (100 mM KCl, 40 mM Hepes; pH7.2) containing ATP (2 mM), phospho(enol)pyruvate (2.5 mM), NADH (0.25 mM), pyruvate kinase (7.5 U), and lactate dehydrogenase (8.0 U). The re-synthesis of ATP consumed by Ca^{2+} ATPase activity was coupled by the pyruvate kinase and lactate dehydrogenase to NADH oxidation, which was recorded at A_{340} (Lambda25 spectrophotometer/UV Winlab software, Perkin Elmer, UK), and ATPase activity (expressed as IU (μmol of ATP hydrolyzed/mg of total protein/min)) was calculated using an extinction coefficient for NADH of 6200 l/mol/cm. Ca^{2+}-ATPase activity was defined as the activation seen on addition of calcium. ATPase activity was measured after a 30-min preincubation (25 °C) with Rosiglitazone (0–20 μM), thapsigargin (100 nM), cyclopiazonic acid (10 μM), or DMSO (0.1% v/v).

SERCA2b mRNA quantitation. MM6 cells were lysed and RNA extracted with Trizol® Reagent according to manufacturer's instructions (Invitrogen, Paisley, UK). RNA samples were converted to cDNA using an Applied Biosystems® High-Capacity cDNA Archive Kit (Invitrogen, Paisley, UK) and stored at −20 °C. SERCA2b mRNA expression was investigated using an Applied Biosystems 7500 Real-time PCR system and assessed semi-quantitatively (relative to Glyceraldehyde Phosphate Dehydrogenase (GAPDH)) via Taqman® Gene Expression Assays (Applied Biosystems, Warrington, UK) for SERCA2b (Gene Expression Assay Hs01566028_g1 [14]: Forward Primer: 5′-GAGATCACAGCTA TGACTGGTGATG-3′; Reverse Primer: 5′-CCCGATTTCCGACTT CTTCA-3′; Probe: 5′-/56-FAM/TGTGAACGACGCGCCCGC/36-TAMRA/-3′) and GAPDH (Gene Expression Assay Hs99999905_m1). Thermocycling was as follows: initial denaturation (2 min; 50 °C/10 min; 95 °C), followed by 50 cycles of denaturation (15 s; 95 °C)/annealing-extension (60 s; 60 °C).

Reporter gene assays. Cultured monocytic cells were transfected with PPRE-Luc plasmid using electroporation. 0.3 ml aliquots from a cell suspension (46×10^6 cells/mL in RPMI 1640) and plasmid (30 μg) were incubated in electroporation cuvettes for 5 min at room temperature before electroporation (975 μF; 250 V; Bio-Rad® Gene Pulser II) using an exponential decay pulse system. Transfected cells were transferred into an ice bath for 20 min, and then resuspended in 10 ml RPMI-1640. 100 μL cell suspension aliquots were then incubated with different stimuli (37 °C; 5% CO_2; 0–72 h). Cell lysis and assay of luciferase activity were performed using a Steady-Glo® Luciferase assay system (Promega, Southampton, UK) following the manufacturer's instructions. Luminescence was quantified using a Dynex MLX Microlitre Plate Luminometer (Dynex technologies, VA, USA).

Statistical analysis. Data are expressed as mean ± standard error of the mean. Multiple and non-multiple comparisons were performed using one-way analysis of variance (ANOVA), and paired or unpaired *t*-tests, as appropriate. Significance levels were set at $P < 0.05$.

Results

Cell viability

Cell viability, as determined by MTB assay and trypan blue exclusion, was not significantly reduced by incubation of cells with maximal doses of Rosiglitazone (20 μM) for >24 h [data not shown; $p < 0.05$].

SERCA2b and PPARγ protein expression in cultured monocytic cells

In subcellular fractionation studies, SERCA2b was detected by Western Blot analysis as a ~105 kDa band that was found predominantly in microsomal membranes from MM6 cells ($n = 3$; Fig. 1A), and which co-fractionated with the ER marker protein Calnexin [data not shown]. In separate Western Blotting experiments ($n = 4$; Fig. 1B), PPARγ was detected in total protein extracts as a doublet of ~55 kDa (non-phosphorylated PPARγ) and ~60 kDa (phosphorylated PPARγ) bands.

SERCA2b Ca^{2+} ATPase activity

In SR preparations from rabbit skeletal muscle, and in microsomes isolated from MM6 cells, maximal Ca^{2+}-ATPase activities were identified (at ~pCa 4.82) of 3.030 ± 0.300 IU ($n = 4$) and 0.061 ± 0.013 IU ($n = 18$) respectively. As expected, maximal activities were higher in SR preparations but Ca^{2+} dependencies and susceptibilities to the SERCA inhibitors thapsigargin and cyclopiazonic acid for the two preparations were almost identical (data not shown), and in approximate agreement with previously published values for SERCA enzymes [17]. Incubation with 0.1% DMSO alone did not cause inhibition (103.6 ± 9.6% maximal activity, $p > 0.05$, $n = 3$). Thus, we conclude that SERCA2b is expressed as an active ER-resident Ca^{2+} pump enzyme in human monocytic cells.

Preincubation (30 min; 25 °C) with Rosiglitazone brought about complete dose-dependent inhibition of SERCA2 b activity in MM6 microsomes (Fig. 2; $IC_{50} = 1.88$ μM; ANOVA $p < 0.05$; $n \geqslant 6$; the apparent negative activity at very high Rosiglitazone concentrations is likely due to variability in Ca^{2+}-independent ATPase activity). Interestingly, these values are similar to that ($IC_{50} = 3.72$ μM) which we have previously reported for Rosiglitazone's Ca^{2+}-dependent actin cytoskeleton remodelling action [4]. Given this similarity, and as the timescale seen for the associated increase in $[Ca^{2+}]_{cyto}$ in both the present study (Fig. 3) and previously [4] is suggestive of leakage of Ca^{2+} ions into the cytoplasm rather than triggering of a specific Ca^{2+} signalling cascade, we propose that inhibition of SERCA2b is responsible for the Rosiglitazone-mediated cytoskeletal remodelling previously seen in monocytic cells [4].

Measurement of $[Ca^{2+}]_{cyto}$

As with our previous study [4], pre-incubation with 10 μM Rosiglitazone for short periods (<1 h) brought about a small but statistically significant increase in resting $[Ca^{2+}]_{cyto}$ in monocytic cells (121.2 ± 2.9% basal; $n = 8$; $p < 0.05$; Fig. 3). This increase was statistically significant after 24 h (140.5 ± 9.5% basal; $n = 3$; $p < 0.05$), but after 72 h, resting $[Ca^{2+}]_{cyto}$ had reverted to basal levels (92.3 ± 7.8% basal; $n = 6$; $p > 0.05$). In contrast, 1 μM Rosiglitazone had no statistically significant effect with any duration of pre-incubation ($n = 15$).

Gene expression in monocytic cells after Rosiglitazone treatment

In reporter gene assays using monocytic cells transfected with a PPRE-luciferase construct, 24 h incubation with 1 or 10 μM Rosiglitazone induced increases in luminescence ($p < 0.05$ vs. basal in both cases; $n = 4$; Fig. 4A), but 1 μM Rosiglitazone produced a significantly greater increase than 10 μM Rosiglitazone (1 μM: 152.5 ± 4.9% basal; 10M: 136.1 ± 5.1% basal ($p < 0.05$)).

Incubation with Rosiglitazone for shorter durations (≤6 h) did not induce a significant change in reporter gene expression (1 μM: 113.9 ± 12.4% basal (6 h); 10 μM: 100.8 ± 3.6% basal ($p > 0.05$; $n = 4$; Fig. 4A)), indicating that PPARγ ligands take several hours to exert their genomic effects. Treatment (24 h; 37 °C) with 100 ng/ml phorbol 12-myristate 13-acetate (PMA), an

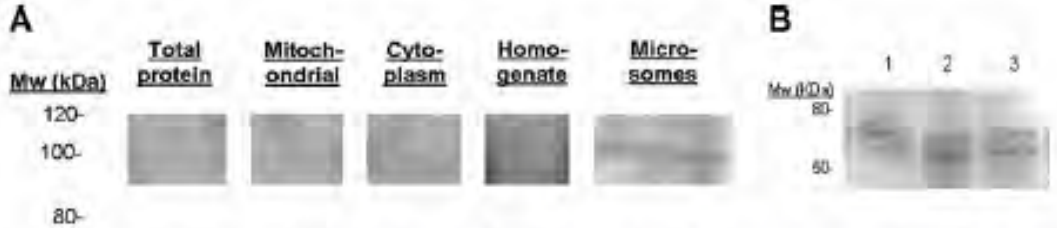

Fig. 1. Western blot detection of SERCA2b and PPARγ in MM6 cells. (A) MM6 subcellular fractions were probed with anti-SERCA2b antibodies (1:1000) and HRP-linked donkey anti-goat 2° antibodies (1:1000); (B) MM6 total protein extracts were probed with anti-PPARγ antibodies (1:1000) and HRP-linked mouse anti-rabbit 2° antibodies (1:1000). Lane 1: 10 μM Rosiglitazone (24 h); Lane 2: 1 μM Rosiglitazone (24 h); Lane 3: Control.

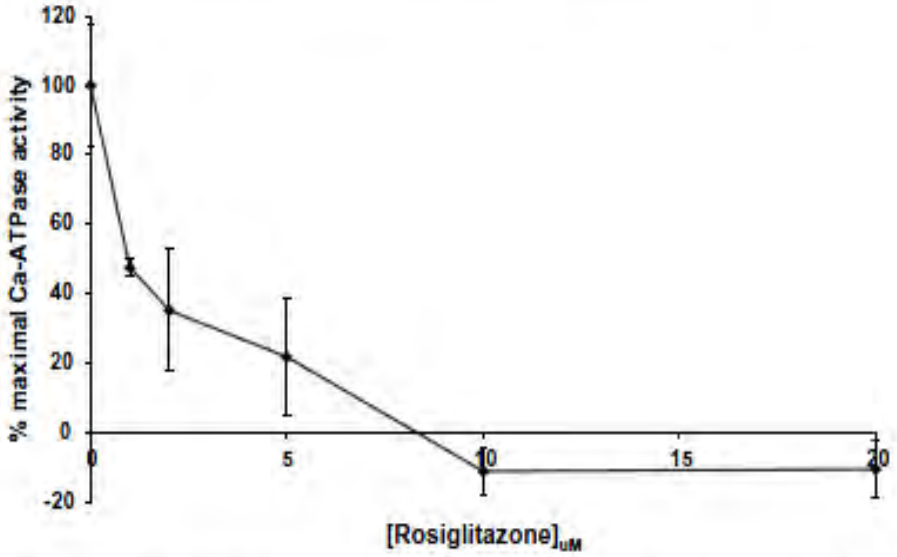

Fig. 2. Ca^{2+} ATPase assay data. Percentages of maximum Ca^{2+} ATPase activity (normalised to maximal activity) are displayed for MM6 microsomes after pre-incubation (30 min) with the indicated concentrations of Rosiglitazone.

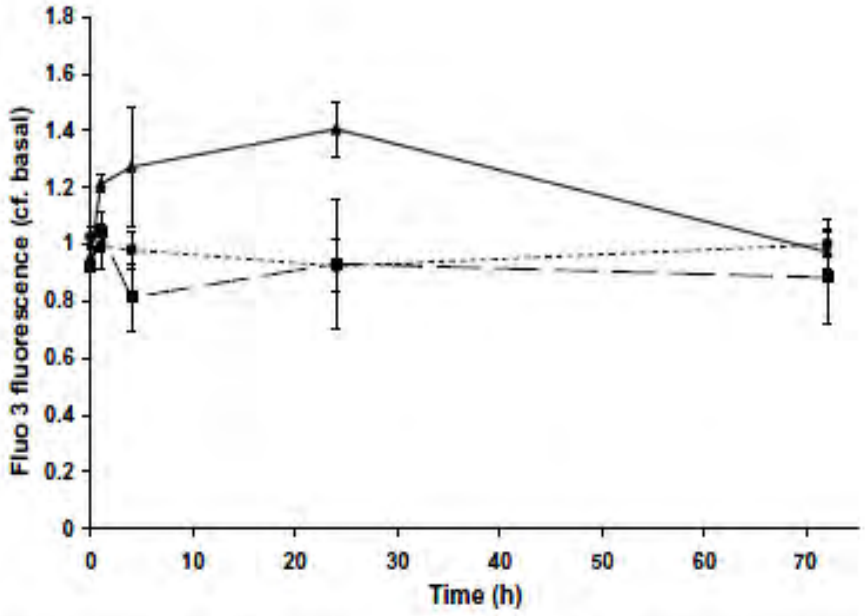

Fig. 3. The effect of Rosiglitazone on intracellular Ca^{2+} concentrations. Ca^{2+}-dependent fluo-3 fluorescence in monocytic cells is displayed relative to basal after incubation for the indicated times with 0.1% v/v DMSO (dotted line; circles), 1 μM Rosiglitazone (dashed line; squares), or 10 μM Rosiglitazone (solid line; triangles).

agent that induces differentiation of monocytic cells into macrophages [18], brought about an increase in luminescence (159.8 ± 4.5% control; $p < 0.05$; $n = 4$; Fig. 4B) that was further increased by incubation with 1 μM Rosiglitazone (182.8 ± 5.4%; $p < 0.05$ vs. PMA alone; $n = 4$), and to a lesser extent by incubation with 10 μM Rosiglitazone (163.1 ± 7.6%; $n = 4$)). As MM6 cells express PPARγ in relatively small quantities, but differentiation is accompanied by increased expression of PPARγ [18], this provides further supporting evidence that reporter gene assay luminescence correlates to PPARγ-dependent genomic actions of Rosiglitazone.

As seen in Fig. 4C, RT-PCR analysis showed that levels of SERCA2b mRNA expression were increased in MM6 cells after ⩾ 24 h incubation with either 1 or 10 μM Rosiglitazone (ANOVA; $n \geqslant 3$; $p \leqslant 0.05$ in both cases), but not by treatment for shorter periods, or with vehicle alone (e.g. 72 h 0.1% DMSO: 100.3 ± 3.2% basal expression; $n \geqslant 3$; $p > 0.05$). In contrast to its effect on PPRE-luc, Rosiglitazone's effect was dose-dependent: at 72 h, 10 μM Rosiglitazone induced a larger upregulation than 1 μM (215.0 ± 30.9% vs. 138.7 ± 5.7% basal; $n \geqslant 3$; $p < 0.05$). Furthermore, PMA-induced increases in expression in PPARγ [18] did not result in increased SERCA2b mRNA

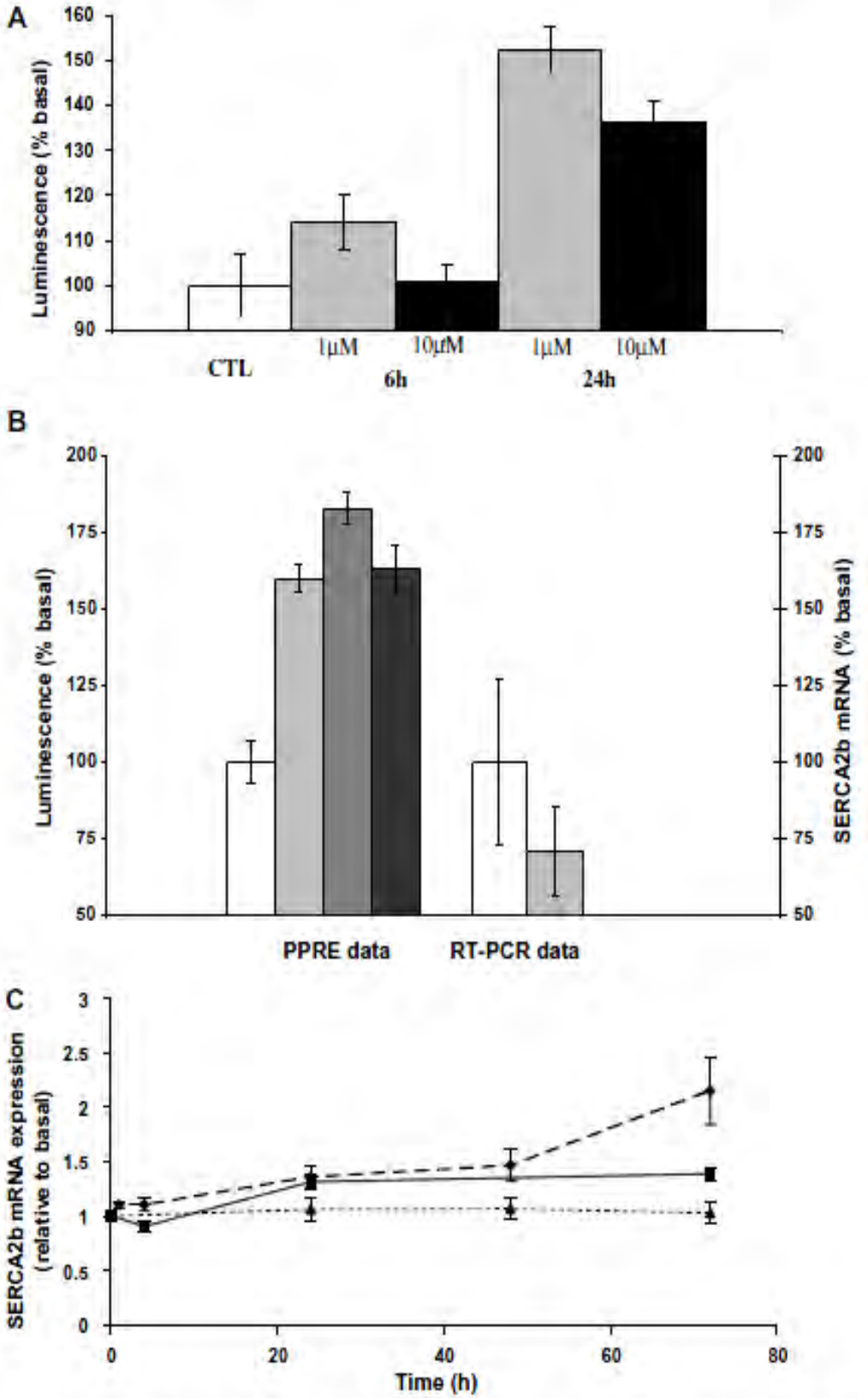

Fig. 4. The effect of Rosiglitazone on PPRE-Luc and SERCA2b expression. MM6 cells (±transfection with PPRE-Luc plasmid) were treated for the indicated times with the indicated concentrations of Rosiglitazone, or with PMA (100 ng/ml) or DMSO (0.1% v/v). (A) PPRE-Luc expression, as reported by luminescence, in control cells (white bar), and cells incubated for the indicated times with 1 μM (grey bars) or 10 μM (black bars) Rosiglitazone; (B) PPRE-Luc or SERCA2b mRNA expression, as determined by luminescence and RT-PCR respectively, in control cells (white bars), cells incubated with PMA (24 h; pale grey bars), and cells incubated with PMA and 1 μM (24 h; dark grey bars) or 10 μM (24 h; black bars) Rosiglitazone (PPRE-Luc only); (C) SERCA2b mRNA expression, as determined by RT-PCR, in DMSO-incubated cells (dotted line; triangles), and cells incubated with 1 μM (solid line; squares) or 10 μM (dashed line; diamonds) Rosiglitazone.

(70.9 ± 14.7% control; 24 h; $p > 0.05$ vs. basal; $n = 3$; Fig. 4B), suggesting that Rosiglitazone's effect on SERCA2b expression is PPARγ-independent (i.e. it is not due to Rosiglitazone-induced activation of PPARγ).

Discussion

This study provides an explanation for the apparent paradox that, while acute doses of Rosiglitazone can disrupt Ca^{2+} homeostasis within monocytes *in vitro* [4], ongoing TZD therapy has not been reported to adversely affect Ca^{2+} signalling within patients' cells. Rosiglitazone's inhibition of SERCA2b's Ca^{2+}ATPase activity (Fig. 2) causes $[Ca^{2+}]_{cyto}$ to increase within ~5 min (Fig. 3), but we propose that this can be linked to a negative feedback process in which cells respond within ⩾24 h by upregulating SERCA2 b expression (Fig. 4B) and restoring normal Ca^{2+} homeostasis in the long-term (Fig. 3).

Several factors suggest that the effects seen in the present study have not been brought about via a genomic mechanism involving interactions between PPARγ, its ligand and PPRE-bearing target gene(s). Firstly, the rapidity of the response (perturbations in $[Ca^{2+}]_{cyto}$ being seen within 5 min); secondly, the fact that inhibition of SERCA2 occurs not only in intact cells, but also in microsomal fractions that lack nuclear proteins such as PPARγ; thirdly, the lack of a PPRE in the SERCA2 gene promoter; and finally, the discrepancies between Rosiglitazone's effects on luciferase reporter gene expression, and its effects on SERCA2b activity and expression.

As shown in Fig. 4A and B, PPARγ-mediated effects of Rosiglitazone in inducing changes in PPRE-bearing target gene expression can be correlated to PPARγ expression, and are optimal at relatively low concentrations (1 μM), with higher doses (>10 μM) exceeding a threshold level beyond which antagonistic non-genomic effects such as MAPK phosphorylation (and therefore inactivation) of PPARγ are initiated [19,20]. Indeed, we observed that incubation of MM6 cells for 24 h with 10 μM (but not 1 μM) Rosiglitazone increased phosphorylation of both MAPK (228.0 ± 32.0% basal (10 μM); $p < 0.05$; $n = 6$; [data not shown]) and PPARγ (phospho-PPARγ = 53.1 ± 1.4% total PPARγ (10 μM Rosiglitazone) vs. 29.1 ± 13.0% total PPARγ (1 μM Rosiglitazone); $n = 4$; $p < 0.05$; Fig. 1B).

This contrasts with the dose-responsive nature of Rosiglitazone's induction of SERCA2b (Fig. 4C), and also with the similar SERCA2b mRNA levels seen in either non-differentiated (low PPARγ) or differentiated (i.e. PMA-treated [high PPARγ]) monocytic cells (Fig. 4B). Thus, we suggest that SERCA2b inhibition and SERCA2b mRNA induction may therefore be PPARγ-independent consequences of a non-genomic interaction between Rosiglitazone and either SERCA2b itself, or else some as-yet-undefined SERCA2b-associated intermediary molecule present in microsomes.

It has been demonstrated that rendering cell membranes leaky to Ca^{2+} using Ca^{2+} ionophore (A_{23187}) results in cytoplasmic Ca^{2+} elevation; this (and possibly the accompanying depletion of ER Ca^{2+} stores) induces increased SERCA2 mRNA and protein levels within 6–10 h via a signalling mechanism involving increased SERCA2 transcription [21]. Our data are in line with these findings, while our sequence analysis [data not shown] supported reports that no PPREs (AGGTCA-n-AGGTCA direct repeat sequences [8]) were present in the SERCA2 gene promoter [12]. However, we and others identified several sequences that resemble other response elements, including two UPREs, a thyroid RE, E-box (glucose RE), two fatty acid REs and nine Sp1-binding sites [data not shown]. The relative contributions of these elements in regulating SERCA2b gene expression remain to be defined [21], as does the precise nature of the mechanism by which SERCA2b is upregulated in response to Rosiglitazone.

In conclusion, it may be relevant to consider the pharmacological concentration range within which Rosiglitazone is found in the body. The peak plasma concentration of Rosiglitazone is estimated to be ~1 μM (e.g. $C_{max} = 285 \pm 50$ ng/ml, or 0.80 ± 0.02 μM [22]). In our experiments, this concentration does partially inhibit SERCA2b: at [Rosiglitazone] = 0.8 μM, SERCA2b is ~65% maximal (Fig. 2). However, we could not detect any effect of 1 μM Rosiglitazone on resting $[Ca^{2+}]_{cyto}$; this may be because cellular Ca^{2+} homeostatic mechanisms are able to buffer the relatively minor leakage of Ca^{2+} that results from partial SERCA2b inhibition. Nevertheless, the fact that 1 μM Rosiglitazone induces upregulation of SERCA2b (e.g. 138.7 ± 5.7% basal at 72 h; Fig. 4C) suggests that 1 μM Rosiglitazone does have an effect in this regard (and also that depletion of $[Ca^{2+}]_{ER}$ rather than increased $[Ca^{2+}]_{cyto}$ may be responsible for triggering SERCA2b upregulation). In any case, the present study demonstrates restoration of normal Ca^{2+} handling *in vitro*, and so we suggest that monocytes of a patient on long-term Rosiglitazone therapy may not undergo chronic perturbations in resting $[Ca^{2+}]_{cyto}$.

The recent publication of meta- and teleo-analyses of clinical Rosiglitazone studies [10,11] has raised safety concerns regarding the increased risk of myocardial infarction, and of death from cardiovascular causes in Rosiglitazone-treated subjects. However, an interim analysis of the RECORD study has refuted this suggestion [23]. Aberrant Ca^{2+} signalling in cardiomyocytes is linked to the pathophysiology of cardiovascular disease [24], but the data presented here suggest that Rosiglitazone does not, in monocytic cells at least, exert detrimental effects on intracellular calcium haemostasis. Indeed, the net effect of Rosiglitazone therapy seems to be increased SERCA2b expression, and as decreased SERCA2b expression/activity levels correlate with both increased resting $[Ca^{2+}]_{cyto}$ and the progression of diabetic complications [6,7], such Rosiglitazone-induced SERCA2b upregulation may constitute a beneficial effect of Rosiglitazone therapy on cellular Ca^{2+} handling.

As the current study consists of *in vitro* investigations into the mechanisms by which cellular effects are brought about, conclusions drawn from the present study should be interpreted cautiously with regard to the clinical setting. The mechanisms by which Ca^{2+} is handled vary widely in different cell types [25], and it remains to be seen whether the mechanisms by which the monocytic cells studied here restore normal Ca^{2+} homeostasis during long-term treatment with Rosiglitazone are also in operation in other cell types that may be more directly relevant to the patient outcomes analysed in recent studies [10,11,23].

Acknowledgment

J.C. and L.A. are recipients of UWIC Ph.D. studentships.

References

[1] A. Advani, S.M. Marshall, T.H. Thomas, Impaired neutrophil store-mediated calcium entry in Type 2 diabetes, Eur. J. Clin. Invest. 34 (2004) 43–49.

[2] D.D. Belke, E.A. Swanson, W.H. Dillmann, Decreased sarcoplasmic reticulum activity and contractility in diabetic *db/db* mouse heart, Diabetes 53 (2004) 3201–3208.

[3] K.R. Bidasee, Y. Zhang, C.H. Shao, M. Wang, K.P. Patel, U.D. Dincer, H.R. Besch, Diabetes increases formation of advanced glycation end products on sarco(endo)plasmic reticulum Ca^{2+}-ATPase, Diabetes 53 (2004) 463–473.

[4] N. Singh, R. Webb, R. Adams, S.A. Evans, A. AlMosawi, M. Evans, A.W. Roberts, A.W. Thomas, The PPAR-γ activator, Rosiglitazone, inhibits actin polymerisation in monocytes: involvement of Akt and intracellular calcium, Biochem. Biophys. Res. Commun. 333 (2005) 455–462.

[5] A. Gunteski-Hamblin, J. Greeb, G.E. Shull, A novel Ca^{2+} pump expressed in brain, kidney, and stomach is encoded by an alternative transcript of the slow-twitch muscle sarcoplasmic reticulum Ca-ATPase gene, J. Biol. Chem. 263 (1988) 15032–15040.

[6] J. Clark, P.M. McDonough, E. Swanson, S.U. Trost, M. Suzuki, M. Fukuda, W.H. Dillmann, Diabetes and the accompanying hyperglycaemia impairs cardiomyocyte cycling through increased nuclear *O*-GlycNAcylation, J. Biol. Chem. 278 (2003) 44230–44237.

[7] Y. Zhong, S. Ahmed, I.L. Grupp, M.A. Matlib, Altered SR protein expression associated with contractile dysfunction in diabetic rat hearts, Am. J. Physiol. Heart Circ. Physiol. 281 (2001) H1137–H1147.

[8] S.A. Smith, Central role of the adipocyte in the insulin-sensitizing and cardiovascular risk modifying actions of the thiazolidinediones, Biochimie 85 (2003) 1219–1230.

[9] J. Hetzel, B. Balletshoffer, K. Rittig, D. Walcher, W. Kratzer, V. Hombach, H-U. Haring, W. Koenig, N. Marx, Rapid effects of Rosiglitazone treatment on endothelial function and inflammatory biomarkers, Arteriosder. Thromb. Vacs. Biol. 25 (2005) 1804–1809.

[10] S.E. Nissen, K. Wolski, Effect of Rosiglitazone on the risk of myocardial infarction and death from cardiovascular causes, N. Eng. J. Med. 356 (2007) 2457–2471.

[11] S. Singh, Y.K. Loke, C.D. Furberg, Thiazolidinediones and Heart Failure: A Teleo-Analysis, Diabetes Care [epub ahead of print].

[12] R.D. Shah, F. Gonzales, E. Golez, D. Augustin, S. Caudillo, A. Abbot, J. Morello, P.M. McDonough, P.J. Paolini, H.E. Shubeita, The antidiabetic agent Rosiglitazone upregulates SERCA2 and enhances TNF-α- and LPS-induced NF-κβ-dependent transcription and TNF-α-induced IL-6 secretion in ventricular myocytes, Cell Physiol. Biochem. 15 (2004) 41–50.

[13] K. Maruyama, D.H. MacLennan, Mutation of aspartic acid-351, lysine-352, and lysine-515 alters the Ca^{21} transport activity of the Ca^{21}-ATPase expressed in COS-1 cells, Proc. Natl. Acad. Sci. USA 85 (1988) 3314–3318.

[14] J. Elsner, J. Norgauer, G.J. Dobos, A. Emmendörffer, E. Schöpf, A. Kapp, J. Roesler, Flow cytometry reveals different lag times in rapid cytoplasmic calcium elevations in human neutrophils in response to *N*-formyl peptide, J. Cell Physiol. 157 (1993) 637–643.

[15] R.J. Webb, Y.M. Khan, M. East, A.G. Lee, The importance of carboxyl groups on the lumenal side of the membrane for the function of the Ca^{21}-ATPase of sarcoplasmic reticulum, J. Biol. Chem. 275 (2000) 977–982.

[16] A.C. Storer, A. Cornish-Bowden, Concentration of $MgATP^2$ and other ions in solution, calculation of the true concentrations of species present in mixtures of associating ions, Biochem. J. 159 (1976) 1–5.

[17] U. Eckstein-Ludwig, R.J. Webb, I.D. van Goethem, J.M. East, A.G. Lee, M. Kimura, P.M. O'Neill, P.G. Bray, S.A. Ward, S. Krishna, Artemisins target the SERCA of *Plasmodium falciparum*, Nature 424 (2003) 957–961.

[18] A. Perez, J.L. Thuillard, C.L. Bentzen, E.J. Niessor, Expression of nuclear receptors and apo E secretion during the differentiation of monocytic THP-1 cells into macrophages, Cell Biol. Toxicol. 19 (2003) 95–105.

[19] W.C. Huang, C.C. Chio, K.H. Chi, H.M. Wu, W.W. Lin, Superoxide anion-dependent Raf/MEK/ERK activation by peroxisome proliferator activated receptor gamma agonists 15-deoxy-delta(12,14)-prostaglandin J(2), ciglitazone, and GW1929, Exp. Cell Res. 277 (2002) 192–200.

[20] J.A. Engelman, M.P. Lisanti, P.E. Scherer, Specific inhibitors of p38 MAPK block 3T3-L1 adipogenesis, J. Biol. Chem. 273 (1998) 32111–32120.

[21] K. Wu, D. Bungard, J. Lytton, Regulation of SERCA Ca^{21} pump expression by cytoplasmic $[Ca^{21}]$ in vascular smooth muscle cells, Am. J. Physiol. Cell Physiol. 280 (2001) 843–851.

[22] M. Niemi, J.T. Backman, M. Granfors, J. Laitila, M. Neuvonen, P.J. Neuvonen, Gemfibrozil considerably increases the plasma concentrations of Rosiglitazone, Diabetologia 46 (2003) 1319–1323.

[23] P.D. Home, S.J. Pocock, H. Beck-Nielsen, R. Gomis, M. Hanefeld, N.P. Jones, M. Komajda, J.J. McMurray, RECORD Study Group, N. Eng. J. Med. 357 (2007) 28–38.

[24] D.M. Bers, Cardiac excitation-contraction coupling, Nature 415 (2002) 198–206.

[25] M. J Berridge, A. Galione, Cytosolic calcium oscillators, FASEB J. 2 (1988) 3074–3082.

Chapter 8

Publications and presentations

Publications and presentations

Peer Reviewed Publications:

Caddy, J., Singh, N., Atkin, L., Ahluwalia, M., Roberts, A.W., Lang, D., Thomas, A.W., & Webb, R.2008, "Rosiglitazone transiently disturbs calcium homeostasis in monocytic cells", *BBRC*, vol. 366, pp. 149-155.

Oral Presentations:

Caddy, J., Thomas, A.W. & Webb, R.J. 02/05/07.
"The anti-diabetic drug Rosiglitazone modulates calcium signalling in monocytic cells".
Speaking of Science 2007. The Graduate Centre, Cardiff University.

Poster Presentations:

Caddy, J., Thomas, A.W. & Webb, R.J. 05/05/06
"Rosiglitazone modulates cytoskeletal remodelling via inhibition of Ca^{2+}ATPase enzymes".
Speaking of Science 2006. The Graduate Centre, Cardiff University.

Caddy, J., Thomas, A.W., Atlin, L., Roberts, A.W., Lang, D., Webb, R. 30/10/08-02/11/08.
"Rosiglitazone induces unfolded protein responses but not apoptosis, in monocytes and vascular smooth muscle cells".
The World Congress on Controversies to Consensus in Diabetes, Obesity and Hypertension (CODHy), October 30 - November 2, 2008, Barcelona, Spain.